Impact of climate change on mean and high streamflow characteristics in Icelandic watersheds: a case study.

Philippe Crochet

Report number:	Date:	Number of pages:	Distribution:
2021-RD-01	December 2021	166	Public

Report title:
Impact of climate change on mean and high streamflow characteristics in Icelandic watersheds: a case study.

Author:
Philippe Crochet
philippec@simnet.is

Abstract:
This study presents an analysis of the hydrological response of three river catchments in Iceland to projected climate change in the 21st century. The catchments are located in the southeast (Geithellnaá), northeast (Selá) and northwest (Vatnsdalsá) of the country and their current hydrological regimes are strongly influenced by snowmelt seasonality. Daily streamflow series were simulated over the period 1981-2100 with the HYPE hydrological model forced with an ensemble of regional climate scenarios. Changes affecting near surface air temperature and precipitation and their impact on mean and extreme streamflow characteristics were analysed. The results suggest that if projected climate scenarios realise, temperature will increase over the next decades and lead to shorter snow seasons combined with less snow accumulation. These changes will in turn impact the hydrological regimes of all studied catchments and lead to a streamflow increase in autumn/winter and a streamflow decrease in spring/summer. The flood regimes of these catchments will also be impacted by the projected warming. In the Vatnsdalsá and Selá catchments, where annual maximum floods are mostly observed in spring in the present climate, a decrease in the magnitude of these extreme events is projected and at the same time, they will gradually tend to occur less frequently in spring and increasingly more frequently in autumn/winter. The Geithellnaá catchment is projected to remain under the main influence of autumn floods and a slight magnitude increase is possible.

Prepared for:
Rannsóknarsjóður Vegagerðarinnar

Keywords:
Iceland - Hydrology - Climate change - HYPE model - CORDEX

Executive summary

This study presents an analysis of the hydrological response of three Icelandic river catchments to projected climate change in the 21st century. The catchments are located in the southeast (Geithellnaá), northeast (Selá) and northwest (Vatnsdalsá) of the country and vary in size from 190 to 700 km^2. The current hydrological regimes of these catchments are strongly influenced by snowmelt seasonality. Daily streamflow series were simulated over the period 1981-2100 with the HYPE hydrological model forced with an ensemble of bias-corrected climate projections under two emission scenarios. The hydrological response of these catchments to projected climate change was analysed within moving 30-year periods and compared to the situation in the reference period (1981-2010).

A significant warming is projected throughout the projection horizon, more or less pronounced depending on the season and catchment location (0.3°C/decade on average for the lower emission scenario and 0.47°C/decade on average for the higher emission scenario). The variability of precipitation projections is mainly characterised by decadal to multi-decadal oscillations. The most noticeable long-term changes concerning mean precipitation are observed in the Vatnsdalsá catchment, where an increase is projected in summer under both emission scenarios, and in the Selá catchment, where an increase is projected in summer and autumn under the higher emission scenario.

In all three catchments, the projected warming is found to gradually lead to shorter snow seasons combined with less snow storage and an increasing fraction of precipitation will fall as rain rather than snow. These changes will, in turn, lead to changes in the seasonality of streamflow, by attenuating the contrast between low winter flows and high spring/summer flows, as observed in the present climate. A gradual streamflow increase is projected in autumn/winter in all catchments; Spring streamflow is projected to decrease in the Vatnsdalsá and Selá catchments but first increase and later decrease in the Geithellnaá catchment; Summer streamflow is projected to decrease in the Selá and Geithellnaá catchments but remain essentially unchanged in the Vatnsdalsá catchment. The changes are more pronounced under the higher emission scenario because it leads to a larger warming and therefore to a larger snowpack reduction than the lower emission scenario.

Projected climate change will also have an impact on the flood regimes of these catchments. As the projected warming will lead to less snow storage and shorter snow seasons, considerable changes are expected to occur in the Vatnsdalsá and Selá catchments, where annual maximum floods are mostly generated by spring snowmelt in the present climate. In these two catchments, these events will increasingly occur in winter in Vatnsdalsá and autumn/winter in Selá, instead of spring and their magnitude is expected to decrease. Toward the end of the 21st century, annual maximum floods will no longer occur primarily in spring but will have a similar or even higher probability of occurring in winter in Vatnsdalsá and autumn/winter in Selá. These changes reflect the decreasing influence of spring snowmelt and the increasing influence of rainfall or the combination of rainfall and snowmelt in autumn/winter driven by the projected warming. The Geithellnaá catchment will remain under the main influence of rainfall-generated annual maximum floods in autumn and their magnitude will possibly increase slightly. Results related to changes in the seasonal frequency of annual maximum floods appear to be relatively consistent and robust while those related to the changes in magnitude are associated with large uncertainties.

1 Introduction

Climate in Iceland is projected to change in the coming decades. In particular, the projected warming is expected to lead to less snow storage and the retreat of glaciers which, in turn, will impact the hydrological regimes of rivers (e.g. Jóhannesson et al., 2007; Einarsson and Jónsson, 2010; Thorsteinsson and Björnsson Eds., 2011; Crochet 2013; Björnsson et al., 2018; Crochet 2020). As a matter of fact, changes are already occurring and records indicate that Icelandic glaciers have essentially been losing mass since the mid-90s (Aðalgeirsdóttir et al., 2020).

Any significant change in the current hydrological regimes of rivers may in turn have an impact on water resources management, the operation of existing hydropower installations and flood risk. Assessing climate change impact on the hydrological characteristics of river basins is therefore very important in order to adapt water management strategies and anticipate mitigating actions that may have to be taken to protect populations and infrastructures. This study is a continuation of the work initiated in Crochet (2020) where the hydrological response of three Icelandic river basins to projected climate change in the 21st century was investigated. The study of Crochet (2020) indicates that the hydrological response varies with each catchment in relation to its physiographic properties and current hydrological regime. Therefore, in order to get a more comprehensive insight into the hydrological response to projected climate change across Iceland, three additional catchments are examined in this study.

The methodology is based on the following impact modelling chain: “emission scenario–global climate model–regional downscaling–bias correction–hydrological modelling–analysis” (see for instance Arheimer and Lindström, 2015). Different strategies of varying complexity have been suggested to address the uncertainty associated with the combination of emission scenarios, climate models, downscaling methods and hydrological modelling (see for instance Habets et al., 2013; Vormoor et al., 2015). The modelling strategy applied in this work is based on the use of two emission scenarios, six different combinations of global and regional climate models, one method for locally correcting the temperature outputs of the regional climate models, two methods for correcting the precipitation outputs, and one hydrological model, leading to an ensemble of twelve hydrological projections for each future emission scenario.

Section 2 presents the studied catchments and Section 3 presents the material and methods. Section 4 is dedicated to the hydrological modelling and Section 5 to the analysis of climate projections. The hydrological response to projected climate change is analysed in Sections 6 and 7 and Section 8 concludes this report.

2 Study catchments

Three mesoscale gauged river basins located in different regions are studied (Figure 1 and Table 1). Vatnsdalsá is located in East-Húnavatnssýsla, in the northwest of Iceland; Selá is located in Vopnafjörður, in the northeast of Iceland; Geithellnaá is located in Álftafjörður, in the southeast of Iceland, east of the Vatnajökull ice-cap. The gauging stations are monitored by Veðurstofa Íslands.

Icelandic rivers are usually classified in three main categories according to the origin of flow: direct runoff rivers (D), glacial fed rivers (J), groundwater fed rivers (L) and whether they flow through lakes (S). In practise, rivers are often a combination of several of these categories. According to Hróðmarsson and Þórarinsdóttir (2018), the Vatnsdalsá river at gauging site vhm45 is a combination of three categories (D, L, S), the Selá river at gauging site vhm48 is a combination of two categories (L, D) and the Geithellnaá river at gauging site vhm149 is classified as direct runoff river but note that its drainage area includes a small part of the Þrándarjökull ice-cap. According to the Corine Land Cover data (Árnason and Matthíasson, 2017), these catchments display a variety of land cover types. The Vatnsdalsá river basin is mainly covered with vegetated land (ca. 57%), barren areas (ca. 21%), wetlands (ca. 18%) and lakes (ca. 3%). The Selá river basin is mainly covered with barren areas (ca. 65%), vegetated land (ca. 29%) and wetlands (ca. 5%). The Geithellnaá river basin is mainly covered with vegetated land (ca. 53%), barren areas (ca. 42%) and an ice cap (ca. 4%).

Table 1: Discharge gauging stations and main characteristics of catchments

Name of river and location of gauging station	ID	River type	Drainage area (km^2)	Mean elevation (m.a.s.l)
Vatnsdalsá í Húnavatnssýslu, Forsæludalur	vhm45	D+L+S	455	555
Selá í Vopnafirði, Hróaldsstaðir	vhm48	L+D	697	546
Geithellnaá í Álftafirði, Geithellur	vhm149	D	188	609

Figure 1: Overview of the studied catchments. Glaciers and coastline from National Land Survey of Iceland. Catchment delineation based on ArcticDEM (Porter et al., 2018).

3 Materials and methods

3-1 Method overview

The same methodology used in Crochet (2020) was applied in this study. Daily hydrologic series were simulated in the three catchments over the period 1981-2100 with the HYPE hydrological model forced with an ensemble of bias-corrected CORDEX regional climate projections, considering two emission scenarios. Using an ensemble of climate projections rather than a single one gives a better representation of possible future states of the climate system and allows a more robust evaluation of the future temporal evolution of the hydrological system under study. Various hydro-climatic variables were then extracted from the ensemble of hydrological projections and their characteristics analysed in moving 30-year periods (1981-2010; 1991-2020; 2001-2030; 2011-2040; 2021-2050; 2031-2060; 2041-2070; 2051-2080; 2061-2090; 2071-2100). The reference period is defined as the 1981-2010 period.

The hydro-climatic variables considered in this study are:

- Temperature, precipitation, rainfall, snowfall, snow accumulation and melt, river discharge.

For each projection (or realisation), monthly, seasonal and annual values were first calculated by averaging daily values from each month, season and water year, respectively, and then the 30-year mean calculated in each period. The water year is defined from October of year *i* to September of year *i*+1 and the four seasons are October to December (OND), January to March (JFM), April to June (AMJ) and July to September (JAS). In order to analyse seasonal changes in more details, 30-year mean daily values were also calculated for each day of the water year.

A two-sided Mann-Whitney test with a 5% significance level was used to evaluate the significance of changes in mean daily, seasonal and annual values from the reference period (1981-2010) to the future periods. The null hypothesis being that the projections in the reference and future periods are drawn from populations having the same distribution and the alternative hypothesis being that the distributions differ by some location shift. Box-plots of the changes from the reference period (1981-2010) to the future periods were also analysed and the significance of changes evaluated from their medians.

The annual maximum of daily discharge simulations (annual maximum floods, AMFs) was also extracted for each water year, within each 30-year period, and changes in the timing and magnitude of these extreme events examined throughout the projection horizon. Changes in the timing of AMFs are analysed in order to examine possible changes in the flood-generating mechanisms. To analyse changes in the magnitude of AMFs, a Gumbel distribution was fitted (Stephenson 2002; Delignette-Muller and Dutang 2015) to the AMFs, and the magnitude of the T-year floods (T=10 and 100 years) estimated in each future period and compared to the T-year floods in the reference period (1981-2010). Finally, the flood magnitude Q was fixed and the corresponding return period T(Q) estimated in each future period and compared to T(Q) in the reference period.

3-2 Hydrological model

HYPE is a semi-distributed hydrological model developed by the Swedish Meteorological and Hydrological Institute to assess water resources and water quality. It is forced with time series of daily precipitation and near surface air temperature to simulate water flow and nutrients concentrations at the catchment scale. The catchment to be modelled may be divided into sub-catchments which, in turn, are divided into land cover and soil type classes. A detailed description of the model can be found in Lindström et al. (2010) and on the HYPE wiki page (http://www.smhi.net/hype/wiki/doku.php). This model has been used in various countries around the world, including in Iceland (Marschollek, 2017; de Niet et al. 2020; Crochet 2020).

3-3 Climate projections

The climate projections for daily precipitation and near surface air temperature used to force the HYPE hydrological model are based on the CORDEX framework (Coordinated Regional Climate Downscaling Experiment) (www.cordex.org). This framework has provided an ensemble of high-resolution regional climate projections over several regions of the world for use in impact and adaptation studies (Giorgi et al., 2009). The CORDEX projections were obtained by dynamical downscaling of a set of coarse global climate simulations made with different global climate models (GCMs), using a set of regional climate models (RCMs), assuming various emission scenarios referred to as representative concentration pathways (RCPs). The set of global climate model simulations used within CORDEX was planned in support of the IPCC Fifth Assessment Report (referred to as CMIP5). The RCPs are a measure of the strength of the anthropogenic greenhouse effect. Two emission scenarios are considered in this study. The first one (RCP4.5) assumes a stabilisation of radiative forcing by the end of the 21st century at 4.5 W/m² relative to pre-industrial conditions and the second one (RCP8.5), more pessimistic, assumes a stabilisation of radiative forcing by the end of 21st century at 8.5 W/m² relative to pre-industrial conditions. In this project, the climate projections are taken from the European branch of CORDEX, EURO-CORDEX (www.euro-cordex.net) (Jacob D., Petersen J., Eggert B. *et al.*, 2014), as this region includes Iceland and is available at a very high horizontal resolution (0.11°, about 12.5 km).

The CORDEX projections consist of a historical period (1976-2005) and a projection period (2006-2100) assuming a given RCP. The projections in the historical period (1976-2005) do not correspond to the actual reality as it happened day after day but represent a possible realisation of what could have taken place. Evaluation series driven by the European Centre for Medium-Range Weather Forecasts (ECMWF) ERA-Interim reanalyses (Dee et al., 2011) and dynamically downscaled with the selected RCMs are also available for the 1981-2010 period and were used in this study to investigate the intrinsic quality of these RCMs.

Tables 2 and 3 present the GCMs and RCMs used in this study. The two selected GCMs are those suggested in Gossling (2017) as the best GCMs for the Icelandic domain, namely MOHC-HadGEM2-ES and MPI-ESM-LR. Each CORDEX projection is considered equally likely.

Table 2: List of CORDEX GCMs and RCMs

Model	Type	Institution	Reference
ERA-Interim	Reanalysis	ECMWF	Dee et al., 2011
MOHC-HadGEM2-ES	GCM	Met Office Hadley Centre	Jones et al., 2011
MPI-ESM-LR	GCM	ESM of the Max-Planck-Institut fur Meteorologie	Giorgetta et al. 2013
CCLM4-8-17	RCM	CLMcom	Rockel et al., 2008
RCA4	RCM	SMHI	Kupiainen et al. 2011 Samuelsson et al. 2011
RACMO22E	RCM	KNMI	Meijgaard van et al. 2012
REMO2009	RCM	MPI-CSC	Jacob et al., 2012

Table 3: List of CORDEX GCM-RCM combinations and emission scenarios (RCP)

		RCP	RCM			
			CCLM4-8-17	RCA4	RACMO22E	REMO2009
Forcing GCM	ERA-Interim (evaluation)		x	x	x	x
	MOHC-HadGEM2-ES	RCP4.5 & RCP8.5	x	x	x	
	MPI-ESM-LR	RCP4.5 & RCP8.5	x	x		x

3-4 Reference weather data

Daily precipitation and 2m-temperature from the high-resolution (2.5 km) ICRA weather reanalysis (Nawri et al., 2017) produced by Veðurstofa Íslands constitute the historical weather data of reference (1981-2017) used i) as input to calibrate the HYPE hydrological model ii) to verify the credibility of the CORDEX climate projections in the historical period and iii) to statistically bias-correct the CORDEX climate projections prior to use them as input to HYPE.

3-5 Hydrological data

Daily-averaged discharge series from three gauging stations monitored by Veðurstofa Íslands were used to calibrate HYPE and verify the credibility of the simulated streamflow series in the historical period when HYPE is forced with the bias-corrected CORDEX projections.

3-6 Other data

The river catchments and sub-catchments delineation was done with QGIS (v.3.6) using a digital elevation model (DEM) with resolution 10m obtained from ArcticDEM (Porter et al., 2018). A DEM with resolution 10m obtained from the download page of the National Land Survey of Iceland (http://atlas.lmi.is/LmiData/) was used to calculate the average elevation of the catchments (cf. Table 1). The hydrological modelling with HYPE requires the use of a landuse map and a soil map. The soil map of Iceland compiled by the Agricultural University of Iceland (Arnalds and Óskarsson, 2009; Arnalds, 2015) was used and downloaded from http://rangarvellir.ru.is. The Corine Land Cover data updated for the reference year 2012 (Árnason and Matthíasson, 2017) were used and obtained from the download page of the National Land Survey of Iceland. Additional information about coastline, glaciers and water bodies were also obtained from the download page of the National Land Survey of Iceland.

3-7 Bias-correction

The same post-processing procedure used in Crochet (2020) was applied to locally bias-correct the daily temperature and precipitation projections. This procedure is necessary in order to guaranty consistency between the CORDEX projections and ICRA reference weather data used in the calibration of the HYPE hydrological model:

- The post-processing of temperature projections is based on quantile mapping (QM) (Gudmundsson et al. 2012; Gudmundsson 2016). A specific correction was defined for each month. The correction coefficients were estimated by comparing ICRA data to the CORDEX historical series in the common period 1981-2005. The correction was then applied to the entire projection period (1976-2100).
- Two post-processing methods were used for bias-correcting the precipitation projections: i) direct quantile mapping as for temperature projections and ii) an analog-based method (not documented yet) based on the analysis of spatial precipitation gradients using the S1 score (see Wilks, 1995), followed by quantile mapping.

4 HYPE model calibration

For the hydrological modelling, the Vatnsdalsá catchment was divided into eight subbasins, the Selá catchment was divided into five subbasins and the Geithellnaá catchment was divided into three subbasins. Daily-averaged discharge series from gauging station vhm45 were used to calibrate HYPE in the Vatnsdalsá catchment, daily-averaged discharge series from gauging station vhm48 were used to calibrate HYPE in the Selá catchment and daily-averaged discharge series from gauging station vhm149 were used to calibrate HYPE in the Geithellnaá catchment.

A spin-up time of one year was used for all catchments. The model calibration was made considering a period of eleven water years (01-Oct-1999 to 30-Sep-2010). Monte Carlo based optimisation methods were used for that purpose, considering a combination of criteria to judge the model performance (Kling-Gupta efficiency and relative bias). The best performing model parameter set was then obtained for each catchment, as in Crochet (2020). The use of a single parameter set to run the HYPE hydrological model implies that the uncertainty related to hydrological modelling is not addressed in this study. Different strategies of varying complexity have been proposed to take into account the uncertainty associated with hydrological modelling and its combination with other sources of uncertainties (climate models, downscaling methods), ranging from the use of an ensemble of parameter sets with the same hydrological model to the use of an ensemble of different hydrological models (see for instance Habets et al., 2013; Vormoor et al., 2015).

Hydrological simulations were then obtained with the calibrated models forced with the ICRA-reanalysis data over the water years 1981-2016 and years which did not belong to the calibration period and for which observed daily discharge was available were used to verify the quality of the simulations (validation). The ability for the simulated daily streamflow series to correctly reproduce the magnitude and timing of annual maximum floods (AMFs) was also examined.

Tables 4 and 5 and Figs. 2 and 3 summarise the results of the daily discharge simulations. The overall NSE was calculated with all valid observed daily discharge data in each period while the annual NSE was only calculated in water years for which observed daily discharge was available in more than 300 days. The overall Nash-Sutcliffe efficiency (NSE) in the validation period is always greater than 0.65. The best results have been obtained with Geithellnaá (vhm149) where the overall NSE reaches 0.725 in the validation period and the annual NSE never falls below 0.55.

For the Vatnsdalsá catchment (vhm45), the years prior to the calibration period are better simulated than those after the calibration period. Three years appear to be poorly calibrated (NSE<0): 1997, 2011 and 2015. These poor performances are likely related to uncertainties in the snowpack estimation and the onset of snowmelt in these years. The seasonality of mean daily streamflow is well reproduced but some underestimation dominates in April.

For the Selá catchment (vhm48), model performances are superior in the validation period than in the calibration period. The seasonality of mean daily streamflow is well reproduced.

For the Geithellnaá catchment (vhm149), model performances are poorer in the years prior to the calibration period than those after the calibration period. The seasonality of mean daily streamflow is well reproduced. Note that the influence of Þrándarjökull glacier on the streamflow of Geithellnaá was found to be relatively limited (9% contribution to JAS streamflow on average with simulations made with the optimum parameter set). The sensitivity of the overall NSE coefficient to variations in glacier melt parameters has also been investigated and found to be very limited, also meaning that the calibration of glacier melt parameters is probably not very robust.

The magnitudes and days of occurrence of annual maximum floods (AMFs) were extracted from the observed and simulated daily discharge series. The plots of the magnitude versus occurrence day are shown in Figs. 4 to 6. The catchments experience AMFs in different seasons, associated with different underlying generating mechanisms (rainfall, snowmelt, combined rainfall and snowmelt). In the Vatnsdalsá catchment (vhm45), a large majority of AMFs occurs during spring. In the Selá catchment (vhm48), the majority of AMFs occurs also during spring. In the Geithellnaá catchment (vhm149), the majority of AMFs occurs in late summer and autumn.

AMFs occurring in spring are expected to be primarily generated by snowmelt, sometimes combined with some rainfall. Summer and autumn AMFs are expected to be primarily generated by rainfall, sometimes combined with some snowmelt. AMFs occurring in winter are expected to be generated by a combination of rainfall and snowmelt.

Overall, despite a few discrepancies, the seasonality of the day of occurrence of AMFs is reasonably well reproduced by the HYPE simulations in all three catchments, meaning that the different types of floods are simulated in the correct proportions. The most noticeable discrepancies are: one event simulated by HYPE in December in the Vatnsdalsá catchment while none was observed in that month; two events simulated by HYPE in Sep-Oct in the Selá catchment while none was observed in that period; one event observed in August in the Selá catchment while none was simulated by HYPE in that month. The results also indicate that the HYPE simulations reproduce the magnitude of observed AMFs reasonably well.

Table 4: Results of the HYPE daily discharge calibration/validation procedure with the best performing parameter set. Overall Nash-Sutcliffe efficiency (NSE) and relative bias (RE). All water years (1981-2016). Validation water years (1981-1998; 2010-2016).

Catchment	**Calibration period**		**Validation period**		**All years**	
	NSE	RE (%)	NSE	RE (%)	NSE	RE (%)
vhm45	0.739	0.54	0.653	-3.2	0.676	-1.98
vhm48	0.667	0.55	0.689	0.07	0.683	0.3
vhm149	0.747	-0.02	0.725	4.76	0.731	3.72

Table 5: Results of the HYPE daily discharge calibration/validation procedure with the best performing parameter set. Annual Nash-Sutcliffe efficiency (NSE) for water years 1981-2016.

Catchment	**Min NSE**	**Median NSE**	**Max NSE**
vhm45	-0.95	0.71	0.84
vhm48	0.12	0.66	0.872
vhm149	0.55	0.719	0.833

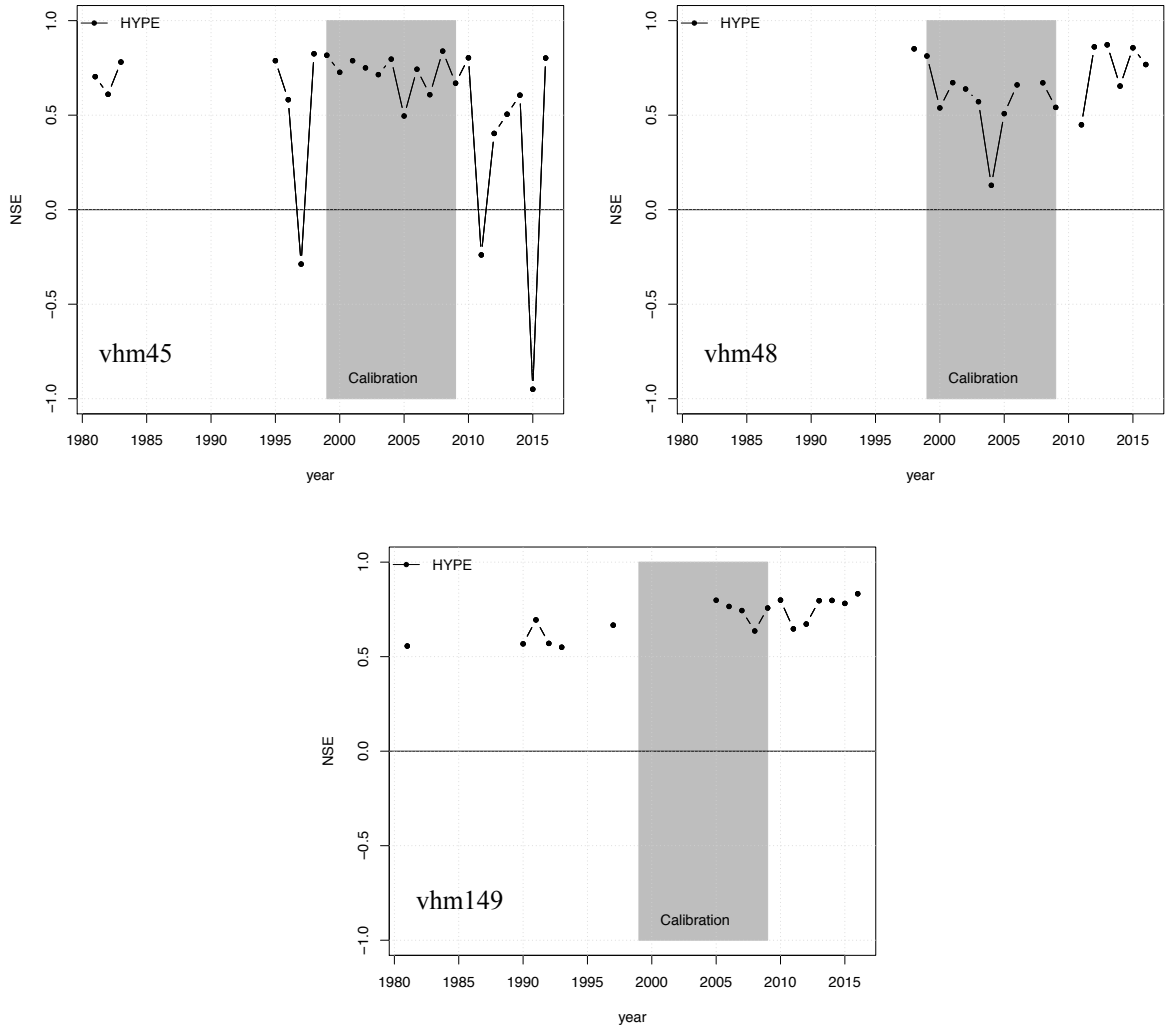

Fig. 2: Annual NSE for years with more than 300 valid daily discharge observations (water years 1981-2016): vhm45 (top-left); vhm48 (top-right); vhm149 (bottom).

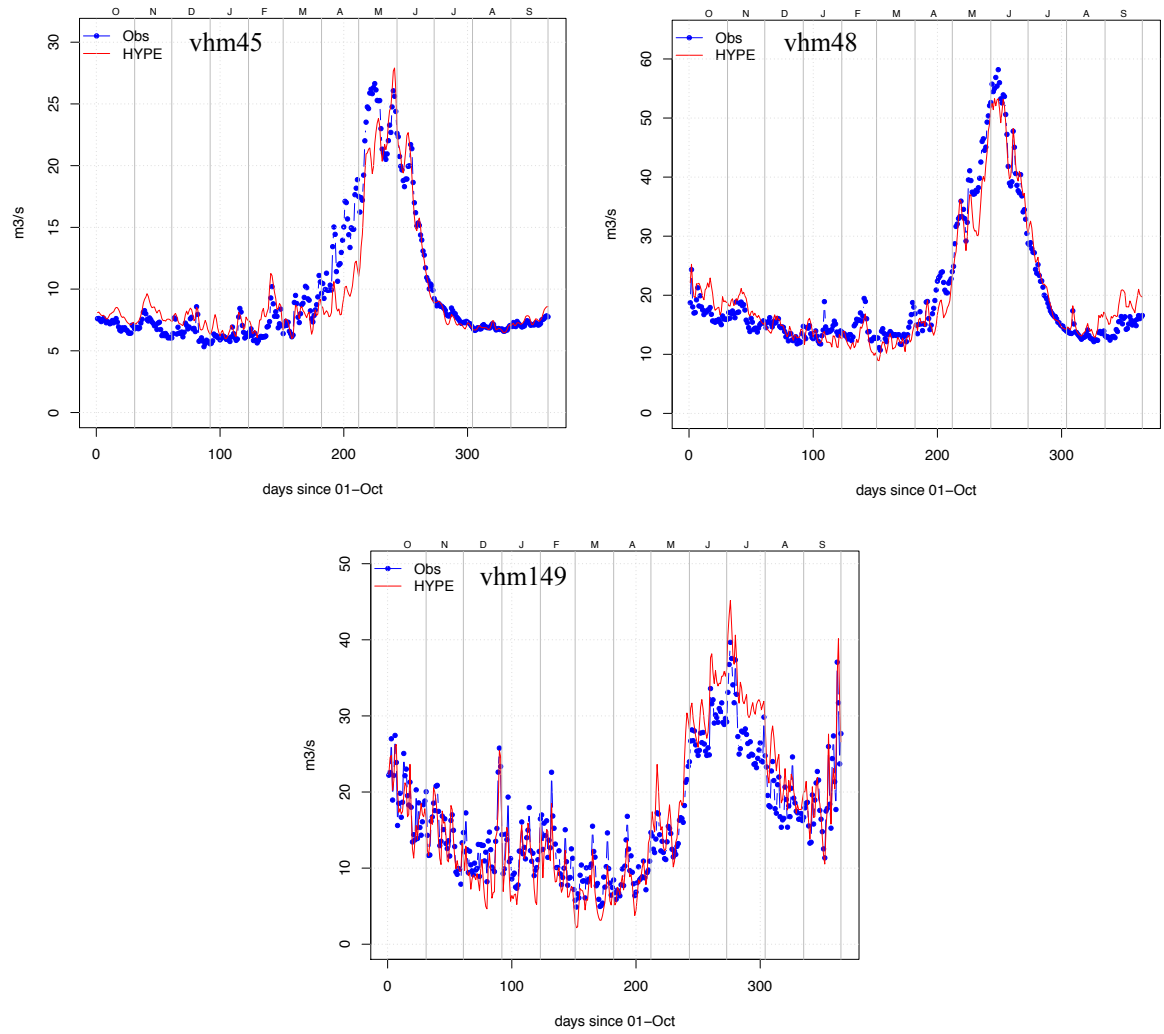

Fig. 3: Seasonality of mean daily discharge in the water years 1981-2016. Observed discharge (blue), HYPE discharge simulations (red); vhm45 (top-left); vhm48 (top-right); vhm149 (bottom). The day = 1 for 1 October and 365 for 30 September.

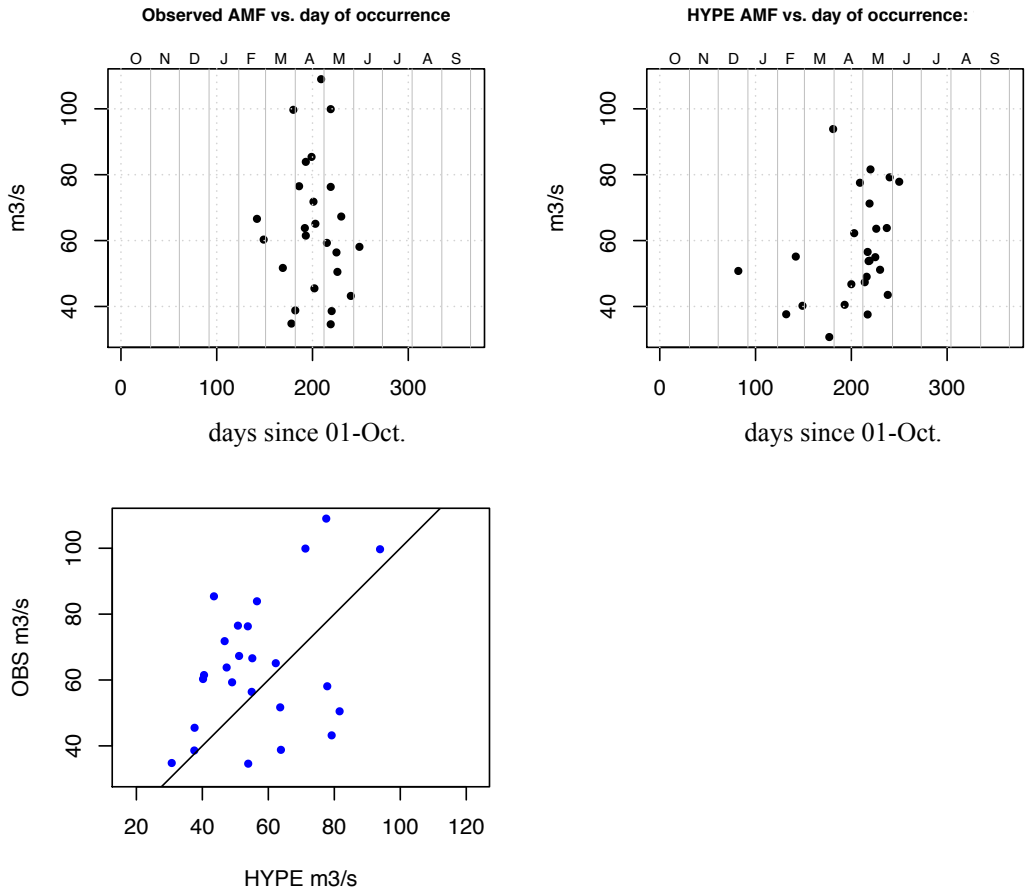

Fig. 4: Annual maximum floods (AMFs) analysis for the Vatnsdalsá catchment (vhm45) (water years 1981-2016). Top-left: magnitude vs. day of occurrence of observed AMFs. Top-right: magnitude vs. day of occurrence of simulated AMFs. Bottom-left: Observed vs. simulated magnitude. Only years with more than 300 valid daily discharge observations are included.

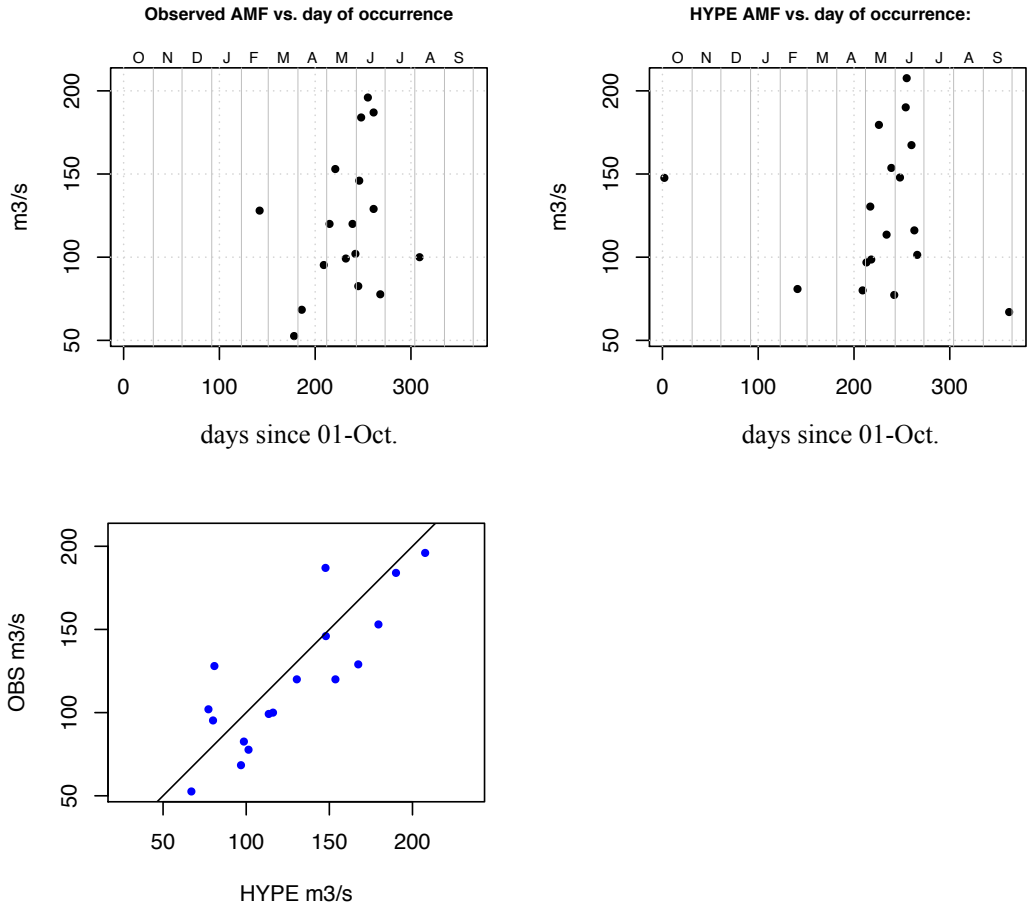

Fig. 5: Annual maximum floods (AMFs) analysis for the Selá catchment (vhm48) (water years 1981-2016). Top-left: magnitude vs. day of occurrence of observed AMFs. Top-right: magnitude vs. day of occurrence of simulated AMFs. Bottom-left: Observed vs. simulated magnitude. Only years with more than 300 valid daily discharge observations are included.

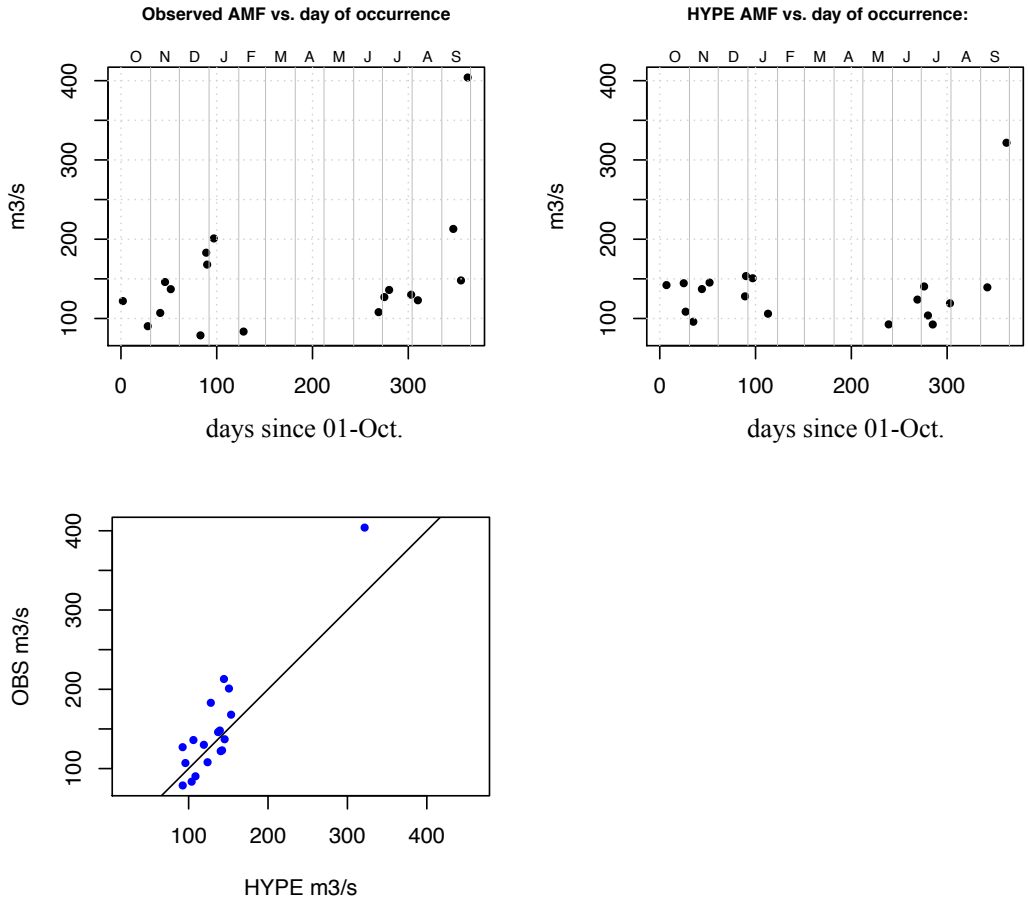

Fig. 6: Annual maximum floods (AMFs) analysis for the Geithellnaá catchment (vhm149) (water years 1981-2016). Top-left: magnitude vs. day of occurrence of observed AMFs. Top-right: magnitude vs. day of occurrence of simulated AMFs. Bottom-left: Observed vs. simulated magnitude. Only years with more than 300 valid daily discharge observations are included.

5 EURO-CORDEX climate projections

CORDEX daily precipitation and temperature projections were area-averaged over the respective catchments and sub-catchments.

5-1 RCMs evaluation and bias-correction skills using the evaluation series

In order to evaluate the intrinsic quality of the different RCMs (see Table 3) and the skills of the bias-correction methods, a comparison was made between the ICRA reanalysis and the CORDEX evaluation series obtained by dynamical downscaling of ERA-interim reanalyses with the selected RCMs. These evaluation series are synchronised with observed climate, making a direct comparison with ICRA reanalysis possible. For sake of simplicity, only results related to daily precipitation and temperature area-averaged over the entire catchments are presented. Quantile mapping correction coefficients were defined by comparing ICRA data in the 1981-2010 period to the CORDEX evaluation series in the available period (1981-2010 or 1989-2008, depending on the RCM). The following evaluation statistics were calculated in the period 1989-2008, common to all evaluation series:

Mean error: ME=E[CORDEX-ICRA]

Root-mean-square error: RMSE= $\sqrt{E[(CORDEX\text{-}ICRA)^2]}$

5-1-1 Temperature

Appendix 1 presents ME and RMSE before and after bias-correction. All evaluation series display a temperature bias in all three catchments, usually more pronounced in summer, except with CCLM-4-8-17 for the Vatnsdalsá catchment (vhm45) which is relatively unbiased in most months. These biases are partly related to differences between the ICRA and CORDEX terrain elevations caused by a difference of spatial resolutions. The ME is mainly negative (underestimation) in most months and catchments with RCA4 and RACMO22E, and mainly positive (overestimation) with CCLM-4-8-17 and REMO2009, except in winter when it is mainly negative or close to zero. These results are in line with those obtained with the three catchments studied in Crochet (2020). Quantile mapping eliminates the bias, on average, and reduces RMSE in months when ME was large. After bias-correction, the different evaluation series are relatively similar in terms of RMSE, with a slight advantage for series obtained with CCLM-4-8-17 and slightly poorer results for series obtained with RCA4.

5-1-2 Precipitation

Appendix 2 presents ME and RMSE before and after bias-correction. All evaluation series display some biases, in most months and all catchments. These biases are not systematic as for temperature and the scatter plots indicate either over- or under-estimation depending on the days (not shown). As a result, precipitation over the Vatnsdalsá catchment (vhm45) tends to be overestimated on average in most months with CCLM-4-8-17 and RCA4, except in summer, slightly underestimated on average with REMO2009 in winter, and relatively unbiased on average with RACMO22E, except in summer. Precipitation over the Selá catchment (vhm48) tends to be

slightly overestimated on average with CCLM-4-8-17 and RCA4, slightly underestimated on average with REMO2009, and mainly unbiased on average with RACMO22E. Precipitation over the Geithellnaá catchment (vhm149) tends to be underestimated on average in most months and with all RCMs, especially in winter, and this underestimation is of more systematic nature than for the other two catchments. Direct quantile mapping eliminates the bias, on average, and either reduces RMSE, when ME is large, or keeps it similar to its original level, when ME is low, meaning that the scatter is not necessarily reduced. The analog-based correction method is efficient at reducing and even eliminating the bias, on average, and at reducing RMSE in months when ME is large. Little or no RMSE reduction is observed for the Geithellnaá catchment (vhm149) after analog-based correction, meaning that the method has corrected systematic biases, on average, but not reduced the scatter. Applying quantile mapping after analog-based correction further reduces ME but does not further reduce RMSE and sometimes slightly re-increases it to a level close to direct quantile mapping.
Overall, the different bias-corrected evaluation series are relatively similar in terms of RMSE, with a slight advantage for CCLM-4-8-17 and RACMO22E. Combining the analog-based method with quantile mapping leads to similar or slightly better results than direct quantile mapping regarding RMSE and similar results regarding ME. Both methods will be used to correct the CORDEX precipitation projections.

5-2 Projections

Comparisons between CORDEX climate projections and ICRA reference climate in the 1981-2010 period confirms i) the presence of biases in the original CORDEX data, as already observed in the evaluation series and ii) the efficiency of the correction methods at eliminating these biases on average (see Appendix 3 and 4). After bias-correction, a temporal trend test based on simple linear regression was applied to monthly temperature and precipitation projections in the entire 1976-2100 period, considering a 5% significance level.

5-2-1 Bias-corrected temperature

A significant warming (linear trend) is observed in all months and all three catchments, more or less pronounced according to the emission scenario and the month under consideration (see Table 6). On average over all catchments, a warming rate of 0.3°C/decade is projected under the RCP4.5 emission scenario and 0.47°C/decade under the RCP8.5 emission scenario. This is slightly larger than the warming rate obtained from the uncorrected CORDEX temperature projections (0.28°C/decade under RCP4.5 and 0.425°C/decade under RCP8.5). The warming rate is usually larger with scenarios driven by HadGEM2ES GCM than with scenarios driven by MPI−ESM−LR GCM (not shown). The largest warming rate is observed in the Selá catchment (vhm48). In addition to the presence of long-term trends, oscillations are observed in the temperature series and reflect the natural climate variability (not shown). The temperature series are more or less grouped according to the driving GCM and the two groups of projections do not necessarily vary in phase with each other, especially between September and May. The projected temperature increase throughout the 21st century is well reflected in the evolution of the seasonal temperature cycle (see Appendix 5).

5-2-2 Bias-corrected precipitation

A large majority of projections does not exhibit any significant linear monthly precipitation trend in most months and catchments. When a significant linear trend is detected, it often concerns one projection only or several projections driven by the same GCM, seldom by both GCMs (see Tables 7 and 8). Significant positive linear precipitation trends were detected in more than 50% of the projections under the RCP8.5 emission scenario only: in Sep. and Oct. for the Vatnsdalsá catchment (vhm45) and in Dec. for the Selá catchment (vhm48).

Similarly to what was already observed in the catchments studied in Crochet (2020), the main features characterising the variability of precipitation projections are decadal to multi-decadal oscillations, especially in autumn-winter, corresponding to a succession of “wet” and “dry” periods. These oscillations are characteristic of the natural variability of precipitation in the Icelandic domain (see for instance Crochet, 2007). The oscillations often depend on the driving GCM and the two groups of precipitation projections driven by the two GCMs do not always vary in phase with each other. The fact that no consistent linear precipitation trend is detected by all ensemble members for a given month does not mean that no change is affecting precipitation in some particular periods. Changes in 30-year mean annual and seasonal precipitation relative to the reference period (1981-2010) are studied in Section 6.

To illustrate the precipitation variability, Appendix 6 presents the time-series of bias-corrected monthly precipitation in February, June and October under the RCP4.5 emission scenario. A 5-year moving average was applied to the monthly series in order to make the oscillations appear more clearly. Similar results were observed for the RCP8.5 scenario (not shown).

Table 6: Average warming rate in degree Celsius/decade estimated from the bias-corrected monthly temperature series (1976-2100). All the ensemble members display a statistically significant linear trend (slope of the linear regression statistically different from zero).

Month	vhm45		vhm48		vhm149	
	RCP4.5	RCP8.5	RCP4.5	RCP8.5	RCP4.5	RCP8.5
Jan	0.295	0.397	0.283	0.380	0.258	0.323
Feb	0.315	0.466	0.282	0.464	0.262	0.418
Mar	0.279	0.436	0.276	0.460	0.246	0.386
Apr	0.286	0.429	0.325	0.523	0.273	0.382
May	0.300	0.447	0.382	0.564	0.316	0.470
Jun	0.260	0.384	0.354	0.520	0.318	0.487
Jul	0.311	0.538	0.370	0.590	0.355	0.554
Agu	0.279	0.498	0.319	0.564	0.372	0.624
Sep	0.321	0.474	0.335	0.506	0.358	0.544
Oct	0.315	0.473	0.332	0.495	0.297	0.447
Nov	0.314	0.515	0.326	0.505	0.282	0.420
Dec	0.277	0.449	0.288	0.474	0.245	0.389
Mean	**0.296**	**0.459**	**0.323**	**0.504**	**0.299**	**0.454**

Table 7: Monthly precipitation projections corrected by direct quantile mapping: Number of members in the ensemble with a significant linear trend (slope of the linear regression statistically different from zero). The average trend (mm/day / decade) is given in brackets when more than 50% of the members have a statistically significant linear trend.

Month	vhm45		vhm48		vhm149	
	RCP4.5	RCP8.5	RCP4.5	RCP8.5	RCP4.5	RCP8.5
Jan	0	2	1	0	2	0
Feb	0	0	1	3	0	0
Mar	0	0	0	3	1	0
Apr	0	0	0	1	1	0
May	0	2	1	2	1	0
Jun	2	1	2	1	2	0
Jul	2	2	2	1	1	0
Agu	1	2	0	0	3	1
Sep	3	6 (0.09)	1	1	0	0
Oct	0	5 (0.11)	0	2	3	0
Nov	1	3	0	0	1	3
Dec	0	3	1	4 (0.098)	2	0

Table 8: Monthly precipitation projections corrected by applying an analog-based method followed by quantile mapping: Number of members in the ensemble with a significant linear trend (slope of the linear regression statistically different from zero). The average trend (mm/day / decade) is given in brackets when more than 50% of the members have a statistically significant linear trend.

Month	vhm45		vhm48		vhm149	
	RCP4.5	RCP8.5	RCP4.5	RCP8.5	RCP4.5	RCP8.5
Jan	0	1	1	1	0	3
Feb	0	1	2	3	0	0
Mar	0	0	0	3	0	1
Apr	0	0	0	1	0	1
May	1	2	1	2	0	1
Jun	1	1	2	2	0	2
Jul	3	1	2	1	0	0
Agu	1	0	0	0	1	3
Sep	1	6 (0.08)	1	0	0	0
Oct	0	4 (0.11)	0	2	0	3
Nov	1	2	0	0	2	1
Dec	0	3	1	4 (0.1)	0	1

6 Hydrological projections

Daily hydrological projections were simulated over the period 1981-2100 by forcing HYPE with the ensemble of bias-corrected daily CORDEX precipitation and temperature projections. Two hydrological simulations were obtained from each original climate projection (cf. Table 3): one by forcing HYPE with temperature and precipitation projections bias-corrected by direct quantile mapping and the other one by forcing HYPE with the temperature projection bias-corrected by direct quantile mapping and the precipitation projection bias-corrected after combining an analog-based method and quantile mapping (cf. Section 3-7), leading to an ensemble of twelve hydrological projections (or members) for each RCP emission scenario.

6-1 Comparison with reference streamflow

In order to evaluate the skills of the bias-correction methods applied to the CORDEX precipitation and temperature projections and their transmission into the hydrological modelling chain, the streamflow simulations made with HYPE forced with CORDEX in the 1981-2010 reference period were compared to those made with HYPE forced with the ICRA reanalysis. Figs 7 to 9 present the seasonality of mean daily discharge in the 1981-2010 period, together with temperature, precipitation and snow accumulation. There is a good agreement between the two sets of hydrological simulations indicating consistency between the HYPE simulations forced with the ICRA reanalysis and those forced with the bias-corrected CORDEX projections in the same period.

The spread of the ensemble reflects the uncertainties associated with the climate projections, the bias-correction methods, and their transmission into the hydrological modelling chain. In conclusion, the seasonality of streamflow projections in the 1981-2010 period offers a reliable estimation of the reference streamflow seasonality in that period, giving credibility to the bias-correction methods applied to the CORDEX projections. It is assumed in the rest of the study that the validity of the bias-correction methods holds for the entire projection period. It is also assumed that the validity of the HYPE best performing parameter set holds for the entire projection period.

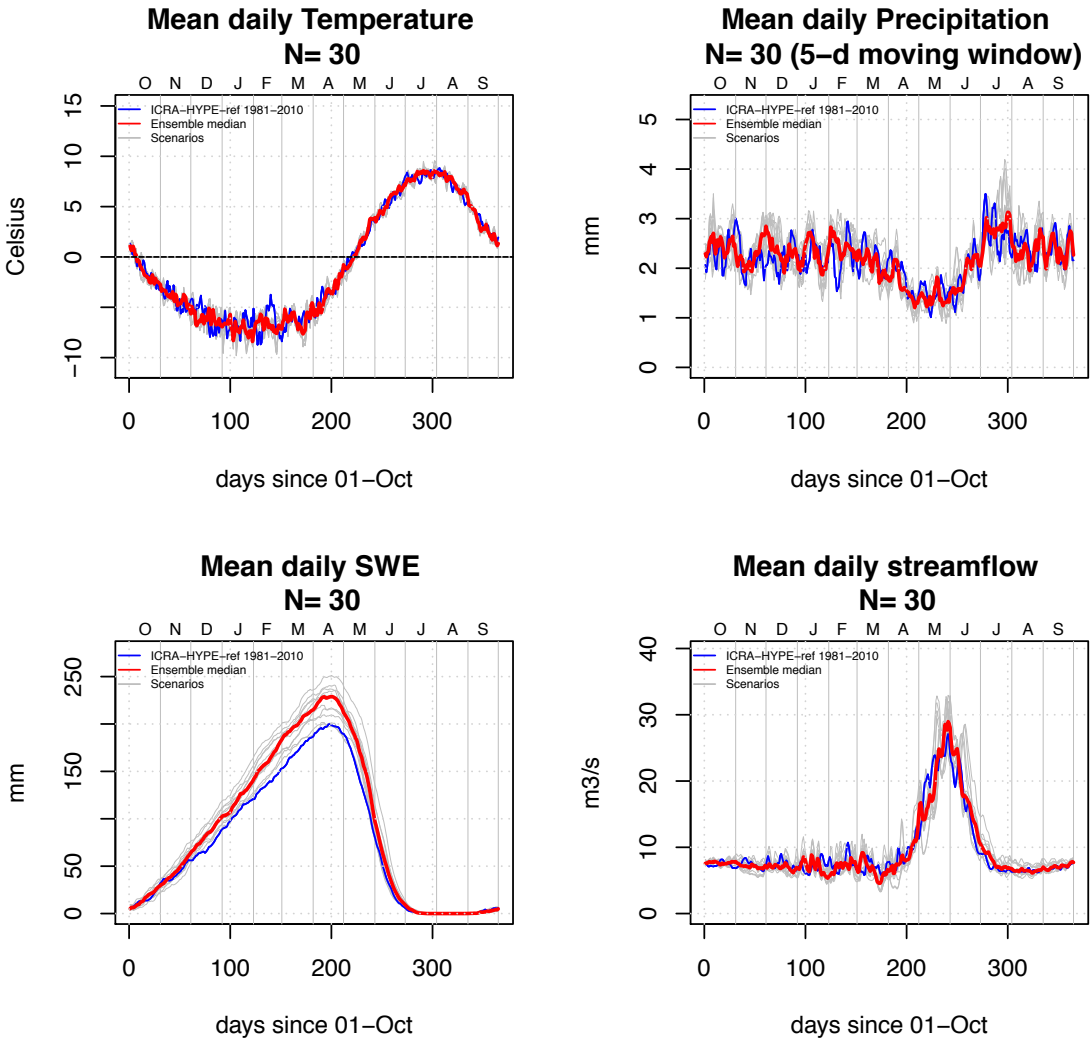

Fig. 7: Vatnsdalsá catchment (vhm45): Mean daily temperature (top-left); Mean daily precipitation (top-right); Mean daily snow accumulation (bottom-left); Mean daily discharge (bottom-right). Estimations derived from HYPE simulations forced with the ICRA reanalysis (blue line) and with the bias-corrected CORDEX projections (grey lines) in the 1981-2010 period. The ensemble median of CORDEX-HYPE projections is coloured in red. (N = number of years in the period).

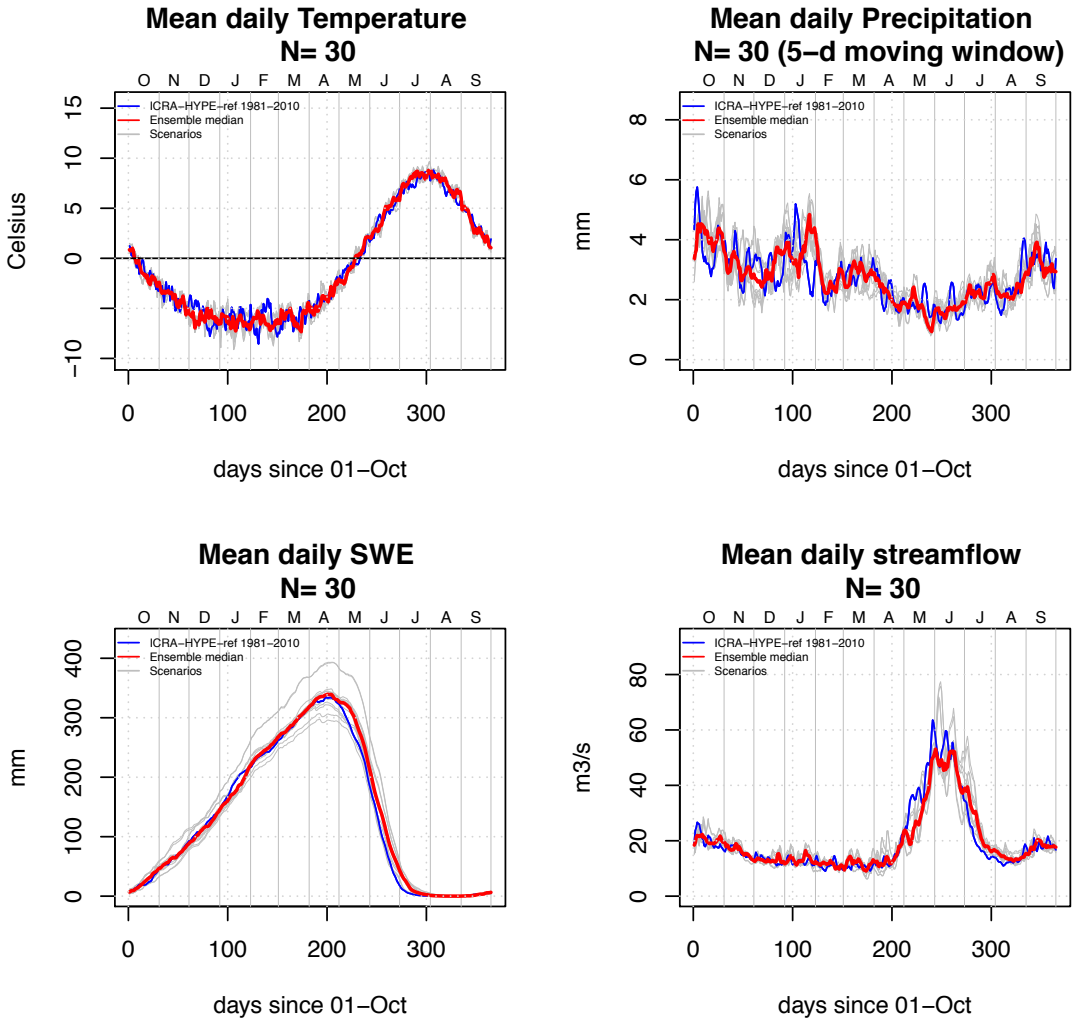

Fig. 8: Selá catchment (vhm48): Mean daily temperature (top-left); Mean daily precipitation (top-right); Mean daily snow accumulation (bottom-left); Mean daily discharge (bottom-right). Estimations derived from HYPE simulations forced with the ICRA reanalysis (blue line) and with the bias-corrected CORDEX projections (grey lines) in the 1981-2010 period. The ensemble median of CORDEX-HYPE projections is coloured in red. (N = number of years in the period).

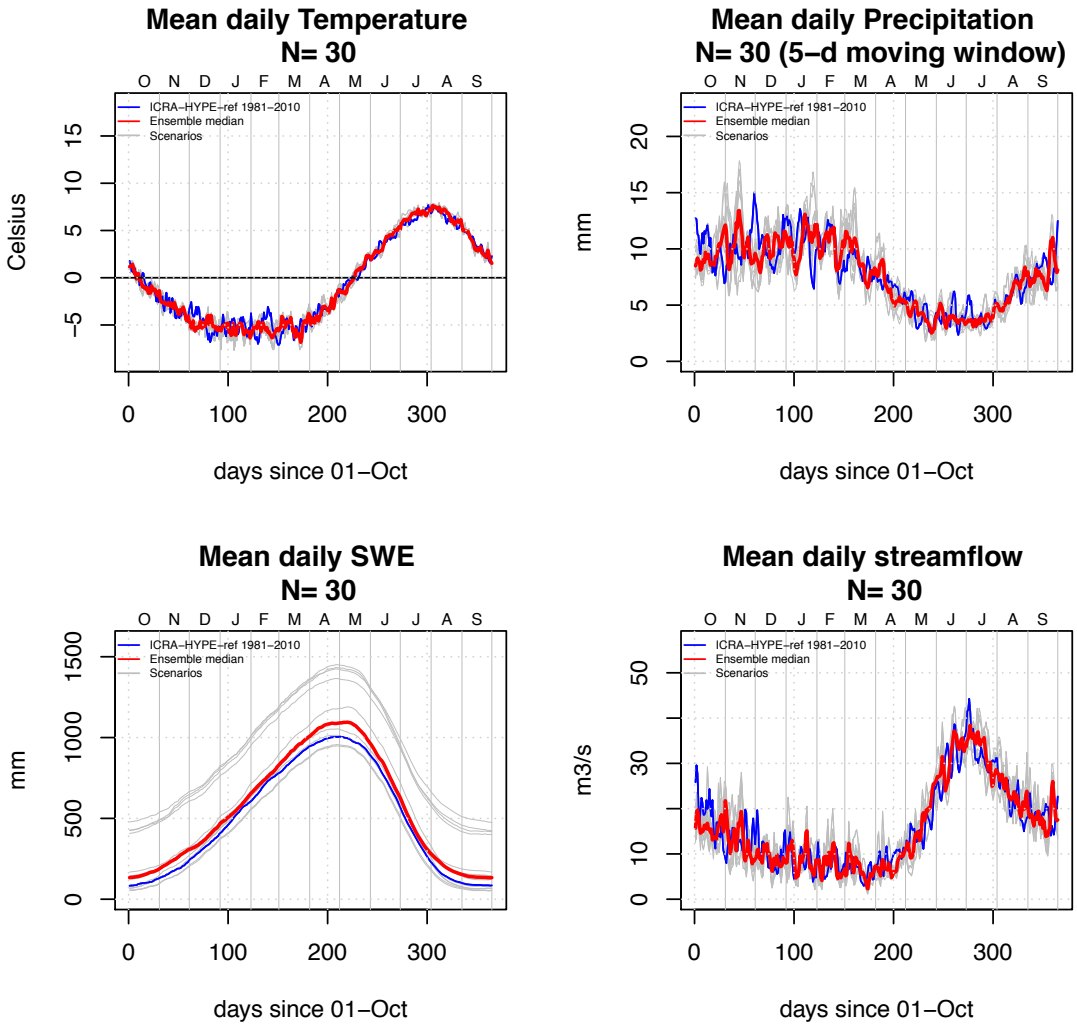

Fig. 9: Geithellnaá catchment (vhm149): Mean daily temperature (top-left); Mean daily precipitation (top-right); Mean daily snow accumulation (bottom-left); Mean daily discharge (bottom-right). Estimations derived from HYPE simulations forced with the ICRA reanalysis (blue line) and with the bias-corrected CORDEX projections (grey lines) in the 1981-2010 period. The ensemble median of CORDEX-HYPE projections is coloured in red. (N = number of years in the period).

6-2 Hydrological response to projected climate change

This section examines the hydrological impact of projected climate change in the 21st century.

6-2-1 Changes in mean daily streamflow and snow storage

The projected seasonality of mean daily streamflow and snow storage in the 2021-2050, 2041-2070 and 2071-2100 periods is presented in Figures 10 to 15 and compared to their seasonality in the reference period (1981-2010). Appendix 7 presents the same figures for the 2041-2070 period only, together with the seasonality of mean daily temperature and precipitation. The spread of all ensemble members provides an estimate of the overall uncertainty associated with the projections. The ensemble median is coloured in red for days when the Mann-Whitney test detected a significant shift between the ensembles of mean daily streamflow or snow storage in the future period and the reference period (1981-2010), and orange otherwise. The percentage of days in the water year affected by a significant shift is also indicated.

In the reference period (1981-2010), the hydrological regimes of the three studied catchments are strongly influenced by snowmelt seasonality, leading to a strong contrast between low flows in winter, when snow accumulates, and high flows in spring/summer, when snow melts. A well defined discharge peak caused by snowmelt in spring can be observed in the three catchments. This peak occurs approximately one month later in the Geithellnaá catchment than in the Vatnsdalsá and Selá catchments. The flow regimes of these catchments are also influenced to varying degrees by rainfall seasonality, especially the Geithellnaá catchment which experiences relatively high flows in late summer and autumn.

The studied river catchments are found to respond to projected climate change and in particular to projected warming (see also Appendix 5). The spread of the ensembles gives information about the projection uncertainty. As the projection horizon increases, increased temperature is projected to gradually lead to shorter snow seasons combined with less snow accumulation. The streamflow pattern will gradually flatten and become more evenly distributed. The larger warming projected under the RCP8.5 emission scenario will lead to larger changes in snow storage and in turn to larger streamflow seasonality changes than under the RCP4.5 emission scenario.

Compared with the reference period (1981-2010), snow storage is projected to decrease in 2021-2050 but snowmelt seasonality will still have a strong influence on the flow regimes of the three catchments under both emission scenarios.

By the mid 21st century (2041-2070), snow storage is projected to decrease further but will still be sufficiently large to maintain a flow regime marked by snowmelt seasonality in all three catchments under both emission scenarios.

By the end of the 21st century (2071-2100), the snowpack is projected to drastically shrink and the snow cover duration is projected to become significantly shorter. The influence of spring

snowmelt on streamflow seasonality will diminish even further especially under the RCP8.5 emission scenario.

On average, i) streamflow will mainly increase in autumn/winter because rainfall and the number of intermittent snowmelt events will likely increase with the projected warming, ii) streamflow will mainly increase in April and decrease in June, while May will either experience a streamflow increase or decrease depending on the catchment and projection period, because of changes in the snowmelt seasonality pattern (shift of the onset of the snowmelt season earlier); the peak of daily streamflow in spring will slowly decrease and shift earlier because snowpack reduction will lead to a decrease in the peak of snowmelt and shift its peak earlier iii) summer streamflow will mainly decrease in the Selá and Geithellnaá catchments because spring/summer snowmelt will decrease and end earlier, while little change is projected in the Vatnsdalsá catchment because snowmelt contribution to summer flow is already limited in the reference period (1981-2010).

In summary, the flow regimes of all three catchments will gradually shift from snowmelt-dominated regimes toward more mixed snowmelt/rainfall regimes, especially under the RCP8.5 emission scenario. The Þrándarjökull ice-cap is projected to retreat throughout the 21st century and its influence on the streamflow of Geithellnaá will become even more limited than initially estimated (not shown).

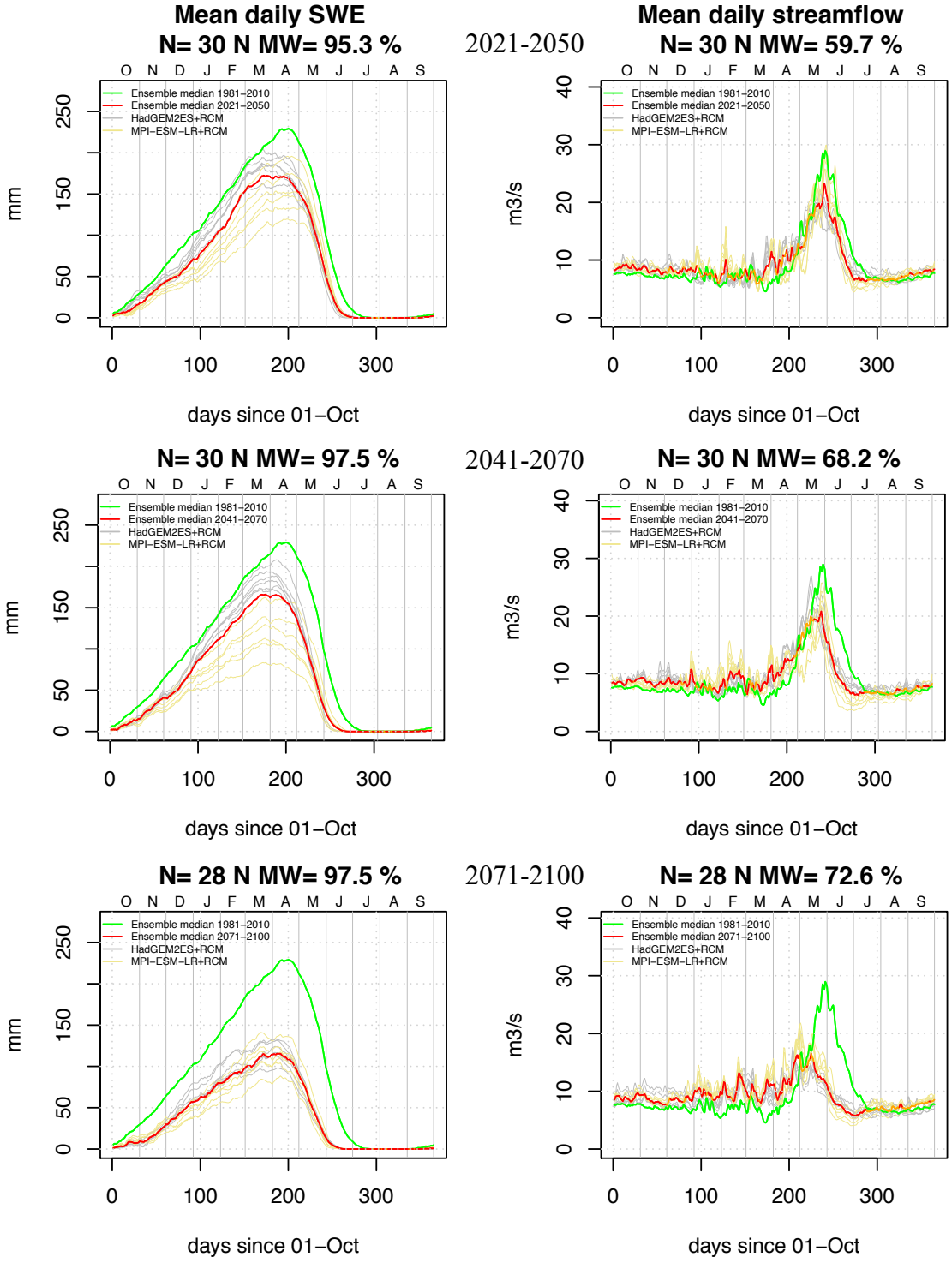

Fig. 10: Vatnsdalsá catchment (vhm45): Projected mean daily snow storage (left-panel) and mean daily discharge (right-panel) under the RCP4.5 emission scenario. Projection periods: 2021-2050 (top), 2041-2070 (middle) and 2071-2100 (bottom). Individual ensemble members are coloured in grey and yellow. The ensemble median in each projection period is coloured in red for days when the Mann-Whitney test detected a significant shift in the mean daily snow storage or discharge ensembles, relative to the reference period (1981-2010) and orange otherwise. Ensemble median in the reference period is shown in green. N = Number of years in the projection period. N MW = Percentage of days in the water year when a significant change in mean daily snow storage or discharge is projected by the Mann-Whitney test.

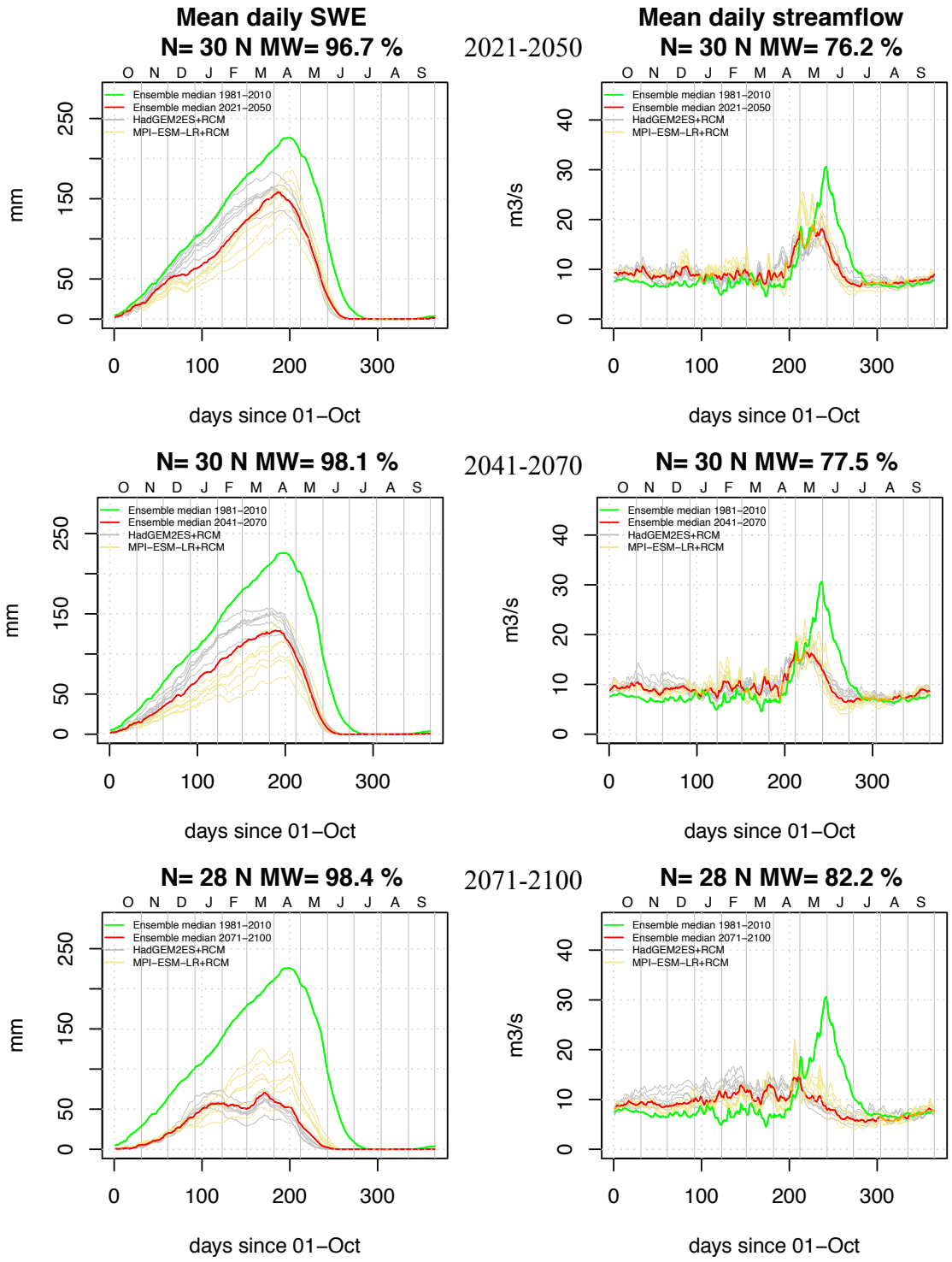

Fig. 11: Vatnsdalsá catchment (vhm45): as Fig. 10 but under the RCP8.5 emission scenario.

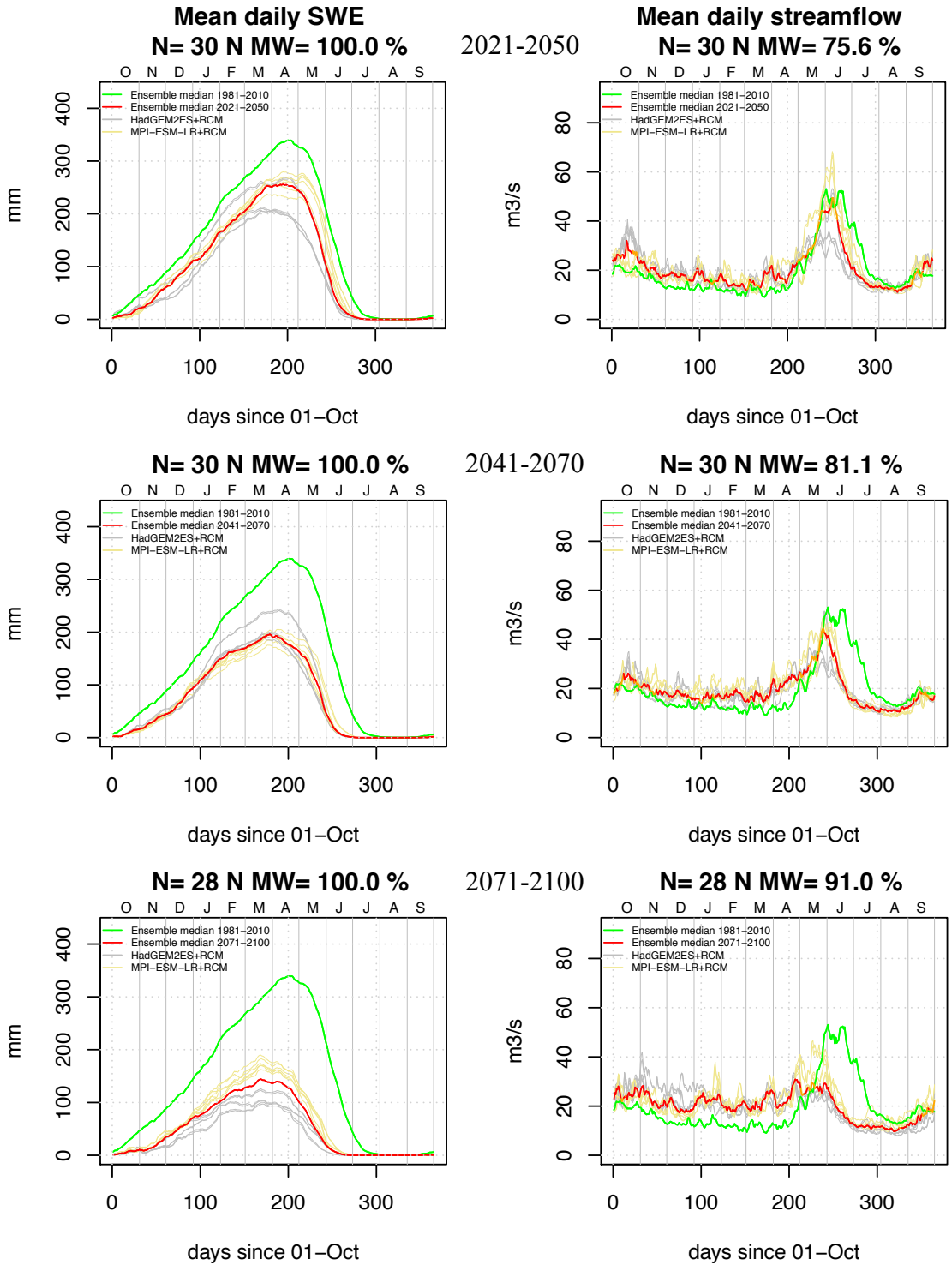

Fig. 12: Selá catchment (vhm48): Projected mean daily snow accumulation (left-panel) and mean daily discharge (right-panel) under the RCP4.5 emission scenario. Projection periods: 2021-2050 (top), 2041-2070 (middle) and 2071-2100 (bottom). Individual ensemble members are coloured in grey and yellow. The ensemble median in each projection period is coloured in red for days when the Mann-Whitney test detected a significant shift in the mean daily snow storage or discharge ensembles, relative to the reference period (1981-2010) and orange otherwise. Ensemble median in the reference period is shown in green. N = Number of years in the projection period. N MW = Percentage of days in the water year when a significant change in mean daily snow storage or discharge is projected by the Mann-Whitney test.

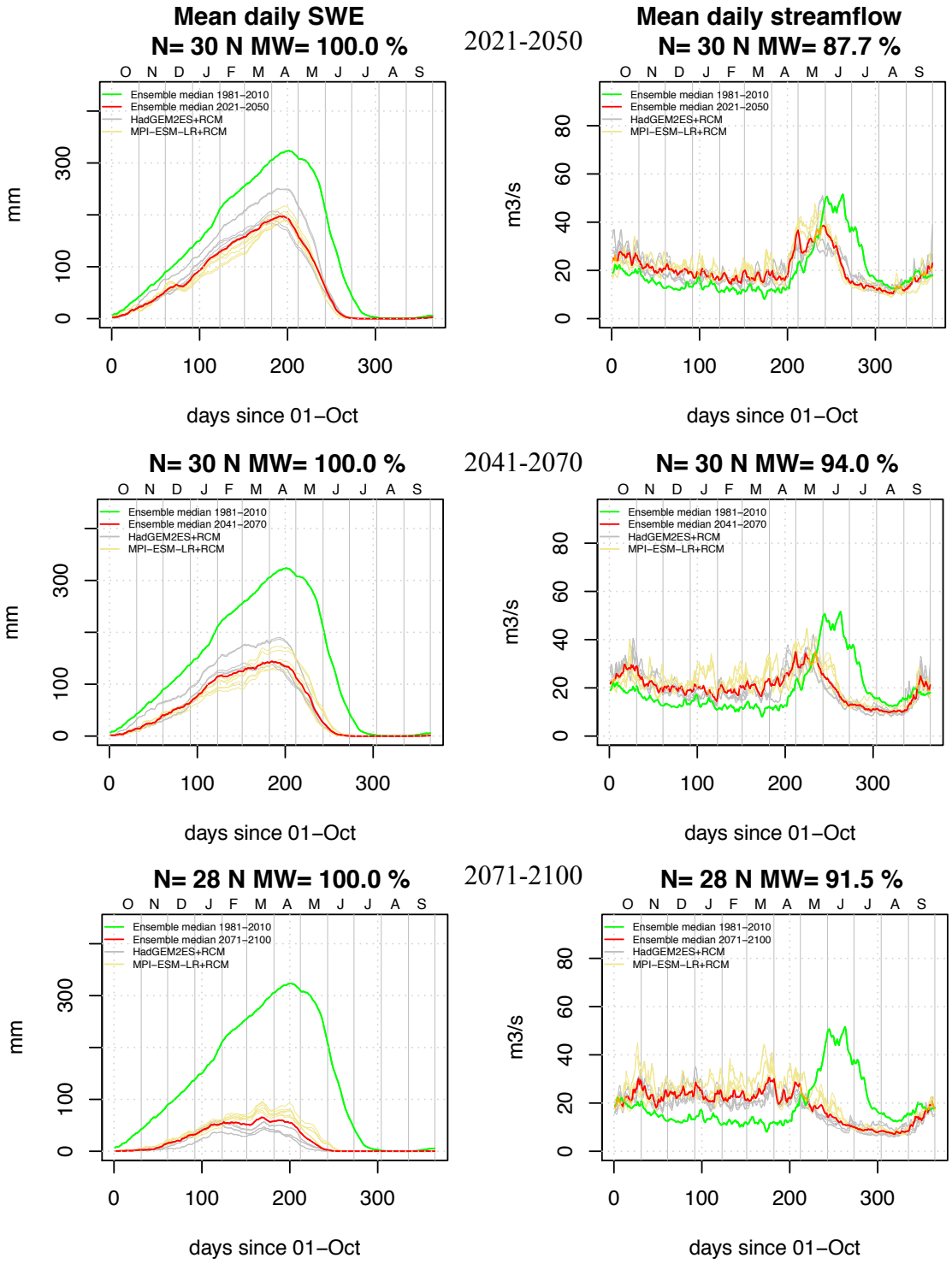

Fig. 13: Selá catchment (vhm48): as Fig. 12 but under the RCP8.5 emission scenario.

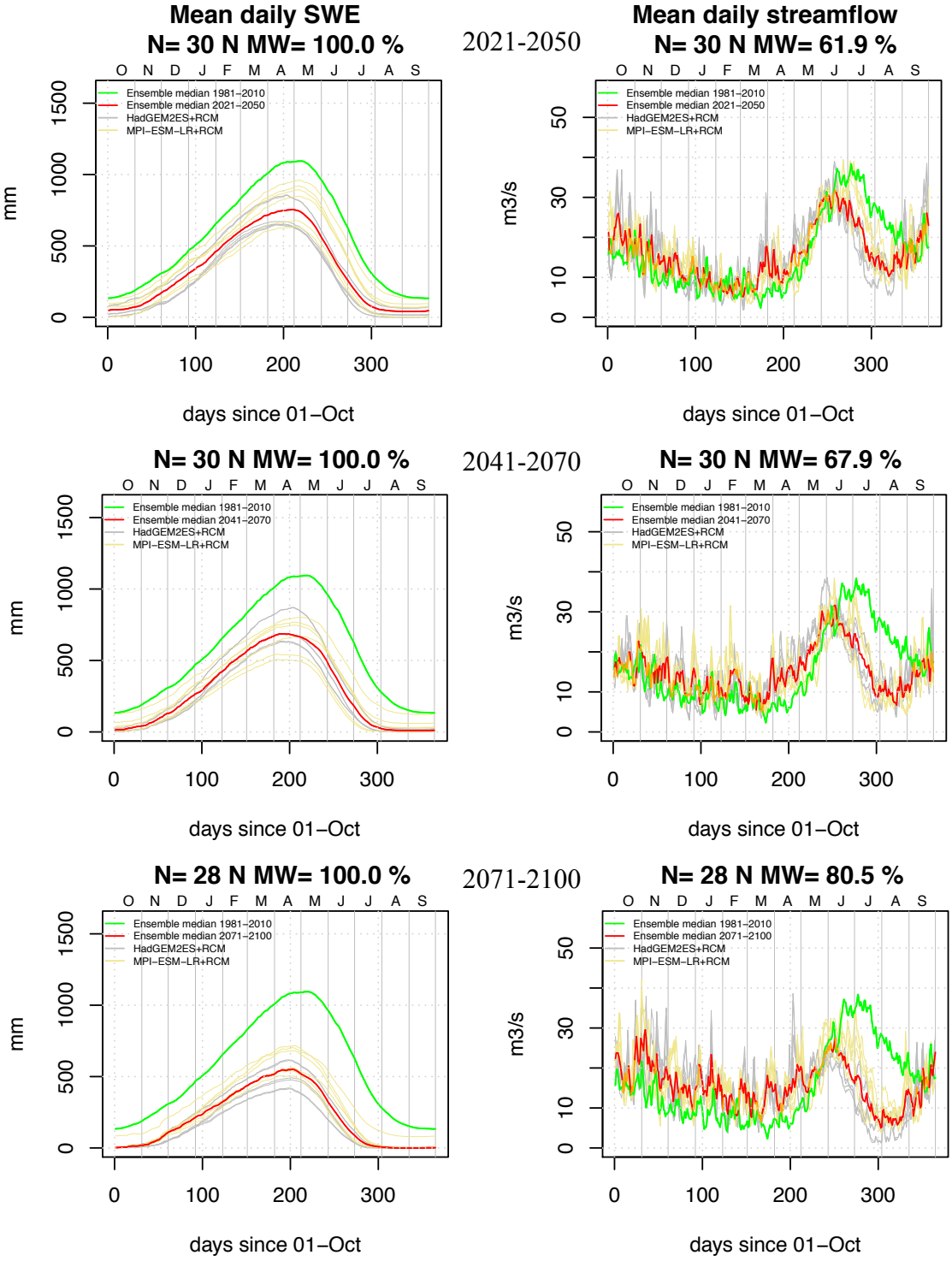

Fig. 14: Geithellnaá catchment (vhm149): Projected mean daily snow accumulation (left-panel) and mean daily discharge (right-panel) under the RCP4.5 emission scenario. Projection periods: 2021-2050 (top), 2041-2070 (middle) and 2071-2100 (bottom). Individual ensemble members are coloured in grey and yellow. The ensemble median in each projection period is coloured in red for days when the Mann-Whitney test detected a significant shift in the mean daily snow storage or discharge ensembles relative to the reference period (1981-2010) and orange otherwise. Ensemble median in the reference period is shown in green. N = Number of years in the projection period. N MW = Percentage of days in the water year when a significant change in mean daily snow storage or discharge is projected by the Mann-Whitney test.

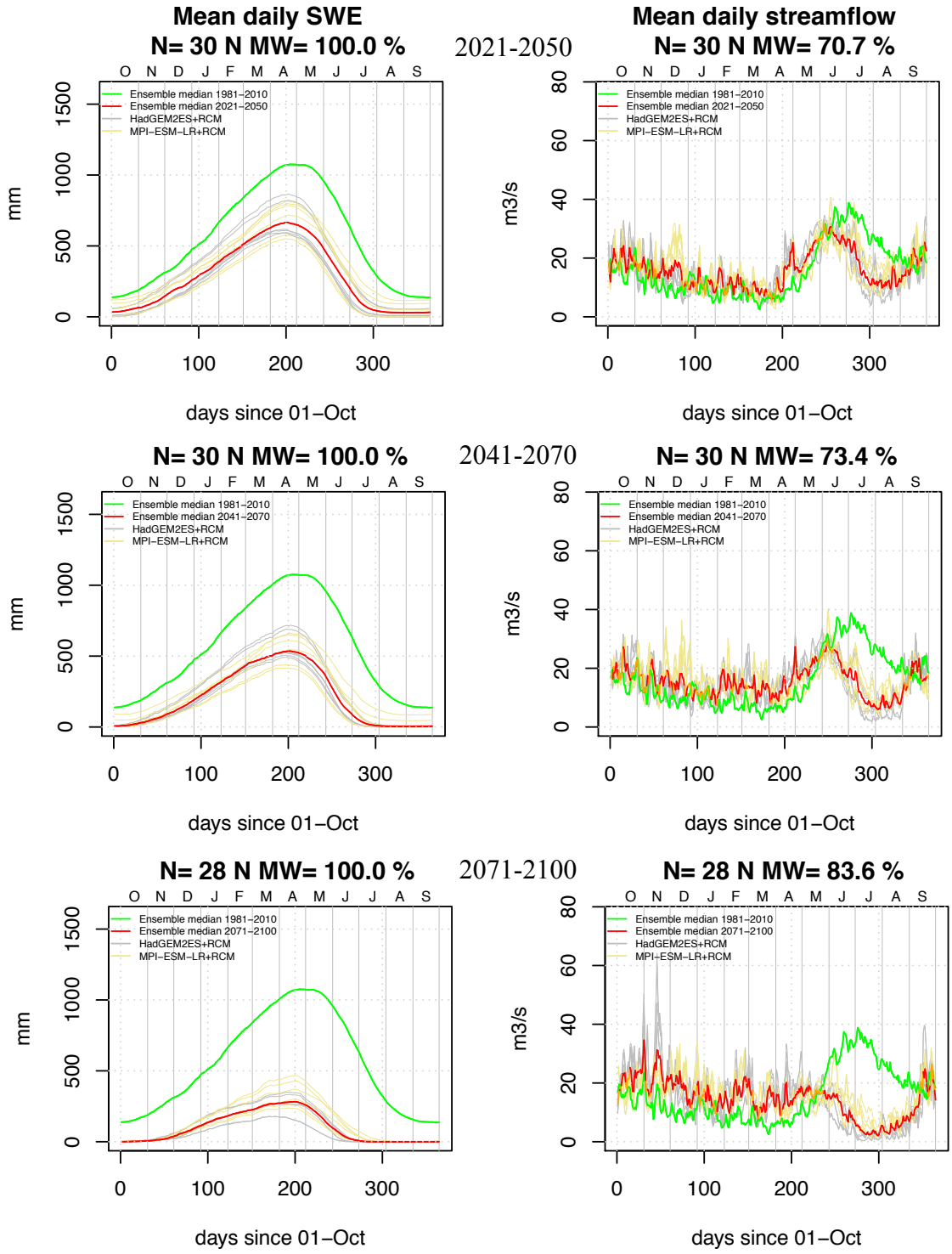

Fig. 15: Geithellnaá catchment (vhm149): as Fig. 14 but under the RCP8.5 emission scenario.

6-2-2 Changes in mean annual and seasonal temperature, precipitation and streamflow

In order to get a better insight into the temporal evolution of the hydrological response to projected climate change, the ensembles of 30-year mean annual and seasonal streamflow projections are analysed together with catchment-averaged temperature, precipitation, rainfall, snowfall and snowmelt. The main results are presented in Figures 16 to 30 (temperature, precipitation and streamflow). The evolution of the 30-year mean seasonal rainfall, snowfall and snowmelt projections are presented in Appendix 8. The significance of changes between the reference period (1981-2010) and each future period is evaluated with a two-sided Mann-Whitney test. This test is first applied to each individual ensemble member to compare the samples of thirty annual and seasonal values in the reference period (1981-2010) to the samples of thirty annual and seasonal values in each future period. Then, the test is applied to compare the ensembles of twelve mean annual and mean seasonal values in the reference period (1981-2010) to those in each future period. Finally, the ensembles of mean annual changes and mean seasonal changes from the reference period (1981-2010) to the future periods are calculated and the median changes estimated (see Appendix 9). The analysis below summarises the main results.

- **Vatnsdalsá catchment (vhm45)**
  - **RCP4.5 emission scenario**
    - Annual (water year)
      - Mean annual temperature is projected to gradually increase throughout the 21st century and the ensemble median becomes positive in 2011-2040. A median warming of 2.6°C is projected from 1981-2010 to 2071-2100.
      - Mean annual precipitation is projected to fluctuate close to its 1981-2010 reference level and no significant change is projected until 2021-2050. Then, a significant shift is projected. The median change is positive and does not exceed 7% in these periods but not all members consistently agree with an increase before 2061-2090.
      - Mean annual streamflow is not projected to change significantly throughout the 21st century and the ensemble median is mainly fluctuating around its 1981-2010 reference level. Increased evapotranspiration caused by increased temperature compensates some of the precipitation increase.
    - Season: OND
      - Mean seasonal temperature is projected to gradually increase but remain negative throughout the 21st century. A median warming of 2.6°C is projected from 1981-2010 to 2071-2100.
      - The trajectory followed by the different mean seasonal precipitation projections depends on the driving GCM. The spread of the ensemble widens with the projection horizon and the ensemble median is projected to remain close to the 1981-2010 reference level throughout the 21st century.
      - A gradual shift toward an increase in mean seasonal streamflow is projected throughout the 21st century. The median increase is ranging from 10 to 20%, mainly driven by

changes affecting one group of projections driven by the same GCM. These changes are driven by the projected warming leading to an increase in the fraction of precipitation falling as rain.

- Season: JFM
  - Mean seasonal temperature is projected to gradually increase throughout the 21st century but remain strongly negative. A median warming of 2.6°C is projected from 1981-2010 to 2071-2100.
  - Mean seasonal precipitation projections oscillate around their respective 1981-2010 reference level. The two groups of projections driven by the two GCMs do not vary in phase with each other, leading to a large ensemble spread. As a result, the ensemble median remains close to its 1981-2010 reference level throughout the 21st century.
  - The trajectory followed by the mean seasonal streamflow projections depends on the driving GCM. No significant change is projected until 2011-2040, then a significant increase is projected. The median increase reaches 40% in 2071-2100. The streamflow increase is driven by the projected warming causing an increase in snowmelt and rainfall.
- Season: AMJ
  - Mean seasonal temperature already positive in 1981-2010 is projected to gradually increase throughout the 21st century. A median warming of 2.6°C is projected from 1981-2010 to 2071-2100.
  - A large spread affects the ensemble of mean seasonal precipitation projections but the ensemble median remains close to its 1981-2010 reference level throughout the entire projection horizon.
  - Mean seasonal streamflow is projected to gradually decrease throughout the 21st century, following a continuous reduction of snowmelt caused by the projected warming. The median decrease reaches 30% in 2071-2100 relative to 1981-2010.
- Season: JAS
  - Mean seasonal temperature is projected to gradually increase throughout the 21st century. A median warming of 2.6°C is projected from 1981-2010 to 2071-2100.
  - A trend toward an increase in mean seasonal precipitation is projected throughout the 21st century although not all members agree with an increase before 2031-2060. The median increase reaches 18% in 2071-2100.
  - Mean seasonal streamflow projections fluctuate around their respective 1981-2010 reference level and there is no statistical evidence suggesting any significant change throughout the 21st century. This result is likely related to the decrease in snowmelt and the increase in evapotranspiration caused by increased temperature, compensating the rainfall increase.

- **RCP8.5 emission scenario**
  - Annual (water year)
    - Mean annual temperature is projected to gradually increase throughout the 21st century and the ensemble median becomes positive in 2001-2030. A median warming of 4.2°C is projected from 1981-2010 to 2071-2100.
    - Regarding mean annual precipitation, projections show a gradual and significant shift toward an increase. The median increase is ranging from 5% to 13% in the periods 2001-2030 to 2071-2100 but the spread of the ensemble widens with the projection horizon making the outcome of the projections increasingly uncertain.
    - Mean annual streamflow projections fluctuate around their respective 1981-2010 reference level. The ensemble median does not significantly change throughout the 21st century despite the projected precipitation increase. This is the result of divergences in the trajectory of individual mean streamflow projections leading the spread of the ensemble to widen with the projection horizon. Increased evapotranspiration caused by increased temperature compensates some of the precipitation increase and contributes to modulate annual streamflow variations.
  - Season: OND
    - Mean seasonal temperature is projected to gradually increase throughout the 21st century and the ensemble median becomes positive in 2071-2100. A median warming of 4.2°C is projected from 1981-2010 to 2071-2100.
    - A large spread widening with the projection horizon affects the mean seasonal precipitation projections. A significant increase is projected in some periods and no significant change is projected in others.
    - A shift toward a mean seasonal streamflow increase is projected throughout the 21st century. The median increase varies between 10% and 30% and becomes relatively stable after 2021-2050 but the spread of the ensemble widens with the projection horizon, increasing the uncertainty of the projected changes. The streamflow increase is related to the projected warming leading to an increase in the fraction of precipitation falling as rain.
  - Season: JFM
    - Mean seasonal temperature is projected to gradually increase but remain negative throughout the entire projection period. A median warming of 4.1°C is projected from 1981-2010 to 2071-2100.
    - Mean seasonal precipitation is projected to oscillate around its 1981-2010 level and the spread of the ensemble is large. The ensemble median remains close to its 1981-2010 reference level. A low but significant median decrease is projected in 2031-2060 and 2041-2070.
    - A gradual shift toward an increase in mean seasonal streamflow is projected throughout the 21st century, especially after 2011-2040. A median increase of 50% is projected from 1981-2010 to 2071-2100. The streamflow increase is caused by the increase in snowmelt and the fraction of precipitation falling as rain, resulting from the projected warming.

- Season: AMJ
  - Mean seasonal temperature, already positive in 1981-2010 is projected to gradually increase throughout the 21st century. A median warming of 4.1°C is projected from 1981-2010 to 2071-2100.
  - The trajectory followed by the different mean seasonal precipitation projections depends on the driving GCM, making the evolution of the ensemble uncertain. The ensemble median is mainly projected to remain close to its 1981-2010 reference level.
  - Mean seasonal streamflow is projected to gradually decrease throughout the 21st century. A median decrease of 40% is projected in 2071-2100 relative to 1981-2010. This decrease is driven by the projected warming leading to a snowpack depletion and a reduction of snowmelt.
- Season: JAS
  - Mean seasonal temperature already positive in 1981-2010 is projected to gradually increase throughout the 21st century. A median warming of 4.5°C is projected from 1981-2010 to 2071-2100.
  - A gradual shift toward an increase in mean seasonal precipitation is projected throughout the 21st century but the spread of the ensemble widens with the projection horizon. A median increase of about 20% is projected in the periods 2041-2070 to 2071-2100, relative to 1981-2010.
  - Mean seasonal streamflow is not projected to significantly change except in 2071-2100 when a median decrease of 15% is projected. This result is likely related to the decrease in snowmelt and the increase in evapotranspiration, caused by increased temperature, compensating the rainfall increase, until the balance becomes negative.

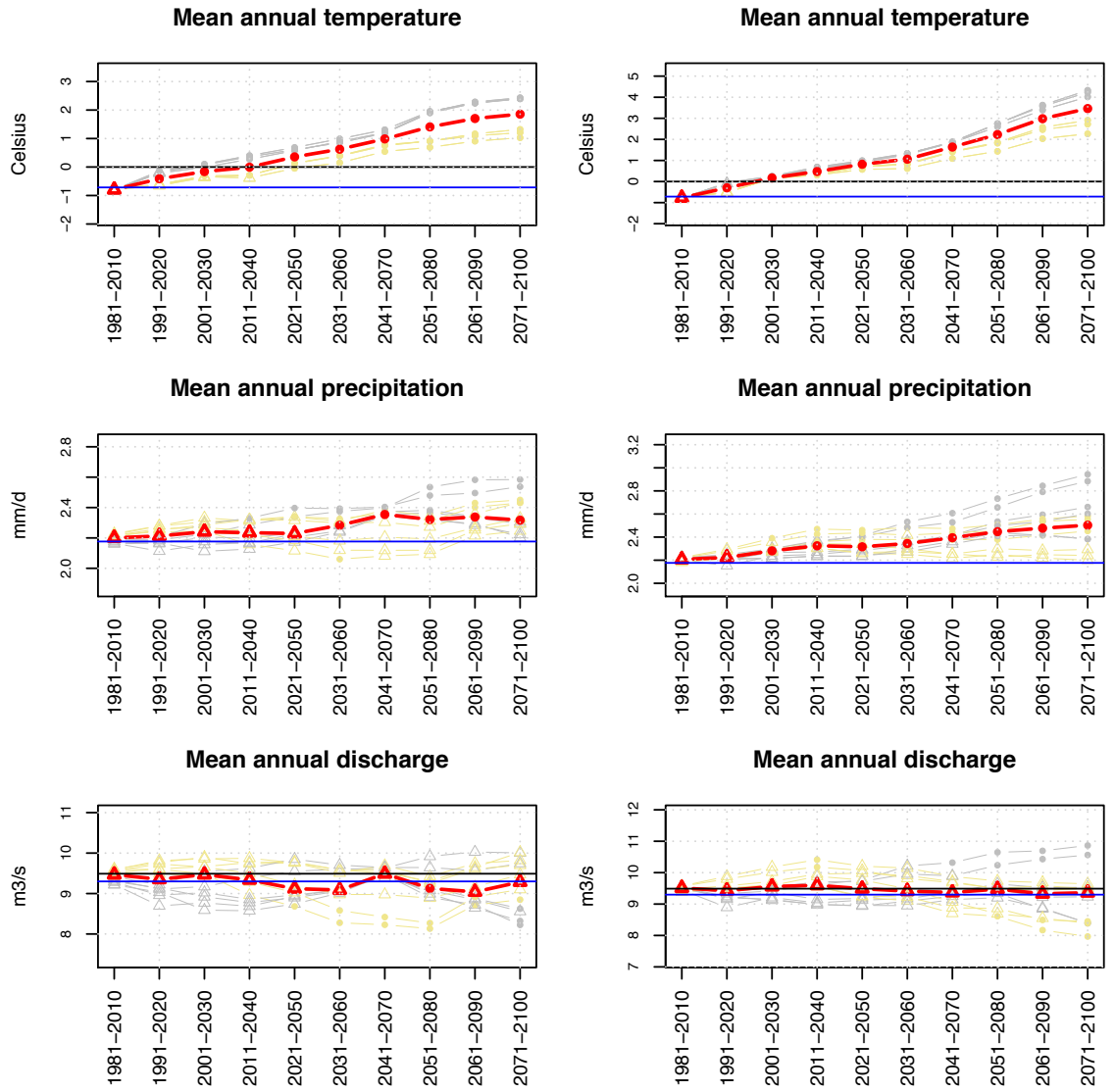

Fig. 16: Vatnsdalsá catchment (vhm45): Projected 30-year mean annual temperature, precipitation and discharge under the RCP4.5 emission scenario (left panel) and RCP8.5 emission scenario (right panel). Projections based on MPI-ESM-LR GCM (yellow lines). Projections based on HadGEM2ES GCM (grey lines). Ensemble median (red line). ICRA reference in the period 1981-2010 (blue line). Mean observed discharge in the period 1981-2010 (black line). Projection periods when a significant change is detected by the Mann-Whitney test compared to the reference period (1981-2010) are marked with a solid circle and with a triangle otherwise. The test is first applied to each ensemble member to compare the thirty annual values in the reference period to those in each projection period (see symbols on individual members) and then it is applied to compare the ensembles of twelve mean annual values in the reference and future periods (see symbols on the ensemble median).

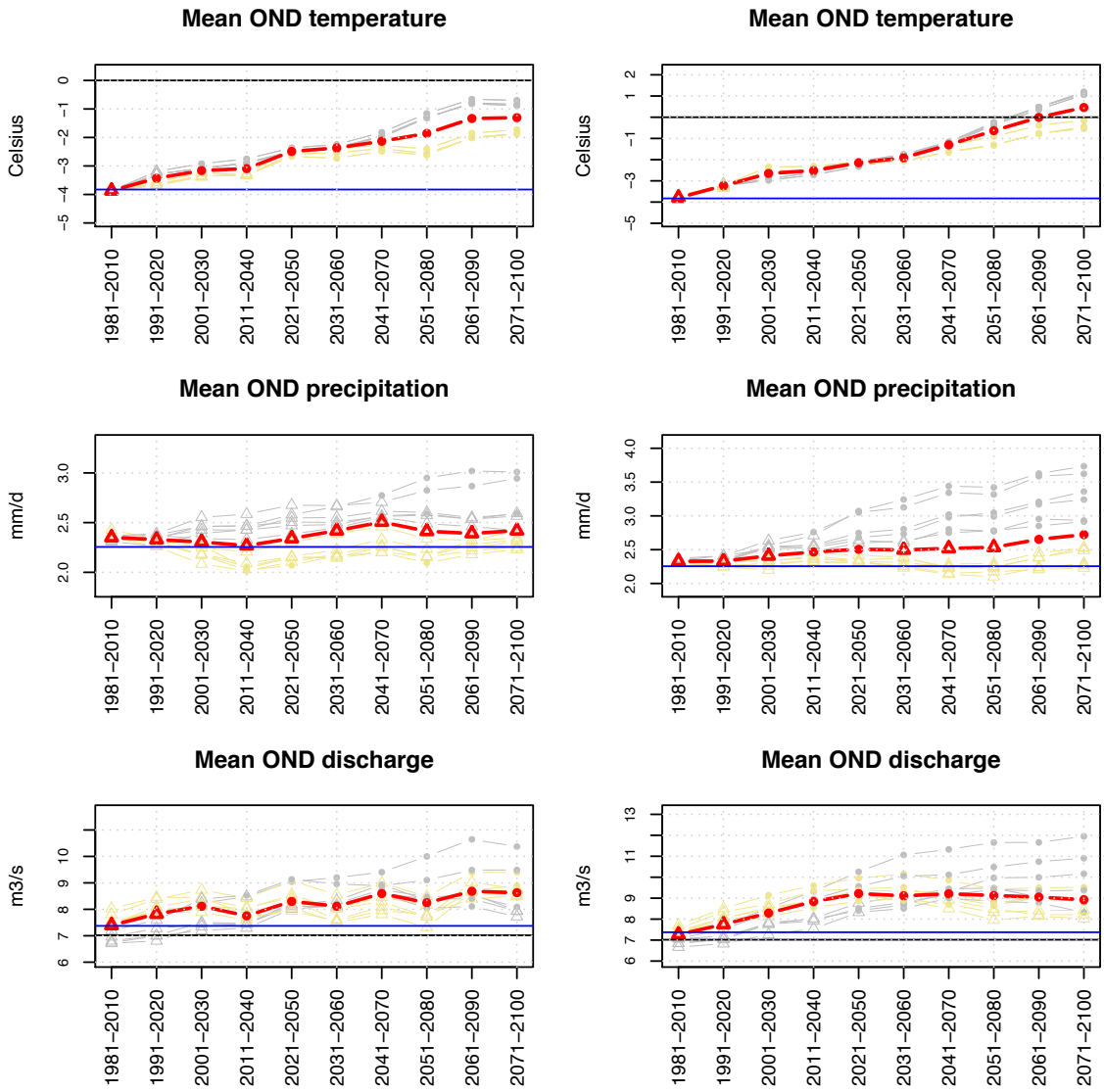

Fig. 17: Vatnsdalsá catchment (vhm45): Projected 30-year mean OND temperature, precipitation and discharge under the RCP4.5 emission scenario (left panel) and RCP8.5 emission scenario (right panel). Projections based on MPI-ESM-LR GCM (yellow lines). Projections based on HadGEM2ES GCM (grey lines). Ensemble median (red line). ICRA reference in the period 1981-2010 (blue line). Mean observed discharge in the period 1981-2010 (black line). Projection periods when a significant change is detected by the Mann-Whitney test compared to the reference period (1981-2010) are marked with a solid circle and with a triangle otherwise. The test is first applied to each ensemble member to compare the thirty seasonal values in the reference period to those in each projection period (see symbols on individual members) and then it is applied to compare the ensembles of twelve mean seasonal values in the reference and future periods (see symbols on the ensemble median).

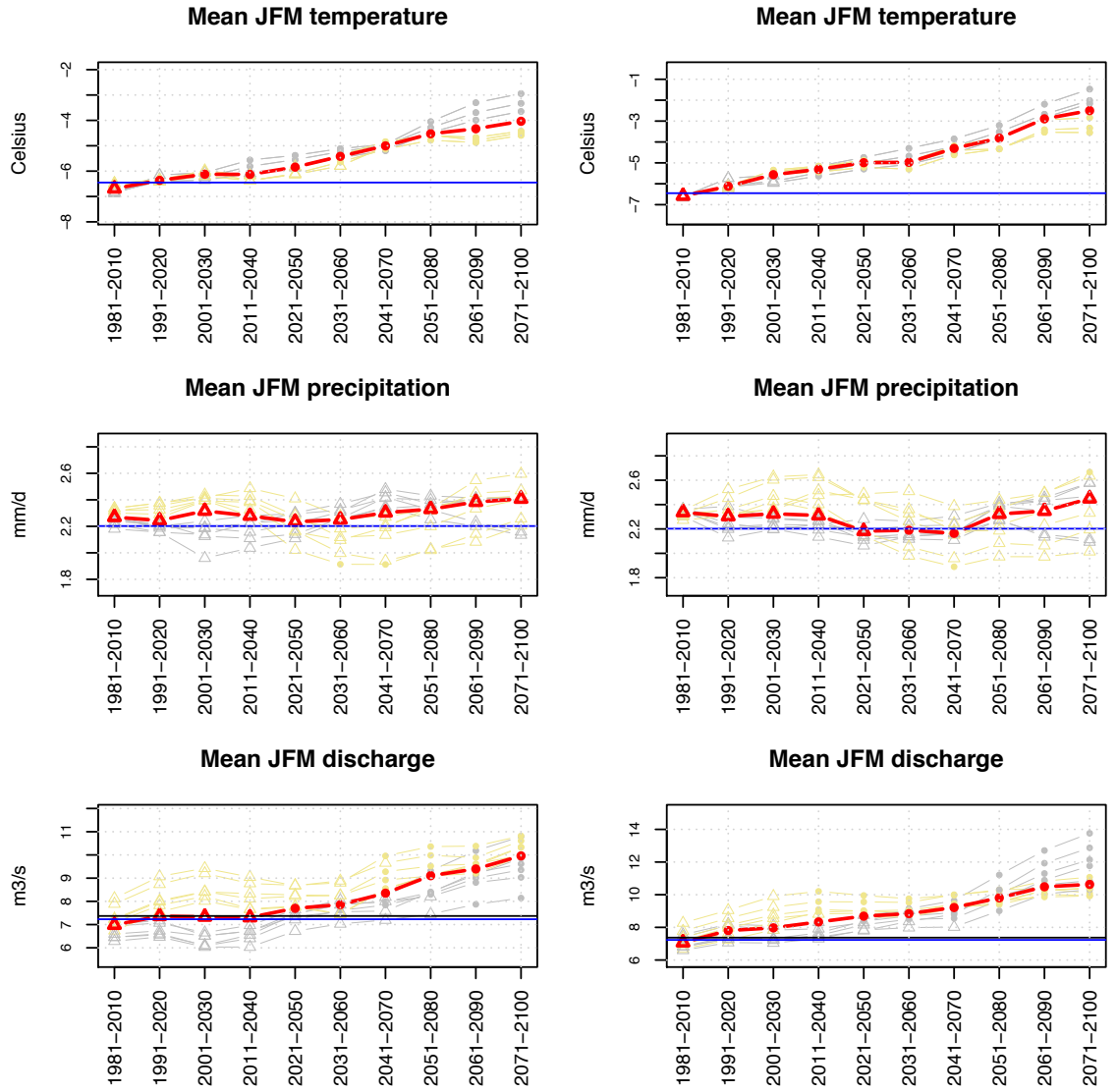

Fig. 18: Vatnsdalsá catchment (vhm45): Projected 30-year mean JFM temperature, precipitation and discharge under the RCP4.5 emission scenario (left panel) and RCP8.5 emission scenario (right panel). Projections based on MPI-ESM-LR GCM (yellow lines). Projections based on HadGEM2ES GCM (grey lines). Ensemble median (red line). ICRA reference in the period 1981-2010 (blue line). Mean observed discharge in the period 1981-2010 (black line). Projection periods when a significant change is detected by the Mann-Whitney test compared to the reference period (1981-2010) are marked with a solid circle and with a triangle otherwise. The test is first applied to each ensemble member to compare the thirty seasonal values in the reference period to those in each projection period (see symbols on individual members) and then it is applied to compare the ensembles of twelve mean seasonal values in the reference and future periods (see symbols on the ensemble median).

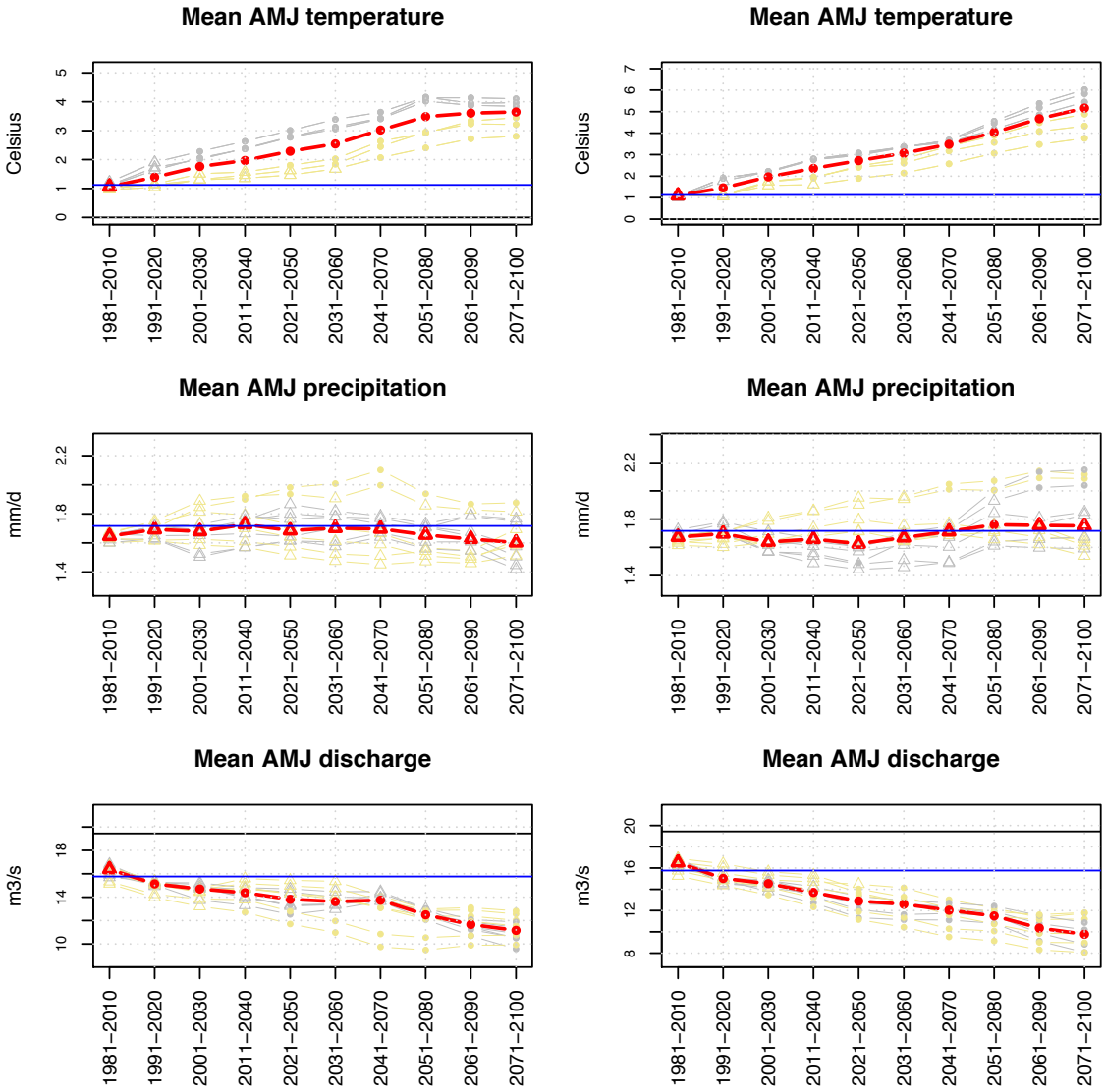

Fig. 19: Vatnsdalsá catchment (vhm45): Projected 30-year mean AMJ temperature, precipitation and discharge under the RCP4.5 emission scenario (left panel) and RCP8.5 emission scenario (right panel). Projections based on MPI-ESM-LR GCM (yellow lines). Projections based on HadGEM2ES GCM (grey lines). Ensemble median (red line). ICRA reference in the period 1981-2010 (blue line). Mean observed discharge in the period 1981-2010 (black line). Projection periods when a significant change is detected by the Mann-Whitney test compared to the reference period (1981-2010) are marked with a solid circle and with a triangle otherwise. The test is first applied to each ensemble member to compare the thirty seasonal values in the reference period to those in each projection period (see symbols on individual members) and then it is applied to compare the ensembles of twelve mean seasonal values in the reference and future periods (see symbols on the ensemble median).

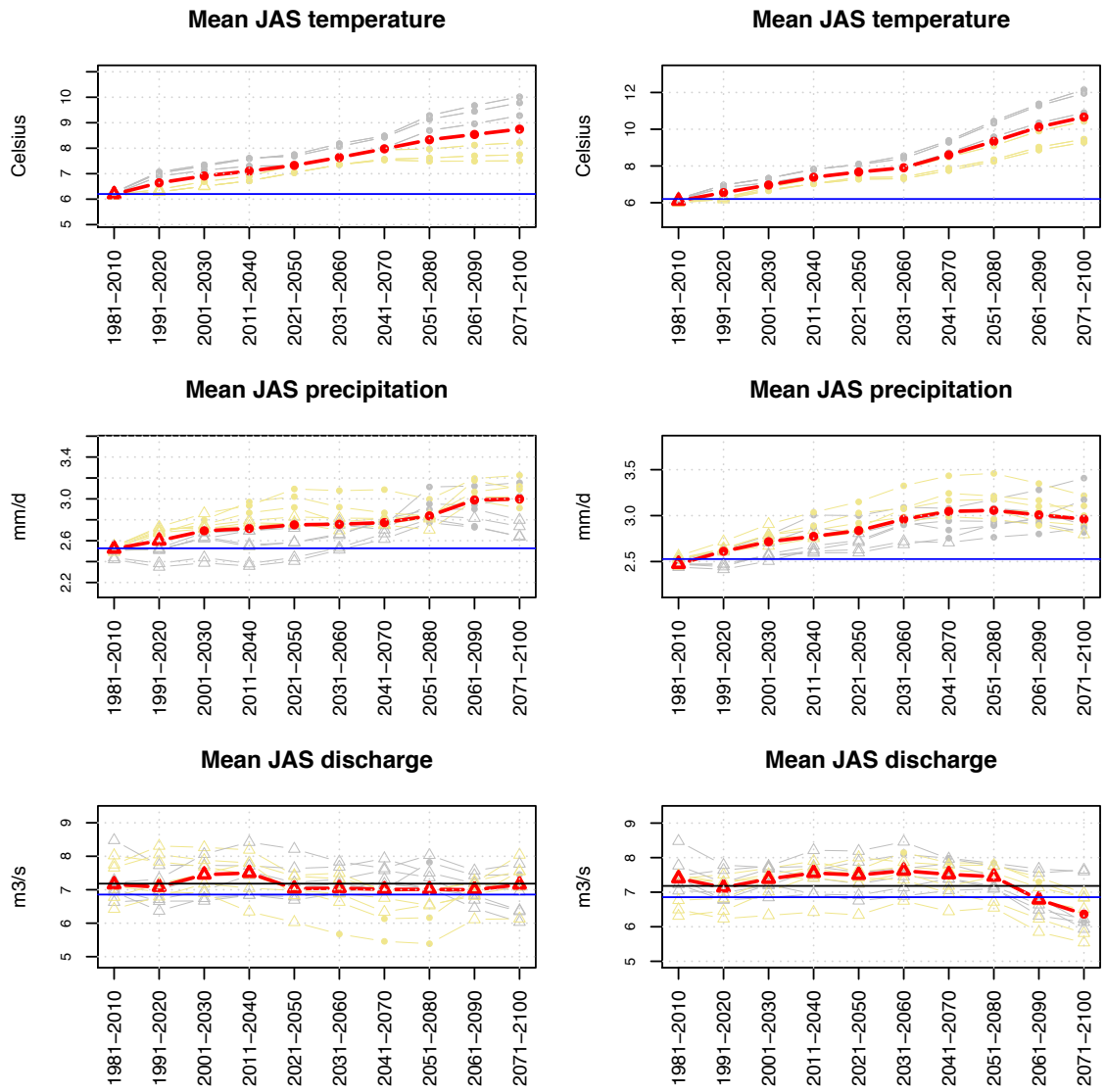

Fig. 20: Vatnsdalsá catchment (vhm45): Projected 30-year mean JAS temperature, precipitation and discharge under the RCP4.5 emission scenario (left panel) and RCP8.5 emission scenario (right panel). Projections based on MPI-ESM-LR GCM (yellow lines). Projections based on HadGEM2ES GCM (grey lines). Ensemble median (red line). ICRA reference in the period 1981-2010 (blue line). Mean observed discharge in the period 1981-2010 (black line). Projection periods when a significant change is detected by the Mann-Whitney test compared to the reference period (1981-2010) are marked with a solid circle and with a triangle otherwise. The test is first applied to each ensemble member to compare the thirty seasonal values in the reference period to those in each projection period (see symbols on individual members) and then it is applied to compare the ensembles of twelve mean seasonal values in the reference and future periods (see symbols on the ensemble median).

- **Selá catchment (vhm48)**
  - **RCP4.5 emission scenario**
    - Annual (water year)
      - Mean annual temperature is projected to gradually increase throughout the 21st century and become positive in 2011-2040. A median warming of 2.9°C is projected from 1981-2010 to 2071-2100.
      - Mean annual precipitation projections oscillate and a significant shift, usually positive, is projected in some periods. When this shift is significant, the median increase does not exceed 7%. The spread of the ensemble widens with the projection horizon.
      - Mean annual streamflow projections follow a pattern similar to precipitation variations. The ensemble median oscillates around its 1981-2010 reference level and the spread of the ensemble widens with the projection horizon. When significant, the median change varies within ± 5% relative to 1981-2010.
    - Season: OND
      - Mean seasonal temperature is projected to gradually increase throughout the 21st century but remain negative. A median warming of 2.7°C is projected from 1981-2010 to 2071-2100.
      - Mean seasonal precipitation projections oscillate around their respective 1981-2010 reference level and the spread of the ensemble widens with the projection horizon. A significant shift, usually positive, is projected in some periods. When this shift is significant, the median increase does not exceed 10%.
      - Mean seasonal streamflow projections reflect precipitation variations. A trend toward an increase in mean seasonal streamflow is projected in all periods. The median increase varies between 15 and 35%. The streamflow increase is driven by the projected warming leading to an increase in the fraction of precipitation falling as rain.
    - Season: JFM
      - Mean seasonal temperature is projected to gradually increase throughout the 21st century but remain negative. A median warming of 2.5°C is projected from 1981-2010 to 2071-2100.
      - Mean seasonal precipitation projections fluctuate and remain close to their respective 1981-2010 reference level. A significant median increase, not exceeding 5%, is projected in the periods 2001-2030 and 2011-2040. The two groups of precipitation projections driven by the two GCMs do not vary in phase with each other, especially after 2051-2080, causing a the ensemble spread to widen with the projection horizon.
      - Mean seasonal streamflow is projected to gradually increase throughout the 21st century. A median increase of 80% is projected from 1981-2010 to 2071-2100. The streamflow increase is driven by the projected warming leading to an increase in snowmelt and rainfall.

- Season: AMJ
  - Mean seasonal temperature is projected to gradually increase throughout the 21st century. A median warming of 3.2°C is projected from 1981-2010 to 2071-2100.
  - Large variations affect the mean seasonal precipitation projections but no trend is emerging. The ensemble median is projected to remain close to its 1981-2010 reference level.
  - A trend toward a mean seasonal streamflow decrease is projected throughout the 21st century. The median change is always negative, but not all members agree with a decrease, especially between 2011-2040 and 2031-2060. A median decrease of 25% is projected from 1981-2010 to 2071-2100. The streamflow decrease is driven by the projected warming leading to a snowpack depletion and a snowmelt reduction. The projected rainfall increase is not large enough to compensate the reduction of snowmelt.
- Season: JAS
  - Mean seasonal temperature is projected to gradually increase throughout the 21st century. A median warming of 3°C is projected from 1981-2010 to 2071-2100.
  - Mean seasonal precipitation is mainly projected to oscillate around its 1981-2010 reference level and a significant shift is detected in some periods. The spread of the ensemble is widening after 2051-2080, making the evolution of precipitation more uncertain. In periods when a significant shift is detected, the median change is always positive but does not exceed 10%.
  - Mean seasonal streamflow is projected to gradually decrease throughout the 21st century. A median decrease of 35% is projected from 1981-2010 to 2071-2100. This decrease is driven by the projected warming leading to a snowpack depletion, snowmelt reduction and increased evapotranspiration.

- **RCP8.5 emission scenario**
  - Annual (water year)
    - Mean annual temperature is projected to gradually increase throughout the 21st century and become positive in 2001-2030. A median warming of 4.7°C is projected from 1981-2010 to 2071-2100.
    - A trend toward an increase in mean annual precipitation is projected after 2001-2030 but the spread of the ensemble widens with the projection horizon. The median increase does not exceed 10%.
    - A large spread, widening with the projection horizon, is observed with the mean annual streamflow projections. No significant change is projected in a majority of members and as a result, the ensemble median remains close to its 1981-2010 reference level.
  - Season: OND
    - Mean seasonal temperature is projected to gradually increase throughout the 21st century and become positive in 2061-2090. A median warming of 4.4°C is projected from 1981-2010 to 2071-2100.

- A trend toward an increase in mean seasonal precipitation is projected throughout the 21st century but the spread of the ensemble widens with the projection horizon. The projected median increase varies between 5 and 15%.
- Mean seasonal streamflow is projected to gradually increase throughout the 21st century. The direction of the change is consistent within the ensemble but the spread of the ensemble widens with projection horizon. The projected median increase varies between approximately 10 and 40%. This streamflow increase is driven by the projected rainfall increase resulting from the combined effects of increased precipitation and warming.

• Season: JFM
- Mean seasonal temperature is projected to gradually increase throughout the 21st century but remain negative. A median warming of 3.8°C is projected from 1981-2010 to 2071-2100.
- No significant shift in mean seasonal precipitation is projected, except from 1991-2020 to 2011-2040 when a significant median decrease, not exceeding 6%, is projected. The spread of the ensemble is widening with the projection horizon and the different ensemble members are grouped according to the driving GCM.
- Mean seasonal streamflow is projected to gradually increase throughout the 21st century. The median increase varies from 8% in 1991-2020 to 95% in 2071-2100, relative to 1981-2010. This increase is driven by the projected warming leading to an increase in snowmelt and the fraction of precipitation falling as rain.

• Season: AMJ
- Mean seasonal temperature is projected to gradually increase throughout the 21st century. A median warming of 5.1°C is projected from 1981-2010 to 2071-2100.
- A large spread is observed in the evolution of mean seasonal precipitation with a lack of consistency in the direction of change between the different members. As a result, the ensemble median remains close to its 1981-2010 reference level.
- A shift toward a mean seasonal streamflow decrease is projected throughout the 21st century. The median decrease varies from 5% in 1991-2020 to 40% in 2071-2100, relative to 1981-2010. This decrease is driven by the projected warming leading to a snowpack depletion and a reduction of snowmelt.

• Season: JAS
- Mean seasonal temperature is projected to gradually increase throughout the 21st century. A median warming of 5.1°C is projected from 1981-2010 to 2071-2100.
- Mean seasonal precipitation is mainly projected to increase, especially after 2001-2030, but the spread of the ensemble is large. When significant, the median increase varies from 5 to 15% and a majority of ensemble members agree with the direction of change.
- A trend toward a decrease in mean seasonal streamflow is projected throughout the 21st century. The median decrease varies from about 10% in 1991-2020 to 40% in 2071-2100, relative to 1981-2010. This trend is driven by the projected warming leading to a snowpack depletion and a decrease of snowmelt. Increased evapotranspiration caused by increased temperature will also contribute to the streamflow decrease.

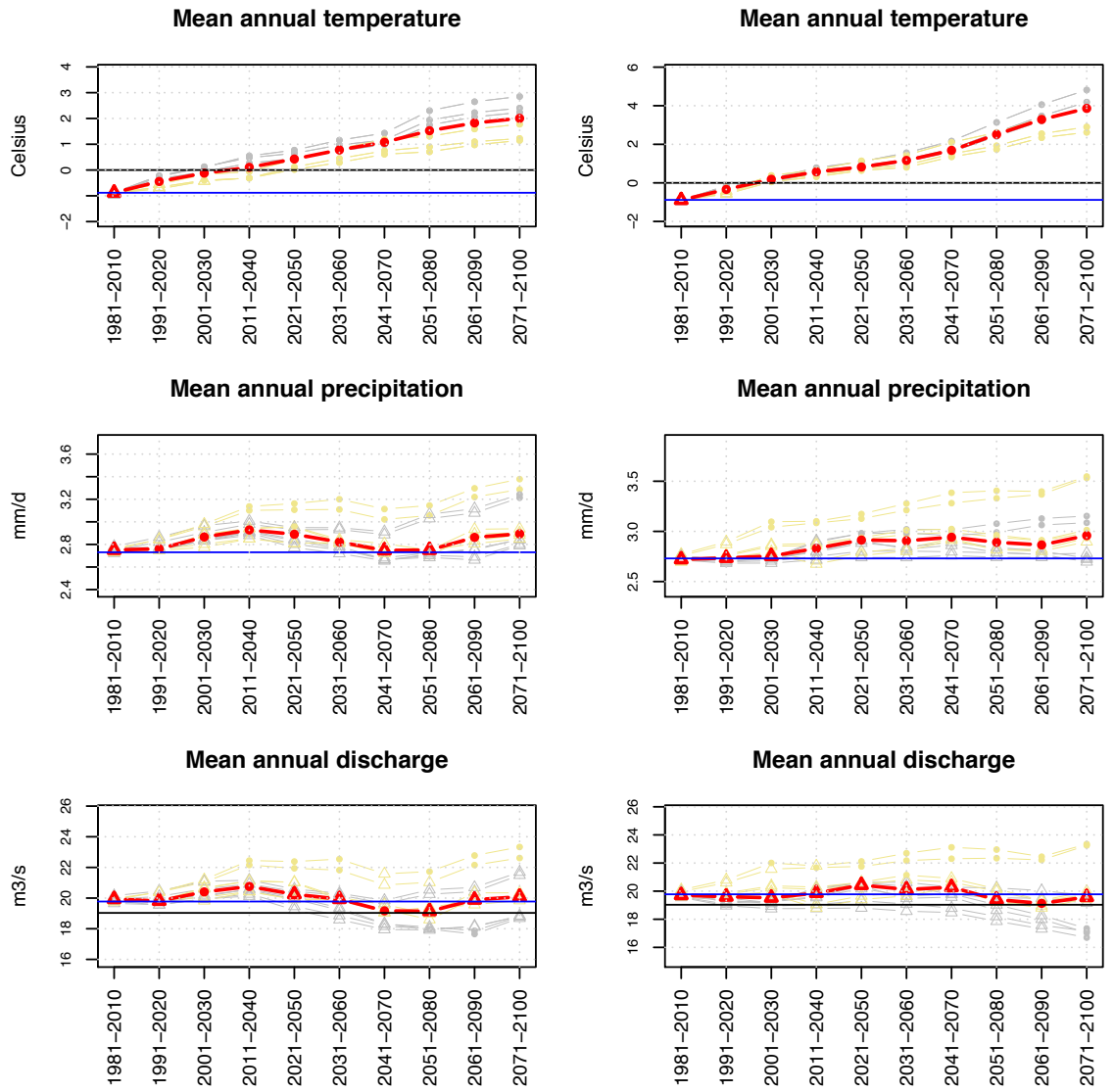

Fig. 21: Selá catchment (vhm48): Projected 30-year mean annual temperature, precipitation and discharge under the RCP4.5 emission scenario (left panel) and RCP8.5 emission scenario (right panel). Projections based on MPI-ESM-LR GCM (yellow lines). Projections based on HadGEM2ES GCM (grey lines). Ensemble median (red line). ICRA reference in the period 1981-2010 (blue line). Mean observed discharge in the period 1981-2010 (black line). Projection periods when a significant change is detected by the Mann-Whitney test compared to the reference period (1981-2010) are marked with a solid circle and with a triangle otherwise. The test is first applied to each ensemble member to compare the thirty annual values in the reference period to those in each projection period (see symbols on individual members) and then it is applied to compare the ensembles of twelve mean annual values in the reference and future periods (see symbols on the ensemble median).

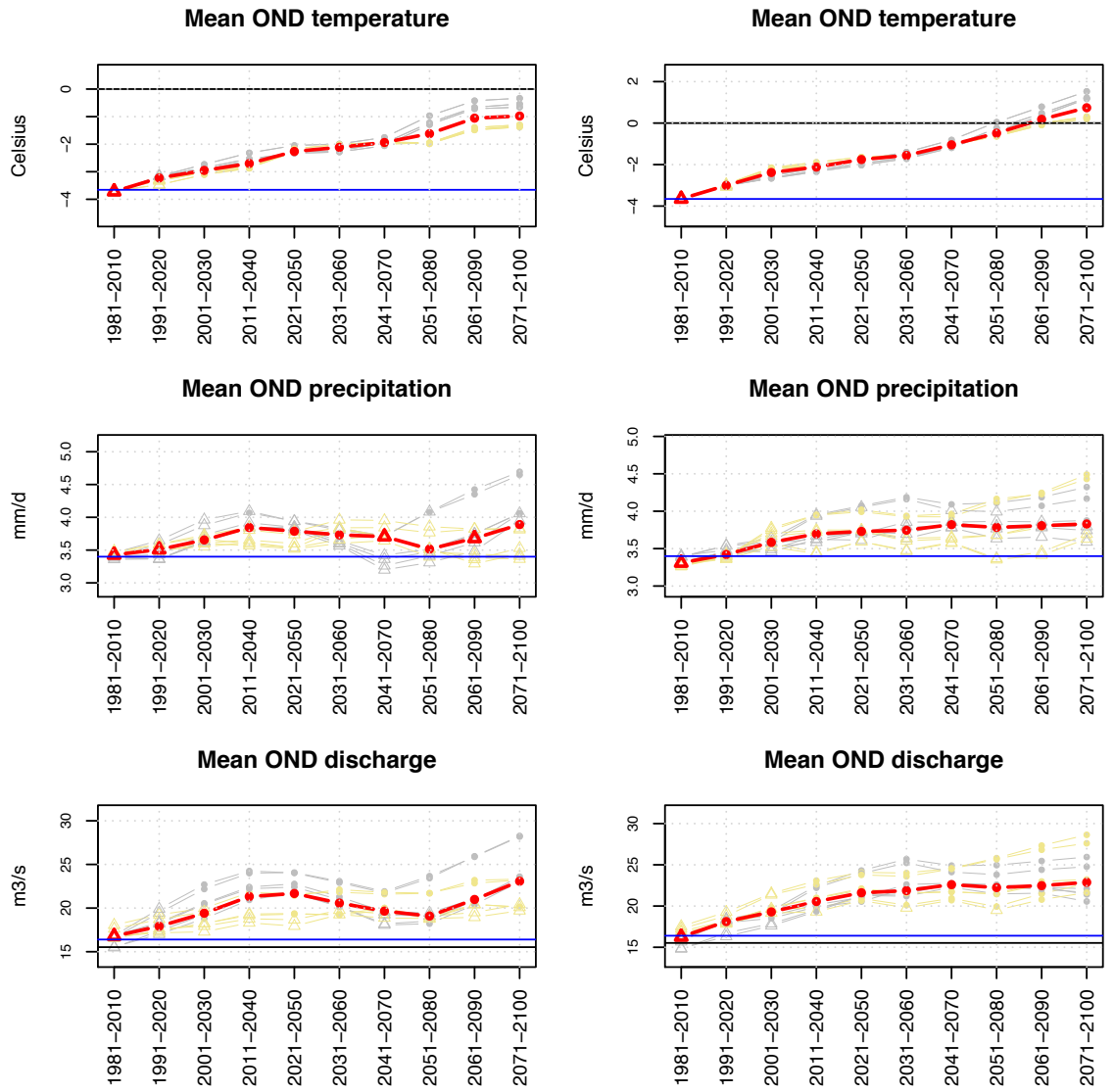

Fig. 22: Selá catchment (vhm48): Projected 30-year mean OND temperature, precipitation and discharge under the RCP4.5 emission scenario (left panel) and RCP8.5 emission scenario (right panel). Projections based on MPI-ESM-LR GCM (yellow lines). Projections based on HadGEM2ES GCM (grey lines). Ensemble median (red line). ICRA reference in the period 1981-2010 (blue line). Mean observed discharge in the period 1981-2010 (black line). Projection periods when a significant change is detected by the Mann-Whitney test compared to the reference period (1981-2010) are marked with a solid circle and with a triangle otherwise. The test is first applied to each ensemble member to compare the thirty seasonal values in the reference period to those in each projection period (see symbols on individual members) and then it is applied to compare the ensembles of twelve mean seasonal values in the reference and future periods (see symbols on the ensemble median).

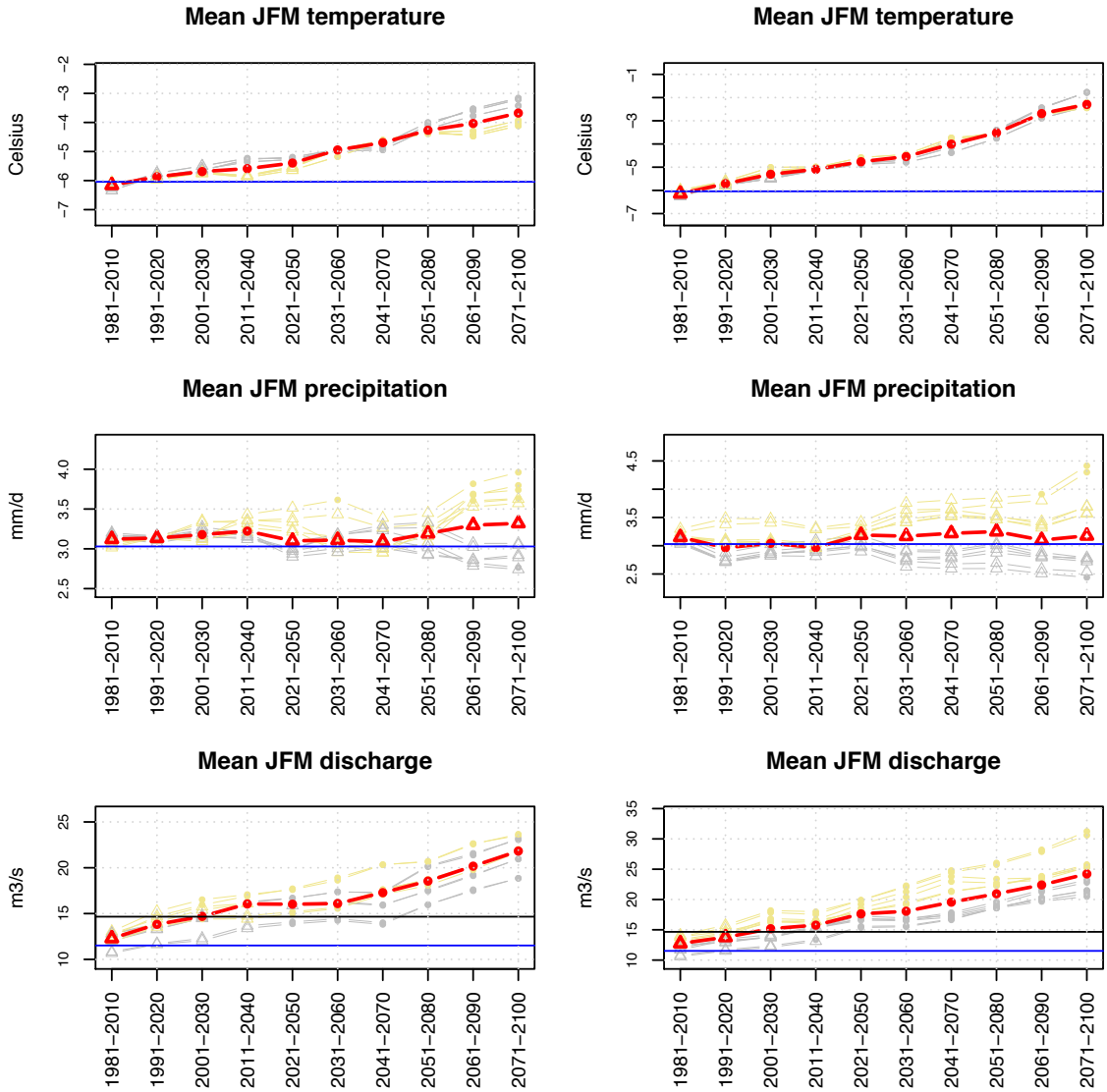

Fig. 23: Selá catchment (vhm48): Projected 30-year mean JFM temperature, precipitation and discharge under the RCP4.5 emission scenario (left panel) and RCP8.5 emission scenario (right panel). Projections based on MPI-ESM-LR GCM (yellow lines). Projections based on HadGEM2ES GCM (grey lines). Ensemble median (red line). ICRA reference in the period 1981-2010 (blue line). Mean observed discharge in the period 1981-2010 (black line). Projection periods when a significant change is detected by the Mann-Whitney test compared to the reference period (1981-2010) are marked with a solid circle and with a triangle otherwise. The test is first applied to each ensemble member to compare the thirty seasonal values in the reference period to those in each projection period (see symbols on individual members) and then it is applied to compare the ensembles of twelve mean seasonal values in the reference and future periods (see symbols on the ensemble median).

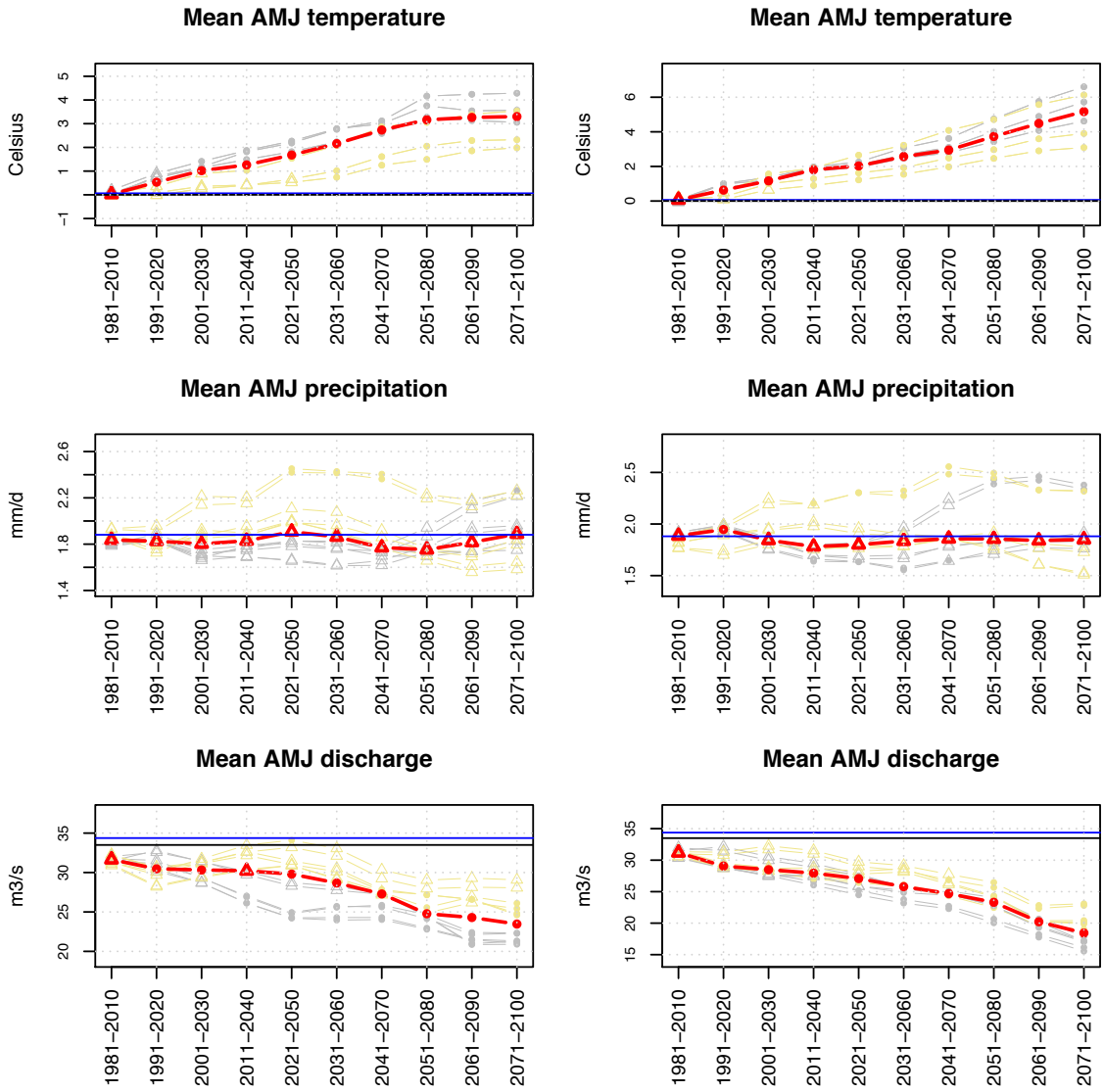

Fig. 24: Selá catchment (vhm48): Projected 30-year mean AMJ temperature, precipitation and discharge under the RCP4.5 emission scenario (left panel) and RCP8.5 emission scenario (right panel). Projections based on MPI-ESM-LR GCM (yellow lines). Projections based on HadGEM2ES GCM (grey lines). Ensemble median (red line). ICRA reference in the period 1981-2010 (blue line). Mean observed discharge in the period 1981-2010 (black line). Projection periods when a significant change is detected by the Mann-Whitney test compared to the reference period (1981-2010) are marked with a solid circle and with a triangle otherwise. The test is first applied to each ensemble member to compare the thirty seasonal values in the reference period to those in each projection period (see symbols on individual members) and then it is applied to compare the ensembles of twelve mean seasonal values in the reference and future periods (see symbols on the ensemble median).

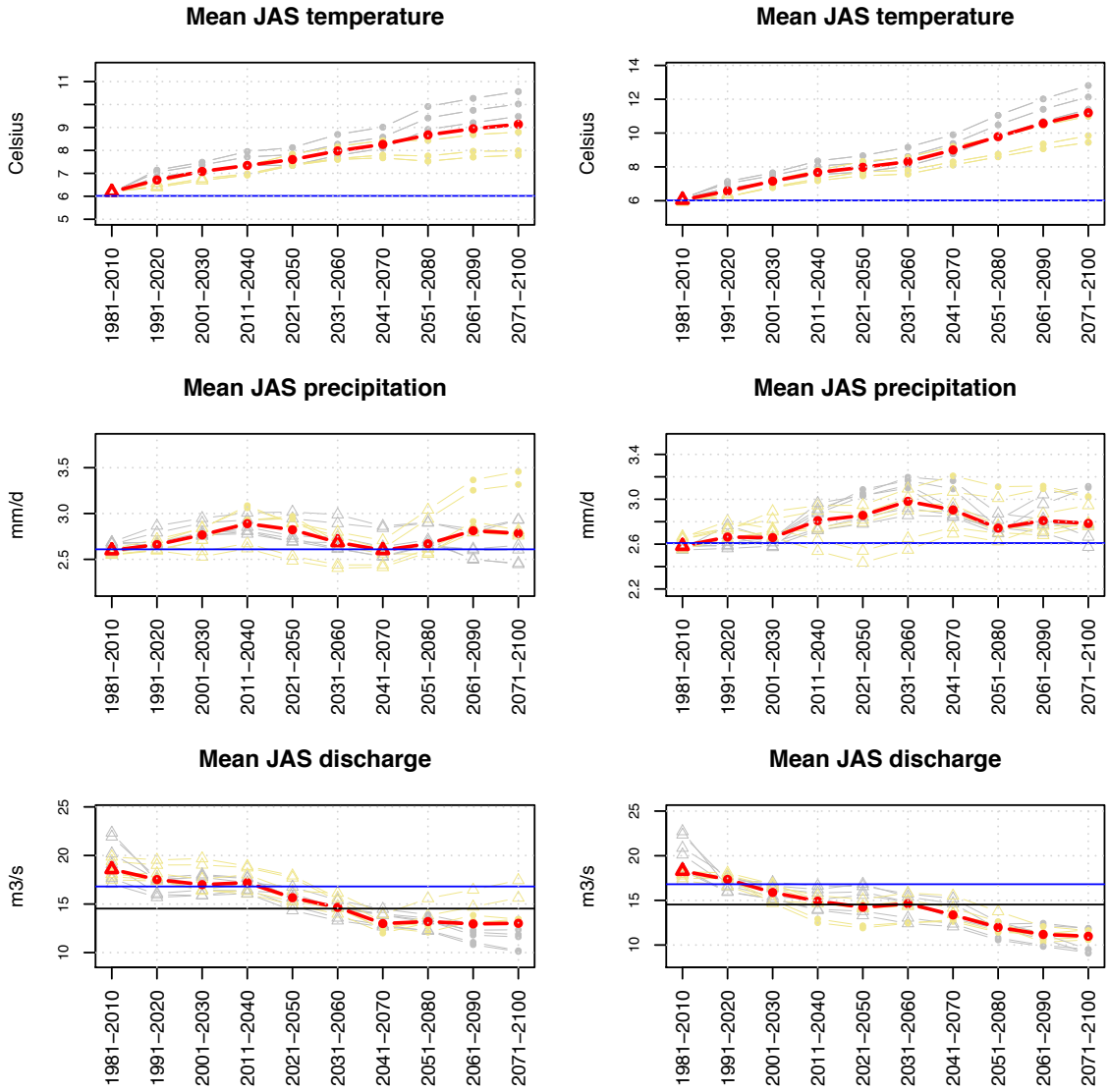

Fig. 25: Selá catchment (vhm48): Projected 30-year mean JAS temperature, precipitation and discharge under the RCP4.5 emission scenario (left panel) and RCP8.5 emission scenario (right panel). Projections based on MPI-ESM-LR GCM (yellow lines). Projections based on HadGEM2ES GCM (grey lines). Ensemble median (red line). ICRA reference in the period 1981-2010 (blue line). Mean observed discharge in the period 1981-2010 (black line). Projection periods when a significant change is detected by the Mann-Whitney test compared to the reference period (1981-2010) are marked with a solid circle and with a triangle otherwise. The test is first applied to each ensemble member to compare the thirty seasonal values in the reference period to those in each projection period (see symbols on individual members) and then it is applied to compare the ensembles of twelve mean seasonal values in the reference and future periods (see symbols on the ensemble median).

- **Geithellnaá catchment (vhm149)**
  - **RCP4.5 emission scenario**
    - Annual (water year)
      - Mean annual temperature is projected to gradually increase throughout the 21st century and become positive in 2001-2030. A median warming of 2.5°C is projected from 1981-2010 to 2071-2100.
      - Mean annual precipitation is projected to oscillate around its 1981-2010 reference level. No significant change is projected except during a few periods when a ± 3% median change is projected.
      - Mean annual streamflow projections follow a trajectory similar to precipitation projections and do not vary much in most cases. The ensemble median is projected to remain close to its 1981-2010 reference level. A small median decrease, not exceeding 5%, is projected in 2041-2070 and 2051-2080.
    - Season: OND
      - Mean seasonal temperature is projected to gradually increase throughout the 21st century but remain negative. A median warming of 2.4°C is projected from 1981-2010 to 2071-2100.
      - Mean seasonal precipitation projections oscillate around their respective 1981-2010 reference level. A significant shift, usually positive, is projected in some periods. The median increase, in these periods, varies between 5 and 10% and a majority of ensemble members agree with the direction of change.
      - A trend toward a mean seasonal streamflow increase is projected throughout the 21st century, modulated by precipitation variations. A median increase of 47% is projected from 1981-2010 to 2071-2100. This increase is driven by the projected warming, causing an increase in the fraction of precipitation falling as rain.
    - Season: JFM
      - Mean seasonal temperature is projected to gradually increase throughout the 21st century but remain negative. A median warming of 2.2°C is projected from 1981-2010 to 2071-2100.
      - Mean seasonal precipitation is projected to oscillate around its 1981-2010 reference level. The trajectory of the ensemble members is linked to the driving GCM and the ensemble spread widens after 2041-2070. A significant median decrease not exceeding 8% is projected in the periods 2011-2040 to 2051-2080.
      - Mean seasonal streamflow is projected to gradually increase throughout the 21st century. A median increase of 70% is projected from 1981-2010 to 2071-2100. This increase is driven by the projected warming, causing an increase in snowmelt and the fraction of precipitation falling as rain.
    - Season: AMJ
      - Mean seasonal temperature is projected to gradually increase throughout the 21st century. A median warming of 2.6°C is projected from 1981-2010 to 2071-2100.

- Mean seasonal precipitation is projected to fluctuate around its 1981-2010 reference level and no significant shift is detected, except in 2061-2090 when a small median decrease is projected but not all members agree with the direction of change.
- A trend toward an increase in mean seasonal streamflow is projected in the periods 2001-2030 to 2051-2080, then the median returns close to its 1981-2010 reference level. The largest median increase is observed in 2031-2060 (13%). These variations are driven by the projected warming leading to a rainfall increase while enough snow will still be available to maintain a stable snowmelt contribution.

• Season: JAS
- Mean seasonal temperature is projected to gradually increase throughout the 21st century. A median warming of 2.6°C is projected from 1981-2010 to 2071-2100.
- Mean seasonal precipitation is projected to oscillate around its 1981-2010 reference level and a significant positive shift is detected in the periods 2001-2030 to 2021-2050. The median increase in these periods does not exceed 15%.
- Mean seasonal streamflow is projected to gradually decrease throughout the 21st century. The median decrease varies from 10% in 1991-2020 to 50% in 2071-2100, relative to 1981-2010. This trend is driven by the projected warming that will gradually reduce snowmelt and increase evapotranspiration, leading to the streamflow decrease.

• **RCP8.5 emission scenario**
• Annual (water year)
- Mean annual temperature is projected to gradually increase throughout the 21st century and become positive in 2001-2030. A median warming of 4°C is projected from 1981-2010 to 2071-2100.
- No significant change in mean annual precipitation is projected throughout the 21st century, but the spread of the ensemble widens with the projection horizon, leading the ensemble median to remain close to its 1981-2010 reference level.
- Mean annual streamflow is projected to remain close to its 1981-2010 reference level until 2041-2070, then a trend toward a decrease is projected. During that period, the median decrease varies from 5 to 8%.

• Season: OND
- Mean seasonal temperature is projected to gradually increase throughout the 21st century and become positive in 2061-2090. A median warming of 3.7°C is projected from 1981-2010 to 2071-2100.
- Mean seasonal precipitation is projected to oscillate around its 1981-2010 reference level and a significant shift, usually positive, is detected in some periods. The median increase does not exceed 10% in these periods but not all members consistently agree with an increase.
- Mean seasonal streamflow is projected to gradually increase throughout the 21st century. A median increase of 50% is projected from 1981-2010 to 2071-2100. This increase is

driven by the projected warming causing an increase in the fraction of precipitation falling as rain and modulated by precipitation variations.

- Season: JFM
  - Mean seasonal temperature is projected to gradually increase throughout the 21st century but remain negative. A median warming of 3.4°C is projected from 1981-2010 to 2071-2100.
  - Mean seasonal precipitation projections oscillate around their respective 1981-2010 reference level and the spread of the ensemble widens with the projection horizon. A significant shift, usually negative, is detected in some periods. The median decrease varying from 8% to 12% in these periods.
  - Mean seasonal streamflow is projected to gradually increase throughout the 21st century but the spread of the ensemble widens with the projection horizon. A median increase of 80% is projected from 1981-2010 to 2071-2100. This increase is driven by the projected warming, leading to an increase in snowmelt and the fraction of precipitation falling as rain.
- Season: AMJ
  - Mean seasonal temperature is projected to gradually increase throughout the 21st century. A median warming of 4°C is projected from 1981-2010 to 2071-2100.
  - Mean seasonal precipitation is projected to fluctuate around its 1981-2010 reference level. The spread of the ensemble widens with the projection horizon. The ensemble median remains close to its 1981-2010 reference level.
  - Mean seasonal streamflow is projected to significantly increase in the periods 2001-2030 to 2031-2060, then to return close to its 1981-2010 reference level until 2051-2080 before significantly decreasing until the end of the century. The spread of the ensemble widens with the projection horizon. The largest median increase is projected in 2011-2040 (13%) and the largest median decrease in 2071-2100 (27%). These variations are driven by the projected warming leading to a rainfall increase while snowmelt will not start decreasing before 2051-2080.
- Season: JAS
  - Mean seasonal temperature is projected to gradually increase throughout the 21st century. A median warming of 4.7°C is projected from 1981-2010 to 2071-2100.
  - Mean seasonal precipitation is projected to fluctuate around its reference level. A significant shift, usually positive, is detected in some periods. The median increase does not exceed 10% in these periods.
  - Mean seasonal streamflow is projected to gradually decrease throughout the 21st century. The median decrease is ranging from 13% in 1991-2020 to 63% in 2071-2100, relative to 1981-2010. This trend is driven by the projected warming leading to a gradual reduction of snowmelt combined with an increase of evapotranspiration while rainfall is not projected to vary much.

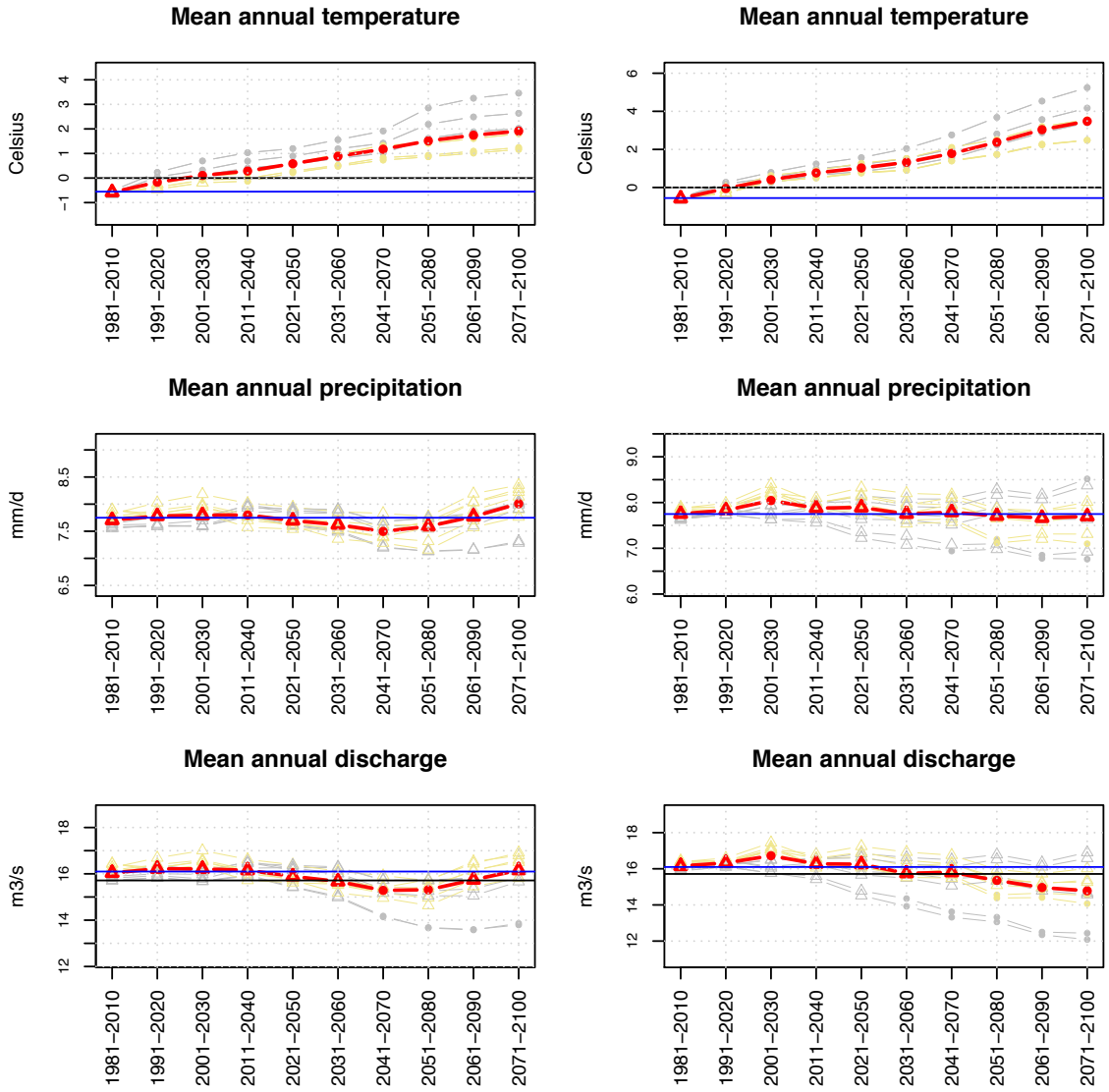

Fig. 26: Geithellnaá catchment (vhm149): Projected 30-year mean annual temperature, precipitation and discharge under the RCP4.5 emission scenario (left panel) and RCP8.5 emission scenario (right panel). Projections based on MPI-ESM-LR GCM (yellow lines). Projections based on HadGEM2ES GCM (grey lines). Ensemble median (red line). ICRA reference in the period 1981-2010 (blue line). Mean observed discharge in the period 1981-2010 (black line). Projection periods when a significant change is detected by the Mann-Whitney test compared to the reference period (1981-2010) are marked with a solid circle and with a triangle otherwise. The test is first applied to each ensemble member to compare the thirty annual values in the reference period to those in each projection period (see symbols on individual members) and then it is applied to compare the ensembles of twelve mean annual values in the reference and future periods (see symbols on the ensemble median).

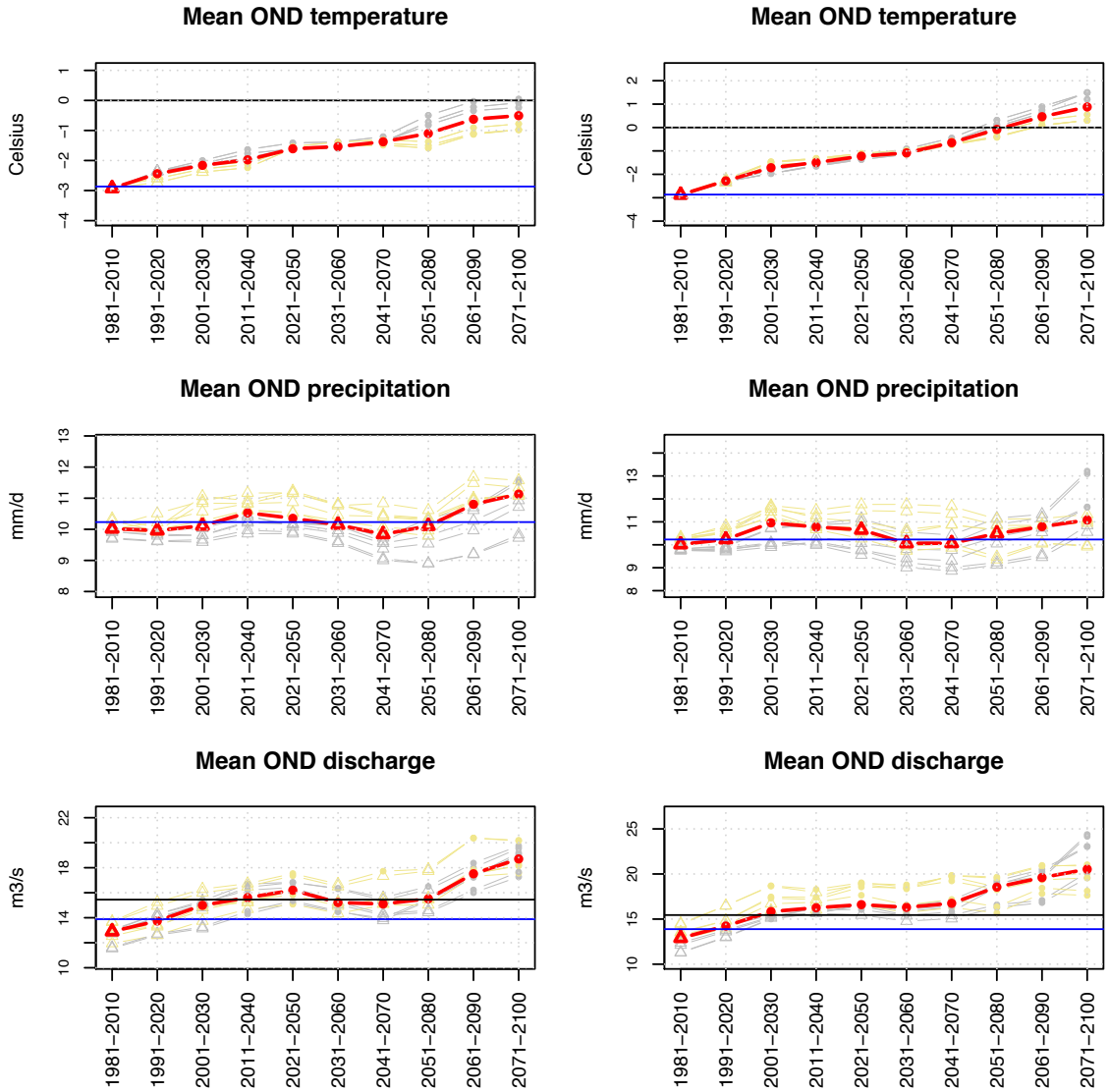

Fig. 27: Geithellnaá catchment (vhm149): Projected 30-year mean OND temperature, precipitation and discharge under the RCP4.5 emission scenario (left panel) and RCP8.5 emission scenario (right panel). Projections based on MPI-ESM-LR GCM (yellow lines). Projections based on HadGEM2ES GCM (grey lines). Ensemble median (red line). ICRA reference in the period 1981-2010 (blue line). Mean observed discharge in the period 1981-2010 (black line). Projection periods when a significant change is detected by the Mann-Whitney test compared to the reference period (1981-2010) are marked with a solid circle and with a triangle otherwise. The test is first applied to each ensemble member to compare the thirty seasonal values in the reference period to those in each projection period (see symbols on individual members) and then it is applied to compare the ensembles of twelve mean seasonal values in the reference and future periods (see symbols on the ensemble median).

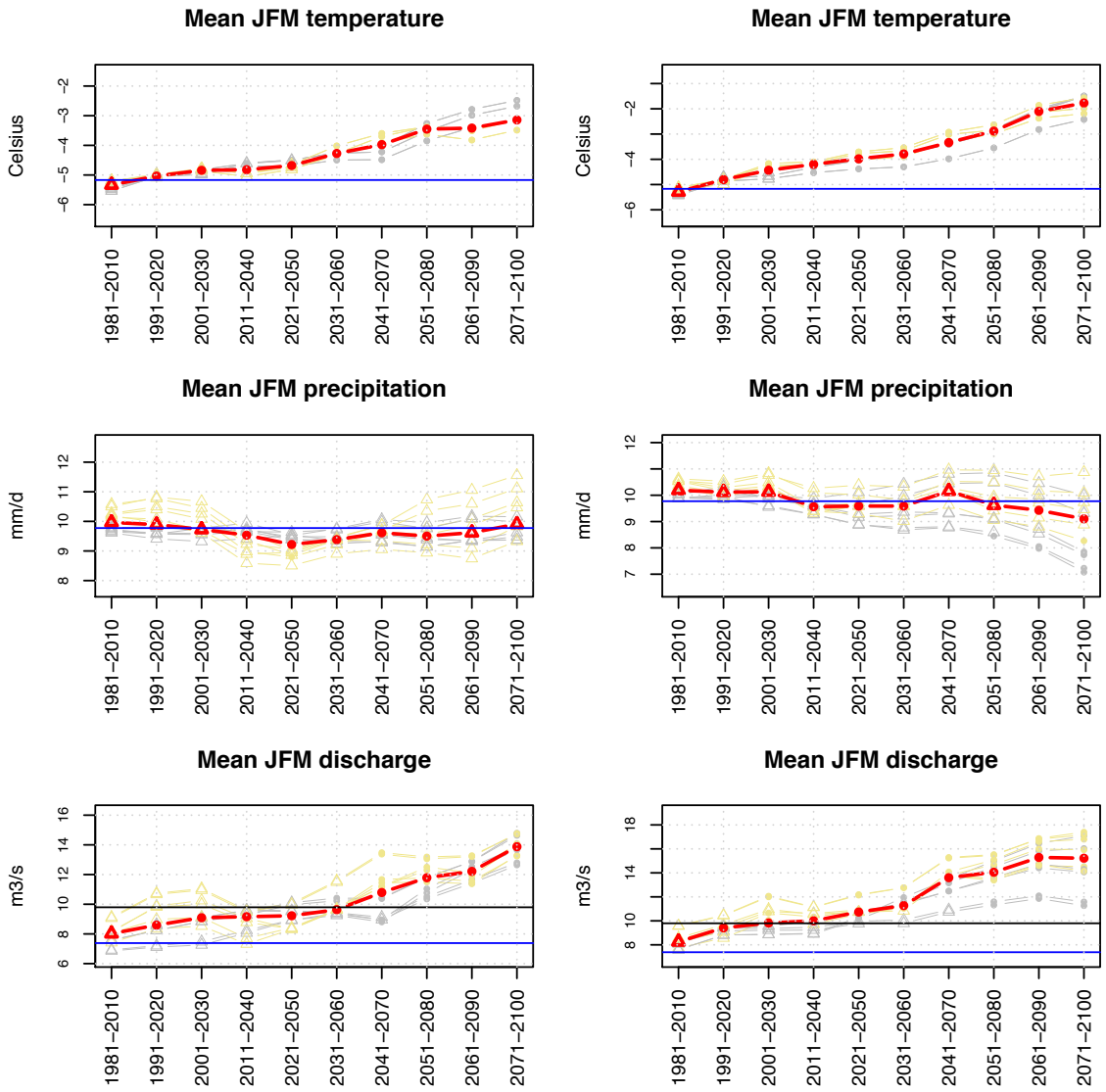

Fig. 28: Geithellnaá catchment (vhm149): Projected 30-year mean JFM temperature, precipitation and discharge under the RCP4.5 emission scenario (left panel) and RCP8.5 emission scenario (right panel). Projections based on MPI-ESM-LR GCM (yellow lines). Projections based on HadGEM2ES GCM (grey lines). Ensemble median (red line). ICRA reference in the period 1981-2010 (blue line). Mean observed discharge in the period 1981-2010 (black line). Projection periods when a significant change is detected by the Mann-Whitney test compared to the reference period (1981-2010) are marked with a solid circle and with a triangle otherwise. The test is first applied to each ensemble member to compare the thirty seasonal values in the reference period to those in each projection period (see symbols on individual members) and then it is applied to compare the ensembles of twelve mean seasonal values in the reference and future periods (see symbols on the ensemble median).

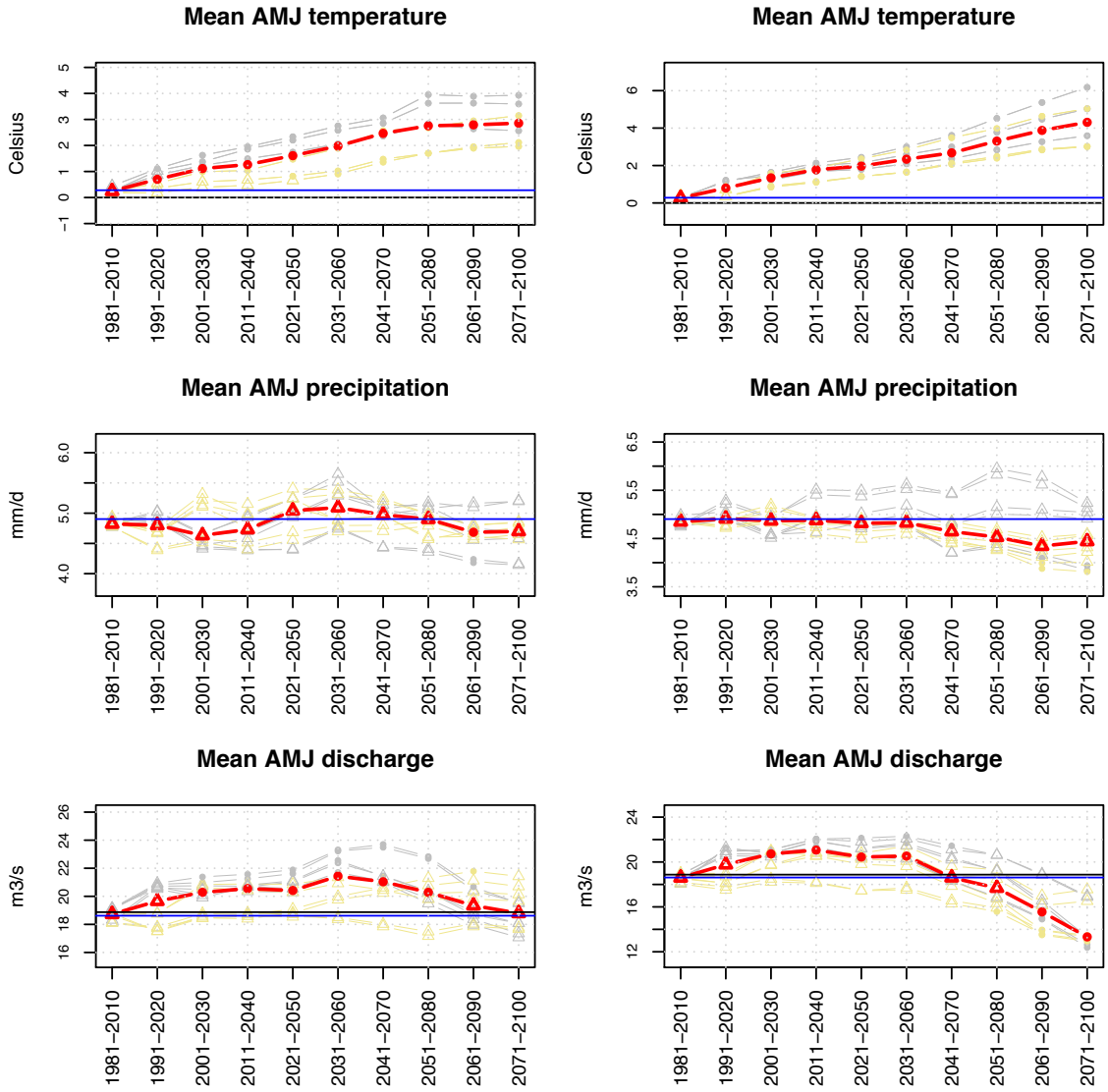

Fig. 29: Geithellnaá catchment (vhm149): Projected 30-year mean AMJ temperature, precipitation and discharge under the RCP4.5 emission scenario (left panel) and RCP8.5 emission scenario (right panel). Projections based on MPI-ESM-LR GCM (yellow lines). Projections based on HadGEM2ES GCM (grey lines). Ensemble median (red line). ICRA reference in the period 1981-2010 (blue line). Mean observed discharge in the period 1981-2010 (black line). Projection periods when a significant change is detected by the Mann-Whitney test compared to the reference period (1981-2010) are marked with a solid circle and with a triangle otherwise. The test is first applied to each ensemble member to compare the thirty seasonal values in the reference period to those in each projection period (see symbols on individual members) and then it is applied to compare the ensembles of twelve mean seasonal values in the reference and future periods (see symbols on the ensemble median).

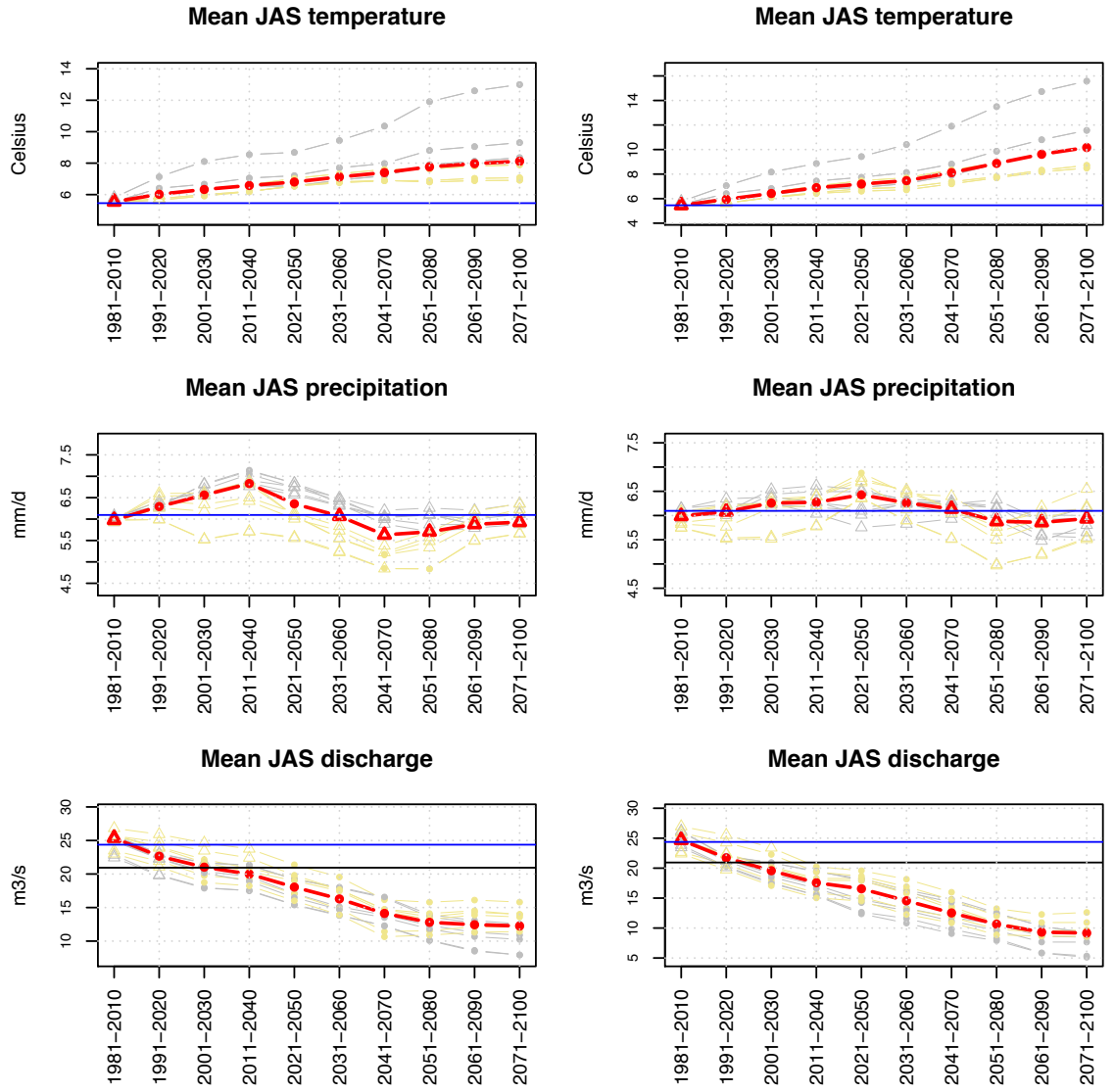

Fig. 30: Geithellnaá catchment (vhm149): Projected 30-year mean JAS temperature, precipitation and discharge under the RCP4.5 emission scenario (left panel) and RCP8.5 emission scenario (right panel). Projections based on MPI-ESM-LR GCM (yellow lines). Projections based on HadGEM2ES GCM (grey lines). Ensemble median (red line). ICRA reference in the period 1981-2010 (blue line). Mean observed discharge in the period 1981-2010 (black line). Projection periods when a significant change is detected by the Mann-Whitney test compared to the reference period (1981-2010) are marked with a solid circle and with a triangle otherwise. The test is first applied to each ensemble member to compare the thirty seasonal values in the reference period to those in each projection period (see symbols on individual members) and then it is applied to compare the ensembles of twelve mean seasonal values in the reference and future periods (see symbols on the ensemble median).

6-2-3 Summary and discussion

The projected warming is relatively homogeneous within the ensemble and relatively linear in all seasons and catchments. As expected, a higher warming is projected under the RCP8.5 emission scenario than under the RCP4.5 emission scenario. Mean annual and seasonal precipitation projections are mainly characterised by oscillations reflecting long-term natural climate variability. The nature of these oscillations often depends on the driving GCM and the different precipitation projections do not always vary in phase with each other, leading sometimes to large uncertainties in some periods and seasons. Significant precipitation changes (positive or negative) are sometimes projected in some periods, depending on the amplitude of these oscillations. Long-term tendencies sometimes dominate the variability of precipitation projections, such as a mean precipitation increase in summer in the Vatnsdalsá catchment under both emission scenarios, and in summer and autumn in the Selá catchment under the RCP8.5 emission scenario, leading to an increase in mean annual precipitation as well. Regardless of precipitation variations, increased temperature will modify the seasonal ratio of rainfall and snowfall: mean seasonal snowfall will gradually decrease while mean seasonal rainfall will increase. The role of snow in the flow regimes of the studied catchments will subsequently be attenuated.

Variations in mean annual streamflow over the course of the projection horizon are mainly driven by variations in mean annual precipitation. Variations in mean seasonal streamflow are driven by variations in mean seasonal rainfall and snowmelt. Increased temperatures are projected to gradually lead to a decrease in the fraction of precipitation falling as snow, which, in turn, will lead to less snow storage and shorter snow seasons. As a result, snowmelt is projected to gradually increase in winter and decrease in spring/summer while rainfall will gradually increase in most seasons. Increased winter snowmelt can be caused by an increase in the number of intermittent snowmelt events and/or a shift of the onset of the snowmelt season from spring to winter. Because of large altitude gradients, daily precipitation does not necessarily fall as 100% rain or 100% snow in the catchments. There are periods in the year during which it is expected that lower portions of the catchments receive precipitation as rainfall and higher portions receive it as snowfall. Changes in mean seasonal rainfall and snowfall on the catchments reflect also changes in the spatial extent of daily rainfall and snowfall events during these periods.

Overall, mean seasonal streamflow is projected to i) gradually increase throughout the 21st century in OND and JFM in all catchments, ii) gradually decrease in AMJ in the Vatnsdalsá and Selá catchments, and first increase and later decrease in the Geithellnaá catchment, iii) gradually decrease in JAS in the Selá and Geithellnaá catchments, but remain mainly unchanged in the Vatnsdalsá catchment. The changes are usually more pronounced and/or more rapid under the RCP8.5 emission scenario because the projected warming is stronger than under RCP4.5 and is leading to more drastic changes in snow storage conditions and in the fraction of precipitation falling as rain. Increased evapotranspiration due to higher temperatures will contribute to reduce streamflow, especially in summer.

7 Climate change impact on flood characteristics

This section examines the impact of projected climate change on the timing and magnitude of annual maximum floods (AMFs).

7-1 Changes in the timing of annual maximum floods

To investigate changes in the timing of AMFs, the day when annual maximum daily discharge occurred in the water year was extracted and assigned to the corresponding season, for each water year in the simulated period (1981-2100). Then, the frequency (relative number) of AMFs occurring in each season within each 30-year period was calculated, and seasonal frequency changes relative to the reference period (1981-2010) analysed. Figs. 31 to 36 present the results for the ensemble median and Appendix 10 presents the results from all ensemble members in form of box-plots.

For all catchments, it is assumed that AMFs occurring in OND are primarily generated by rainfall; AMFs occurring in JFM are generated by a combination of rainfall and snowmelt; AMFs occurring in AMJ are primarily generated by snowmelt but some rainfall can be combined with snowmelt; AMFs occurring in JAS are primarily generated by rainfall, except in Geithellnaá where early summer events are probably generated by rainfall and snowmelt.

- **Vatnsdalsá catchment (vhm45)**

In the reference period (1981-2010), AMFs occur mainly in AMJ and only a minor fraction occurs in JFM, while practically no event is simulated in JAS and OND.

- RCP4.5 emission scenario

As the projection horizon increases, AMFs are projected to gradually occur less frequently in AMJ and at the same time, increasingly more frequently in JFM. The main flood season will remain AMJ but the difference between the median frequency of AMFs in AMJ and JFM will be strongly reduced. A few AMFs are also projected to occur in OND toward the end of the century.

- RCP8.5 emission scenario

Results are similar to those observed under the RCP4.5 emission scenario except that the amplitude of the frequency changes in AMJ and JFM will be stronger (AMJ/decrease; JFM/increase). As a result, JFM will become the main flood season in 2071-2100 in terms of frequency of AMFs. A small frequency increase is also projected in OND throughout the projection horizon, and in JAS after 2031-2060.

- **Selá catchment (vhm48)**

In the reference period (1981-2010), AMFs occur mainly in AMJ and only a small fraction occurs in other seasons and in relative similar proportions.

- RCP4.5 emission scenario

As the projection horizon increases, AMFs are projected to gradually occur less frequently in AMJ and at the same time, increasingly more frequently in OND and JFM, while no change is projected

in JAS. In 2071-2100, AMJ will no longer be the main flood season and AMFs will occur as frequently in AMJ and OND, closely followed by JFM while very few events will occur in JAS, according to the ensemble median.

- RCP8.5 emission scenario

Results are similar to those observed under the RCP4.5 emission scenario except that the frequency of AMFs in AMJ is projected to decrease faster. In 2071-2100, AMJ will no longer be the main flood season, and slightly more AMFs will occur in OND and JFM than in AMJ, while very few events will occur in JAS, according to the ensemble median.

- **Geithellnaá catchment (vhm149)**

In the reference period (1981-2010), AMFs occur mainly in OND, followed by JAS and then by the other two seasons. Note that the median frequency of simulated events in JAS in the reference period (1981-2010) is slightly lower than the observed frequency (cf. Fig. 6).

- RCP4.5 emission scenario

The prevalence of OND will persist in the future. Only little changes are projected to take place under this emission scenario: in the periods 2041-2070 to 2071-2100, the frequency of AMFs is projected to slightly decrease in JAS and increase in JFM.

- RCP8.5 emission scenario

Results are similar to those observed under the RCP4.5 emission scenario.

- **Discussion**

Catchments most affected by changes in the seasonal frequency of AMFs are those where these events are primarily generated by snowmelt and occurring in spring in the reference period (Vatnsdalsá and Selá). Due to the increase in temperature, the flood regimes of these catchments will gradually become less governed by spring snowmelt and more influenced by rainfall or a combination of rainfall and snowmelt in autumn/winter. In the Geithellnaá catchment, AMFs will continue to occur most frequently in autumn in the future, as these events are triggered by rainfall in both reference and future periods, but some intensification is expected in winter, whereas a few less AMFs will occur in summer, probably because fewer events will be triggered by combined rain and snowmelt in early summer as compared to the reference period (1981-2010).

For the Vatnsdalsá and Selá catchments, the seasonal frequency changes imply that spring floods will tend to become smaller than autumn/winter floods, so that autumn/winter floods will sometimes be selected as AMFs instead of spring floods. This means that magnitude changes are either occurring simultaneously in the different seasons (i.e. decrease in spring and increase in autumn/winter) or in one season mainly (i.e. decrease in spring or increase in autumn/winter). As projected warming will lead to a considerable reduction of snowmelt in spring and a decrease in mean daily discharge, a decrease in the magnitude of spring floods is vey likely. An increase in the magnitude of autumn/winter floods is not excluded either. A seasonal flood analysis would be required to study in more details these changes and the underlying causes.

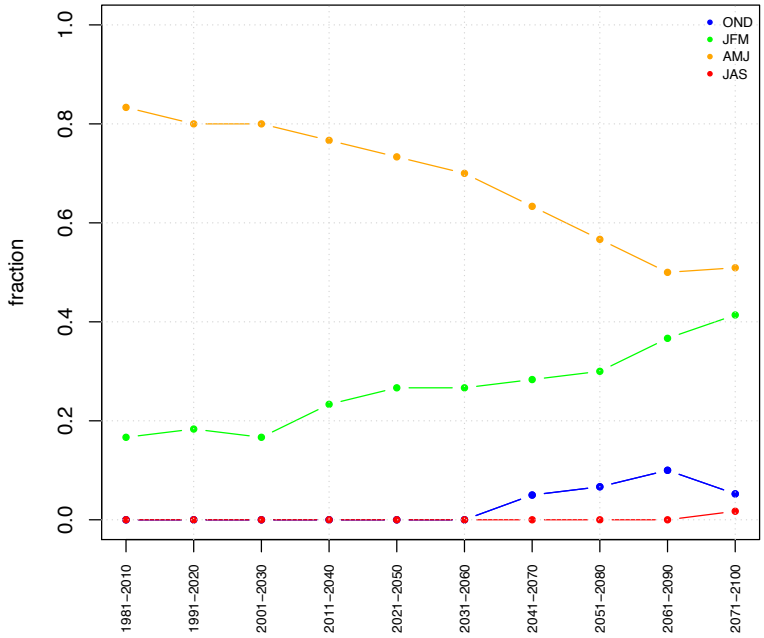

Fig. 31: Vatnsdalsá catchment (vhm45): Ensemble median of the projected frequency (relative number) of annual maximum floods occurring in each season and period, under the RCP4.5 emission scenario. OND (blue), JFM (green), AMJ (orange), JAS (red).

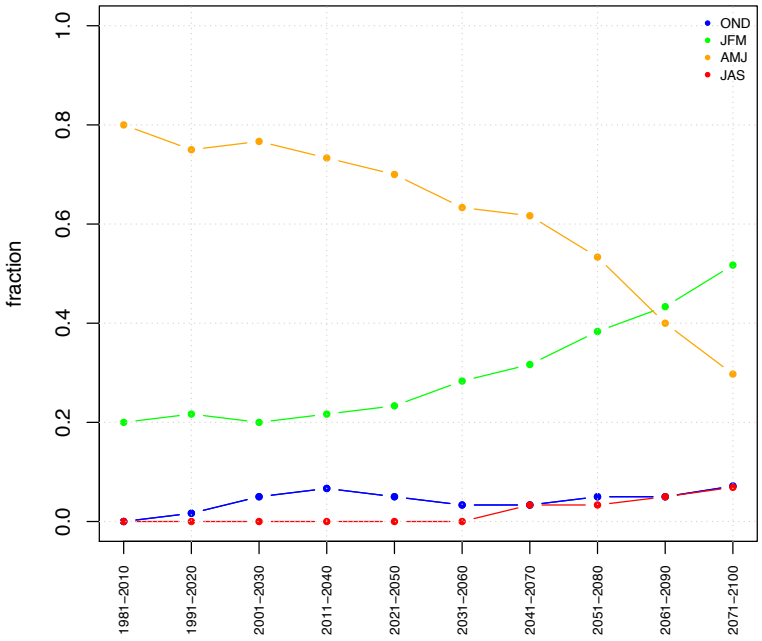

Fig. 32: Vatnsdalsá catchment (vhm45): as Fig. 31 but under the RCP8.5 emission scenario.

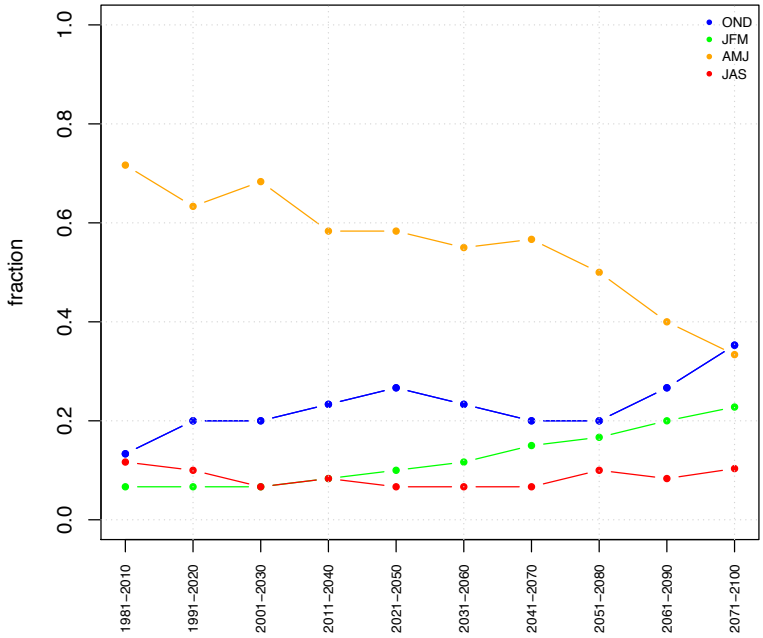

Fig. 33: Selá catchment (vhm48): Ensemble median of the projected frequency (relative number) of annual maximum floods occurring in each season and period, under the RCP4.5 emission scenario. OND (blue), JFM (green), AMJ (orange), JAS (red).

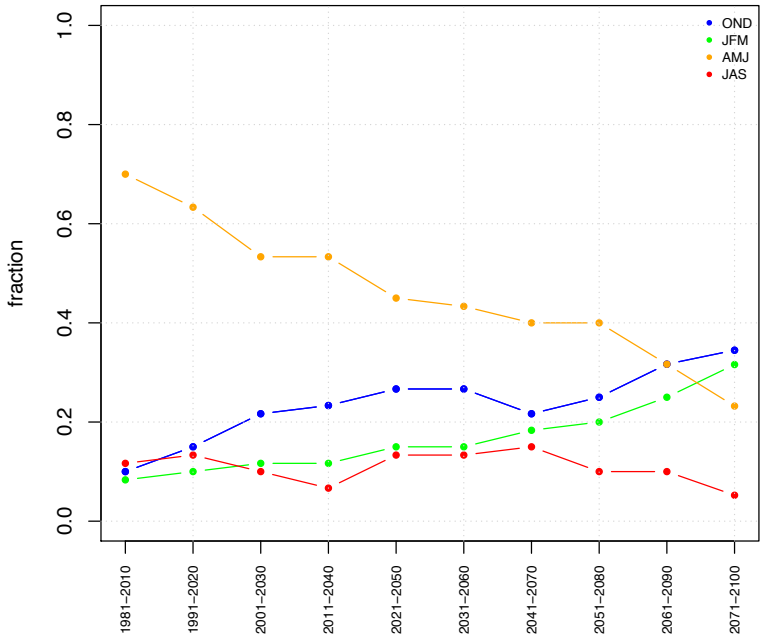

Fig. 34: Selá catchment (vhm48): as Fig. 33 but under the RCP8.5 emission scenario.

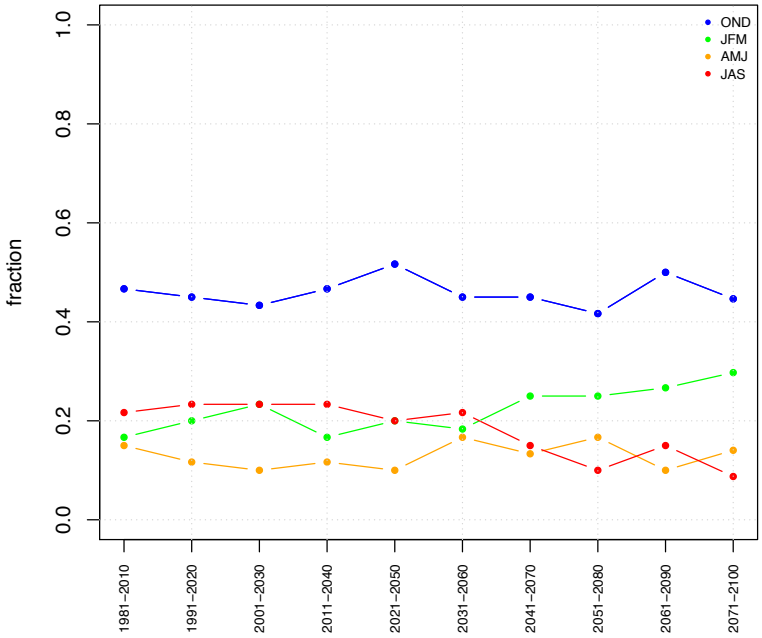

Fig. 35: Geithellnaá catchment (vhm149): Ensemble median of the projected frequency (relative number) of annual maximum floods occurring in each season and period, under the RCP4.5 emission scenario. OND (blue), JFM (green), AMJ (orange), JAS (red).

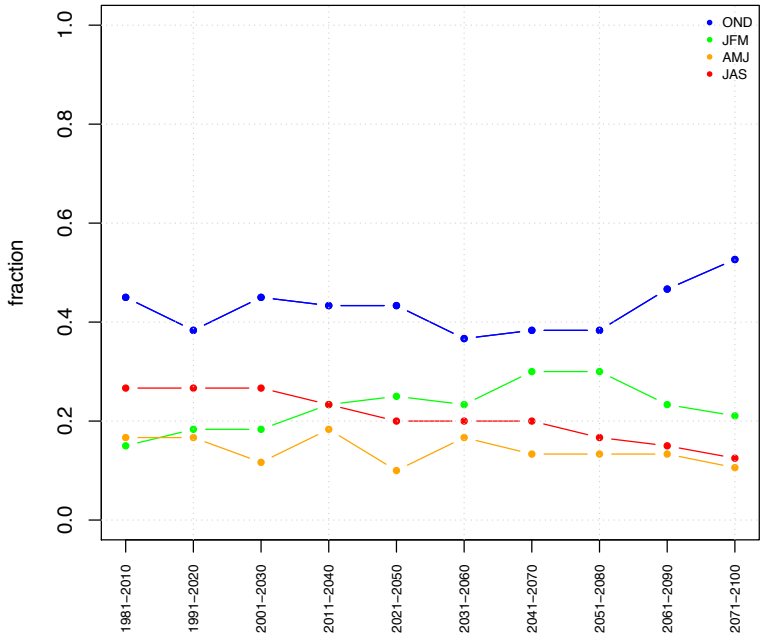

Fig. 36: Geithellnaá catchment (vhm149): as Fig. 35 but under the RCP8.5 emission scenario.

7-2 Changes in the magnitude of annual maximum floods

This section examines the impact of projected climate change on the magnitude of annual maximum floods (AMFs).

7-2-1 Changes in the magnitude of T-year floods

A Gumbel distribution was fitted to the AMFs series, within each 30-year period (not shown) and the magnitude of T-year floods estimated for return periods T=10 and 100 years. The uncertainty associated with the T-year flood estimation increases with the return period T and projection horizon. Changes in the magnitude of T-year floods, relative to the magnitude of T-year floods in the reference period (1981-2010) were then calculated. Figs. 37 to 42 present the evolution of the relative changes in 10-year and 100-year floods and Appendix 11 presents these results in form of box-plots.

- **Vatnsdalsá catchment (vhm45)**

See Figs. 37 and 38.

- RCP4.5 emission scenario

Apart from very few members projecting an increase in some periods, a consistent and gradual decrease in the magnitude of T-year floods is projected by a majority of realisations forming the ensemble, throughout the 21st century, but the uncertainty of the projected change is large. The median decrease varies in similar proportions for the two return periods, from 5% to 30%. Note in Fig. 37 that the different ensemble members tend to be grouped according to the driving GCM, with a tendency for the changes derived from projections driven by the HadGEM2ES GCM to be larger than those derived from projections driven by the MPI-ESM-LR GCM.

- RCP8.5 emission scenario

The magnitude of T-year floods is mainly projected to gradually decrease throughout the 21st century. Here too, the different ensemble members tend to be grouped according to the driving GCM. The median decrease varies from 5% to 45%, in similar proportions for the two return periods.

- Discussion

Spring snowmelt plays a primary role in the generation of annual maximum floods in this catchment in the reference period (1981-2010). Snowpack depletion, shorter snow seasons and the reduction of spring snowmelt caused by the projected warming are very likely responsible for the projected decrease in the magnitude of T-year floods in this catchment.

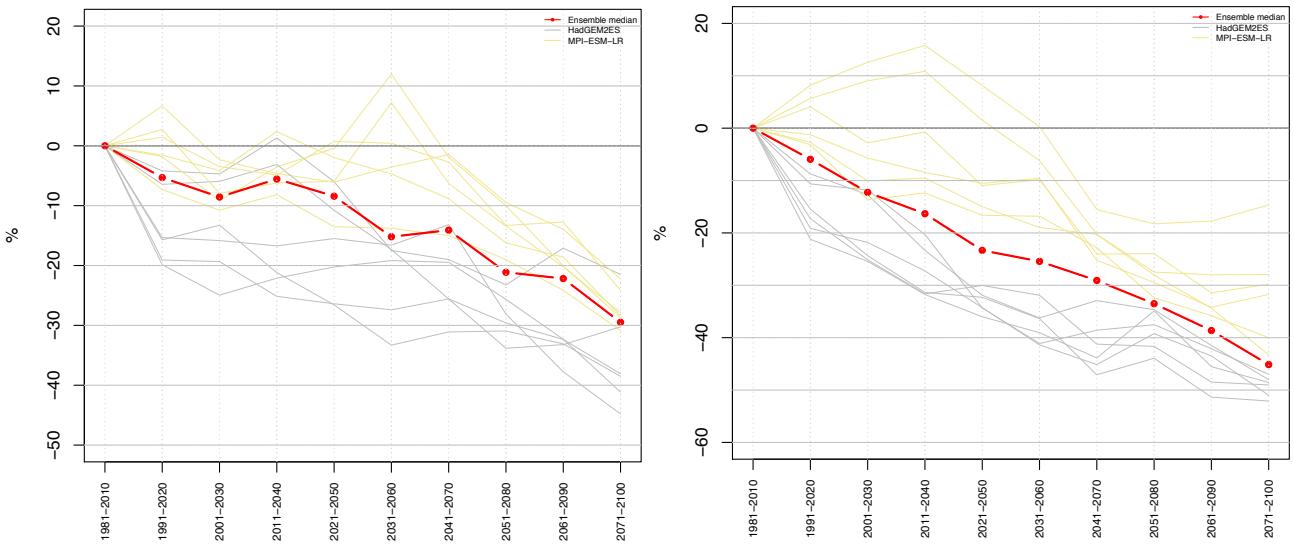

Fig. 37: Vatnsdalsá catchment (vhm45): Projected changes (in percent) in the magnitude of the 10-year flood relative to its 1981-2010 reference level (each ensemble member has its own reference 10-year flood). RCP4.5 emission scenario (left) and RCP8.5 emission scenario (right). Individual ensemble members (grey and yellow lines) and ensemble median (red line).

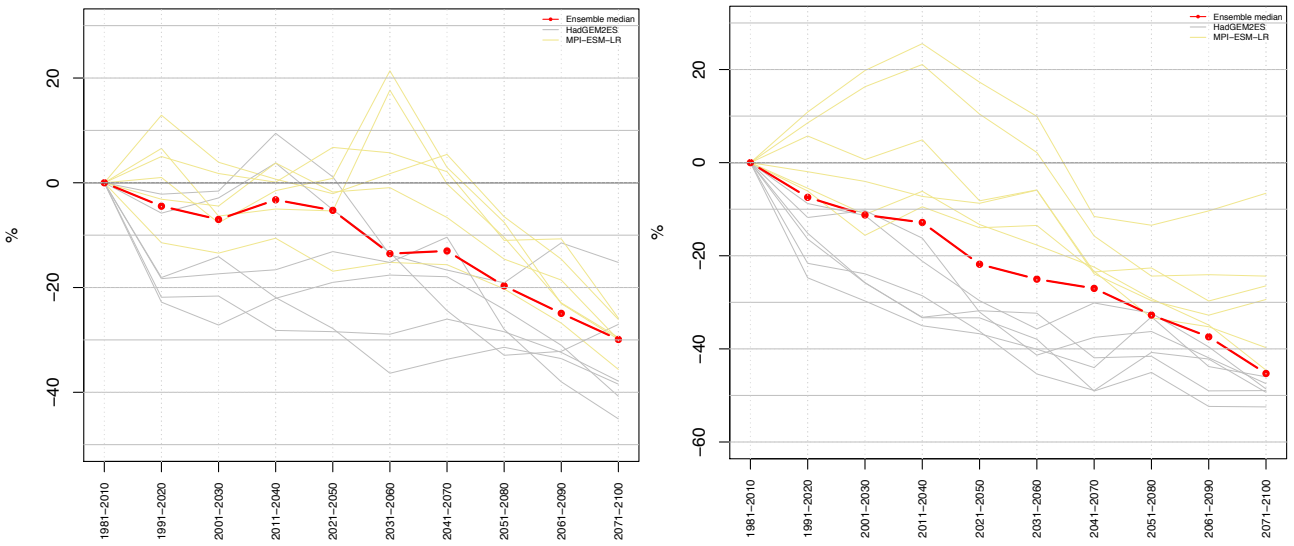

Fig. 38: Vatnsdalsá catchment (vhm45): Projected changes (in percent) in the magnitude of the 100-year flood relative to its 1981-2010 reference level (each ensemble member has its own reference 100-year flood). RCP4.5 emission scenario (left) and RCP8.5 emission scenario (right). Individual ensemble members (grey and yellow lines) and ensemble median (red line).

- **Selá catchment (vhm48)**

See Figs. 39 and 40.

- RCP4.5 emission scenario

Changes in the magnitude of T-year floods are projected to fluctuate in the future, with a trend toward a decrease for a majority of ensemble members and periods but a large ensemble spread is observed, making difficult to draw clear conclusions. The median change is always negative and varies approximately from -15% to -30% but the direction of change within the ensemble is not always consistent and no clear enough signal seems to emerge in the periods 2061-2090 and 2071-2100.

- RCP8.5 emission scenario

Similar results are observed under this emission scenario: changes in the magnitude of T-year floods are projected to fluctuate in the future, with a trend toward a decrease but a large spread is observed, making difficult to draw clear conclusions. The median change is always negative and varies approximately from -10% to -25%, but the direction of change within the ensemble is not always consistent and no clear enough signal seems to emerge in the periods 2041-2070 to 2051-2080.

- Discussion

Large uncertainties affect the temporal evolution of projected changes in the magnitude of T-year floods. A lack of consensus regarding the likely direction of change is sometimes observed in some periods in this catchment. Some of the uncertainty could originate from the large variability affecting the ensemble of T-year flood estimations in the reference period (1981-2010) (not shown). Following the projected warming, the flood regime of this catchment is projected to gradually become less influenced by spring snowmelt and more influenced by rainfall or a combination of rainfall and snowmelt in autumn/winter (cf. Figs. 33 and 34). The projected snowpack depletion caused by higher temperatures is expected to lead to a decrease in the magnitude of snowmelt-generated floods in spring, however an intensification of rainfall-generated floods in autumn/winter cannot be ruled out to explain some of the projected fluctuations. A more detailed seasonal analysis of the magnitude of floods would be required to help interpreting these results further.

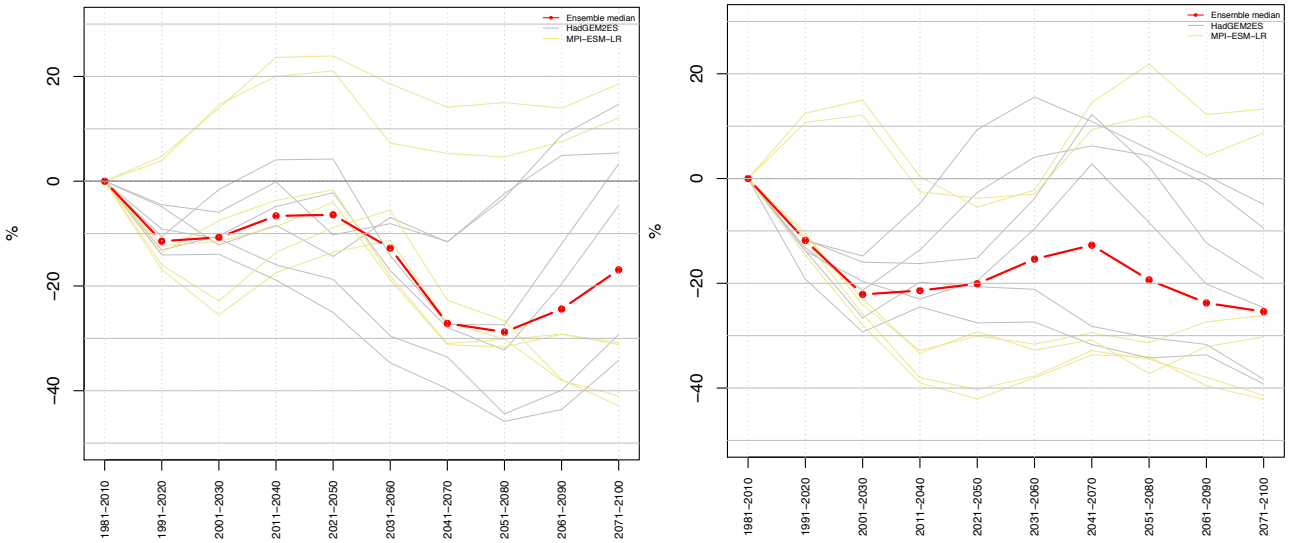

Fig. 39: Selá catchment (vhm48): Projected changes (in percent) in the magnitude of the 10-year flood relative to its 1981-2010 reference level (each ensemble member has its own reference 10-year flood). RCP4.5 emission scenario (left) and RCP8.5 emission scenario (right). Individual ensemble members (grey and yellow lines) and ensemble median (red line).

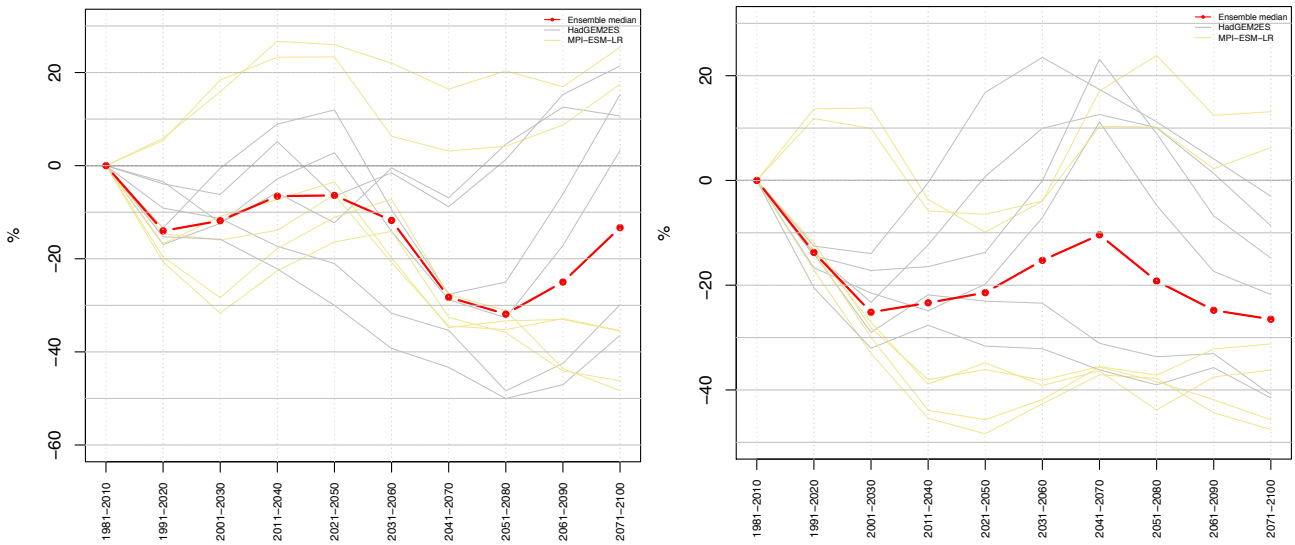

Fig. 40: Selá catchment (vhm48): Projected changes (in percent) in the magnitude of the 100-year flood relative to its 1981-2010 reference level (each ensemble member has its own reference 100-year flood). RCP4.5 emission scenario (left) and RCP8.5 emission scenario (right). Individual ensemble members (grey and yellow lines) and ensemble median (red line).

- **Geithellnaá catchment (vhm149)**

See Figs. 41 and 42.

- RCP4.5 emission scenario

Projected changes in the magnitude of T-year floods are uncertain but a trend toward an increase is emerging. The changes are not linear and oscillations are observed over the projection horizon. The median change varies in similar proportions for the two return periods. The largest median increase is projected in 2011-2040 (ca. 25%) and the lowest one in 2041-2070 (less than 5%). A few ensemble members project a decrease, especially in 2021-2050 and 2031-2060 but the median change is positive in all projection periods.

- RCP8.5 emission scenario

Projected changes in the magnitude of T-year floods are uncertain. The median change is always positive and varies in similar proportions for the two return periods. However, the direction of change within the ensemble is not consistent enough before 2041-2070 to draw clear conclusions during that period. A more consistent pattern of T-year flood increase is projected in the periods 2041-2070 to 2071-2100 with a median increase varying approximately between 10% and 15%.

- Discussion

Large uncertainties affect the temporal evolution of projected changes in the magnitude of T-year floods. A lack of consensus regarding the likely direction of change is sometimes observed in some periods. However, a trend toward an increase in the magnitude of T-year floods seems to emerge, possibly as the result of an intensification of autumn rainfall.

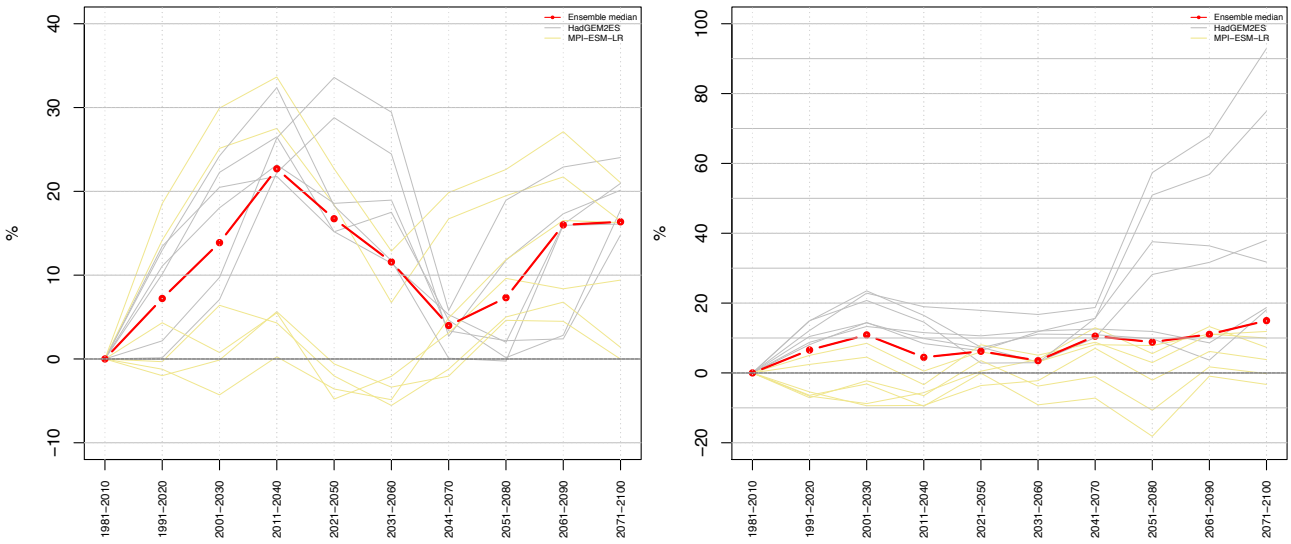

Fig. 41: Geithellnaá catchment (vhm149): Projected changes (in percent) in the magnitude of the 10-year flood relative to its 1981-2010 reference level (each ensemble member has its own reference 10-year flood). RCP4.5 emission scenario (left) and RCP8.5 emission scenario (right). Individual ensemble members (grey and yellow lines) and ensemble median (red line).

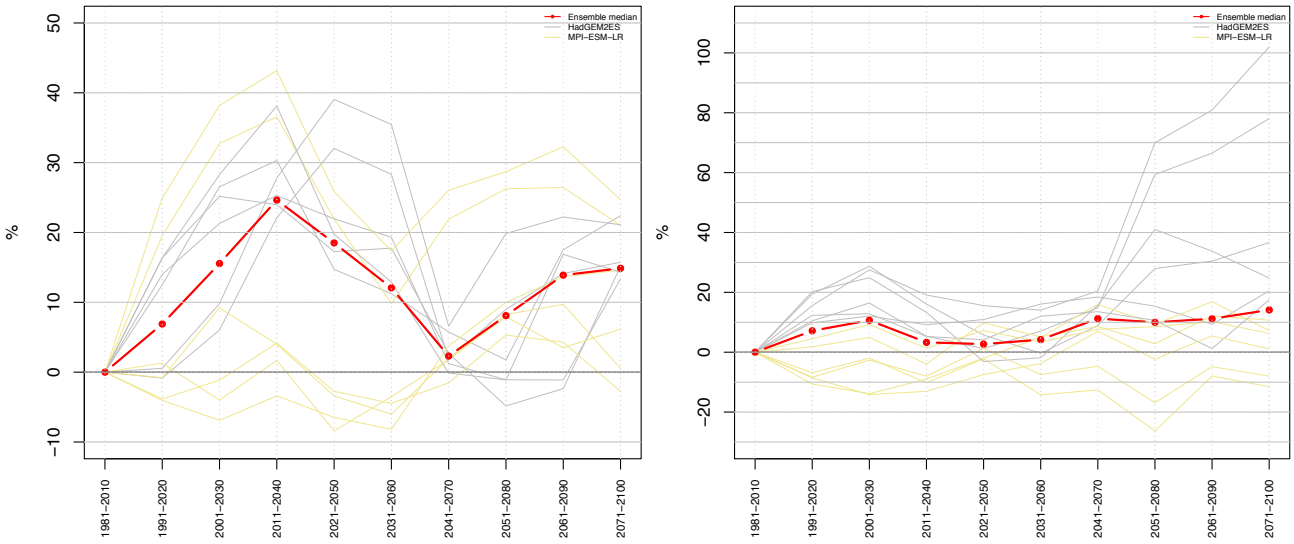

Fig. 42: Geithellnaá catchment (vhm149): Projected changes (in percent) in the magnitude of the 100-year flood relative to its 1981-2010 reference level (each ensemble member has its own reference 100-year flood). RCP4.5 emission scenario (left) and RCP8.5 emission scenario (right). Individual ensemble members (grey and yellow lines) and ensemble median (red line).

7-2-2 Changes in the return period of annual maximum floods

After having examined the projected changes in the magnitude of T-year floods throughout the 21st century for fixed T values, the flood magnitude (Q) is now fixed and the corresponding return period T(Q) estimated, considering moving 30-year periods, and compared to T(Q) in the reference period (1981-2010).

If the flood frequency distribution is projected to shift toward larger flood discharges in the future then the return period associated with a flood of magnitude Q should decrease:

$$Q(T)_{future} > Q(T)_{1981\text{-}2010}$$
$$T(Q)_{future} < T(Q)_{1981\text{-}2010}$$

If the flood frequency distribution is projected to shift toward lower flood discharges in the future then the return period associated with a flood of magnitude Q should increase:

$$Q(T)_{future} < Q(T)_{1981\text{-}2010}$$
$$T(Q)_{future} > T(Q)_{1981\text{-}2010}$$

The reference flood magnitude (Q) is taken as the magnitude of the 10-year flood in the reference period (1981-2010) (each ensemble member has its own reference 10-year flood). The temporal evolution of the T(Q) ensembles throughout the projection horizon is presented in Figs. 43 to 45. As expected, the results are found to mirror the projected evolution of 10-year floods analysed in Section 7-2-1 above.

- **Vatnsdalsá catchment (vhm45)**

See Fig. 43.

- RCP4.5 emission scenario

The return period associated with the reference flood is projected to strongly increase throughout the 21st century. This implies that the 10-year flood estimated in the reference period (1981-2010) is projected to be exceeded less than once every 10-years on average in the future. The ensemble spread is large and increases with the projection horizon, making the projected median return period increasingly uncertain. The projected return period is also subject to increasing uncertainty as T increases, especially when T > 50 or 100 years, because the estimation is often obtained by extrapolation of the Gumbel distribution beyond the range of simulated discharges. However, the direction of change is usually consistent for a large majority of members forming the ensemble, especially from 2041-2070 to 2071-2100 when all ensemble members project a return period increase.

- RCP8.5 emission scenario

Results are similar to those obtained under the RCP4.5 emission scenario but changes are more pronounced and even more consistent. In the periods 2031-2060 to 2071-2100, all ensemble members project an increase of the return period associated with the reference flood. This implies that the 10-year flood estimated in the reference period (1981-2010) is projected to be exceeded less than once every 10-years on average in the future.

- **Selá catchment (vhm48)**

See Fig. 44.

- RCP4.5 emission scenario

A majority (60% to 80%) of members projects an increase in the return period associated with the reference flood, over most of the projection horizon, but the uncertainty is very large. The median return period is systematically projected to increase, especially after 2031-2060. Theses results imply that the 10-year flood estimated in the reference period (1981-2010) is projected to be exceeded less than once every 10-years on average in the future.

- RCP8.5 emission scenario

Similar results are obtained under this emission scenario. A majority (50% to 90%) of members projects an increase in the return period associated with the reference flood, over most of the projection horizon, but the spread of the ensemble is large making the projected median return period very uncertain.

- **Geithellnaá catchment (vhm149)**

See Fig. 45.

- RCP4.5 emission scenario

A majority of members projects a decrease in the return period associated with the reference flood, over most of the projection horizon, especially from 2041-2070 to 2071-2100. The spread of the ensemble is large, especially from 2001-2030 to 2031-2060 making the median estimation very uncertain in these periods. Theses results imply that the 10-year flood estimated in the reference period (1981-2010) is projected to be exceeded more than once every 10-years on average in the future.

- RCP8.5 emission scenario

The spread of the return period ensemble is large. In particular, projections driven by the MPI-ESM-LR GCM are more scattered than those driven by HadGEM2ES GCM. The direction of change varies within the ensemble but a majority of members projects a decrease in the return period associated with the reference flood, especially from 2041-2070 to 2071-2100. These results imply that the 10-year flood estimated in the reference period (1981-2010) is projected to be exceeded more than once every 10-years on average in the future.

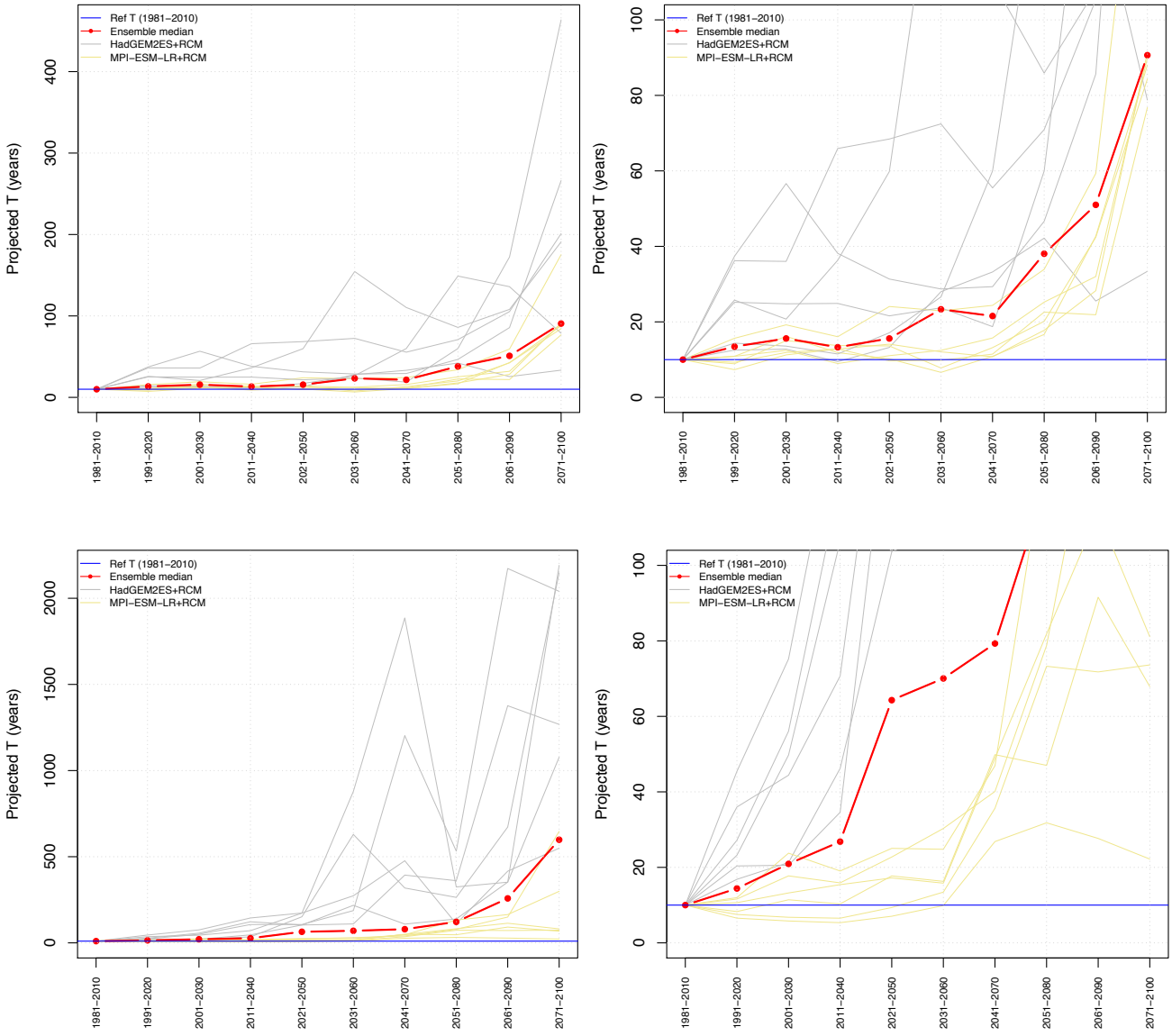

Fig. 43: Vatnsdalsá catchment (vhm45): Evolution of the projected return period T(Q) associated with a reference flood Q. The reference flood corresponds to the 10-year flood in the period 1981-2010. Top-panel: RCP4.5 emission scenario; bottom-panel: RCP8.5 emission scenario. Individual ensemble members (grey and yellow lines) and ensemble median (red line). Left-panel: full T range; right-panel: same as left panel but the range of projected Ts is limited to 100 years for better readability of the median.

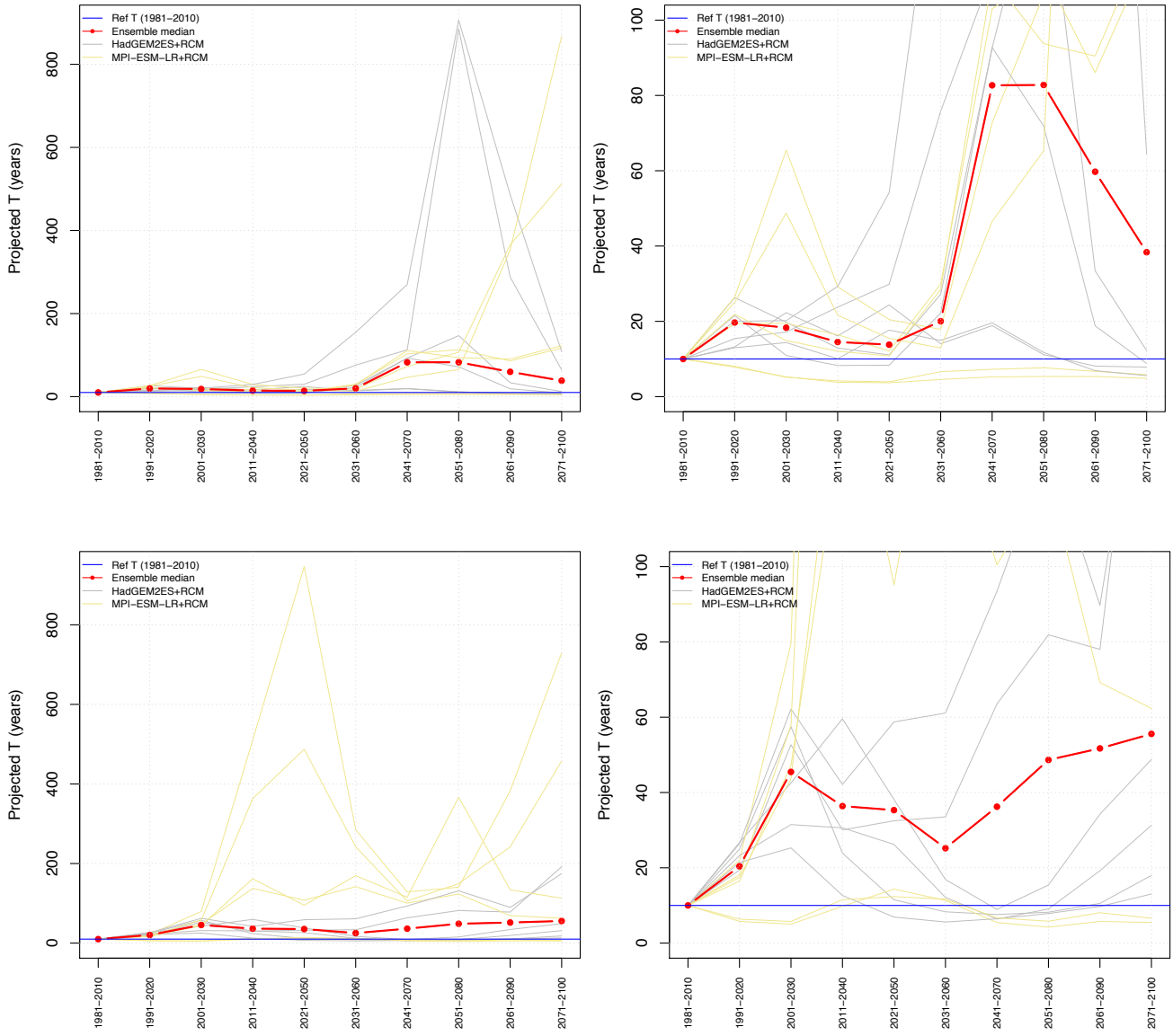

Fig. 44: Selá catchment (vhm48): Evolution of the projected return period T(Q) associated with a reference flood Q. The reference flood corresponds to the 10-year flood in the period 1981-2010. Top-panel: RCP4.5 emission scenario; bottom-panel: RCP8.5 emission scenario. Individual ensemble members (grey and yellow lines) and ensemble median (red line). Left-panel: full T range; right-panel: same as left panel but the range of projected Ts is limited to 100 years for better readability of the median.

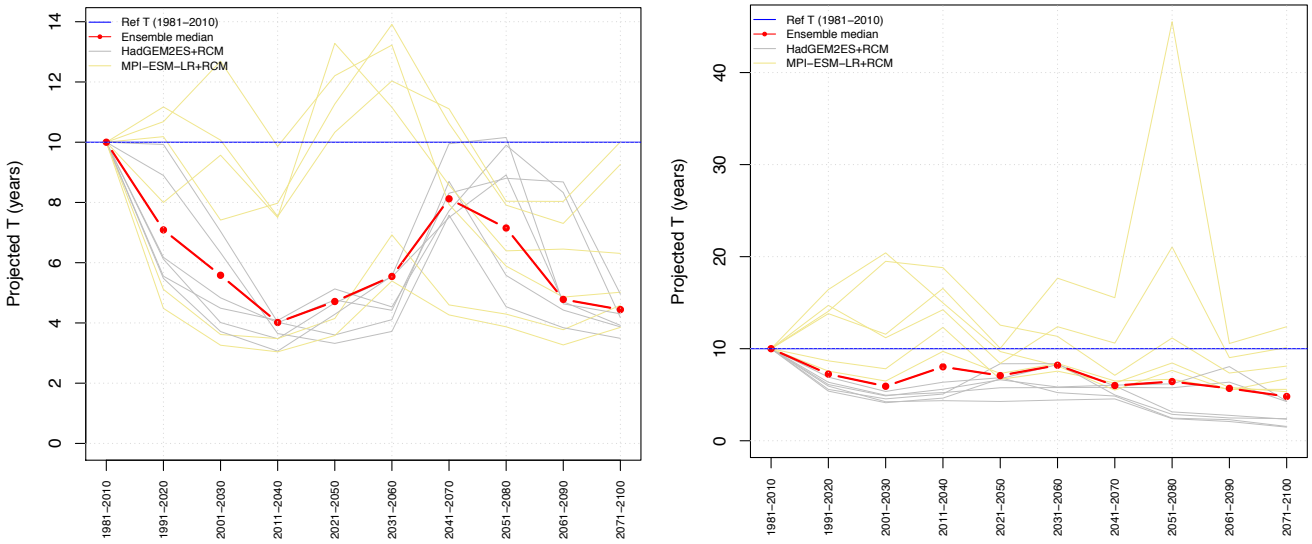

Fig. 45: Geithellnaá catchment (vhm149): Evolution of the projected return period T(Q) associated with a reference flood Q. The reference flood corresponds to the 10-year flood in the period 1981-2010. Left: RCP4.5 emission scenario; right: RCP8.5 emission scenario. Individual ensemble members (grey and yellow lines) and ensemble median (red line).

7-3 Summary

Climate change is projected to have an impact on the flood regimes of the studied catchments, especially those where snowmelt currently plays a central role in the generation of floods. In the Selá and Vatnsdalsá catchments, the strong influence of spring snowmelt will gradually decrease and the influence of rainfall and/or combined rainfall and snowmelt in autumn/winter increase, due to the projected increase in temperature. As a result, the magnitude of annual maximum floods will tend to decrease. The Geithellnaá catchment is projected to remain mainly governed by rainfall-generated annual maximum floods in autumn and their magnitude is expected to increase slightly, likely because of some rainfall intensification.

These results are consistent with findings from hydrological projections for Norway (Vormoor et al., 2015) and Sweden (Arheimer and Lindström, 2015) suggesting a decreasing influence of snowmelt and an increasing influence of rainfall in the generation of floods, due to increased temperature in the future.

Quantifying changes in the magnitude of T-year floods in the future remains a challenging task because the uncertainty associated with their estimation is very large, especially when there is a lack of consensus within the ensemble regarding the direction of change, so these results have to be interpreted with caution. The overall uncertainty is related to uncertainties affecting extreme discharge simulations and uncertainties related to the fitting of the Gumbel distribution with a limited data sample (30-year periods and twelve ensemble members only). The use of 30-year periods is the result of a compromise between having large enough samples to derive robust statistics while limiting the risk of non-stationarity within the periods. Uncertainties affecting extreme discharge simulations are related to uncertainties affecting the hydrological modelling, the climate projections and the local statistical downscaling.

Fixing the flood magnitude and estimating its future return period turned out to be a challenging task as well, especially when projected return periods were estimated by extrapolation of the fitted Gumbel distribution beyond the range of simulated streamflow values, so these results have to be interpreted with caution.

8 Conclusions

A rigorous methodology has been applied to investigate the impact of projected climate change on the hydrological characteristics of three catchments located in different regions in Iceland.

A significant warming is projected throughout the 21st century, more or less pronounced depending on the season and catchment location (0.3°C/decade under the RCP4.5 emission scenario and 0.47°C/decade under the RCP8.5 emission scenario, on average over all months and catchments). The temporal variability of precipitation projections is mainly characterised by decadal to multi-decadal oscillations. The nature of these oscillations often depends on the driving GCM and the different precipitation projections do not always vary in phase with each other, leading sometimes to large uncertainties in some periods and seasons. Significant mean precipitation changes (positive or negative) are sometimes projected in some seasons and periods, depending on the amplitude of these oscillations. Long-term tendencies sometimes dominate, such as a projected mean precipitation increase in summer in the Vatnsdalsá catchment under both emission scenarios, and in summer and autumn in the Selá catchment under the RCP8.5 emission scenario, leading then to an increase in mean annual precipitation.

The hydrological response of the catchments to projected climate change depends on their geographic location, current hydrological regime and physical characteristics. In the reference period (1981-2010), snow storage and melt strongly affect the streamflow seasonality pattern of all studied catchments, leading to a strong contrast between the low winter flows and the peak of discharge in spring/summer. The projected warming will gradually lead to shorter snow seasons, less snow storage and a shift earlier of the onset of the snowmelt season, leading to some snowmelt increase in winter and a strong snowmelt decrease in spring/summer, combined with an increase in the fraction of precipitation falling as rain in all seasons. Changes in the relative contributions of rainfall and snowmelt to streamflow will, in turn, lead to changes in the seasonality of streamflow, by attenuating the contrast between low winter flows and high spring/summer flows, as observed in the present climate.

Hydrological simulations project a gradual change as the projection horizon increases, toward a streamflow increase in autumn/winter in all studied catchments. Spring streamflow is mainly projected to decrease in the Vatnsdalsá and Selá catchments and first increase and later decrease in the Geithellnaá catchment. The peak of mean daily discharge caused by snowmelt in spring is projected to decrease and shift earlier in all studied catchments, and eventually vanish toward the end of the 21st century under the RCP8.5 emission scenario. Summer streamflow is projected to decrease in the Selá and Geithellnaá catchments but remain essentially unchanged in the Vatnsdalsá catchment. The changes are usually more pronounced and/or more rapid under the RCP8.5 emission scenario than under the RCP4.5 emission scenario because projected warming is stronger and will lead to larger changes in snow storage. Uncertainties related to the hydrological modelling contribute to the overall uncertainty of streamflow projections, but this aspect was not included in this study.

Climate change, is also projected to have an impact on the flood regimes of the studied catchments. The nature of this impact is linked to the flood-generating mechanisms that prevail in each catchment under the present climate. Assuming that each season is currently associated with a main flood-generating mechanism (rainfall in summer/autumn, snowmelt in spring, combined rainfall and snowmelt in winter), results of the hydrological projections suggest that:

- Considerable changes are expected to occur in the Vatnsdalsá and Selá catchments, where annual maximum floods are mostly generated by spring snowmelt under the present climate. Annual maximum floods will increasingly occur in winter in Vatnsdalsá and autumn/winter in Selá, instead of spring and their magnitude is expected to decrease. Toward the end of the 21st century, these events will no longer occur primarily in spring but will have a similar or even higher probability of occurring in winter in Vatnsdalsá and autumn/winter in Selá. These changes reflect the decreasing influence of spring snowmelt and the increasing influence of rainfall or the combination of rainfall and snowmelt in autumn/winter resulting from the projected warming and its impact on snow storage.
- The Geithellnaá catchment will remain under the main influence of rainfall-generated annual maximum floods in autumn and a slight magnitude increase in the future is possible, probably because of rainfall intensification.
- The nature of the flood risk is likely to change in the future in all three catchments.
- The implicit assumption of stationarity of the flood frequency distribution, used in design flood studies, will no longer be valid if the magnitude of T-year floods is likely to change over the next decades.
- The uncertainties associated with the estimation of T-year floods are large, especially for the Selá and Geithellnaá catchments, so these projections should be interpreted with caution.

In conclusion, if either one of the climate scenarios realises (RCP4.5 or RCP8.5), it is likely that it will have an impact on the hydrological characteristics of the studied catchments and, in turn, on water resources management and flood risk. As the nature of the hydrological response to projected climate change is specific to each catchment, other catchments should be investigated in order to obtain a more comprehensive overview across Iceland.

Acknowledgements

This project was funded by the Icelandic Road and Coastal Administration Research Fund (Rannsóknarsjóður Vegagerðarinnar).

The author acknowledges the World Climate Research Programme's Working Group on Regional Climate, and the Working Group on Coupled Modelling, former coordinating body of CORDEX and responsible panel for CMIP5. The author also thanks the climate modelling groups (listed in Table 2 of this report) for producing and making available their model output. The author also acknowledges the Earth System Grid Federation infrastructure an international effort led by the U.S. Department of Energy's Program for Climate Model Diagnosis and Intercomparison, the European Network for Earth System Modelling and other partners in the Global Organisation for Earth System Science Portals (GO-ESSP).

The author acknowledges Veðurstofa Íslands for providing the ICRA reanalysis weather data.

Discharge observations were obtained from Veðurstofa Íslands (IMO database, service no. 2019-11-01 / 01).

DEMs were created from DigitalGlobe, Inc., imagery and funded under National Science Foundation awards 1043681, 1559691, and 1542736.

The author acknowledges the Swedish Meteorological and Hydrological Institute for making HYPE freely available.

Data analysis was performed with the R software (R Core Team, 2016).

9 References

Aðalgeirsdóttir G., Magnússon E., Pálsson F., Thorsteinsson T., Belart J.M.C., Jóhannesson T., Hannesdóttir H., Sigurðsson O., Gunnarsson A., Einarsson B., Berthier E., Steffensen Schmidt L., Haraldsson H. H., and Björnsson H. (2020). Glacier Changes in Iceland From ~1890 to 2019. *Front. Earth Sci.* , 8, 1-15, doi: 10.3389/feart.2020.523646.

Arheimer B. and Lindström G. (2015). Climate impact on floods: changes in high flows in Sweden in the past and the future (1911–2100). *Hydrol. Earth Syst. Sci.*, 19, 771–784, 2015. doi: 10.5194/hess-19-771-2015.

Arnalds O. (2015). The Soils of Iceland. World Soils Book Series. Springer Netherlands.

Árnason K. and Matthíasson I. (2017). CORINE - landflokkun 2012. Landgerðabreytingar á Íslandi 2006-2012. Landmælingar Íslands.

Arnalds Ó. and Óskarsson H. (2009). Íslenskt jarðvegskort (Soil map of Iceland). Nátturufræðingurinn 78:107-121.

Björnsson H., Sigurðsson B. D., Davíðsdóttir B., Ólafsson J., Ástþórssson Ó. S., Ólafsdóttir S., Baldursson T., Jónsson T. (2018). Loftslagsbreytingar og áhrif þeirra á Íslandi – Skýrsla vísindanefndar um loftslagsbreytingar 2018. Veðurstofa Íslands.

Climate Change and Energy Systems. Impacts, risks and adaptation in the Nordic and Baltic countries. Th. Thorsteinsson and H. Björnsson Eds. TemaNord (2011):502, 226 pp.

Crochet P. (2007). A study of regional precipitation trends in Iceland using a high quality gauge network and ERA-40. *J. Climate,* 20(18), 4659-4677.

Crochet P. (2013). Sensitivity of Icelandic river basins to recent climate variations. *Jökull*, 63, 71-90.

Crochet P. (2020). Flood frequency analysis in a changing climate - Climate change impact on design flood (160p). Report prepared for Rannsóknarsjóður Vegagerðarinnar. https://www.vegagerdin.is/link_to_report

Dee D. P., Uppala S. M., Simmons A. J., Berrisford P., Poli P., Kobayashi S., Andrae U., Balmaseda M. A., Balsamo G., Bauer P., Bechtold P., Beljaars A. C. M., van de Berg L., Bidlot J., Bormann N., Delsol C., Dragani R., Fuentes M., Geer A. J., Haimberger L., Healy S. B., Hersbach H., Hólm E. V., Isaksen L., Kållberg P., Köhler M., Matricardi M., McNally A. P., Monge-Sanz B. M., Morcrette J.-J., Park B.-K., Peubey C., de Rosnay P., Tavolato C., Thépaut J.-N. and Vitart, F. (2011). The ERA-Interim reanalysis: configuration and performance of the data assimilation system, *Q.J.R. Meteorol. Soc.*, 137(656), 553–597, doi:10.1002/qj.828.

Delignette-Muller M.L. and Dutang C. (2015). "fitdistrplus: An R Package for Fitting Distributions." *Journal of Statistical Software*, **64**(4), 1–34.

de Niet J., Finger D.C., Bring A., Egilson D., Gustafson D. and Kalantari Z. (2020): Benefits of combining satellite-derived snow cover data and discharge data to calibrate a glaciated catchment in sub-arctic Iceland. *Water* 2020, *12*, 975; doi:10.3390/w12040975

Einarsson B. and Jónsson S. (2010). The effect of climate change on runoff from two watersheds in Iceland. VÍ-2010-016 report, 34 pp.

Giorgetta M.A., Jungclaus J., Reick C., Legutke S., Bader J., Böttinger M., Brovkin V., Crueger T., Esch M., Fieg K., Glushak K., Gayler V., Haak H., Hollweg H., Ilyina T., Kinne S., Kornblueh L., Matei D., Mauritsen T., Mikolajewicz U., Mueller W., Notz D., Pithan F., Raddatz T., Rast S., Redler R., Roeckner E., Schmid H., Schnur R., Segschneider J., Six K.D., Stockhause M., Timmreck C., Wegner J., Widmann H., Weiners K., Claussen M., Marotzke J. and Stevens B. (2013). Climate and carbon cycle changes from 1850 to 2100 in MPI-ESM simulations for the coupled model intercomparison project phase 5. *Journal of Advances in Modeling Earth Systems* 5:572–597. https://doi.org/10.1002/jame.20038.

Giorgi F., Jones C. and Asrar G. R. (2009). Addressing climate information needs at the regional level: the CORDEX framework, World Meteorological Organization (WMO) Bulletin, 58(3), 175-183.

Gosseling M. (2017). CORDEX climate trends for Iceland in the 21st century. VI-report 2017-009.

Gudmundsson L., Bremnes J. B., Haugen J. E. and Engen-Skaugen T. (2012). Technical Note: Downscaling RCM precipitation to the station scale using statistical transformations – a comparison of methods, *Hydrol. Earth Syst. Sci.*, 16, 3383–3390, https://doi.org/10.5194/hess-16-3383-2012.

Gudmundsson, L. (2016). qmap: Statistical transformations for post-processing climate model output. R package version 1.0-4.

Habets, F., Boé J., Déqué M., Ducharne, A., Gascoin S., Hachour A., Martin E., Pagé C., Sauquet E., Terray L., Thiéry D., Oudin L., Viennot P. (2013). Impact of climate change on the hydrogeology of two basins in northern France. *Climatic Change*, 121: 771-785. DOI 10.1007/s10584-013-0934-x

Hróðmarsson H.B. and Þórarinsdóttir T. (2018). Flóð íslanskra vatnsfalla, Flóðagreining rennslisraða. VÍ-2018-003 report, 144 pp.

Jacob D., Elizalde A., Haensler A., Hagemann S., Kumar P., Podzun R., Rechid D., Remedio A.R., Saeed F., Sieck K., Teichmann C. and Wilhelm C. (2012). Assessing the transferability of the regional climate model REMO to different coordinated regional climate downscaling experiment (CORDEX) regions. *Atmosphere* 3(1): 181-199. https://doi.org/10.3390/atmos3010181.

Jacob D., Petersen J., Eggert B., Alias A., Christensen O.B., Bouwer L.M., Braun A., Colette A., Déqué M., Georgievski G., Georgopoulou E., Gobiet A., Menut L., Nikulin G., Haensler A., Hempelmann N., Jones C., Keuler K., Kovats S., Kröner N., Kotlarski S., Kriegsmann A., Martin E., van Meijgaard E., Moseley C., Pfeifer S., Preuschmann S., Radermacher C., Radtke K., Rechid D., Rounsevell M., Samuelsson P., Somot S., Soussana J.-F., Teichmann C., Valentini R., Vautard R., Weber B. and Yiou P. (2014). EURO-CORDEX: new high-resolution climate change projections for European impact research. *Reg Environ Change* 14:563–578. https://doi.org/10.1007/s10113-013-0499-2.

Jones C. D., Hughes J. K., Bellouin N., Hardiman S. C., Jones G. S., Knight J., Liddicoat S., O'Connor F. M., Andres R. J., Bell C., Boo K.-O., Bozzo A., Butchart N., Cadule P., Corbin K. D., Doutriaux-Boucher M., Friedlingstein P., Gornall J., Gray L., Halloran P. R., Hurtt G., Ingram W. J., Lamarque J.-F., Law R. M., Meinshausen M., Osprey S., Palin E. J., Parsons Chini L., Raddatz T., Sanderson M. G., Sellar A. A., Schurer A., Valdes P., Wood N., Woodward S., Yoshioka M. and Zerroukat M. (2011). The HadGEM2-ES implementation of CMIP5 centennial simulations. *Geosci. Model Dev*., 4, 543-570. doi:10.5194/gmd-4-543-2011.

Jóhannesson T. and co-authors (2007). Effect of climate change on hydrology and hydro-resources in Iceland. OS-2007/011, 91 pp.

Kupiainen M., Samuelsson P., Jones C., Jansson C., Willén U., Hansson U., Ullerstig A., Wang S., and Döscher R. (2011). Rossby Centre regional atmospheric model, RCA4. Rossby Centre Newsletter.

Lindström G., Pers C., Rosberg J., Strömqvist J. and Arheimer B. (2010). Development and testing of the HYPE (Hydrological Predictions for the Environment) water quality model for different spatial scales. *Hydrology Research*, 41, 3-4, 295-319.

Marschollek S. (2017). Discharge Modelling of the Tungnaá River in Iceland using the HYPE Model. Faculty of Civil and Environmental Engineering School of Engineering and Natural Sciences University of Iceland, Reykjavik.

Meijgaard E. van, Van Ulft L.H., Lenderink G., de Roode S.R., Wipfler L., Boers R. and Timmermans R.M.A. (2012). Refinement and application of a regional atmospheric model for climate scenario calculations of Western Europe. Climate changes Spatial Planning publication: KvR 054/12, ISBN/EAN 978-90-8815-046-3, pp 44.

Nawri N., Pálmason B., Petersen G.N., Björnsson H. and Þorsteinsson S. (2017). The ICRA atmospheric reanalysis project for Iceland. VÍ Report, 2017-005, Veðurstofa Íslands.

Porter C., Morin P., Howat I., Noh M.-J., Bates B., Peterman K, Keesey S., Schlenk M., Gardiner J., Tomko K., Willis M., Kelleher C., Cloutier M., Husby E., Foga S., Nakamura H., Platson M., Wethington M. Jr., Williamson C., Bauer G., Enos J., Arnold G., Kramer W., Becker P., Doshi A., D'Souza C., Cummens P., Laurier F. and Bojesen M. (2018). "ArcticDEM", https://doi.org/10.7910/DVN/OHHUKH, Harvard Dataverse, V1, [Accessed Nov. 2019].

R Core Team (2016). R: A language and environment for statistical computing. R Foundation for Statistical Computing, Vienna, Austria. URL https://www.R-project.org/.

Rockel B., Will A. and Hense A. (2008). Special issue regional climate modelling with COSMO-CLM (CCLM). *Meteorol Z* 17:347–348. doi:10.1127/0941-2948/2008/0309.

Samuelsson P., Jones C., Willén U., Ullerstig A., Gollvik S., Hansson U., Jansson C., Kjellström E., Nikulin G. and Wyser K. (2011). The Rossby Centre Regional Climate Model RCA3: model description and performance. *Tellus* 63A. doi:10.1111/j.1600-0870.2010.00478.x.

Stephenson, A.G (2002). evd: Extreme Value Distributions. R News, 2(2):31-32, June 2002. URL: http://CRAN.R-project.org/doc/Rnews/.

Vormoor, K., Lawrence D., Heistermann M., and Bronstert, A. (2015). Climate change impacts on the seasonality and generation processes of floods – projections and uncertainties for catchments with mixed snowmelt/rainfall regimes. *Hydrol. Earth Syst. Sci.*, 19, 913-931, doi:10.5194/hess-19-913-2015.

Wilks, D.S. (1995). Statistical methods in the atmospheric sciences: an introduction. Academic Press. International geophysics series v. 59.

Appendix 1

CORDEX daily temperature evaluation series: Bias-correction skills

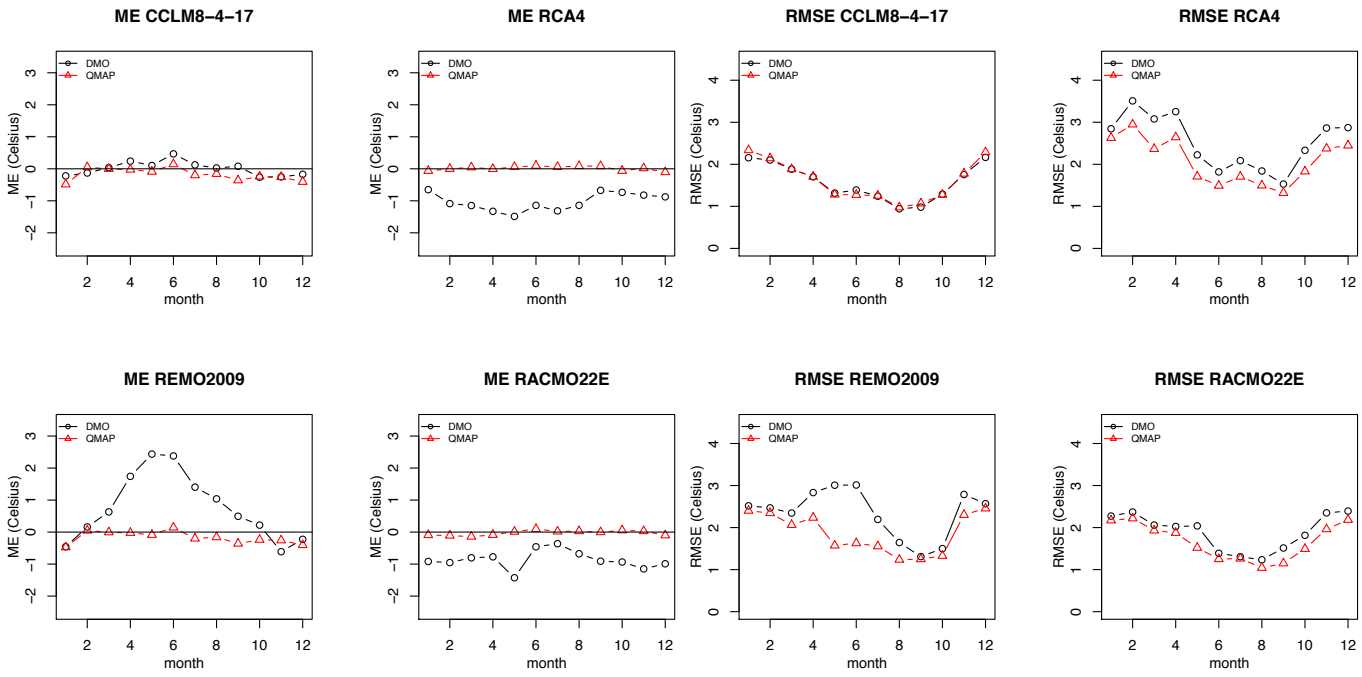

Fig. I-1: Catchment vhm45: Mean error (ME) and root-mean-square error (RMSE) between CORDEX temperature evaluation series and ICRA reference temperature. DMO=original CORDEX; QMAP=bias-corrected CORDEX. Period 1989-2008.

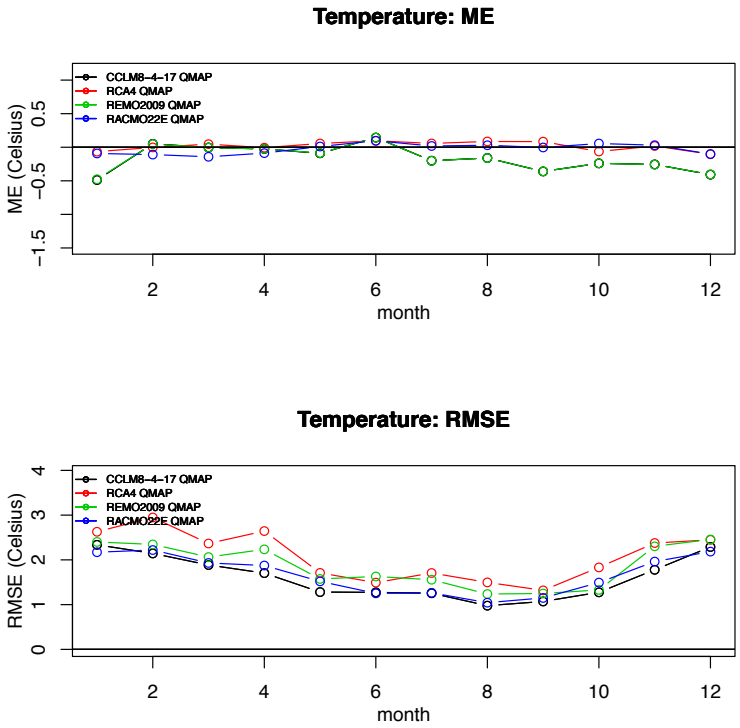

Fig. I-2: Catchment vhm45: Mean error (ME) and root-mean-square error (RMSE) between bias-corrected CORDEX temperature evaluation series and ICRA reference temperature. Each colour corresponds to a RCM (cf. Table 3).

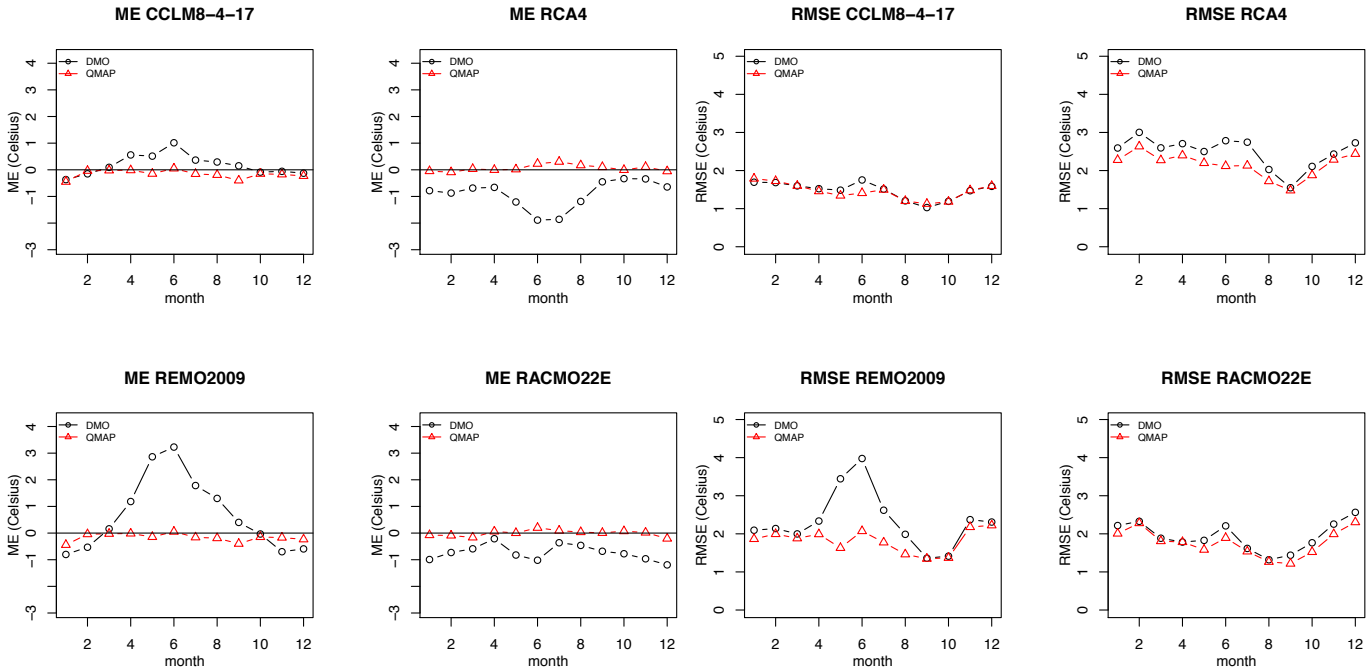

Fig. I-3: Catchment vhm48: Mean error (ME) and root-mean-square error (RMSE) between CORDEX temperature evaluation series and ICRA reference temperature. DMO=original CORDEX; QMAP=bias-corrected CORDEX. Period 1989-2008.

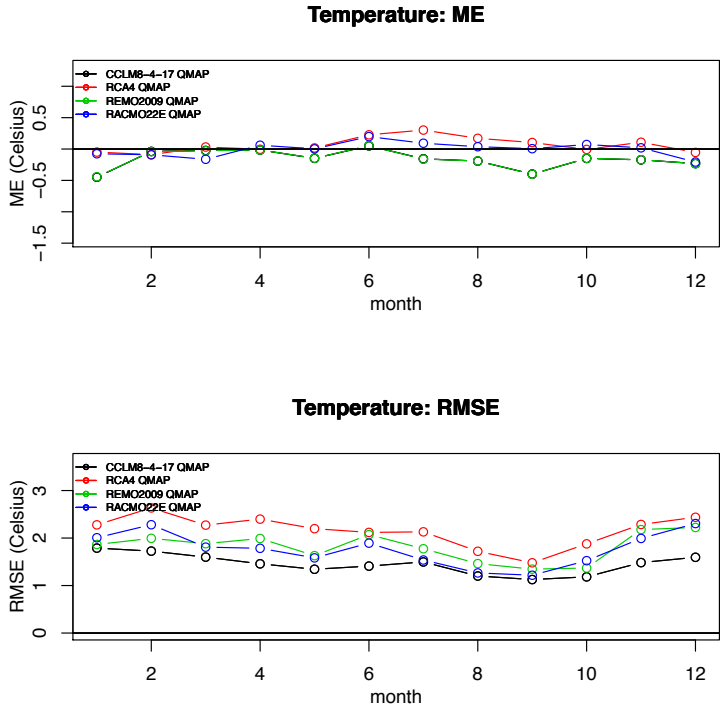

Fig. I-4: Catchment vhm48: Mean error (ME) and root-mean-square error (RMSE) between bias-corrected CORDEX temperature evaluation series and ICRA reference temperature. Each colour corresponds to a RCM (cf. Table 3).

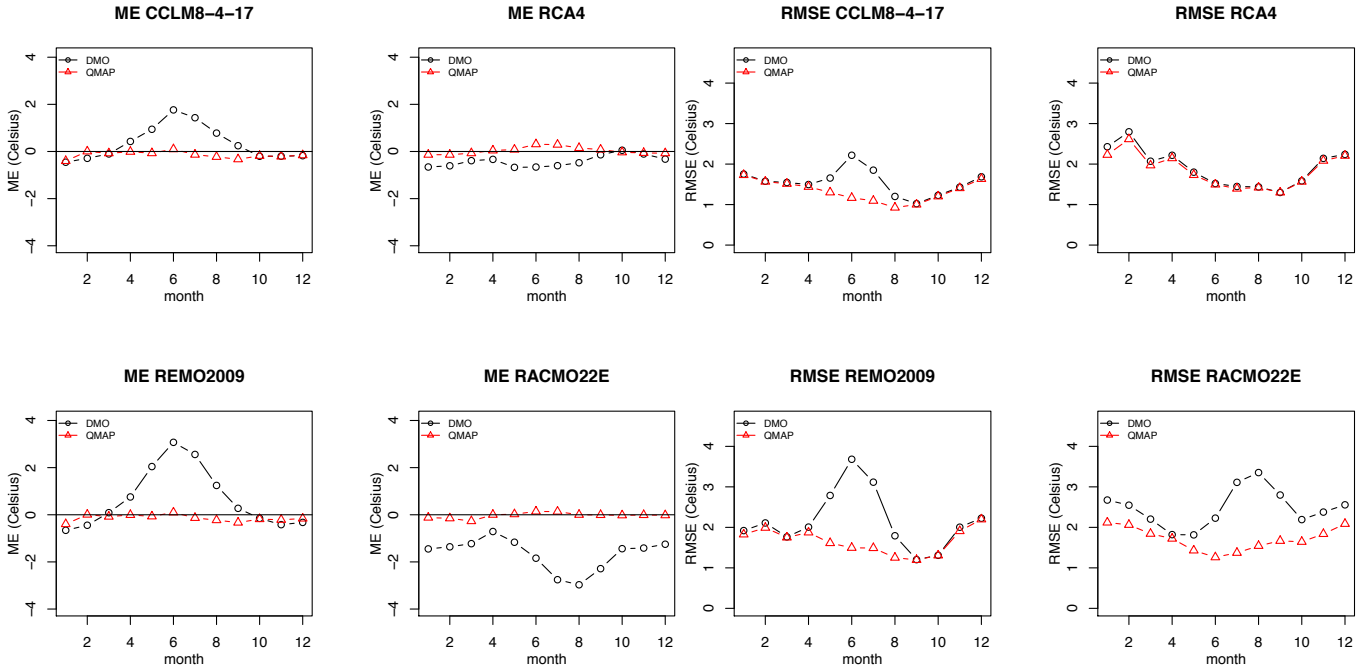

Fig. I-5: Catchment vhm149: Mean error (ME) and root-mean-square error (RMSE) between CORDEX temperature evaluation series and ICRA reference temperature. DMO=original CORDEX; QMAP=bias-corrected CORDEX. Period 1989-2008.

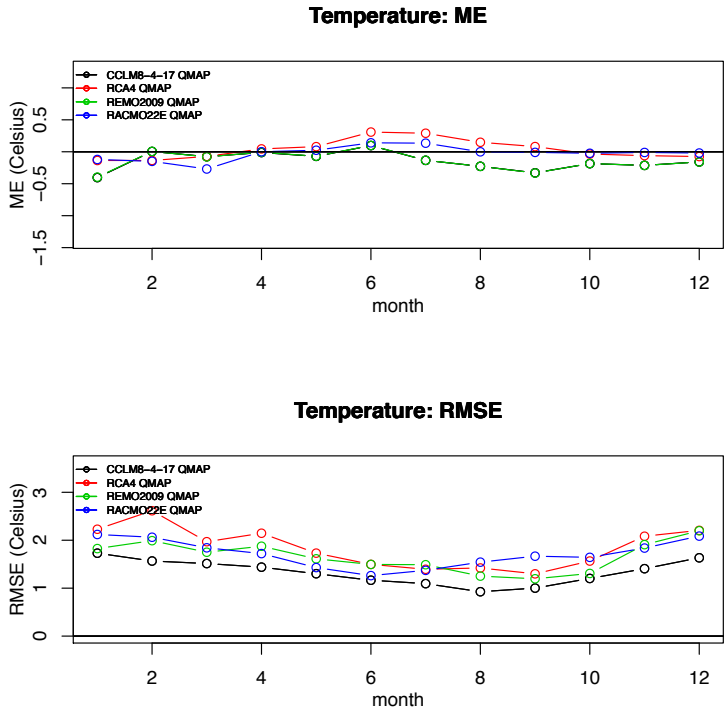

Fig. I-6: Catchment vhm149: Mean error (ME) and root-mean-square error (RMSE) between bias-corrected CORDEX temperature evaluation series and ICRA reference temperature. Each colour corresponds to a RCM (cf. Table 3).

Appendix 2

CORDEX daily precipitation evaluation series: Bias-correction skills

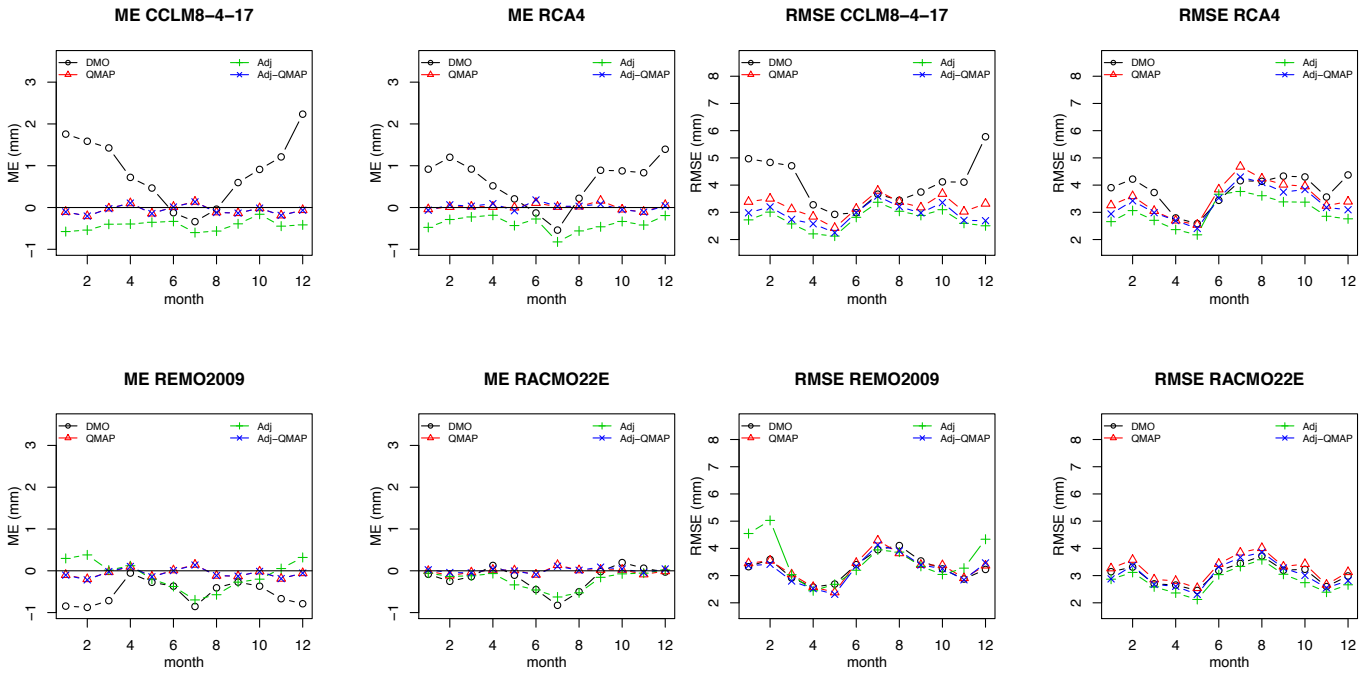

Fig. II-1: Catchment vhm45: Mean error (ME) and root-mean-square error (RMSE) between CORDEX daily precipitation evaluation series and ICRA reference precipitation (mm/d). DMO=original CORDEX (black); QMAP=direct quantile mapping (red); Adj=analog-based correction (green); Adj-QMAP= analog-based correction + quantile mapping (blue). Period 1989-2008.

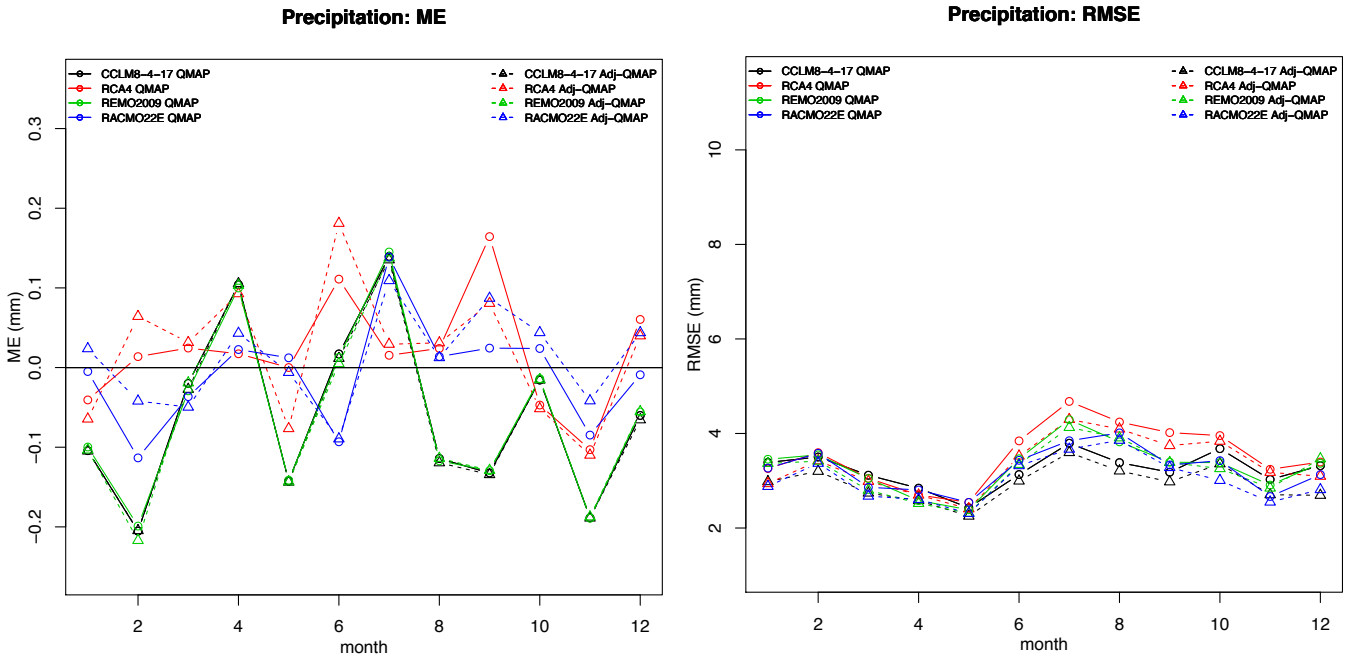

Fig. II-2: Catchment vhm45: Mean error (ME) and root-mean-square error (RMSE) between bias-corrected CORDEX daily precipitation evaluation series and ICRA reference precipitation (mm/d). QMAP=direct quantile mapping (solid lines); Adj-QMAP=analog-based correction + quantile mapping (dashed lines). Each colour corresponds to a RCM (cf. Table 3).

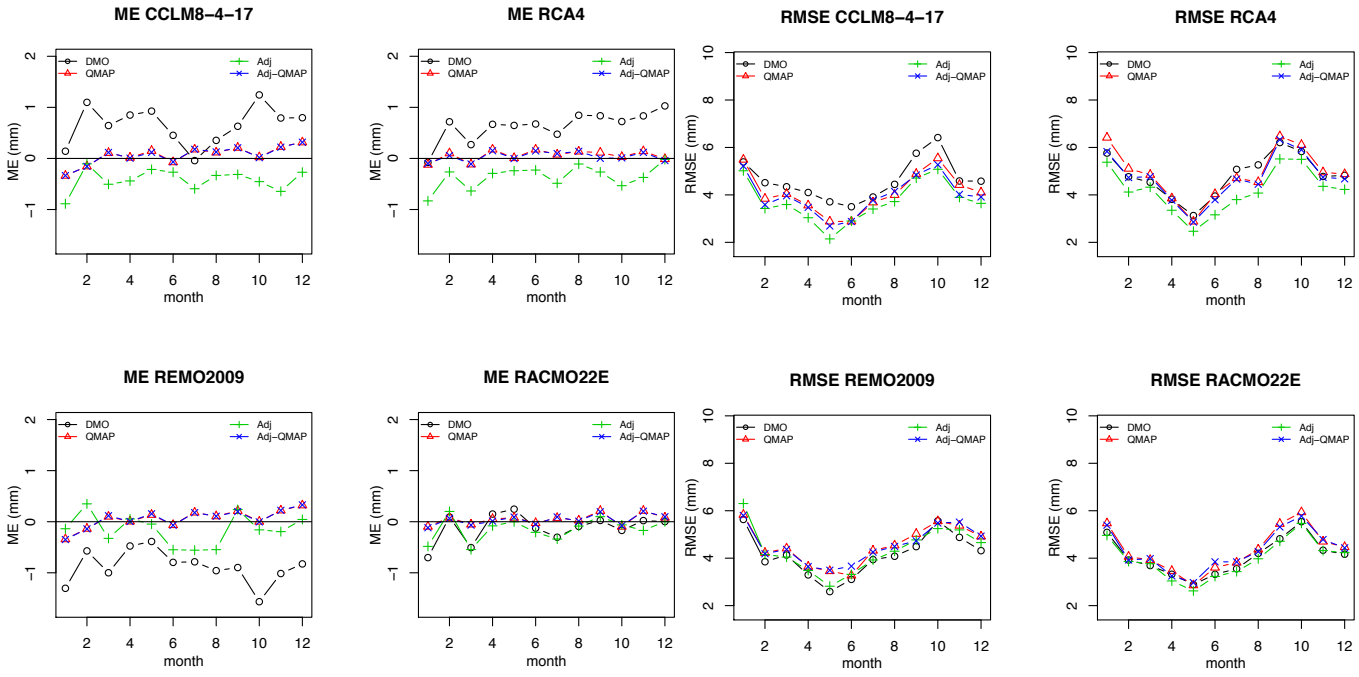

Fig. II-3: Catchment vhm48: Mean error (ME) and root-mean-square error (RMSE) between CORDEX daily precipitation evaluation series and ICRA reference precipitation (mm/d). DMO=original CORDEX (black); QMAP=direct quantile mapping (red); Adj=analog-based correction (green); Adj-QMAP= analog-based correction + quantile mapping (blue). Period 1989-2008.

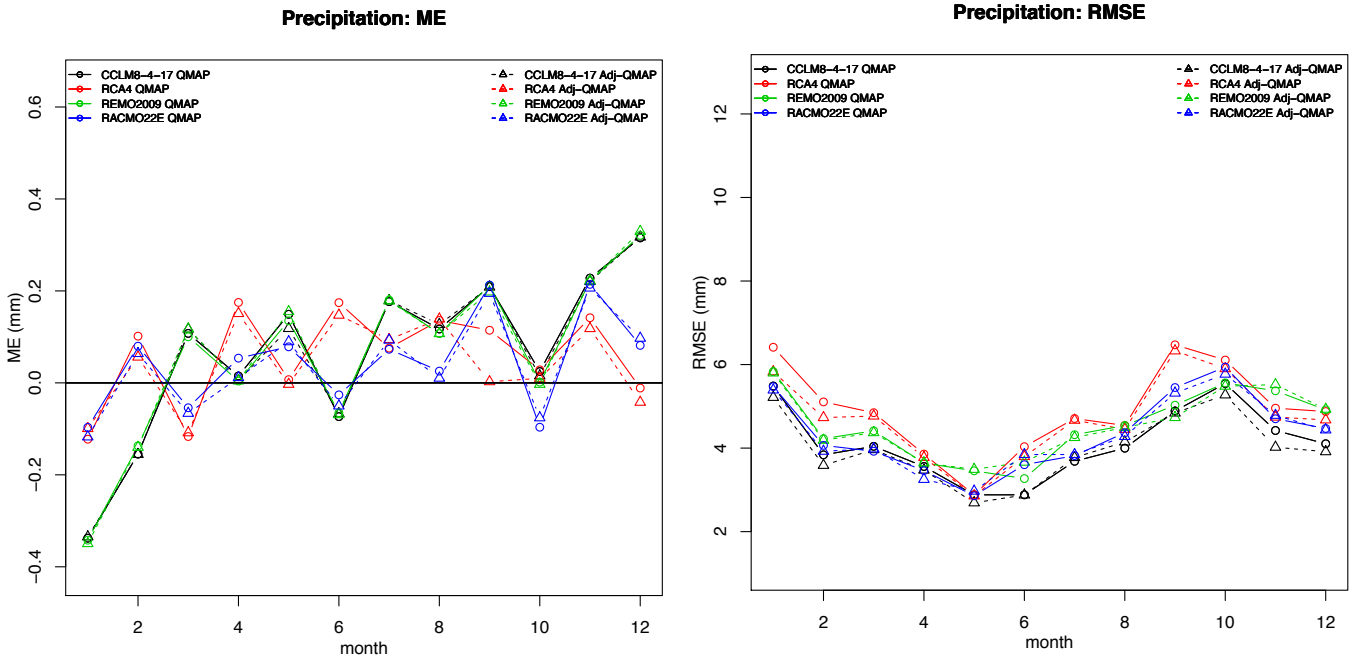

Fig. II-4: Catchment vhm48: Mean error (ME) and root-mean-square error (RMSE) between bias-corrected CORDEX daily precipitation evaluation series and ICRA reference precipitation (mm/d). QMAP=direct quantile mapping (solid lines); Adj-QMAP=analog-based correction + quantile mapping (dashed lines). Each colour corresponds to a RCM (cf. Table 3).

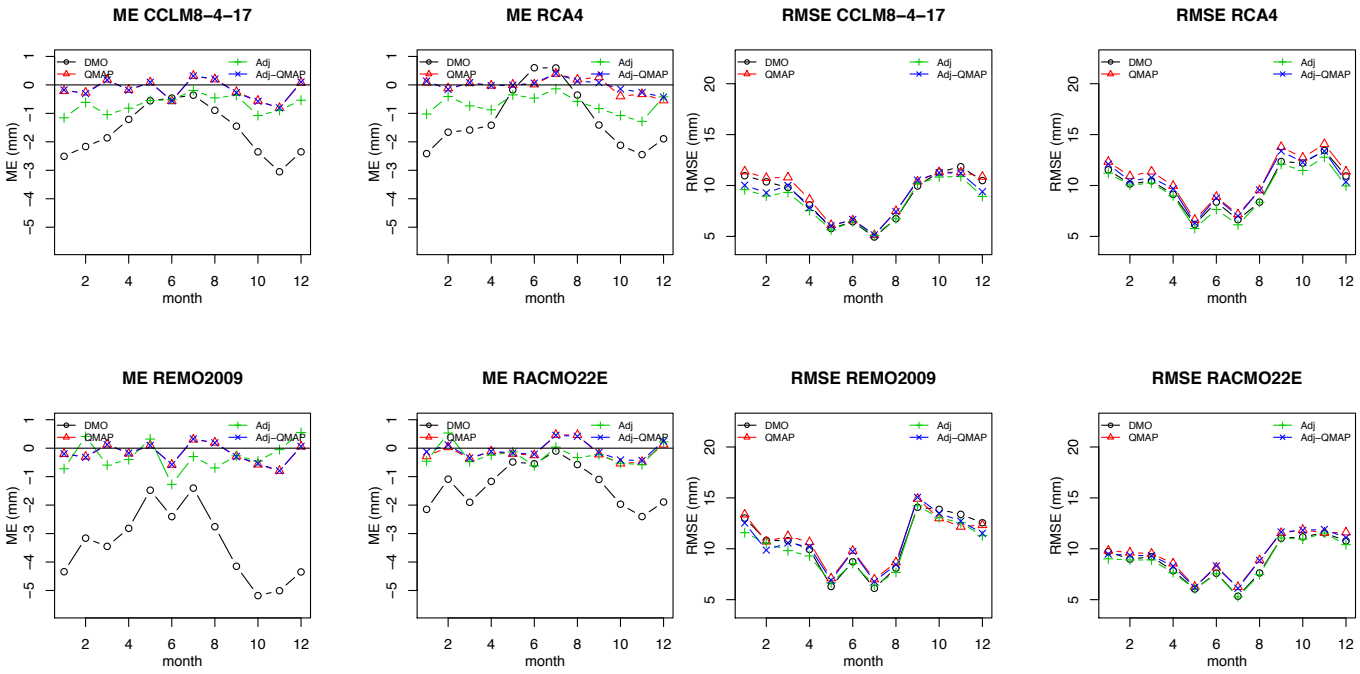

Fig. II-5: Catchment vhm149: Mean error (ME) and root-mean-square error (RMSE) between CORDEX daily precipitation evaluation series and ICRA reference precipitation (mm/d). DMO=original CORDEX (black); QMAP=direct quantile mapping (red); Adj=analog-based correction (green); Adj-QMAP= analog-based correction + quantile mapping (blue). Period 1989-2008.

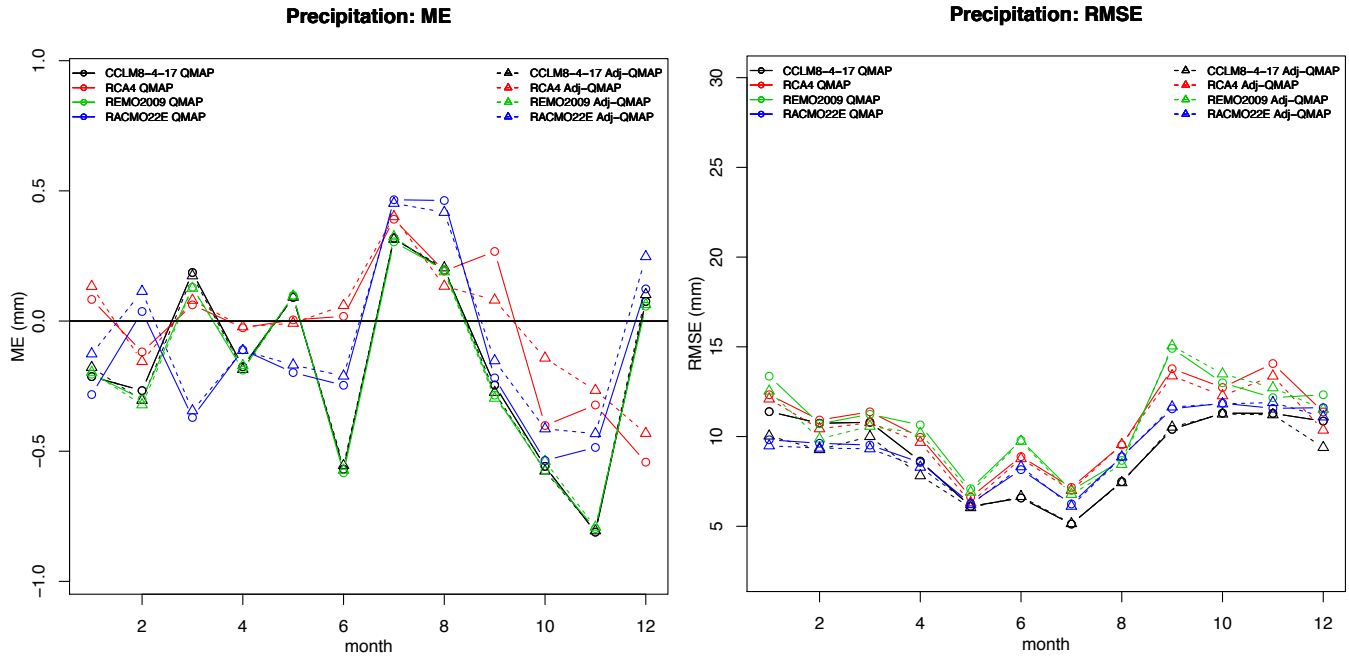

Fig. II-6: Catchment vhm149: Mean error (ME) and root-mean-square error (RMSE) between bias-corrected CORDEX daily precipitation evaluation series and ICRA reference precipitation (mm/d). QMAP=direct quantile mapping (solid lines); Adj-QMAP=analog-based correction + quantile mapping (dashed lines). Each colour corresponds to a RCM (cf. Table 3).

Appendix 3

Mean monthly temperature in the reference period (1981-2010)

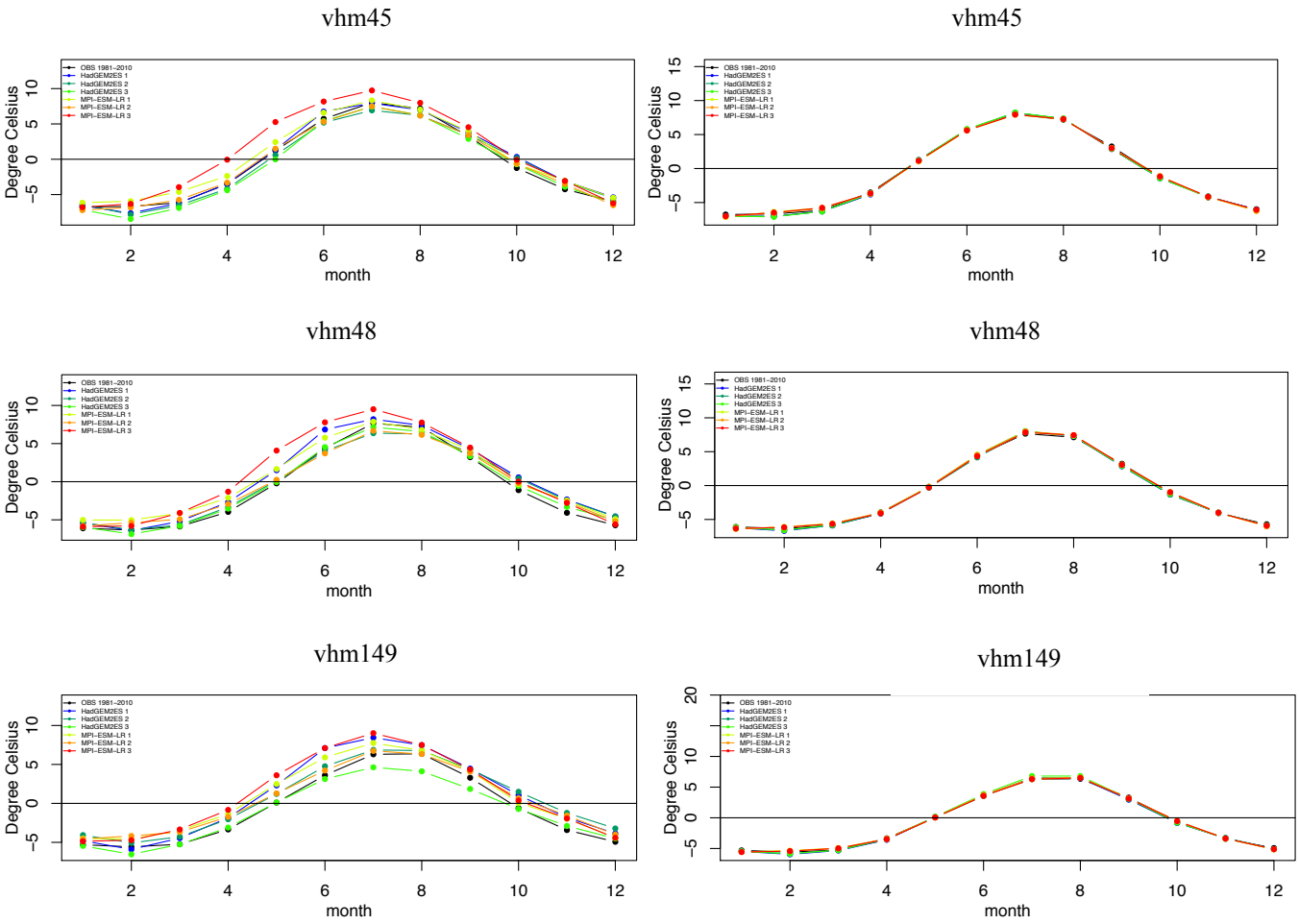

Fig. III-1: Mean monthly CORDEX temperature in the reference period (1981-2010). Left-panel: CORDEX original; Right-panel: after bias-correction by quantile mapping. Each colour corresponds to a GCM-RCM combination (cf. Table 3). ICRA-reference (black line). Top-panel: catchment vhm45; middle-panel: catchment vhm48; bottom-panel: catchment vhm149.

Appendix 4

Mean monthly precipitation in the reference period (1981-2010)

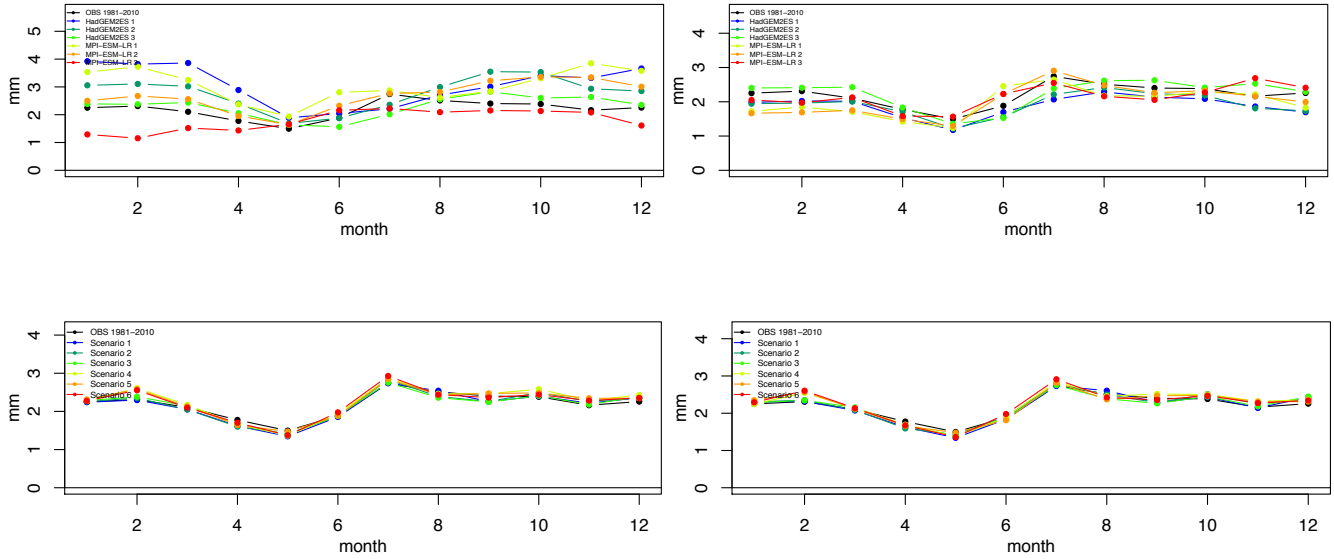

Fig. IV-1: Catchment vhm45: Mean monthly CORDEX precipitation (mm/d) in the reference period (1981-2010). Top-left: CORDEX original; Bottom-left: bias-corrected with direct quantile mapping; Top-right: analog-based correction; Bottom-right: analog-based correction + quantile mapping. Each colour corresponds to a GCM-RCM combination (cf. Table 3). ICRA-reference (black line).

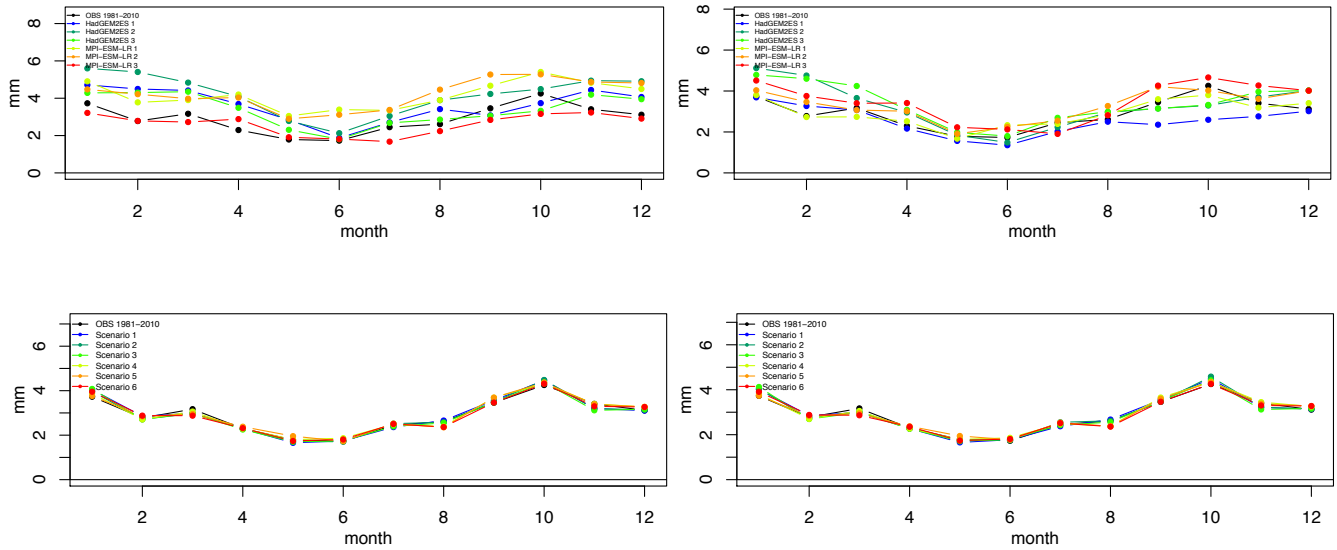

Fig. IV-2: As Fig. IV-1 but for catchment vhm48.

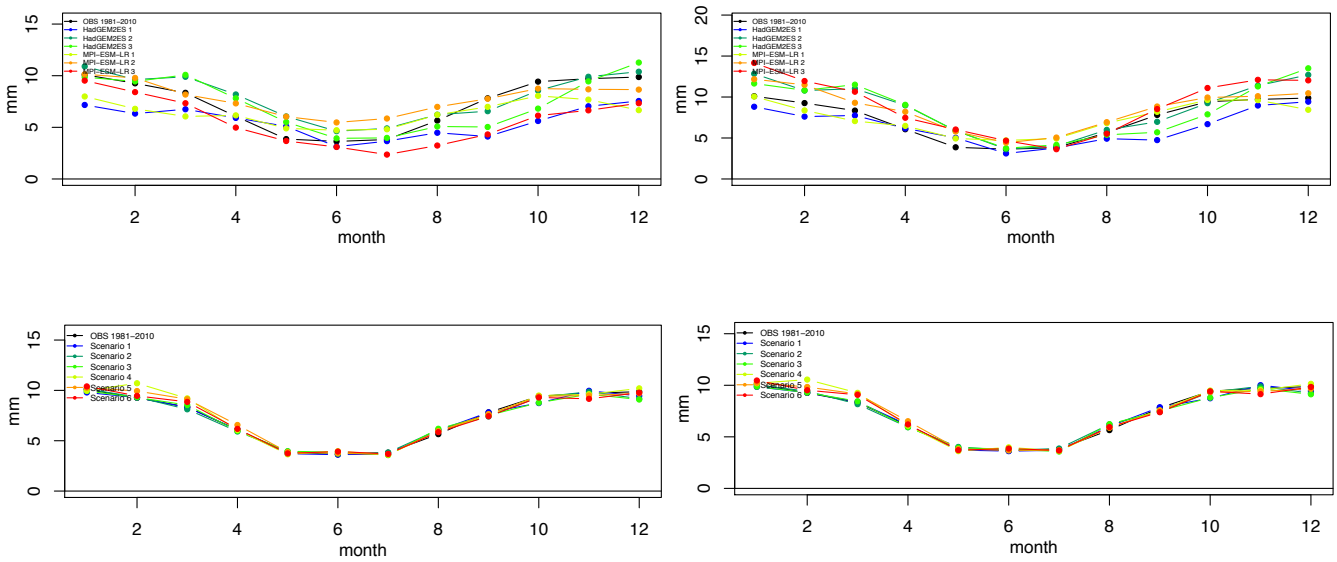

Fig. IV-3: As Fig. IV-1 but for catchment vhm149.

Appendix 5

Projected bias-corrected 30-year mean monthly temperature

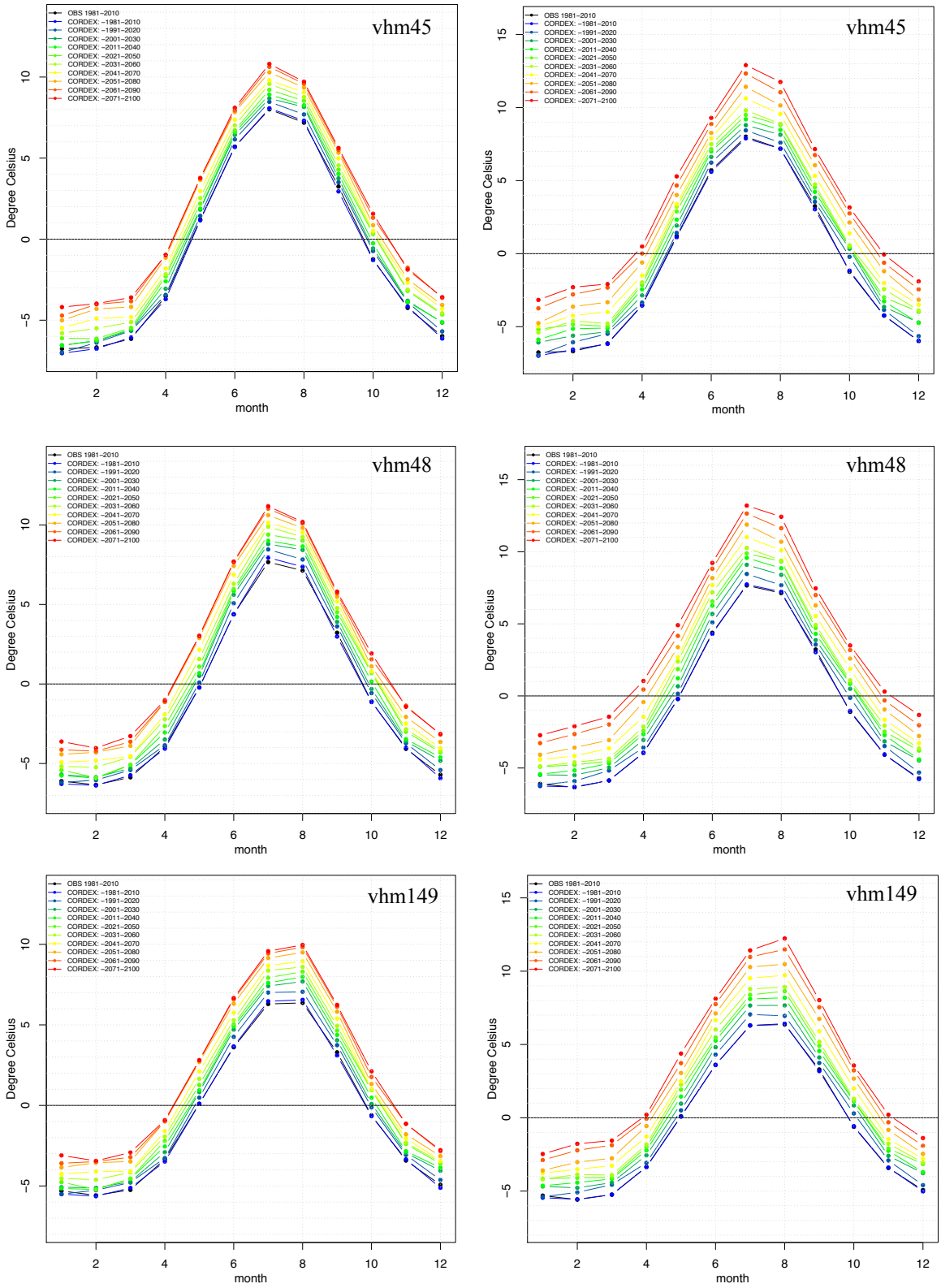

Fig. V-1: Ensemble median of projected 30-year mean monthly CORDEX temperature under the RCP4.5 emission scenario (left panel) and RCP8.5 emission scenario (right panel). Catchments vhm45 (top panel), vhm48 (middle panel), vhm149 (bottom panel). ICRA-reference (1981-2010) (black line). Each colour corresponds to a 30-year period: from dark blue (1981-2010) to red (2071-2100).

Appendix 6

Projected bias-corrected monthly precipitation under the RCP4.5 emission scenario

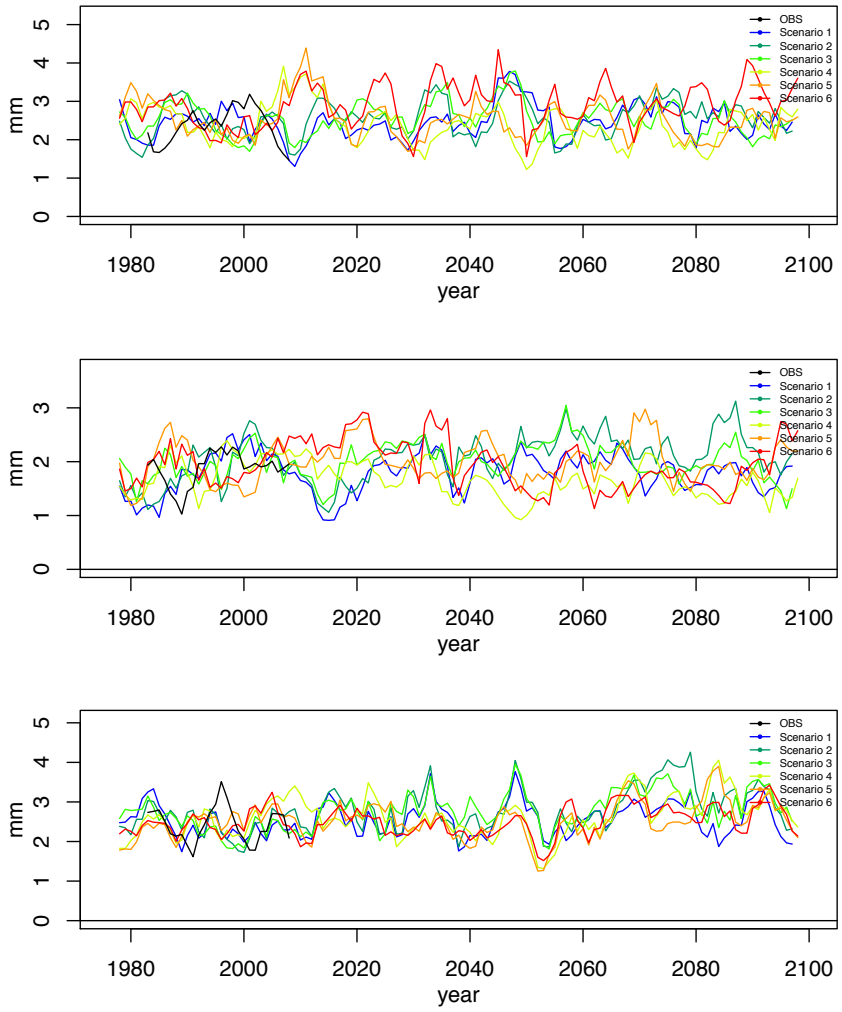

Fig. VI-1: Catchment vhm45: Projected CORDEX monthly precipitation (mm/d) under the RCP4.5 emission scenario. Top (February); Middle (June); Bottom (October). A 5-year running mean was applied. Each colour corresponds to a GCM-RCM combination (cf. Table 3). ICRA-reference (black line).

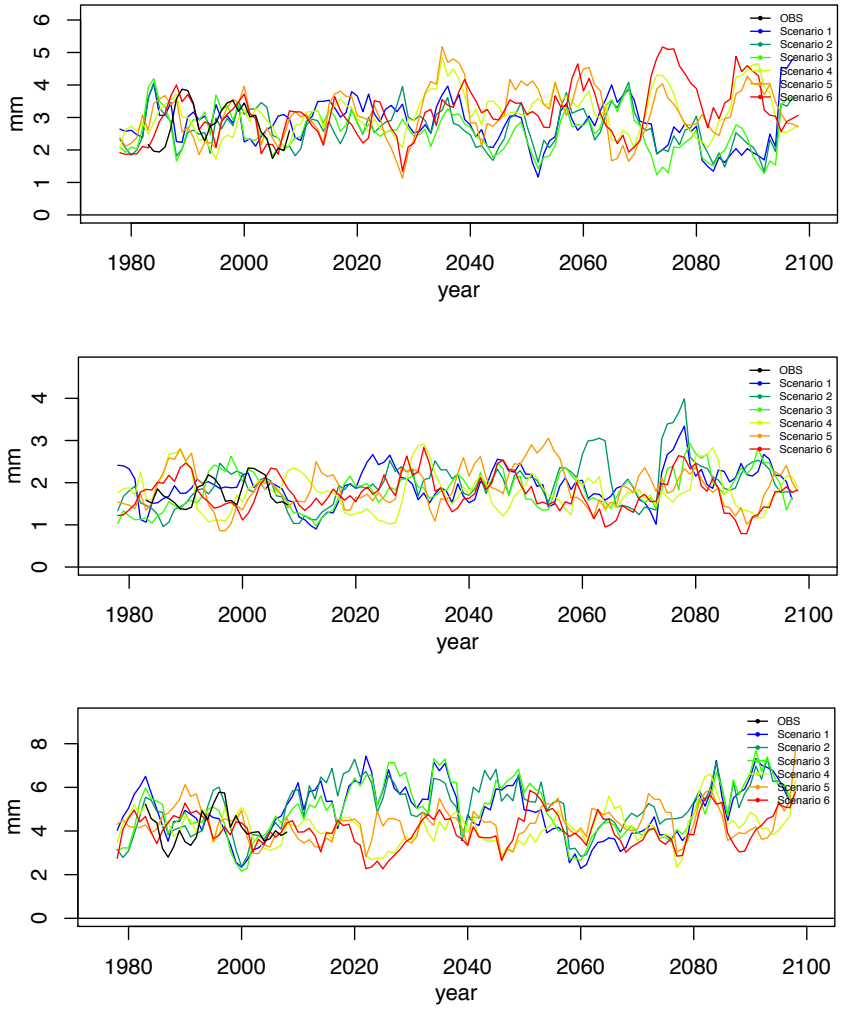

Fig. VI-2: Catchment vhm48: Projected CORDEX monthly precipitation (mm/d) under the RCP4.5 emission scenario. Top (February); Middle (June); Bottom (October). A 5-year running mean was applied. Each colour corresponds to a GCM-RCM combination (cf. Table 3). ICRA-reference (black line).

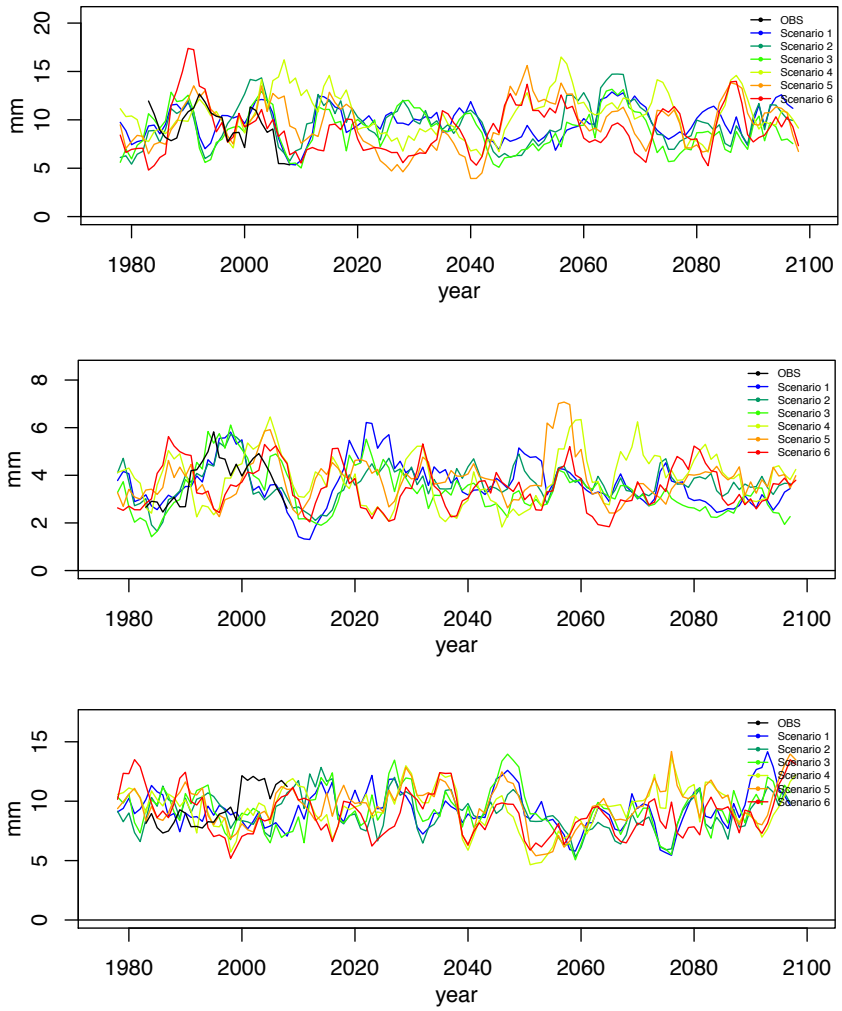

Fig. VI-3: Catchment vhm149: Projected CORDEX monthly precipitation (mm/d) under the RCP4.5 emission scenario. Top (February); Middle (June); Bottom (October). A 5-year running mean was applied. Each colour corresponds to a GCM-RCM combination (cf. Table 3). ICRA-reference (black line).

Appendix 7

Projected mean daily temperature, precipitation, snow accumulation and discharge in 2041-2070

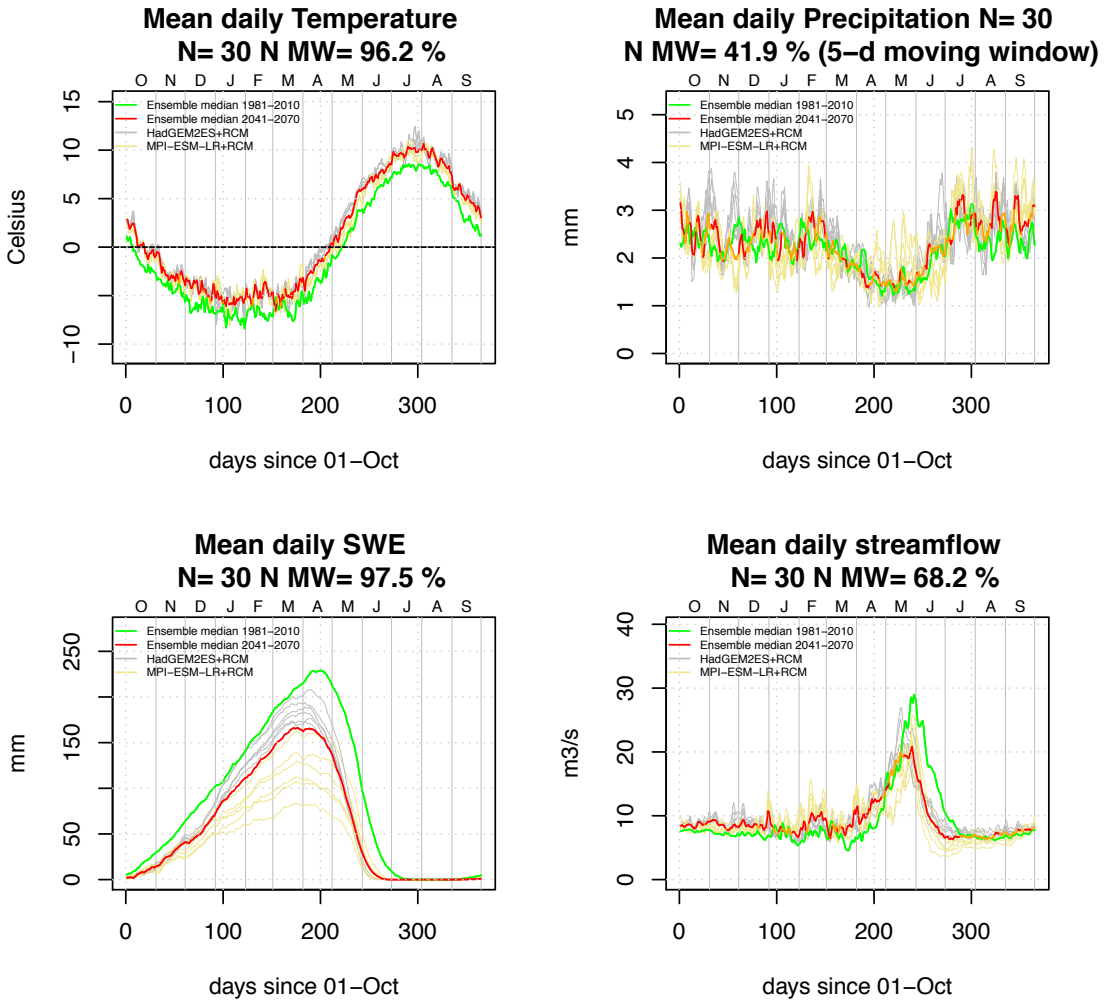

Fig. VII-1: Catchment vhm45: Projected mean daily temperature (top-left), precipitation (top-right), snow accumulation (bottom-left) and discharge (bottom-right) in the period 2041-2070 under the RCP4.5 emission scenario. Individual ensemble members are coloured in grey and yellow. The ensemble median is coloured in red for days when the Mann-Whitney test detected a significant shift in the ensemble of mean daily values relative to the ensemble in the reference period (1981-2010) and orange otherwise. The ensemble median in the reference period (1981-2010) is shown in green. N = Number of years in the projection period. N MW = Percentage of days in the water year when a significant shift was detected by the Mann-Whitney test.

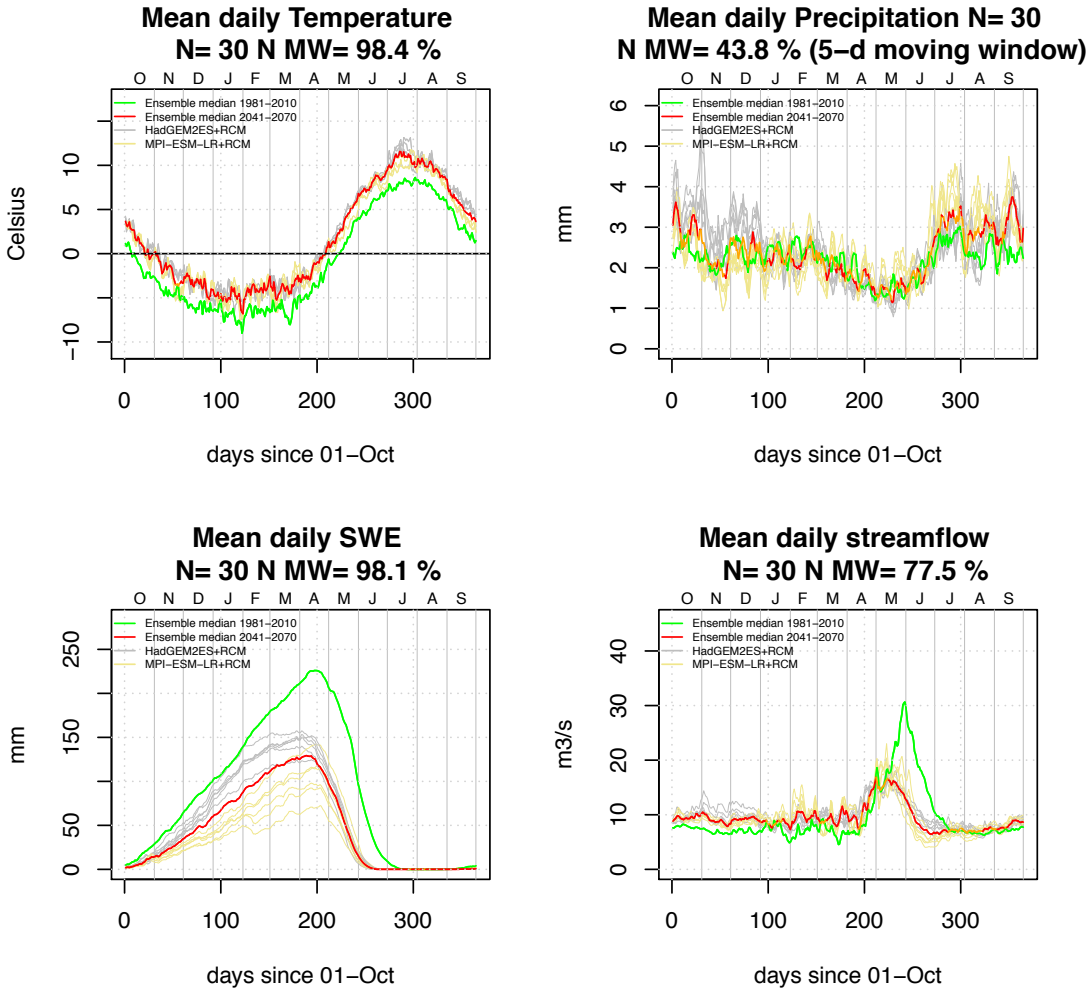

Fig. VII-2: Catchment vhm45: As Fig. VII-1 but under the RCP8.5 emission scenario.

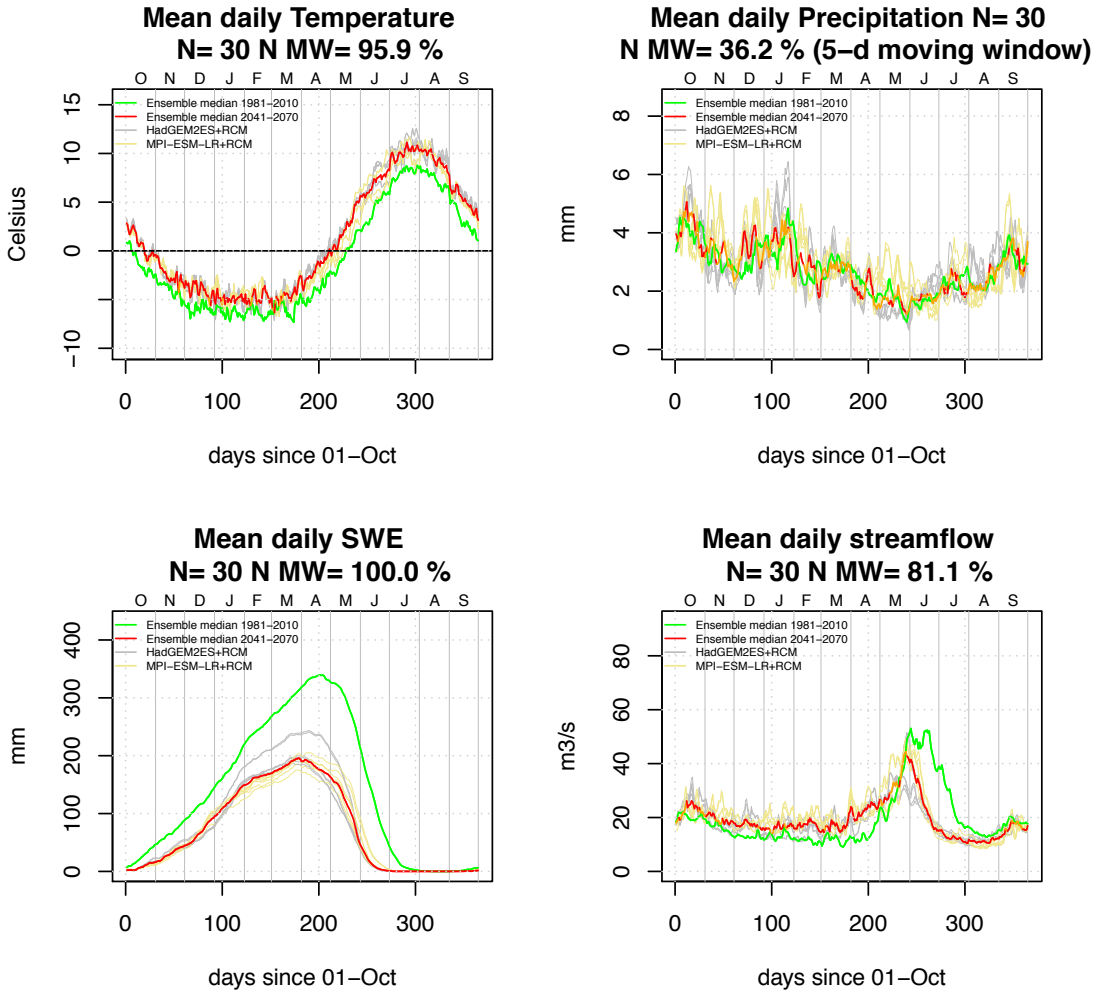

Fig. VII-3: Catchment vhm48: Projected mean daily temperature (top-left), precipitation (top-right), snow accumulation (bottom-left) and discharge (bottom-right) in the period 2041-2070 under the RCP4.5 emission scenario. Individual ensemble members are coloured in grey and yellow. The ensemble median is coloured in red for days when the Mann-Whitney test detected a significant shift in the ensemble of mean daily values relative to the ensemble in the reference period (1981-2010) and orange otherwise. The ensemble median in the reference period (1981-2010) is shown in green. N = Number of years in the projection period. N MW = Percentage of days in the water year when a significant shift was detected by the Mann-Whitney test.

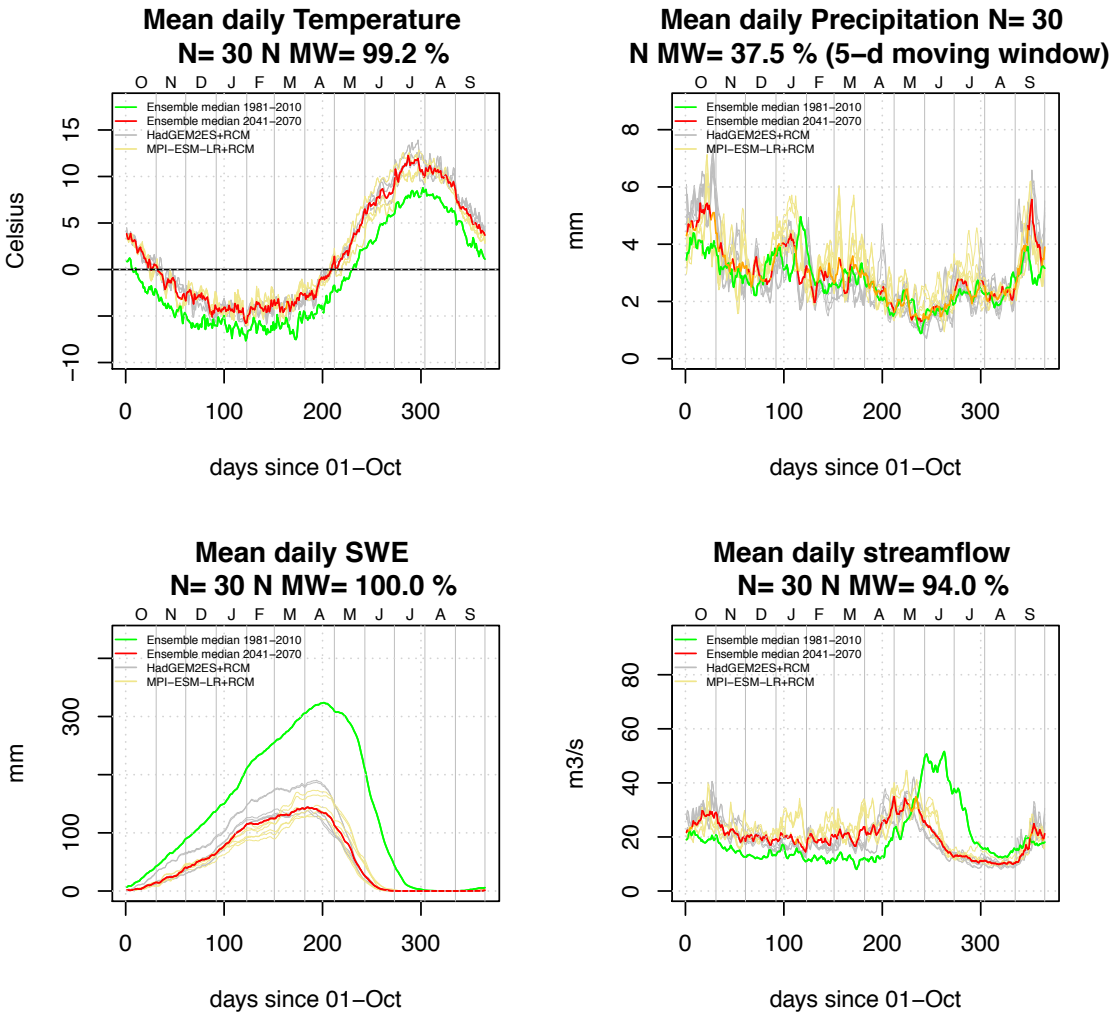

Fig. VII-4: Catchment vhm48: As Fig. VII-3 but under the RCP8.5 emission scenario.

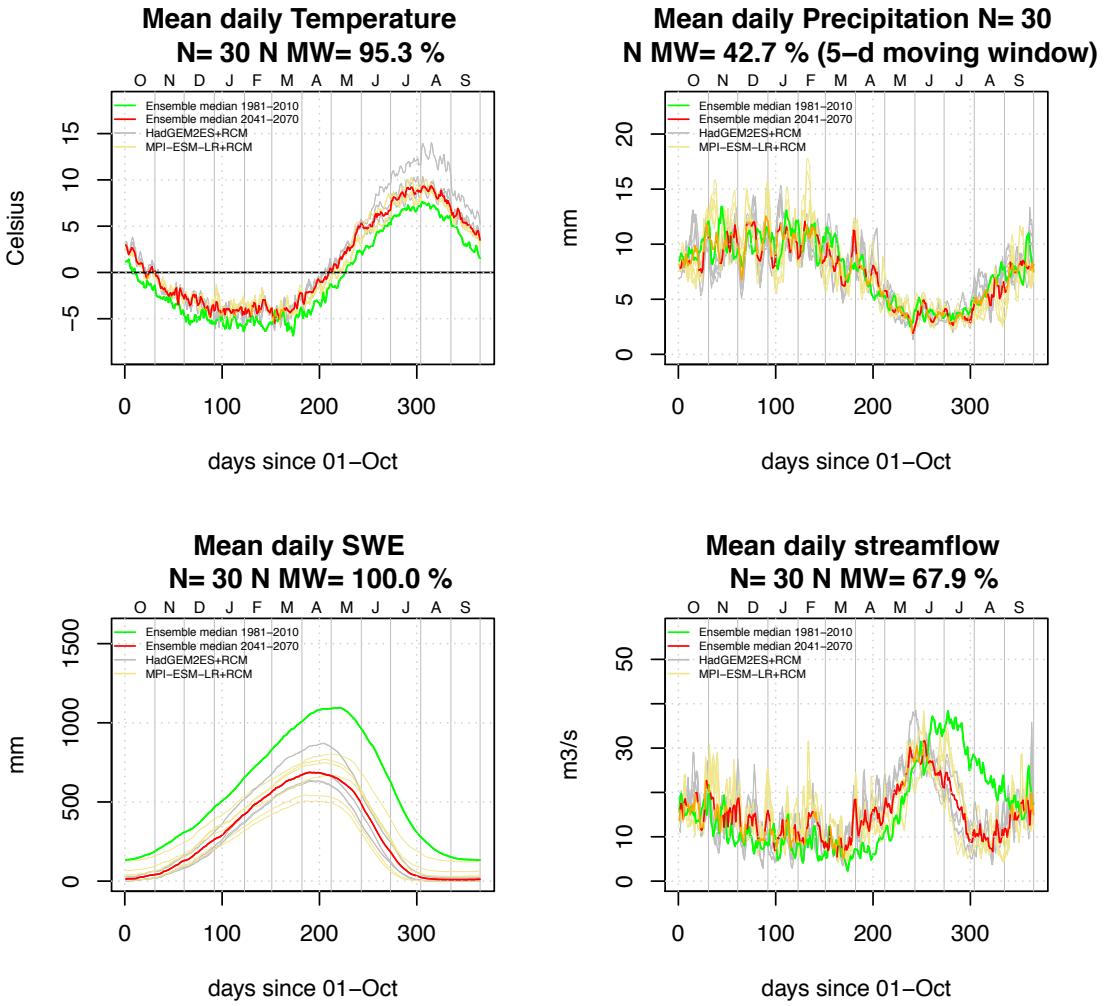

Fig. VII-5: Catchment vhm149: Projected mean daily temperature (top-left), precipitation (top-right), snow accumulation (bottom-left) and discharge (bottom-right) in the period 2041-2070 under the RCP4.5 emission scenario. Individual ensemble members are coloured in grey and yellow. The ensemble median is coloured in red for days when the Mann-Whitney test detected a significant shift in the ensemble of mean daily values relative to the ensemble in the reference period (1981-2010) and orange otherwise. The ensemble median in the reference period (1981-2010) is shown in green. N = Number of years in the projection period. N MW = Percentage of days in the water year when a significant shift was detected by the Mann-Whitney test.

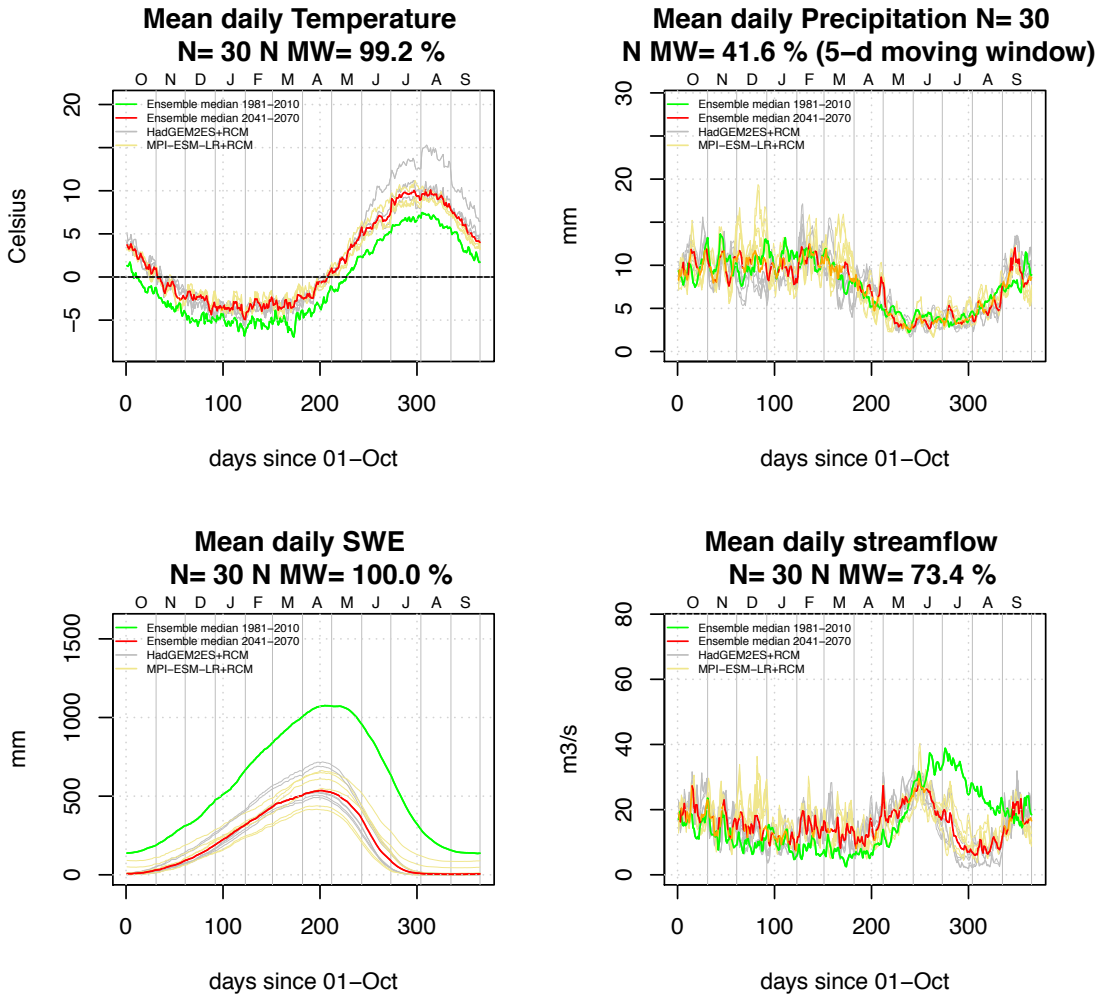

Fig. VII-6: Catchment vhm149: As Fig. VII-5 but under the RCP8.5 emission scenario.

Appendix 8

Projected 30-year mean seasonal rainfall, snowfall, snowmelt, and fraction of precipitation falling as rain, for all ensemble members

Projections based on MPI-ESM-LR GCM (yellow lines). Projections based on HadGEM2ES GCM (grey lines). Ensemble median (red line). Simulations based on the ICRA-reanalysis in the period 1981-2010 are given for comparison (blue line).

The significance of changes in seasonal values between the reference period (1981-2010) and each projection period is evaluated with a two-sided Mann-Whitney test. This test is first applied to each ensemble member (or realisation) to compare the sample of thirty seasonal values in the reference period (1981-2010) to the sample of thirty seasonal values in each 30-year projection period. Periods when a significant change is detected with this test are marked with a solid circle and with a triangle otherwise.

Then, the test is applied to compare the ensemble of twelve mean seasonal values in the reference period (1981-2010) to the ensemble of twelve mean seasonal values in each projection period and the results of this test are shown on the ensemble median (red line with solid circle if change is significant and triangle otherwise).

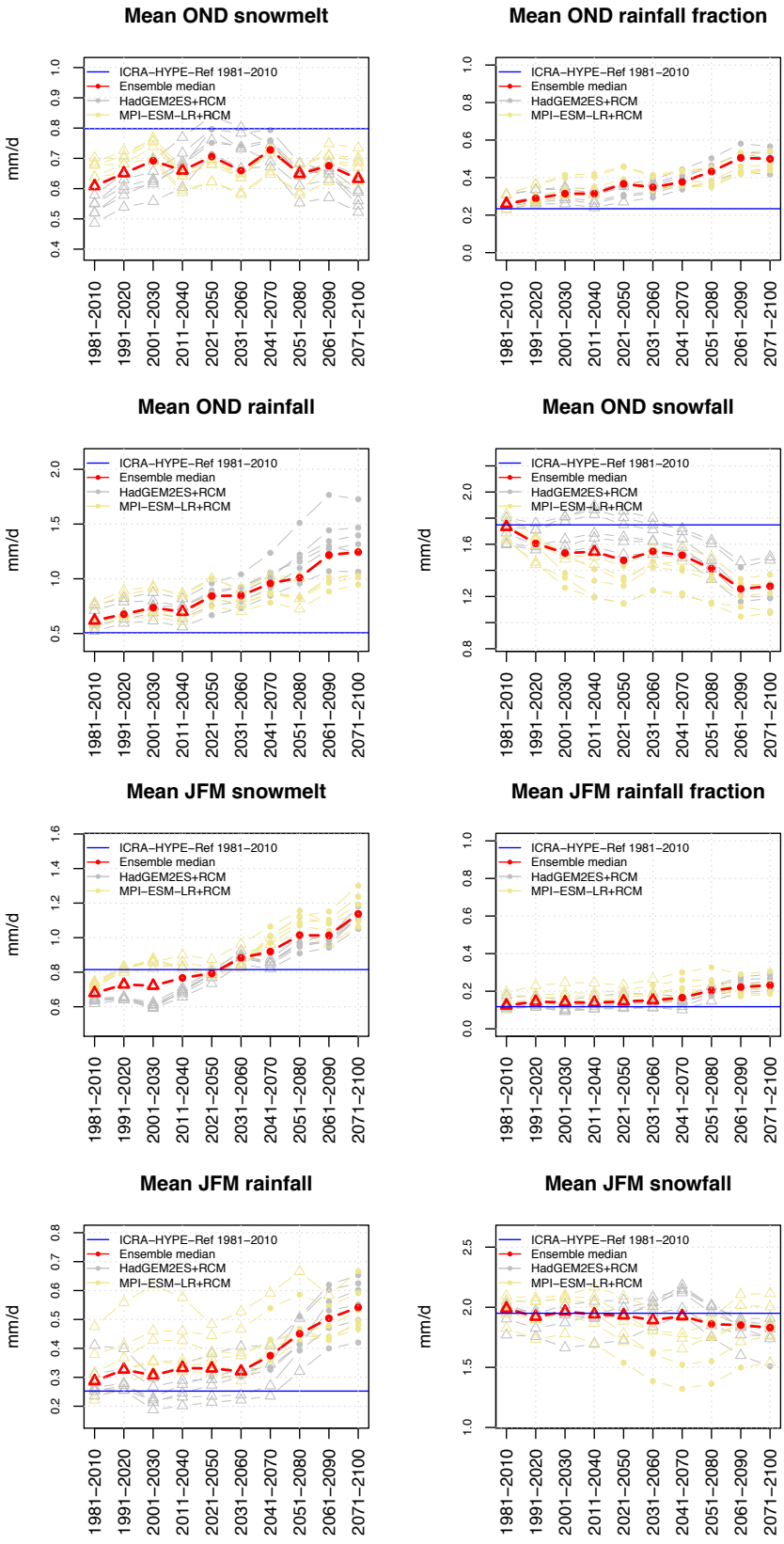

Fig. VIII-1: Catchment vhm45: OND and JFM projections under the RCP4.5 emission scenario.

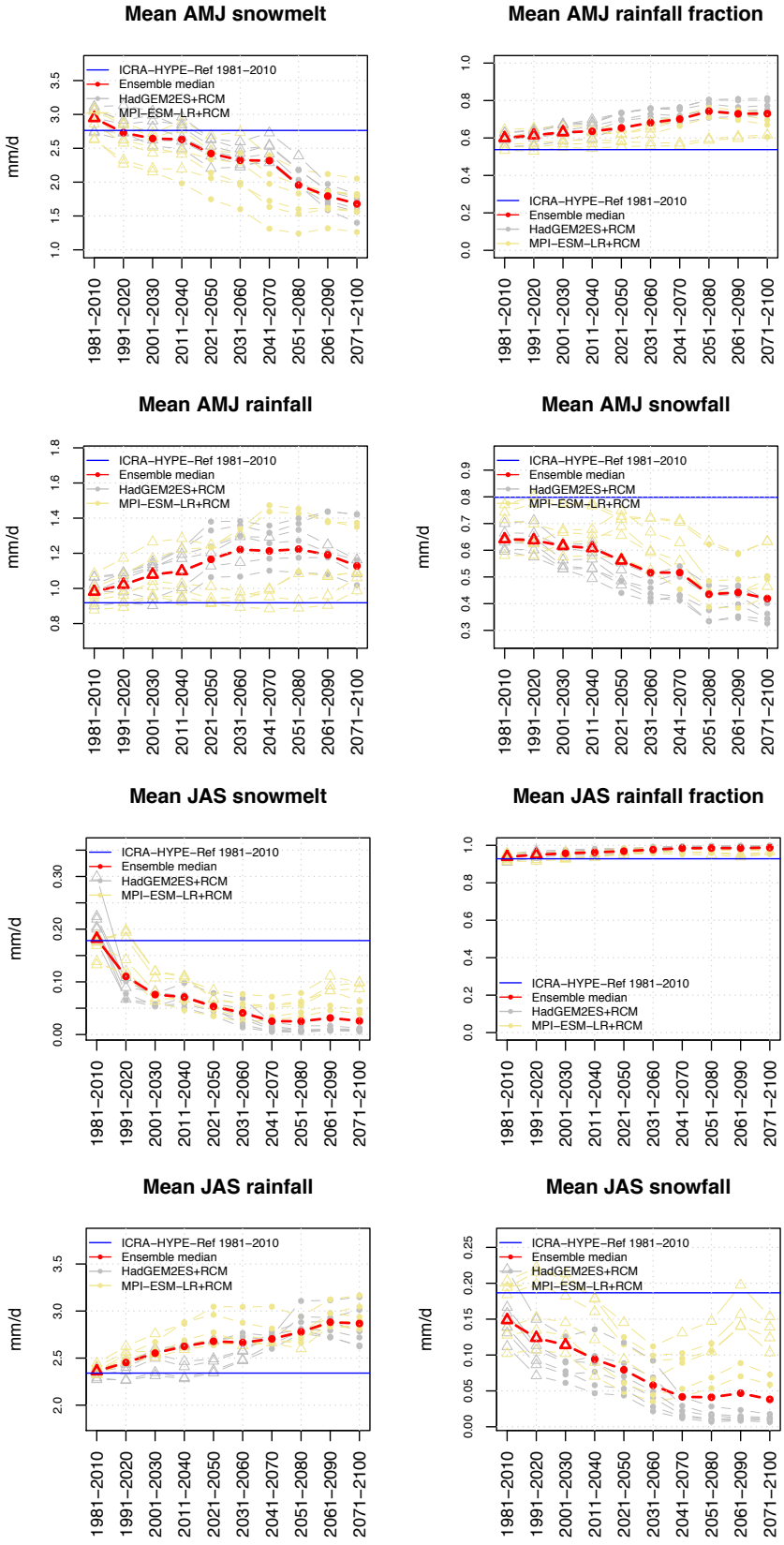

Fig. VIII-2: Catchment vhm45: AMJ and JAS projections under the RCP4.5 emission scenario.

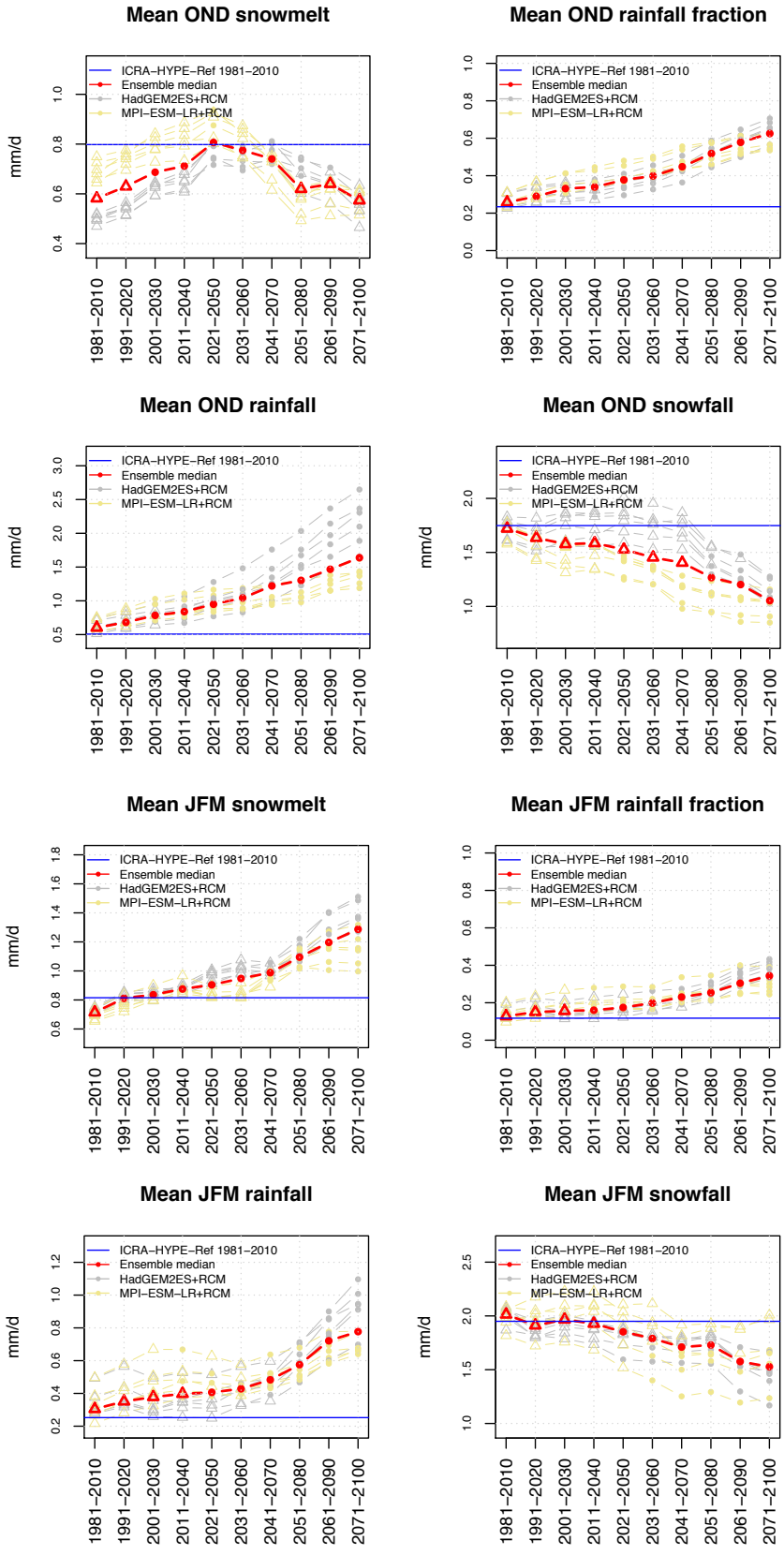

Fig. VIII-3: Catchment vhm45: OND and JFM projections under the RCP8.5 emission scenario.

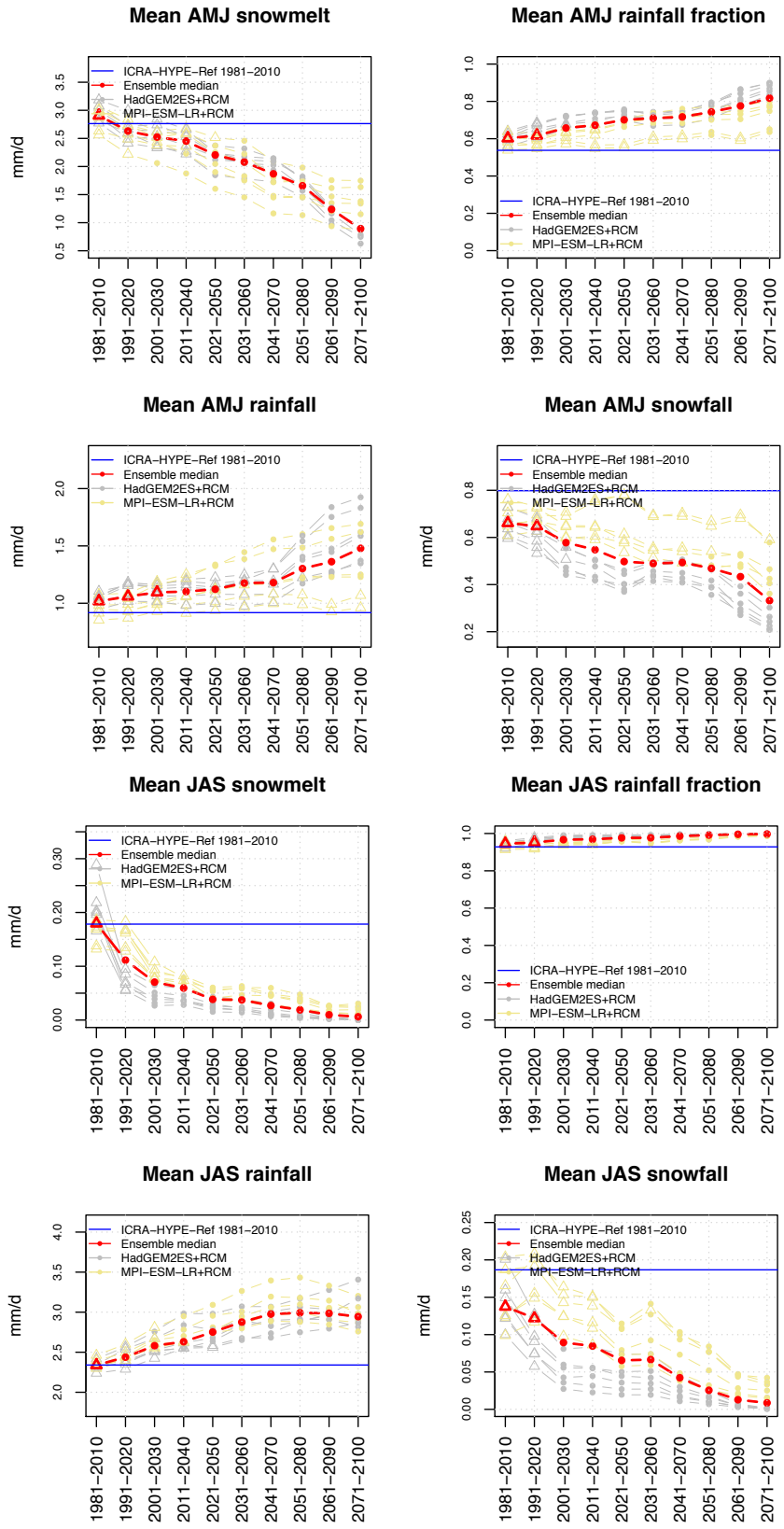

Fig. VIII-4: Catchment vhm45: AMJ and JAS projections under the RCP8.5 emission scenario.

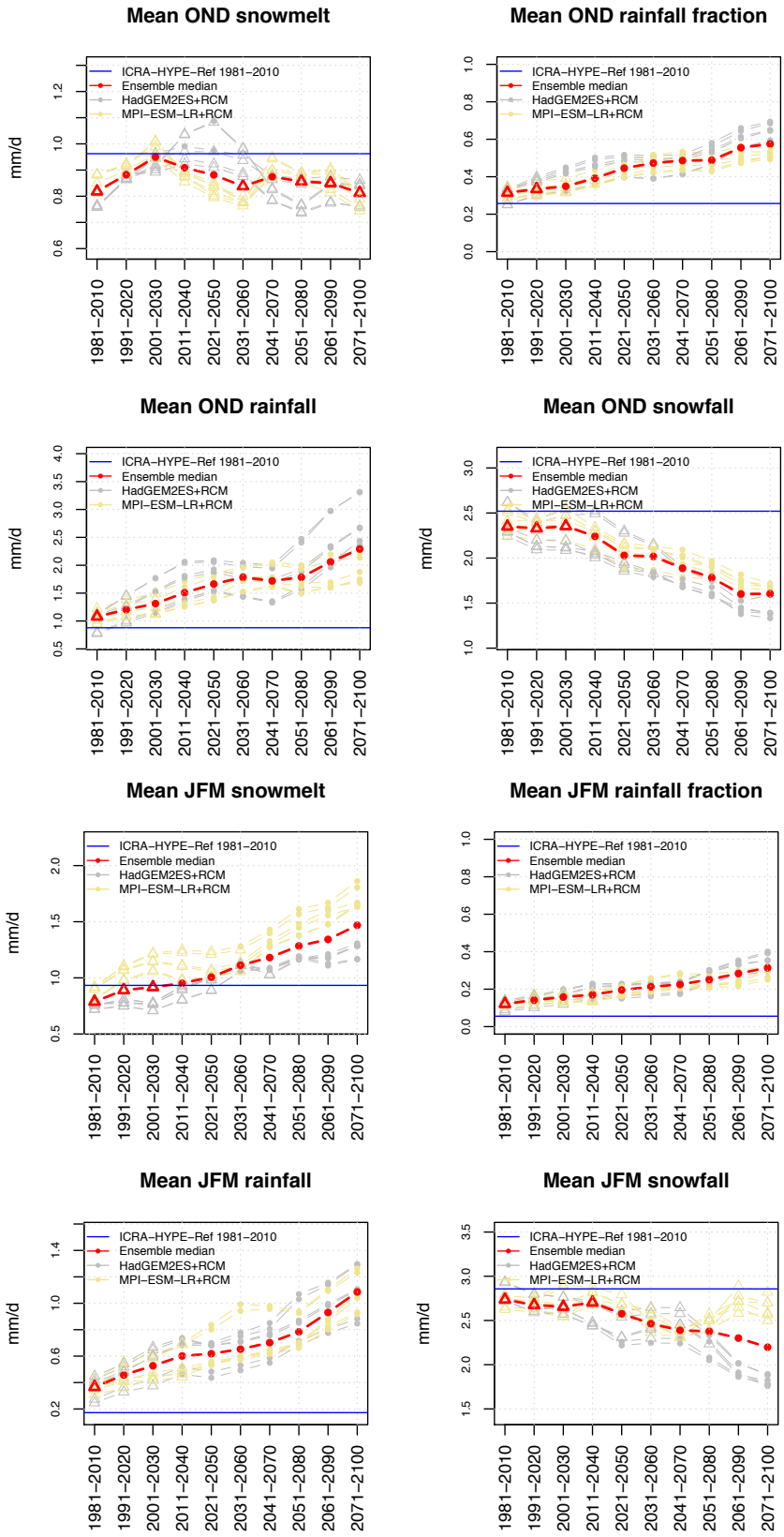

Fig. VIII-5: Catchment vhm48: OND and JFM projections under the RCP4.5 emission scenario.

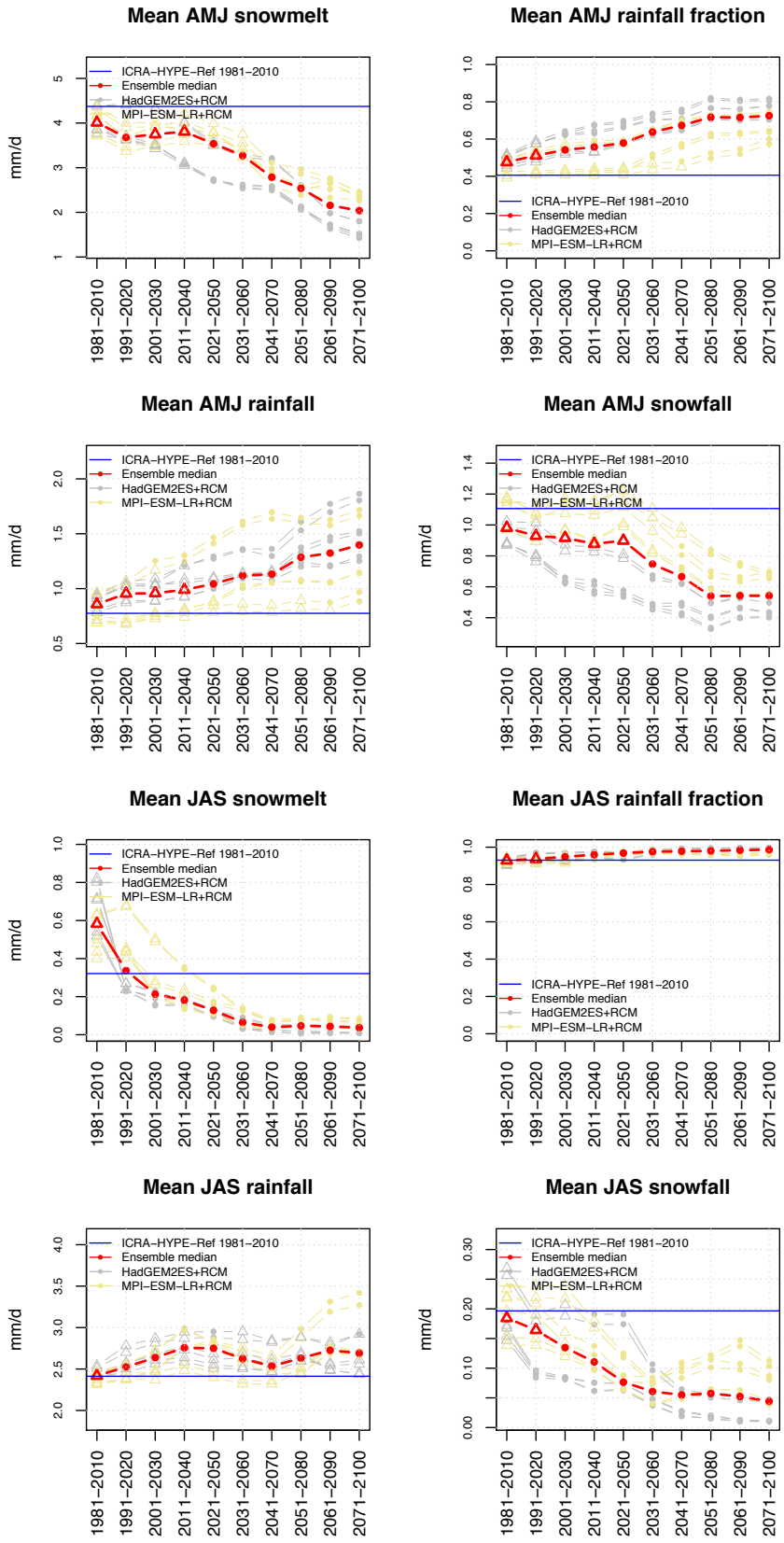

Fig. VIII-6: Catchment vhm48: AMJ and JAS projections under the RCP4.5 emission scenario.

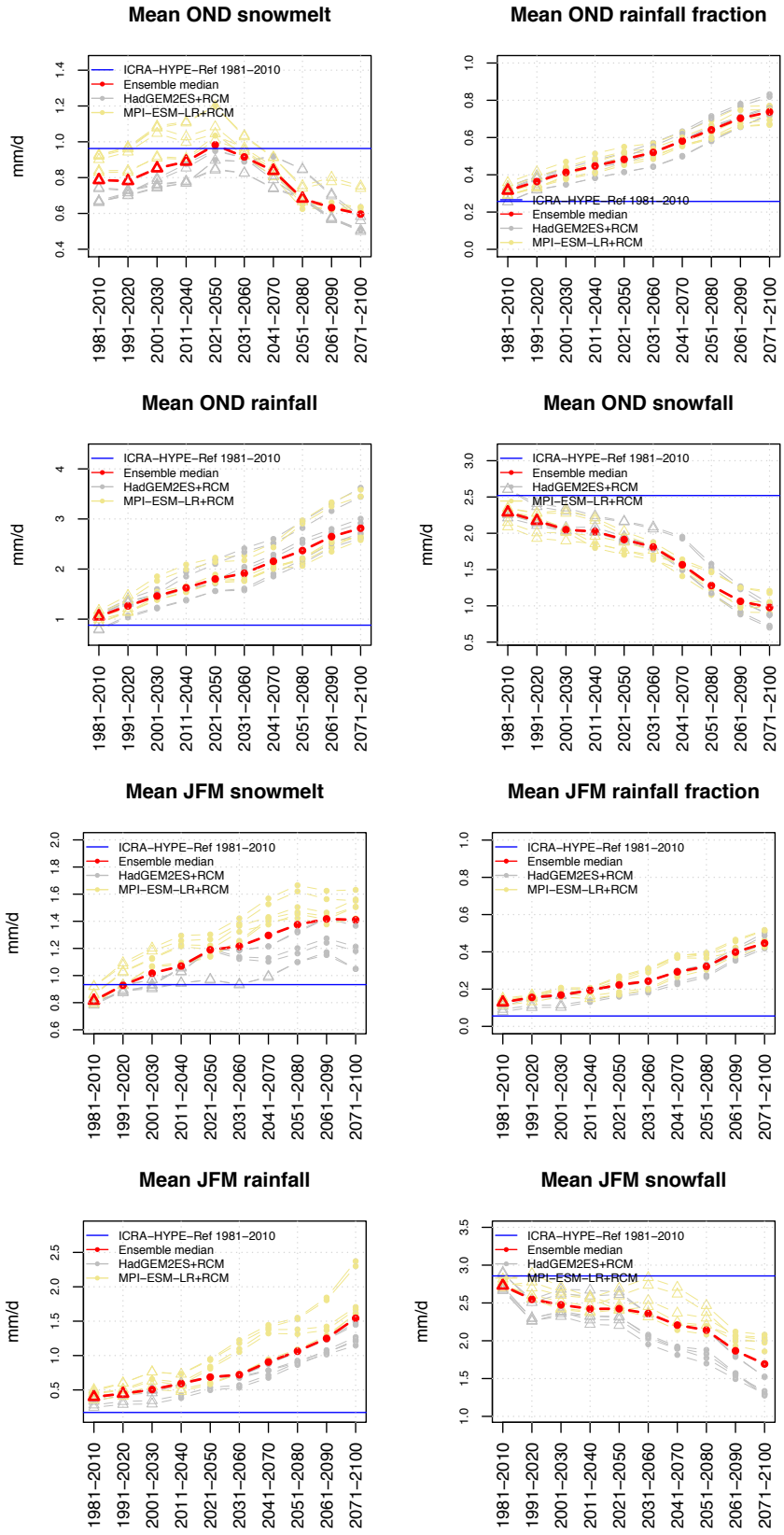

Fig. VIII-7: Catchment vhm48: OND and JFM projections under the RCP8.5 emission scenario.

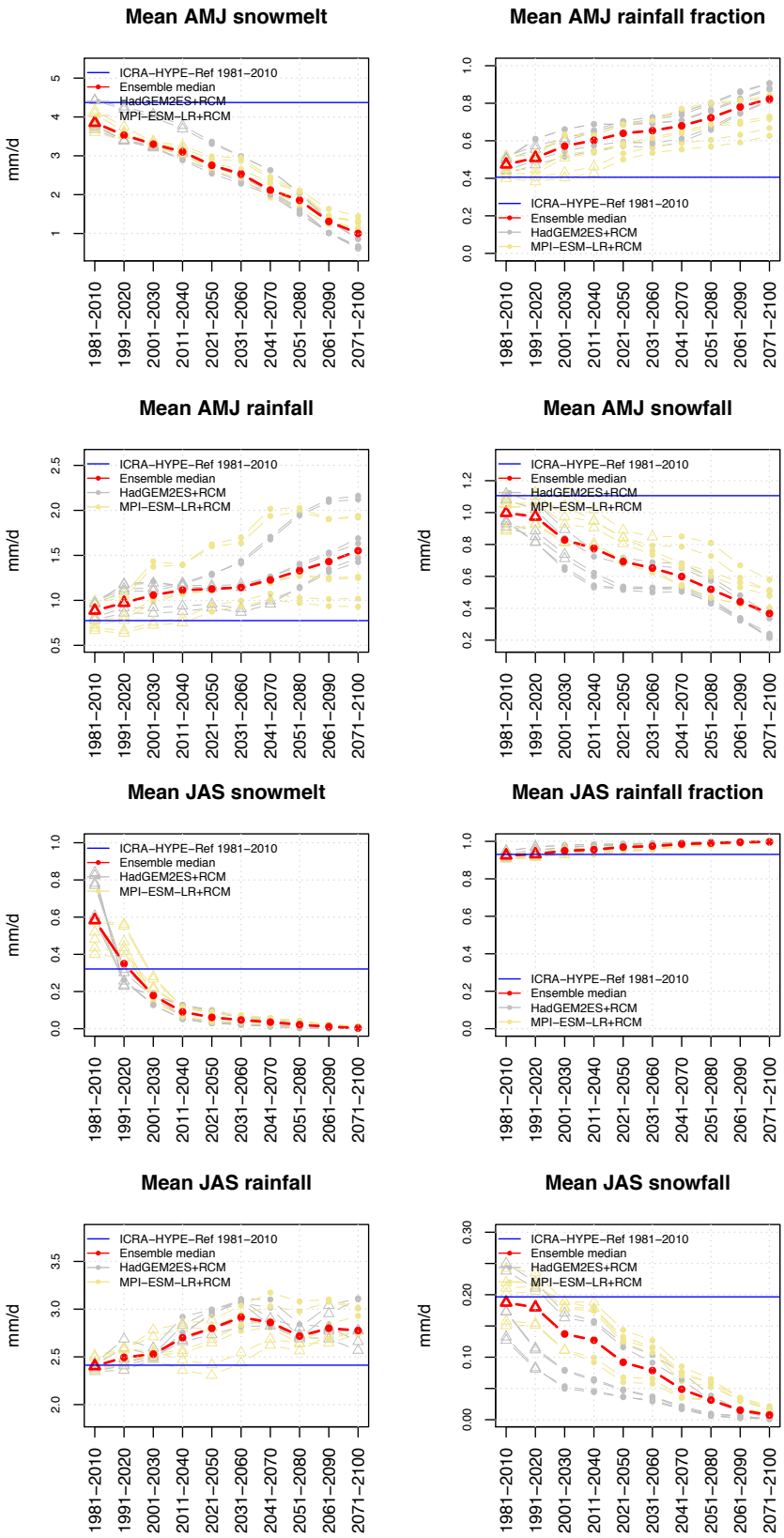

Fig. VIII-8: Catchment vhm48: AMJ and JAS projections under the RCP8.5 emission scenario.

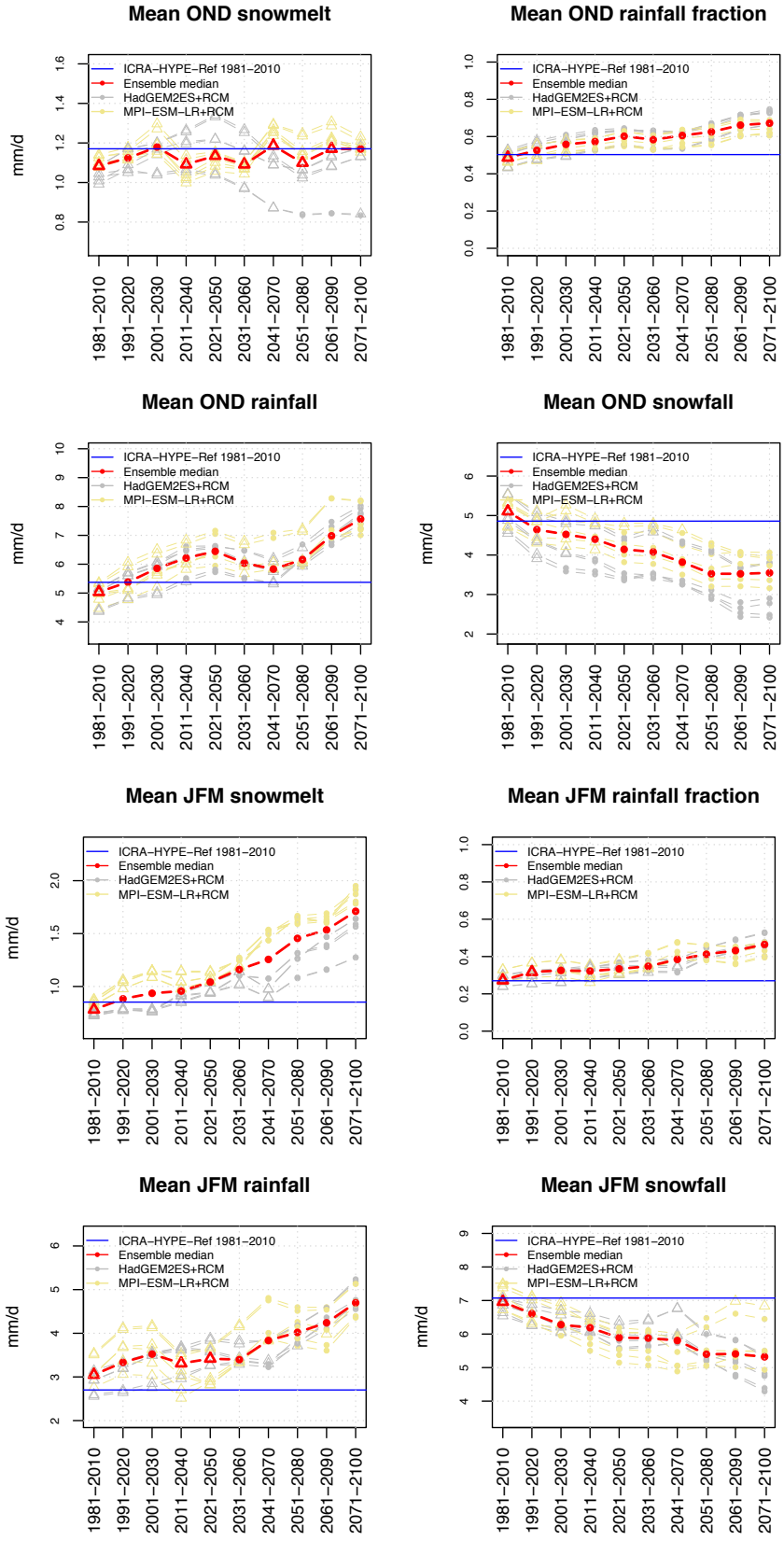

Fig. VIII-9: Catchment vhm149: OND and JFM projections under the RCP4.5 emission scenario.

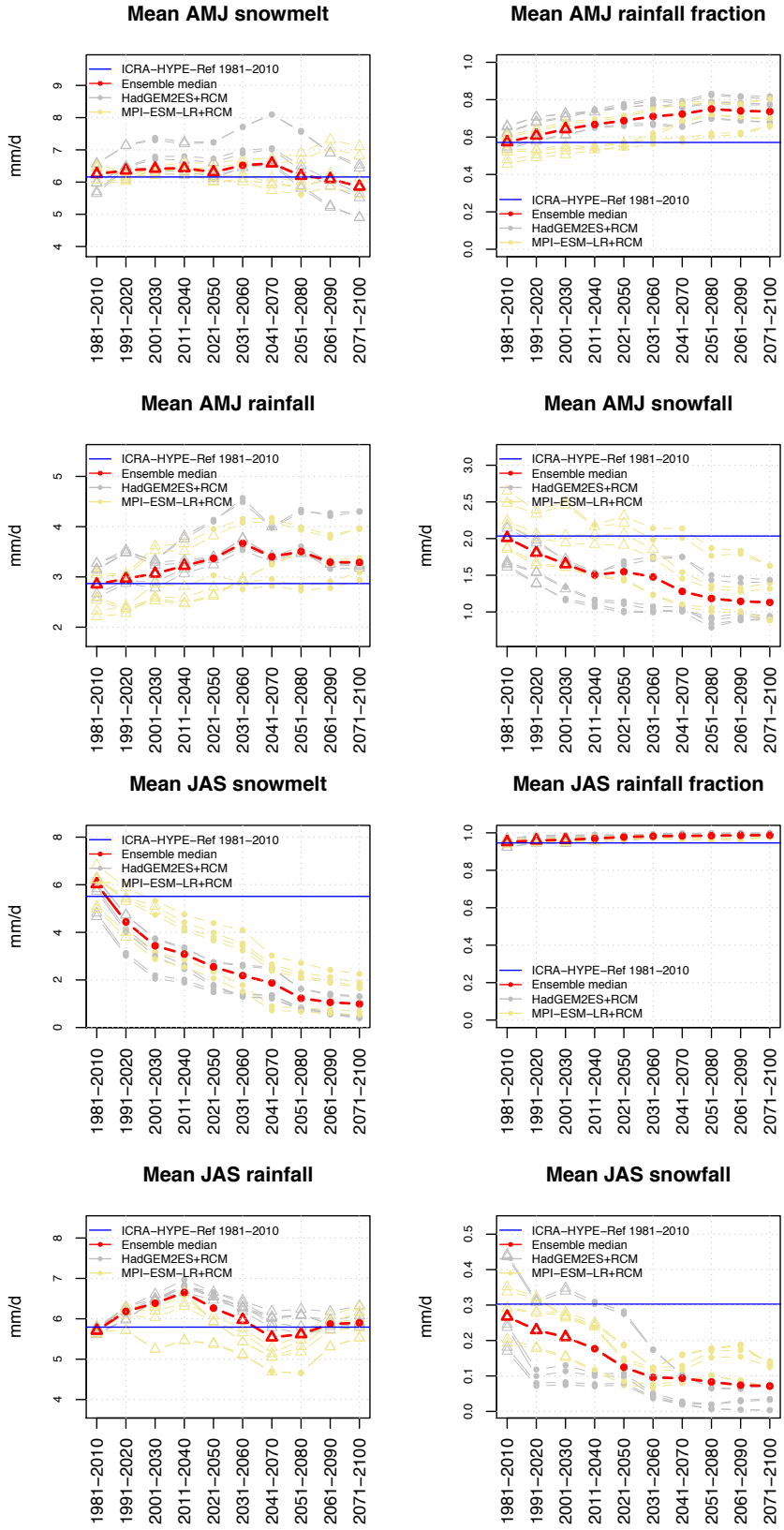

Fig. VIII-10: Catchment vhm149: AMJ and JAS projections under the RCP4.5 emission scenario.

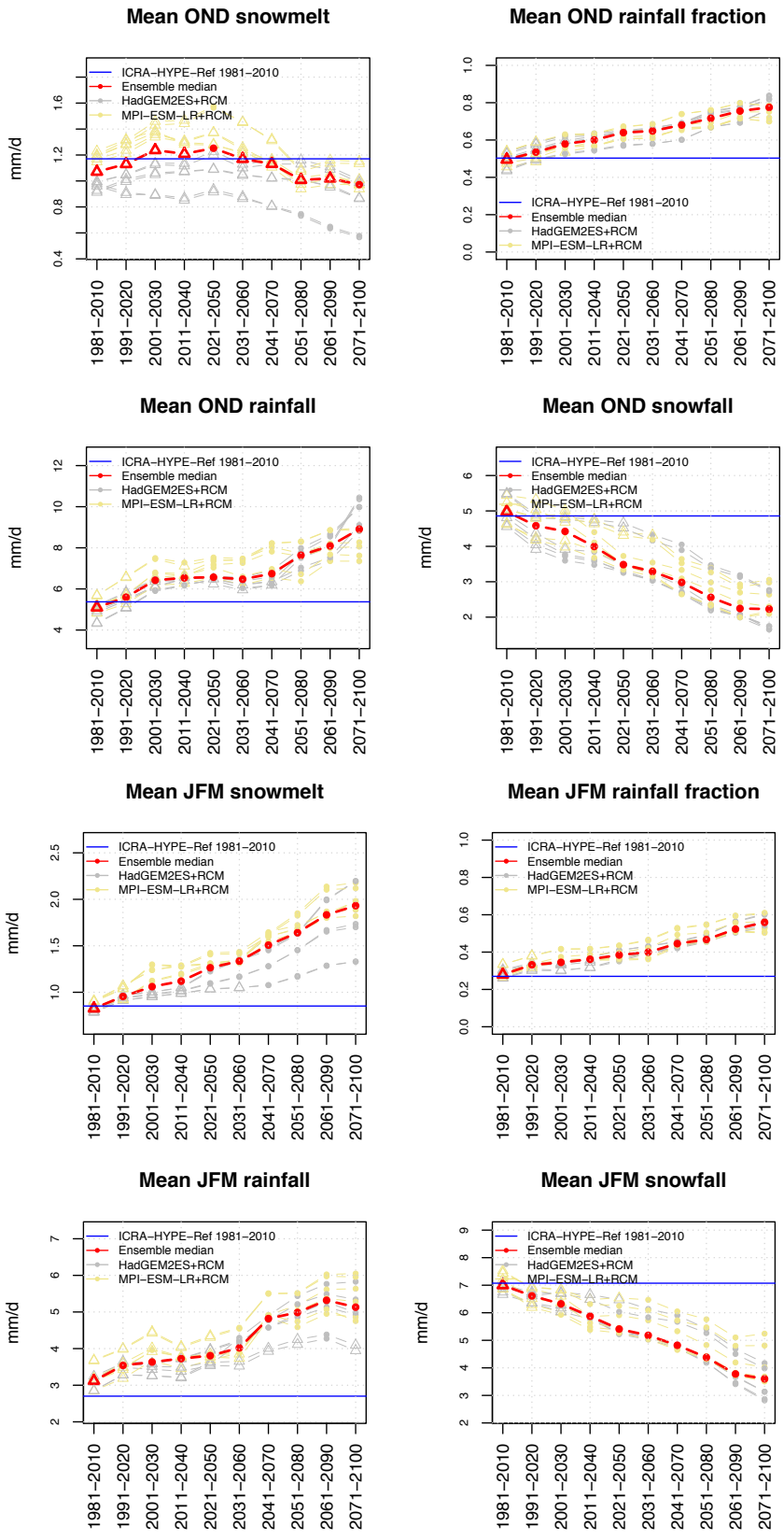

Fig. VIII-11: Catchment vhm149: OND and JFM projections under the RCP8.5 emission scenario.

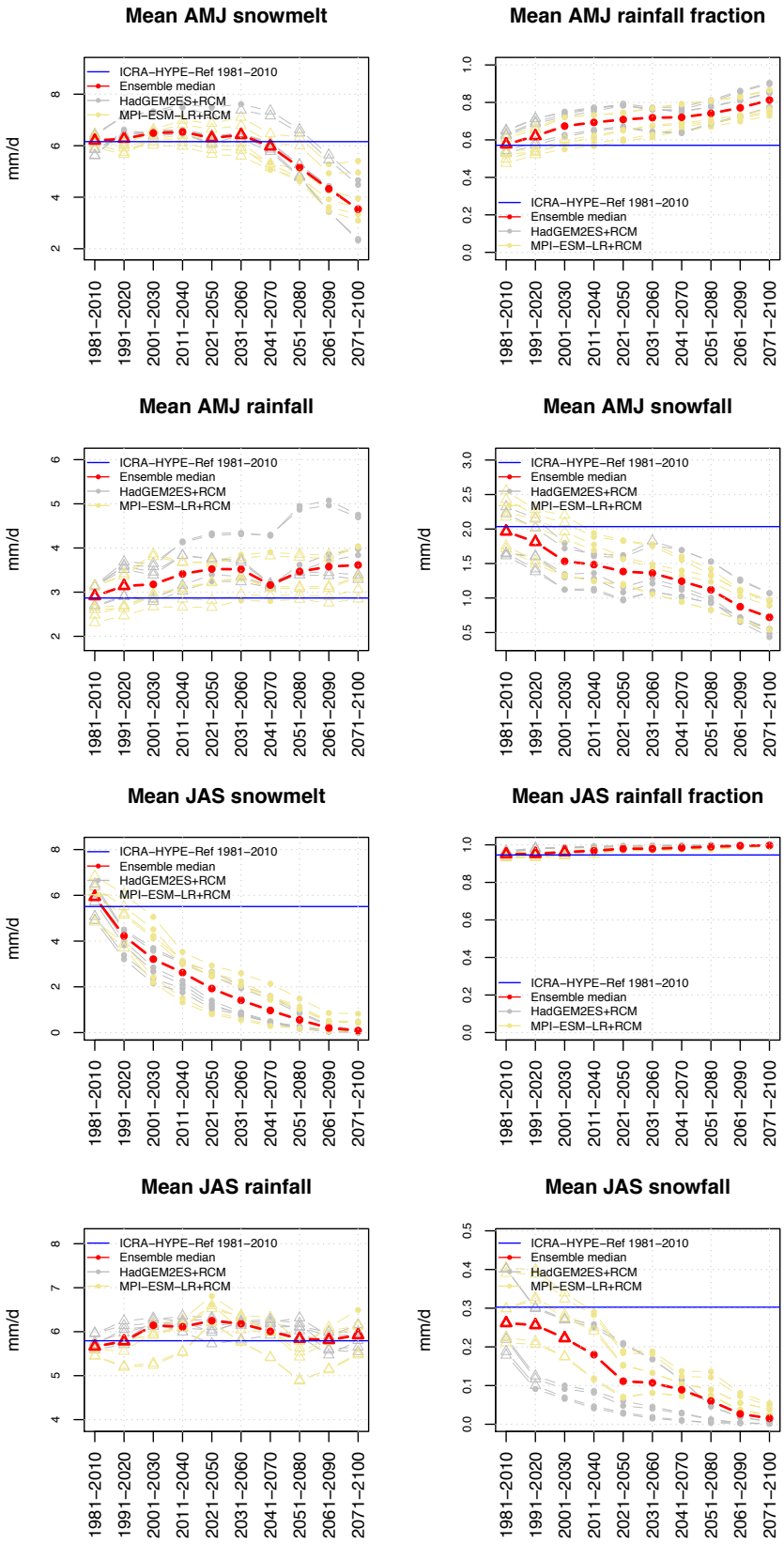

Fig. VIII-12: Catchment vhm149: AMJ and JAS projections under the RCP8.5 emission scenario.

Appendix 9

Box-plots of the projected changes in 30-year mean annual and mean seasonal temperature, precipitation and discharge for all ensemble members

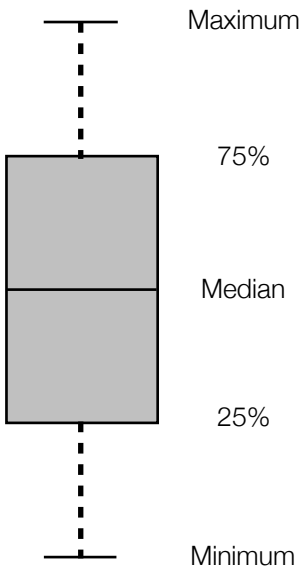

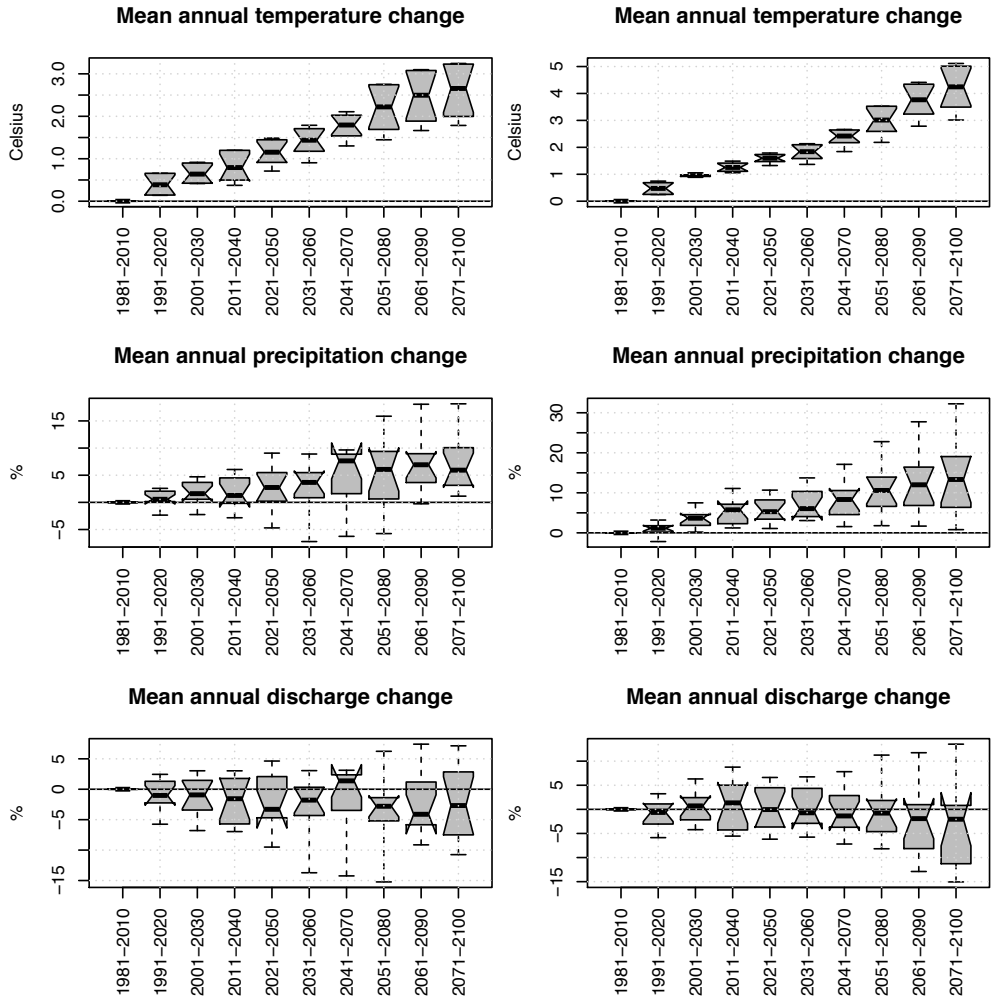

Fig. IX-1: Catchment vhm45: Projected changes in mean annual temperature, precipitation and discharge relative to the reference period (1981-2010), under the RCP4.5 emission scenario (left panel) and RCP8.5 emission scenario (right panel). The notches give an estimate of the 95% confidence interval (CI) of the median. The 95% CI sometimes exceeds the interquartile range.

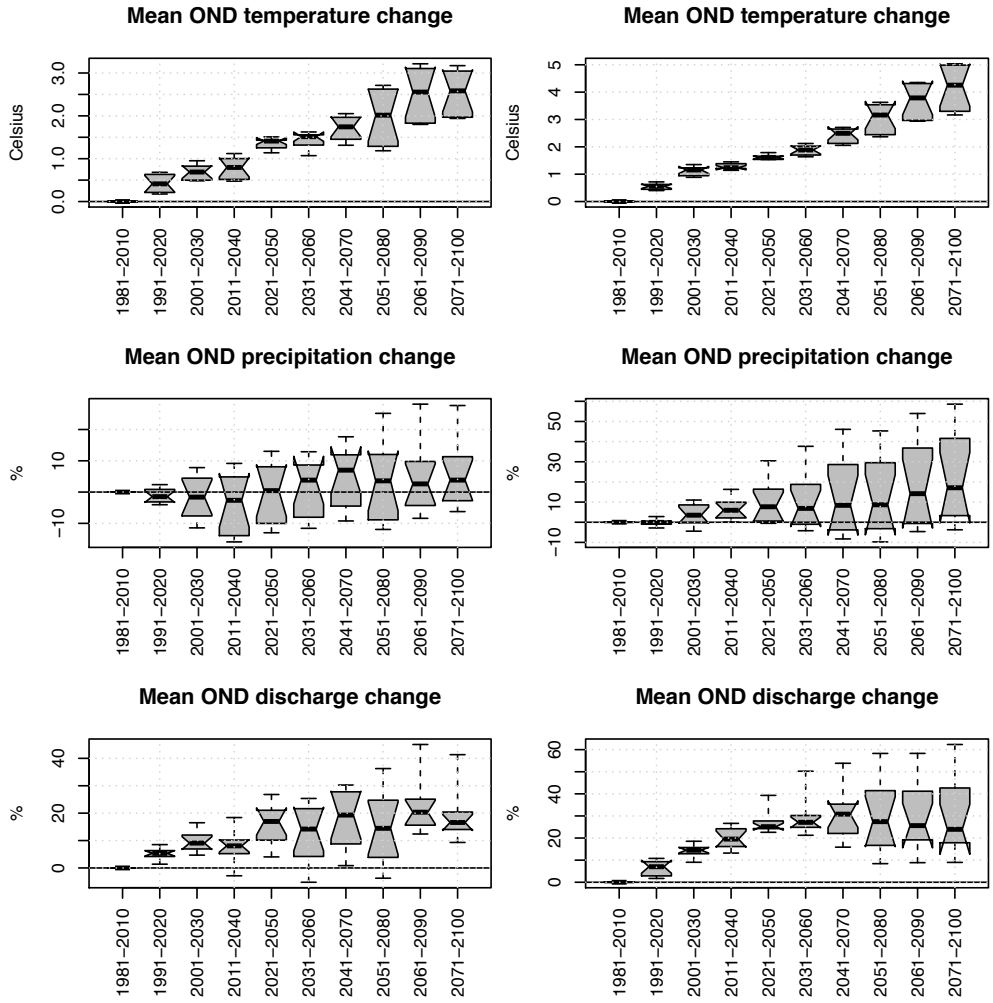

Fig. IX-2: Catchment vhm45: Projected changes in mean OND temperature, precipitation and discharge relative to the reference period (1981-2010), under the RCP4.5 emission scenario (left panel) and RCP8.5 emission scenario (right panel). The notches give an estimate of the 95% confidence interval (CI) of the median. The 95% CI sometimes exceeds the interquartile range.

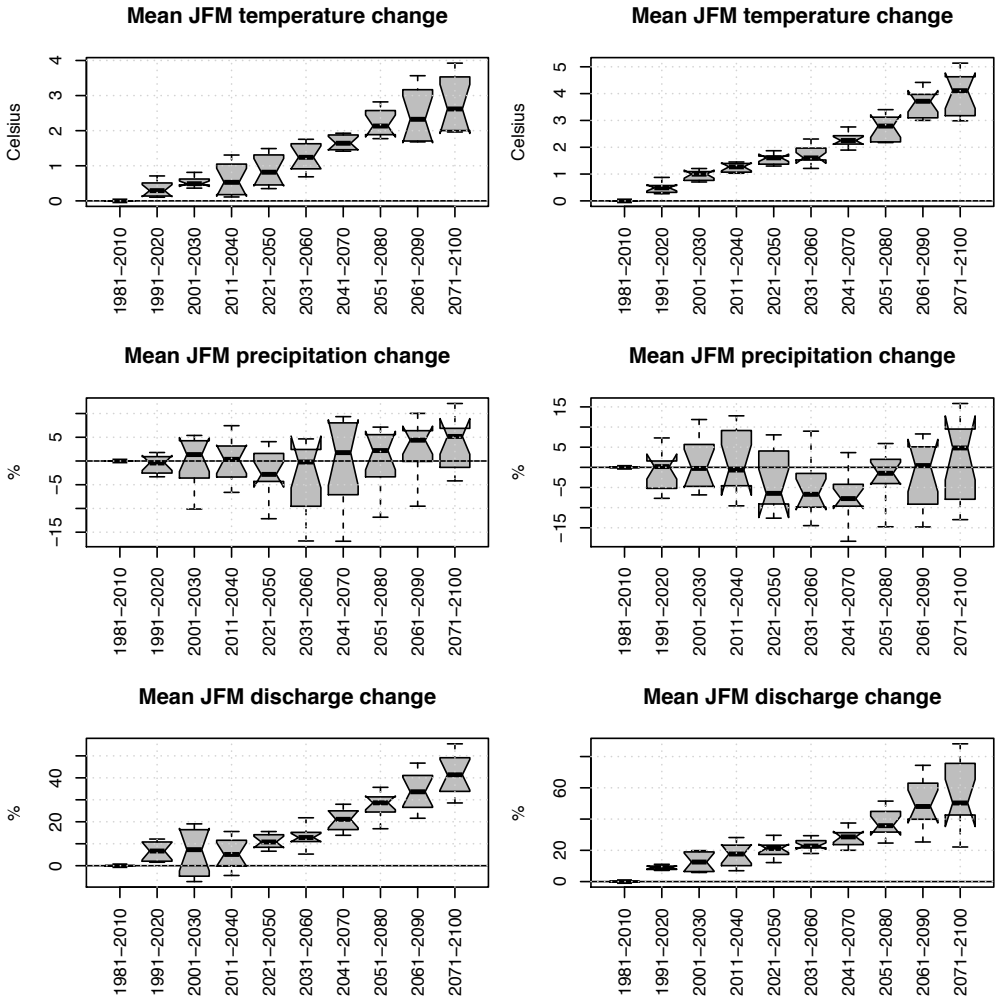

Fig. IX-3: Catchment vhm45: Projected changes in mean JFM temperature, precipitation and discharge relative to the reference period (1981-2010), under the RCP4.5 emission scenario (left panel) and RCP8.5 emission scenario (right panel). The notches give an estimate of the 95% confidence interval (CI) of the median. The 95% CI sometimes exceeds the interquartile range.

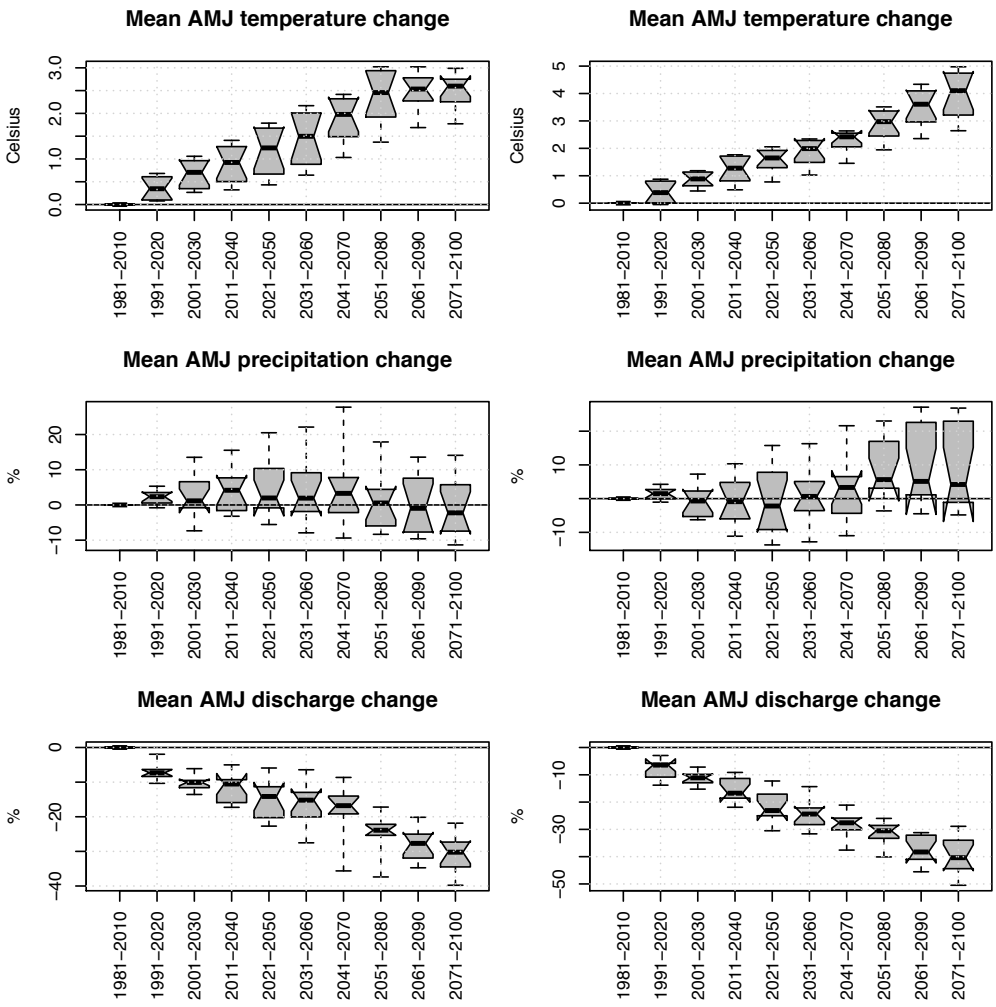

Fig. IX-4: Catchment vhm45: Projected changes in mean AMJ temperature, precipitation and discharge relative to the reference period (1981-2010), under the RCP4.5 emission scenario (left panel) and RCP8.5 emission scenario (right panel). The notches give an estimate of the 95% confidence interval (CI) of the median. The 95% CI sometimes exceeds the interquartile range.

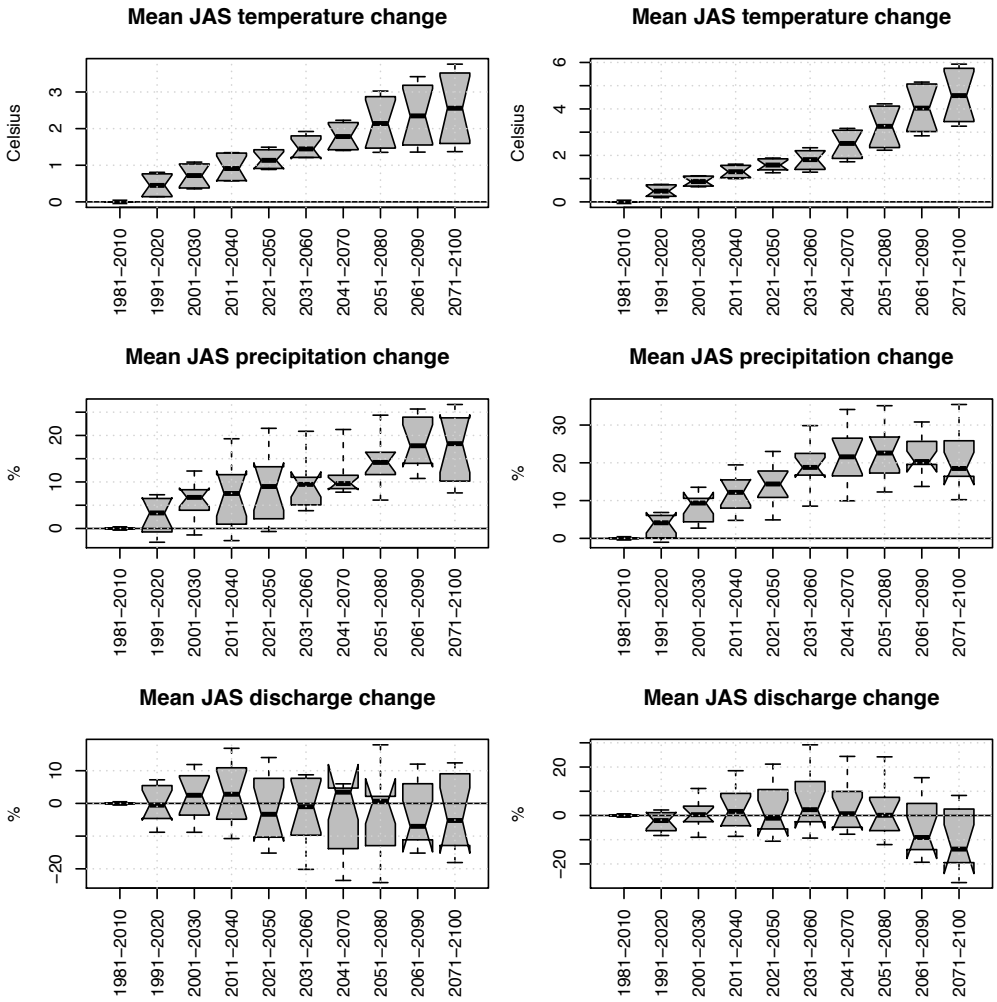

Fig. IX-5: Catchment vhm45: Projected changes in mean JAS temperature, precipitation and discharge relative to the reference period (1981-2010), under the RCP4.5 emission scenario (left panel) and RCP8.5 emission scenario (right panel). The notches give an estimate of the 95% confidence interval (CI) of the median. The 95% CI sometimes exceeds the interquartile range.

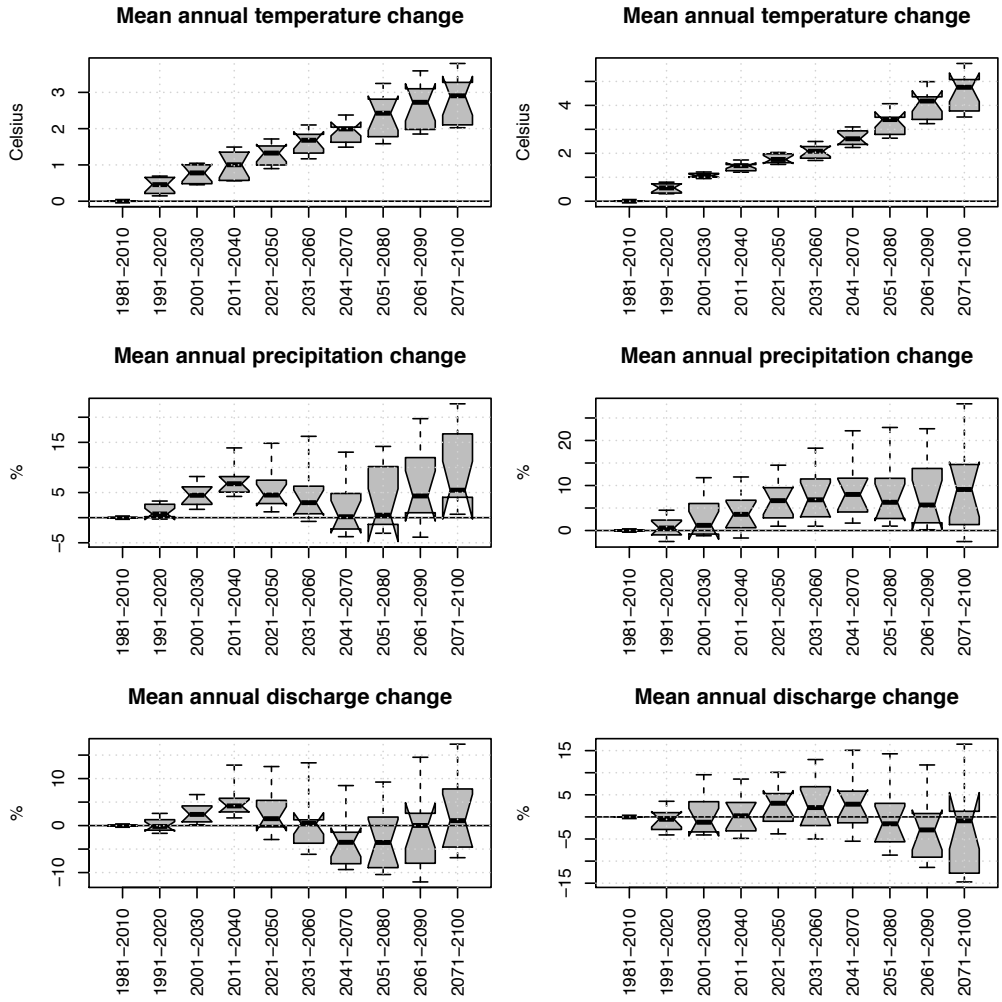

Fig. IX-6: Catchment vhm48: Projected changes in mean annual temperature, precipitation and discharge relative to the reference period (1981-2010), under the RCP4.5 emission scenario (left panel) and RCP8.5 emission scenario (right panel). The notches give an estimate of the 95% confidence interval (CI) of the median. The 95% CI sometimes exceeds the interquartile range.

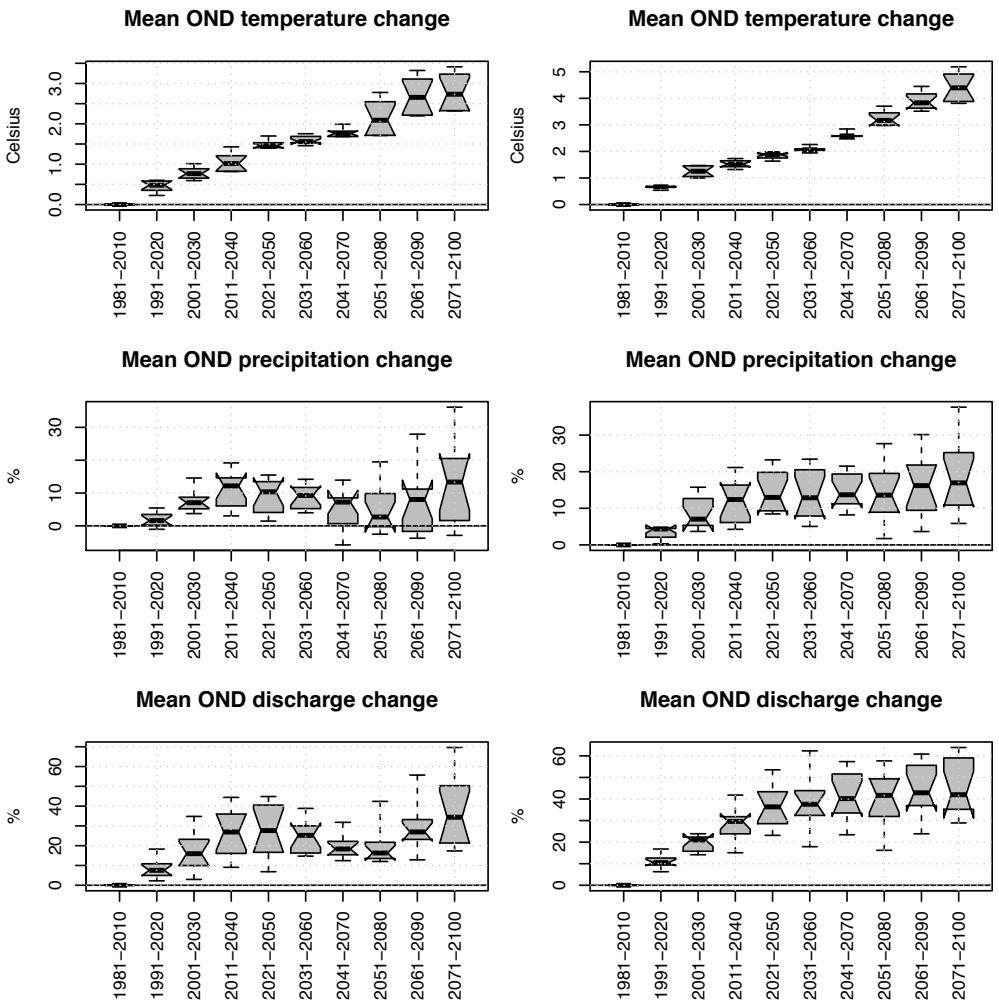

Fig. IX-7: Catchment vhm48: Projected changes in mean OND temperature, precipitation and discharge relative to the reference period (1981-2010), under the RCP4.5 emission scenario (left panel) and RCP8.5 emission scenario (right panel). The notches give an estimate of the 95% confidence interval (CI) of the median. The 95% CI sometimes exceeds the interquartile range.

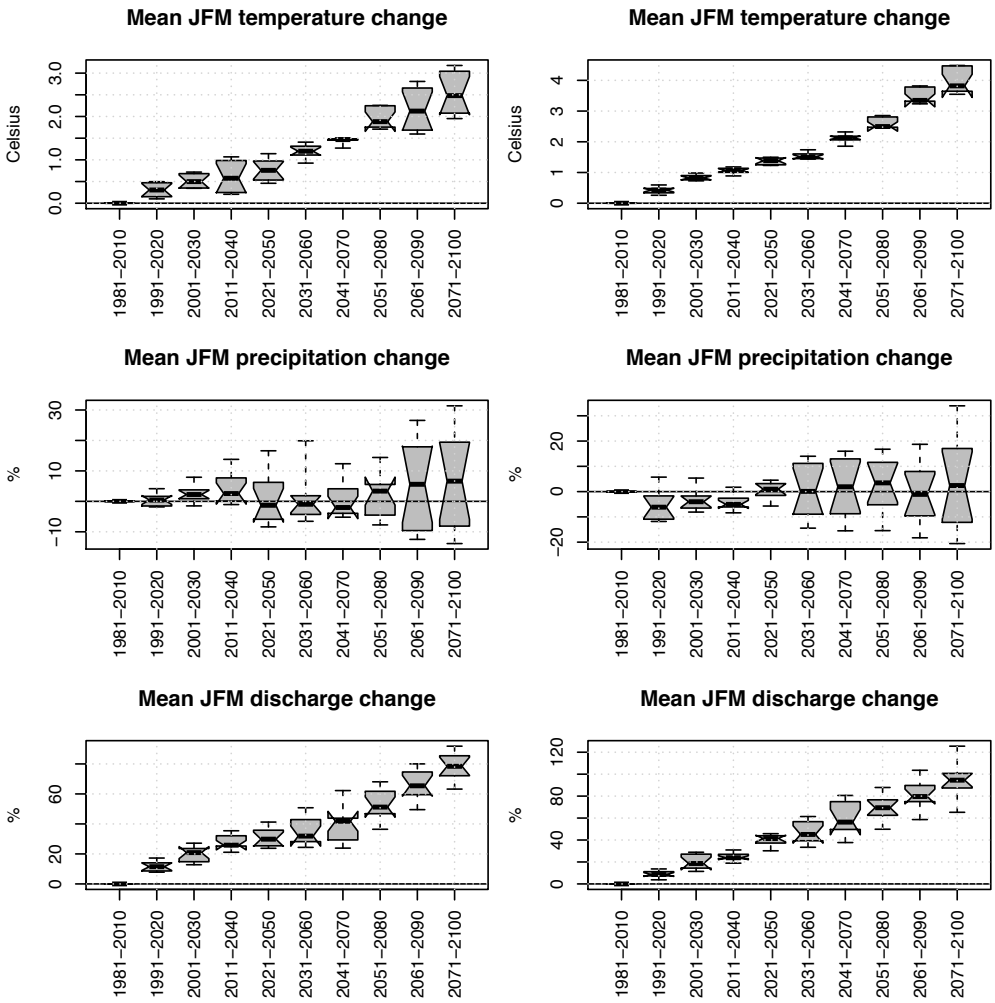

Fig. IX-8: Catchment vhm48: Projected changes in mean JFM temperature, precipitation and discharge relative to the reference period (1981-2010), under the RCP4.5 emission scenario (left panel) and RCP8.5 emission scenario (right panel). The notches give an estimate of the 95% confidence interval (CI) of the median. The 95% CI sometimes exceeds the interquartile range.

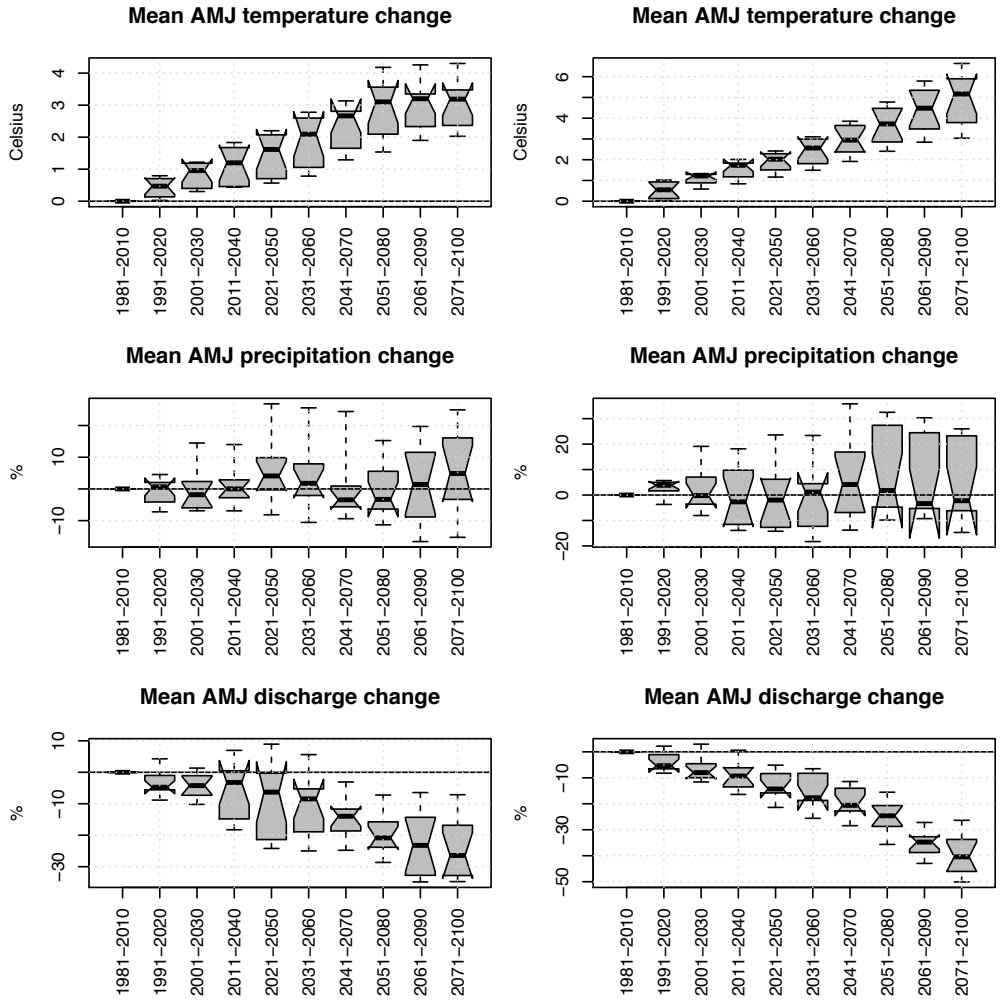

Fig. IX-9: Catchment vhm48: Projected changes in mean AMJ temperature, precipitation and discharge relative to the reference period (1981-2010), under the RCP4.5 emission scenario (left panel) and RCP8.5 emission scenario (right panel). The notches give an estimate of the 95% confidence interval (CI) of the median. The 95% CI sometimes exceeds the interquartile range.

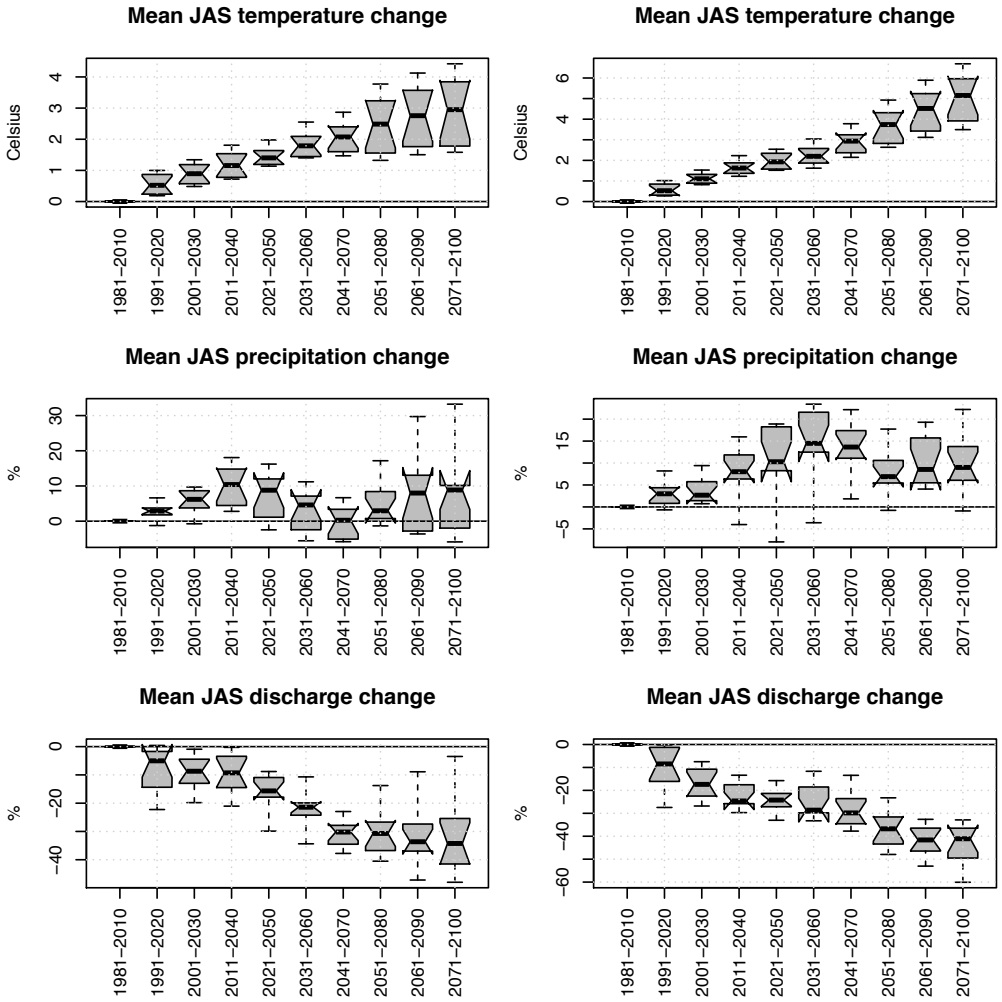

Fig. IX-10: Catchment vhm48: Projected changes in mean JAS temperature, precipitation and discharge relative to the reference period (1981-2010), under the RCP4.5 emission scenario (left panel) and RCP8.5 emission scenario (right panel). The notches give an estimate of the 95% confidence interval (CI) of the median. The 95% CI sometimes exceeds the interquartile range.

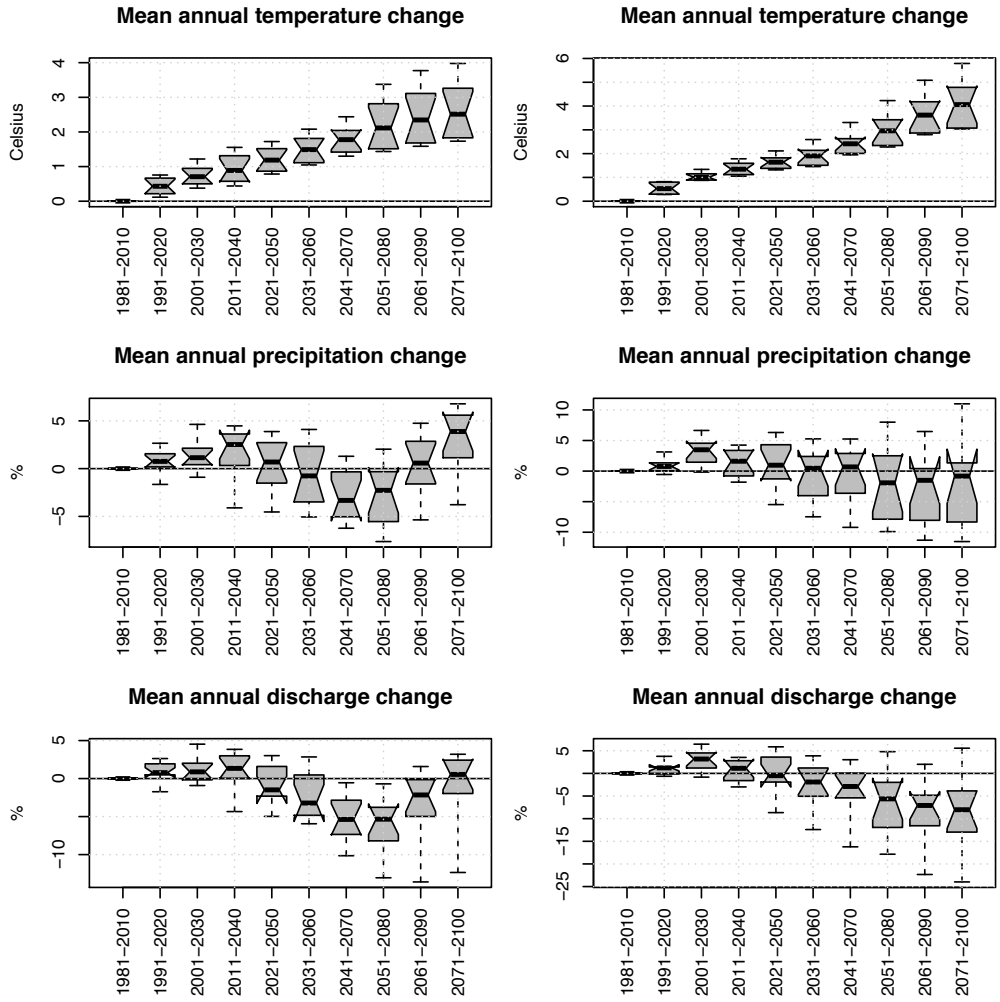

Fig. IX-11: Catchment vhm149: Projected changes in mean annual temperature, precipitation and discharge relative to the reference period (1981-2010), under the RCP4.5 emission scenario (left panel) and RCP8.5 emission scenario (right panel). The notches give an estimate of the 95% confidence interval (CI) of the median. The 95% CI sometimes exceeds the interquartile range.

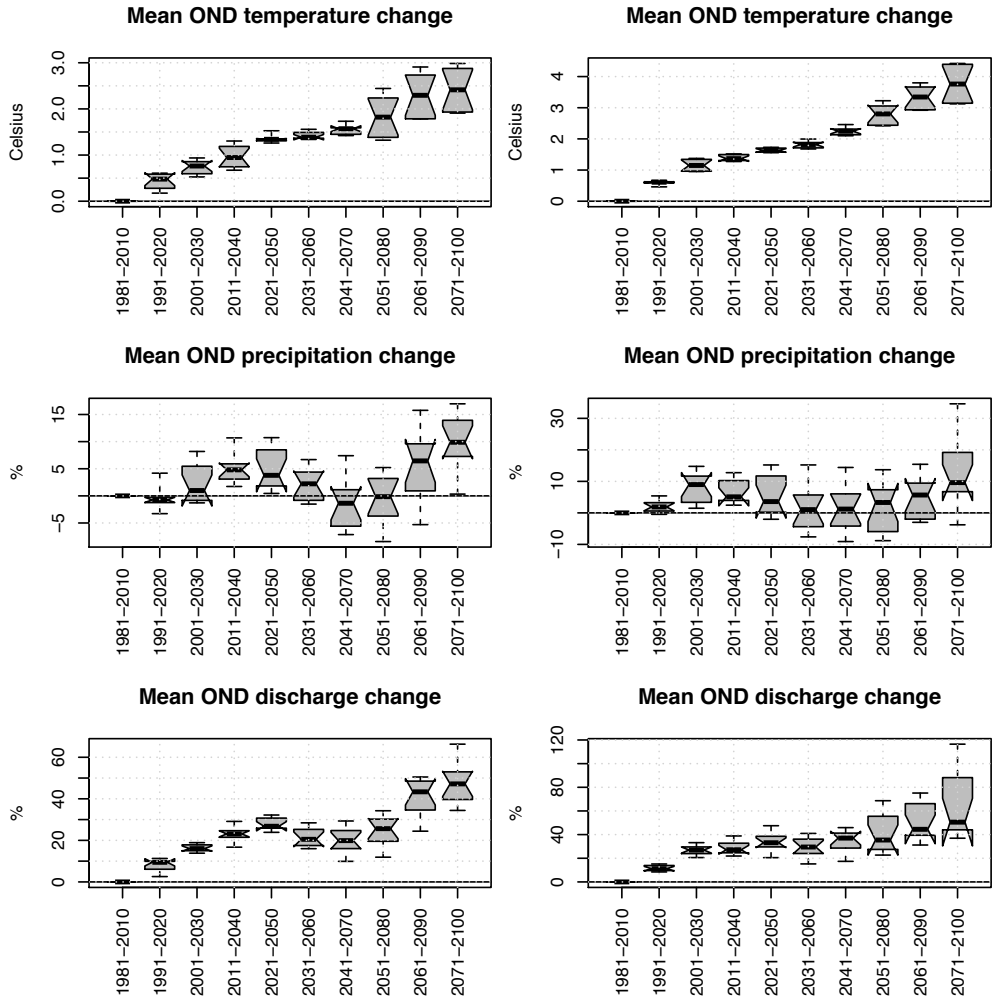

Fig. IX-12: Catchment vhm149: Projected changes in mean OND temperature, precipitation and discharge relative to the reference period (1981-2010), under the RCP4.5 emission scenario (left panel) and RCP8.5 emission scenario (right panel). The notches give an estimate of the 95% confidence interval (CI) of the median. The 95% CI sometimes exceeds the interquartile range.

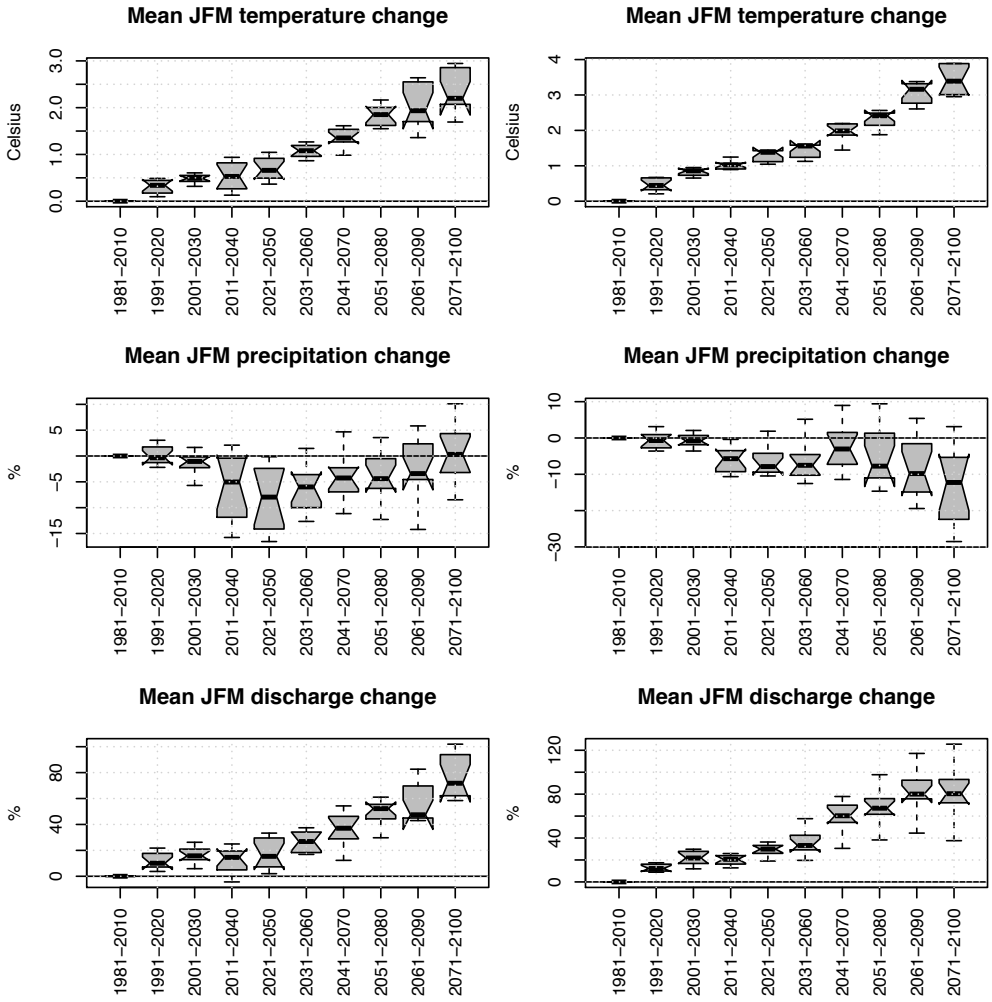

Fig. IX-13: Catchment vhm149: Projected changes in mean JFM temperature, precipitation and discharge, under the RCP4.5 emission scenario (left panel) and RCP8.5 emission scenario (right panel), relative to the reference period (1981-2010). The notches give an estimate of the 95% confidence interval (CI) of the median. The 95% CI sometimes exceeds the interquartile range.

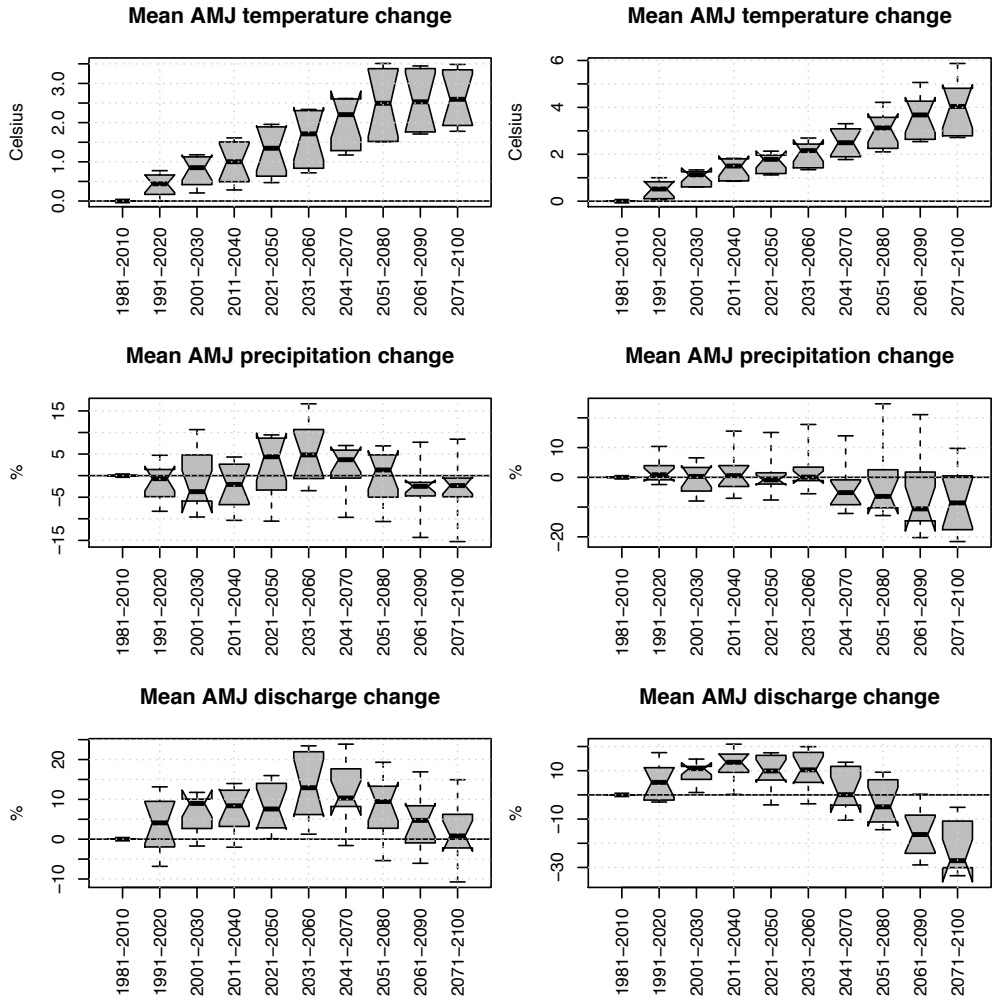

Fig. IX-14: Catchment vhm149: Projected changes in mean AMJ temperature, precipitation and discharge, under the RCP4.5 emission scenario (left panel) and RCP8.5 emission scenario (right panel), relative to the reference period (1981-2010). The notches give an estimate of the 95% confidence interval (CI) of the median. The 95% CI sometimes exceeds the interquartile range.

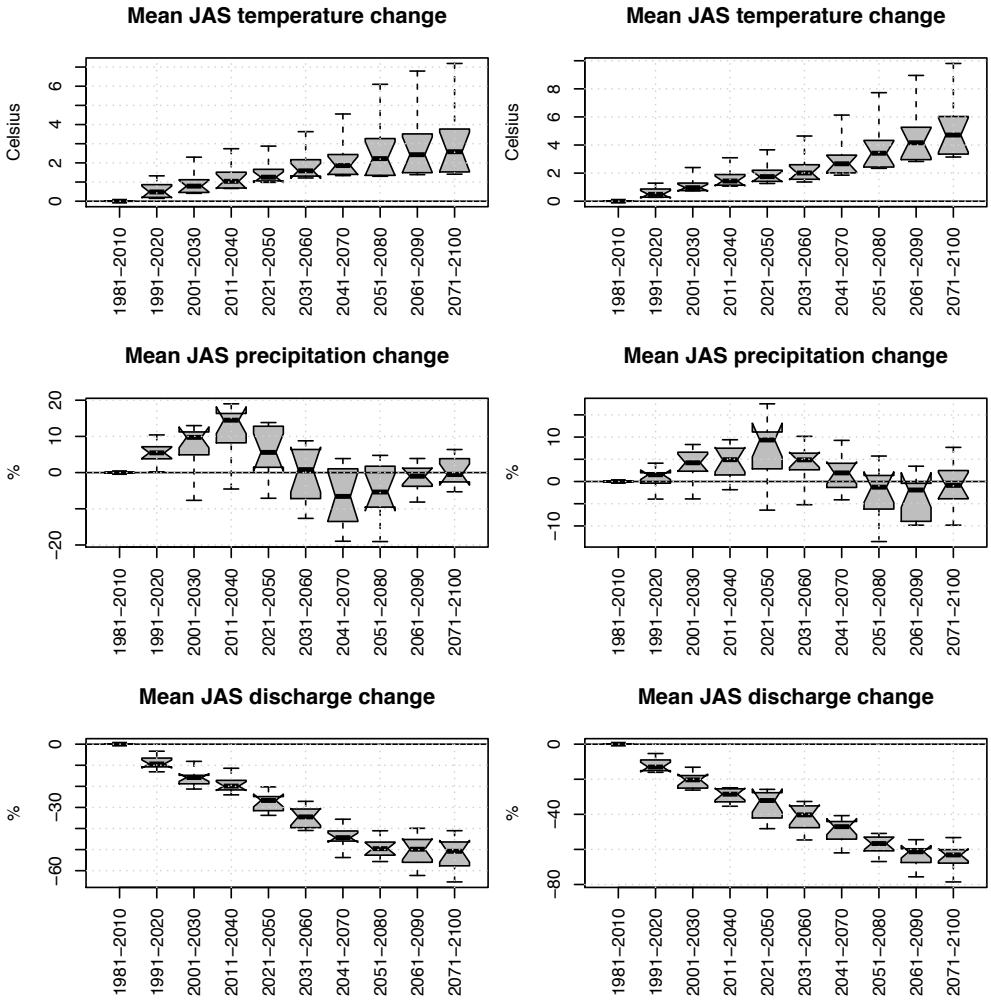

Fig. IX-15: Catchment vhm149: Projected changes in mean JAS temperature, precipitation and discharge, under the RCP4.5 emission scenario (left panel) and RCP8.5 emission scenario (right panel), relative to the reference period (1981-2010). The notches give an estimate of the 95% confidence interval (CI) of the median. The 95% CI sometimes exceeds the interquartile range.

Appendix 10

Box-plots of the projected seasonal frequency of AMFs for all ensemble members

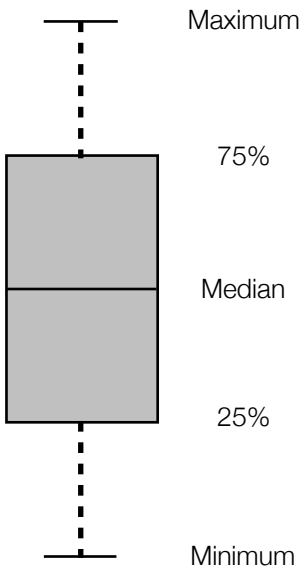

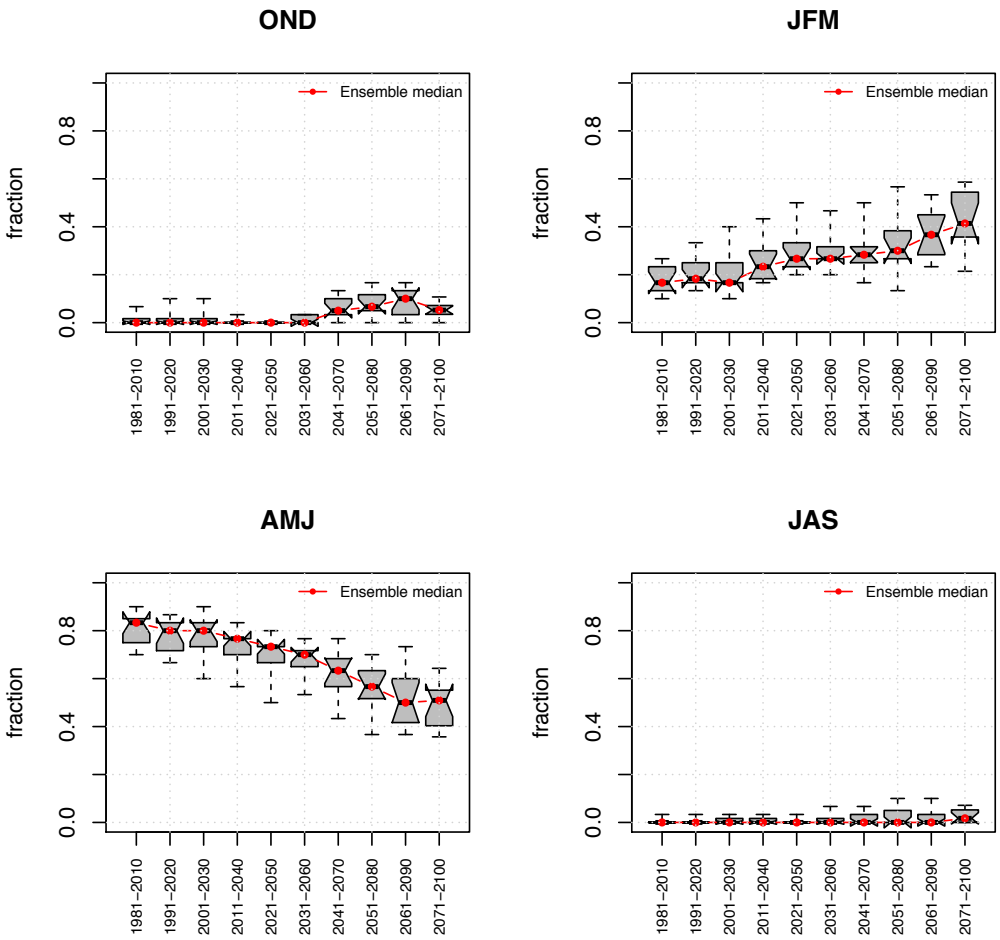

Fig. X-1: Catchment vhm45: Box-plots of the projected frequency (relative number) of AMFs in each season under the RCP4.5 emission scenario. The notches give an estimate of the 95% confidence interval (CI) of the median. The 95% CI sometimes exceeds the interquartile range. Projected medians from the reference and future periods significantly differ if their CIs do not overlap.

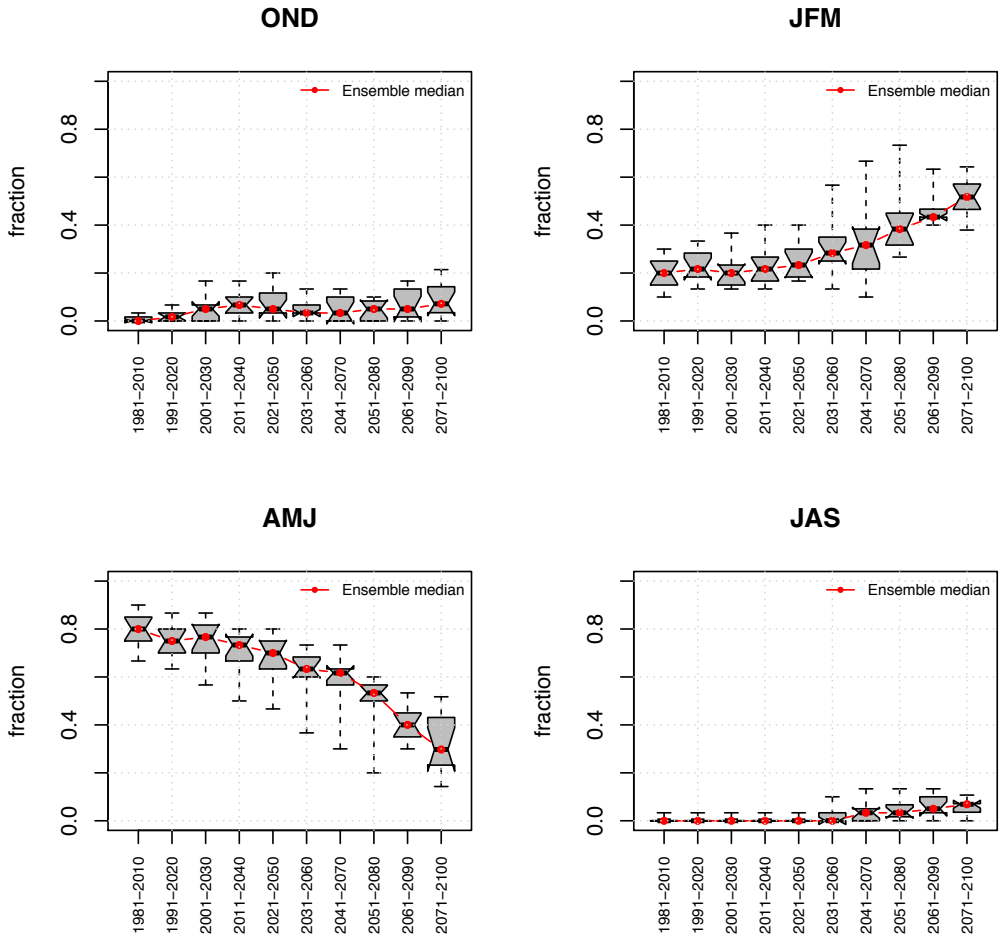

Fig. X-2: Catchment vhm45: Box-plots of the projected frequency (relative number) of AMFs in each season under the RCP8.5 emission scenario. The notches give an estimate of the 95% confidence interval (CI) of the median. The 95% CI sometimes exceeds the interquartile range. Projected medians from the reference and future periods significantly differ if their CIs do not overlap.

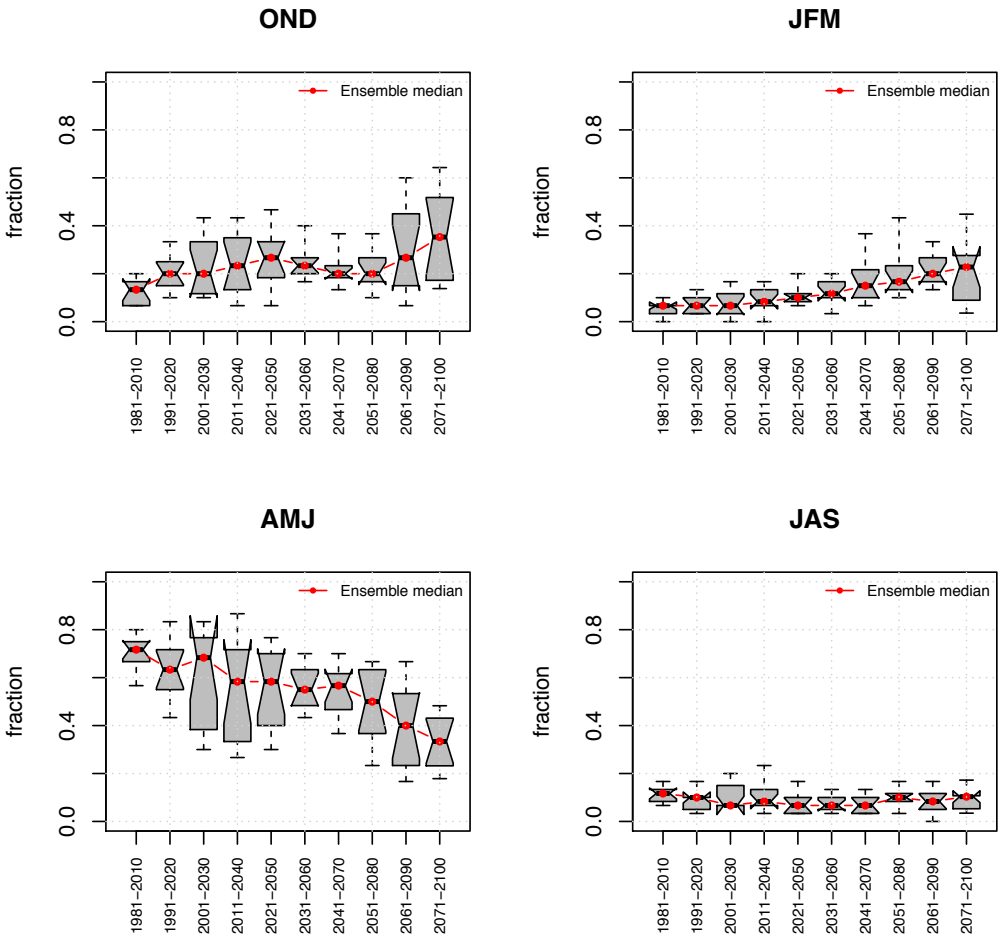

Fig. X-3: Catchment vhm48: Box-plots of the projected frequency (relative number) of AMFs in each season under the RCP4.5 emission scenario. The notches give an estimate of the 95% confidence interval (CI) of the median. The 95% CI sometimes exceeds the interquartile range. Projected medians from the reference and future periods significantly differ if their CIs do not overlap.

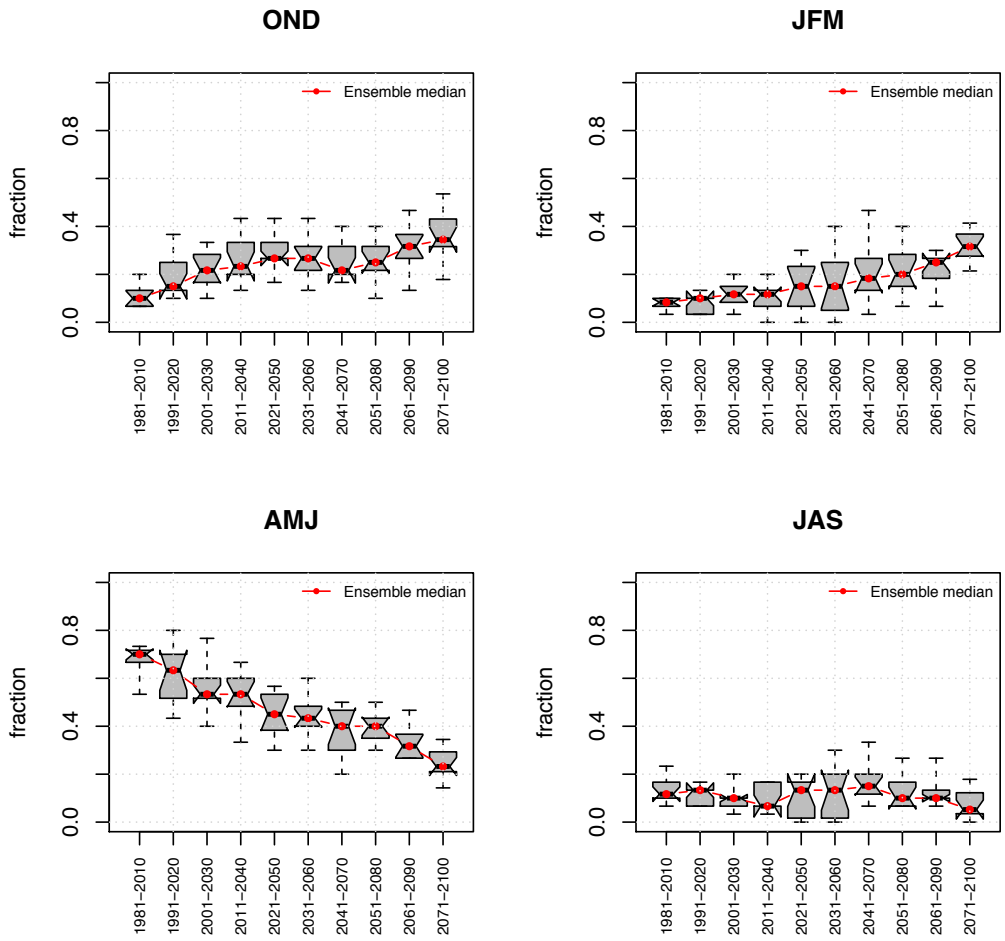

Fig. X-4: Catchment vhm48: Box-plots of the projected frequency (relative number) of AMFs in each season under the RCP8.5 emission scenario. The notches give an estimate of the 95% confidence interval (CI) of the median. The 95% CI sometimes exceeds the interquartile range. Projected medians from the reference and future periods significantly differ if their CIs do not overlap.

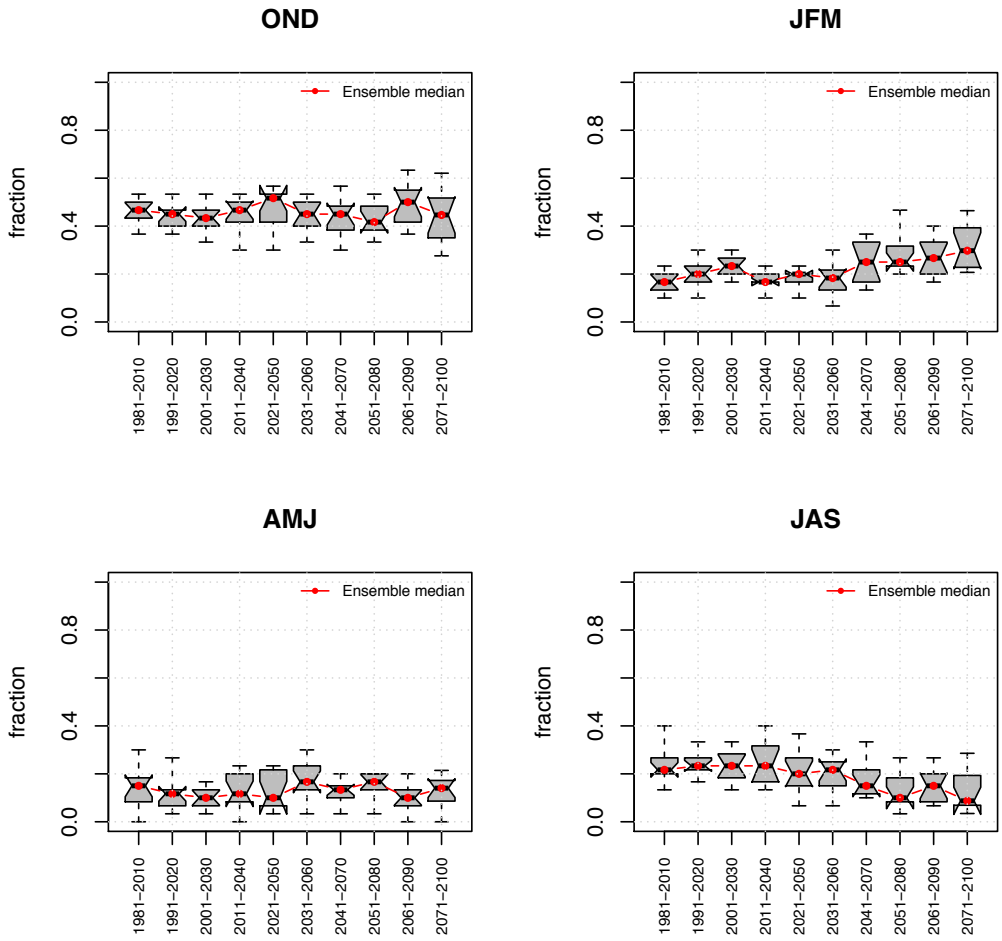

Fig. X-5: Catchment vhm149: Box-plots of the projected frequency (relative number) of AMFs in each season under the RCP4.5 emission scenario. The notches give an estimate of the 95% confidence interval (CI) of the median. The 95% CI sometimes exceeds the interquartile range. Projected medians from the reference and future periods significantly differ if their CIs do not overlap.

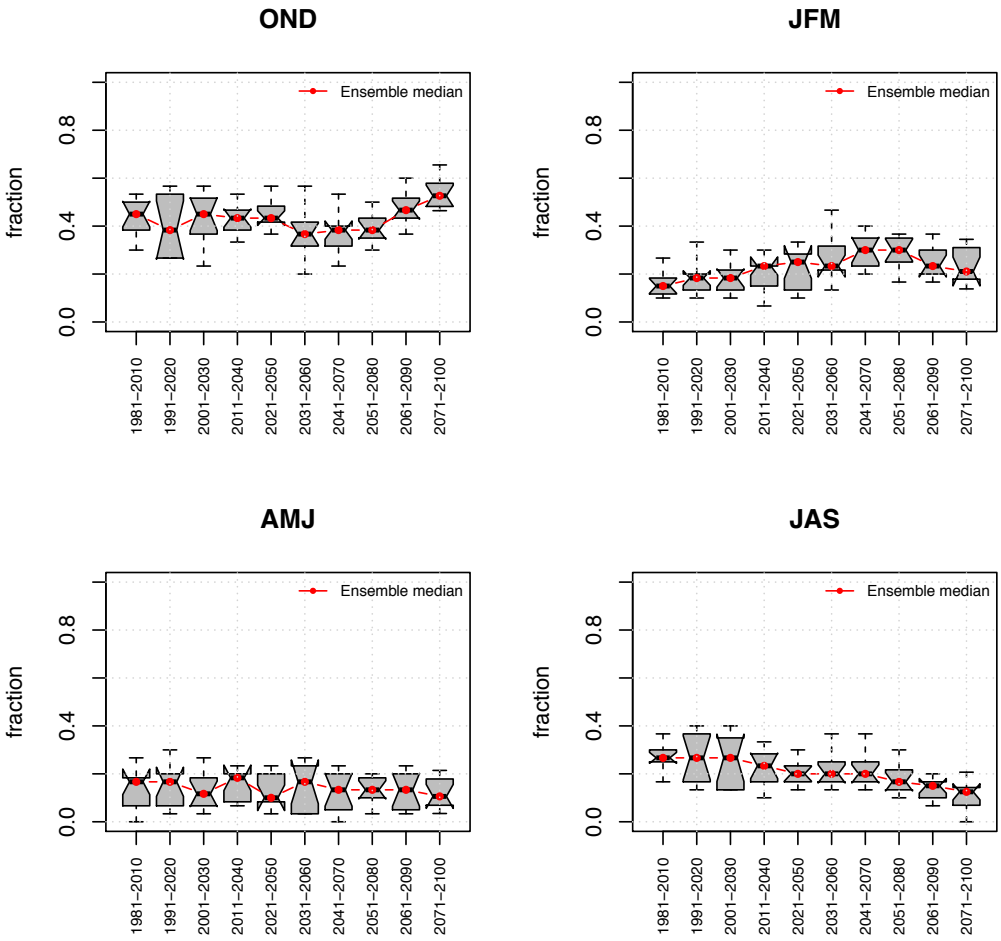

Fig. X-6: Catchment vhm149: Box-plots of the projected frequency (relative number) of AMFs in each season under the RCP8.5 emission scenario. The notches give an estimate of the 95% confidence interval (CI) of the median. The 95% CI sometimes exceeds the interquartile range. Projected medians from the reference and future periods significantly differ if their CIs do not overlap.

Appendix 11

Box-plots of the projected changes in the magnitude of T-year floods for all ensemble members

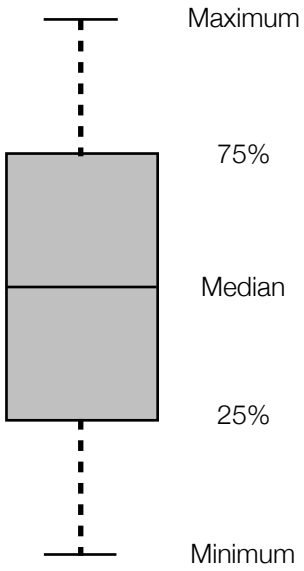

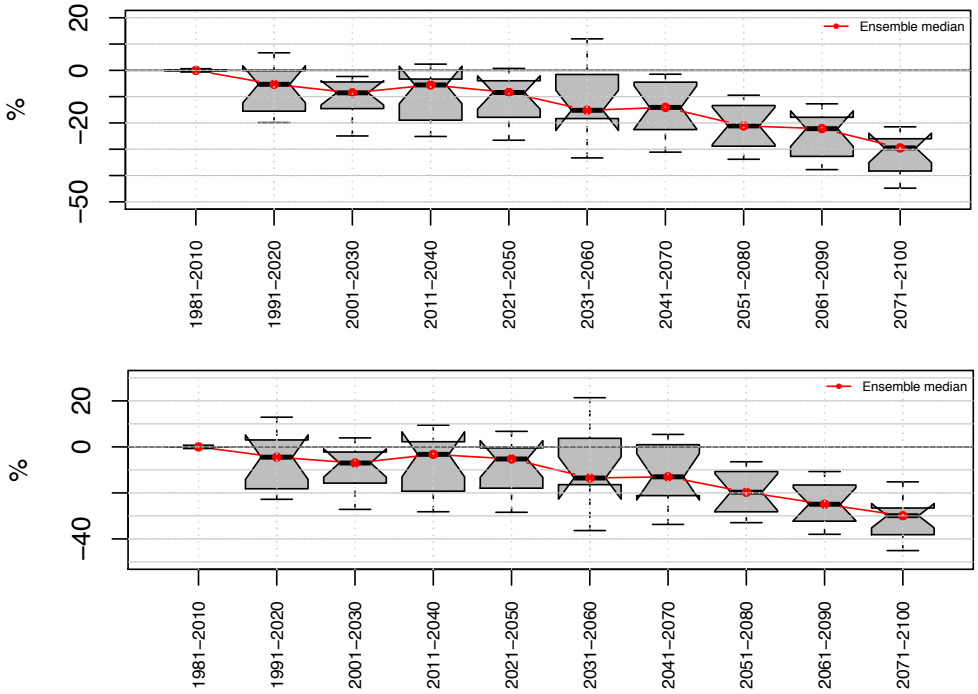

Fig. XI-1: Catchment vhm45, RCP4.5 emission scenario: Projected changes (in percent) in the magnitude of the 10-year flood (top) and 100-year flood (bottom) relative to the reference period (1981-2010). The notches give an estimate of the 95% confidence interval (CI) of the median. The 95% CI sometimes exceeds the interquartile range.

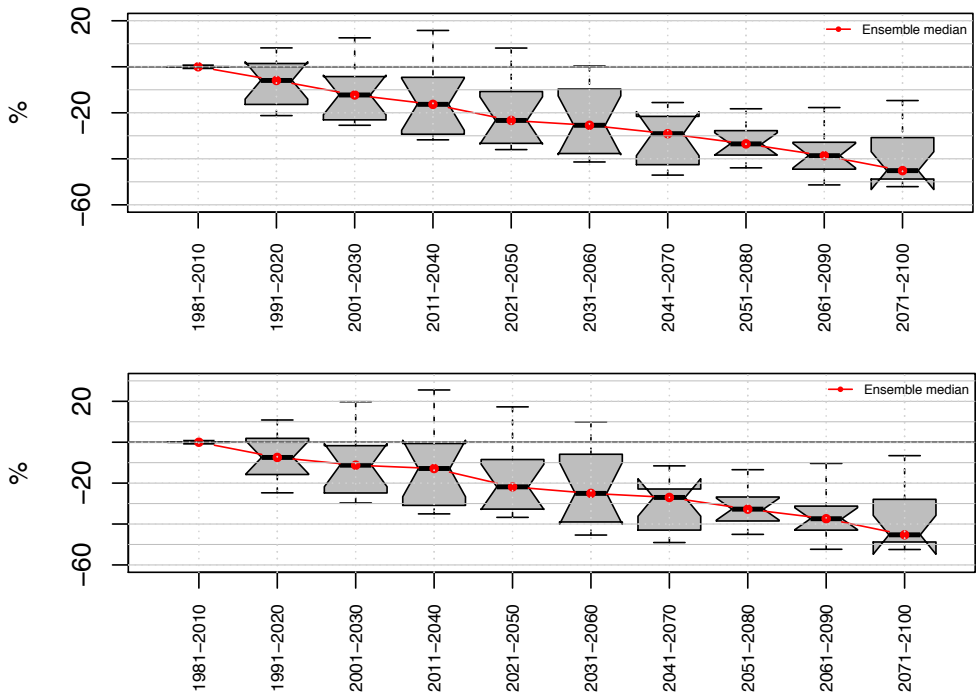

Fig. XI-2: Catchment vhm45, RCP8.5 emission scenario: Projected changes (in percent) in the magnitude of the 10-year flood (top) and 100-year flood (bottom) relative to the reference period (1981-2010). The notches give an estimate of the 95% confidence interval (CI) of the median. The 95% CI sometimes exceeds the interquartile range.

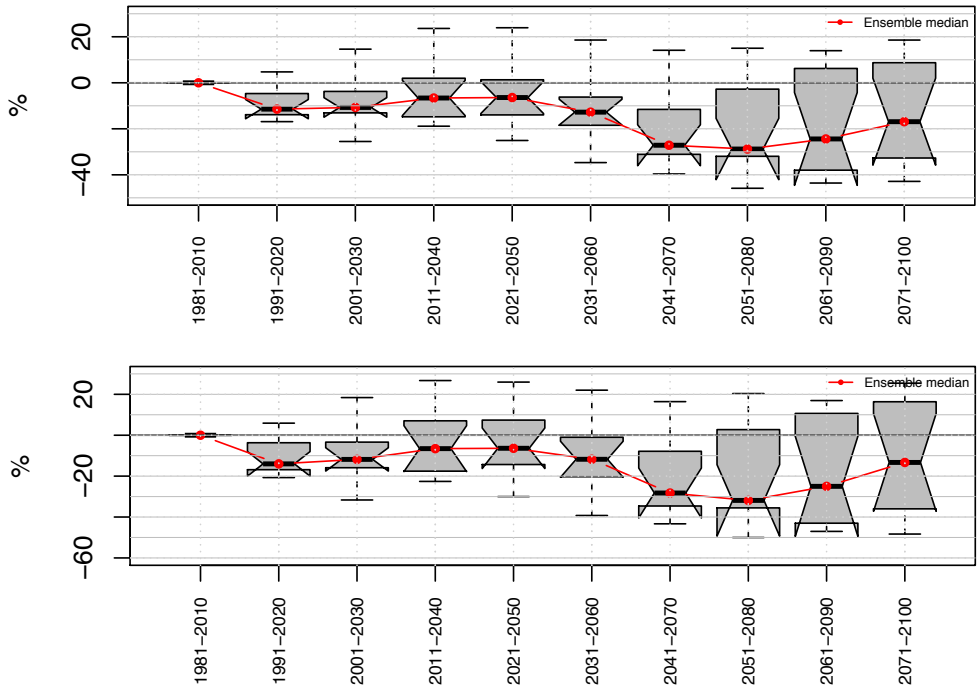

Fig. XI-3: Catchment vhm48, RCP4.5 emission scenario: Projected changes (in percent) in the magnitude of the 10-year flood (top) and 100-year flood (bottom) relative to the reference period (1981-2010). The notches give an estimate of the 95% confidence interval (CI) of the median. The 95% CI sometimes exceeds the interquartile range.

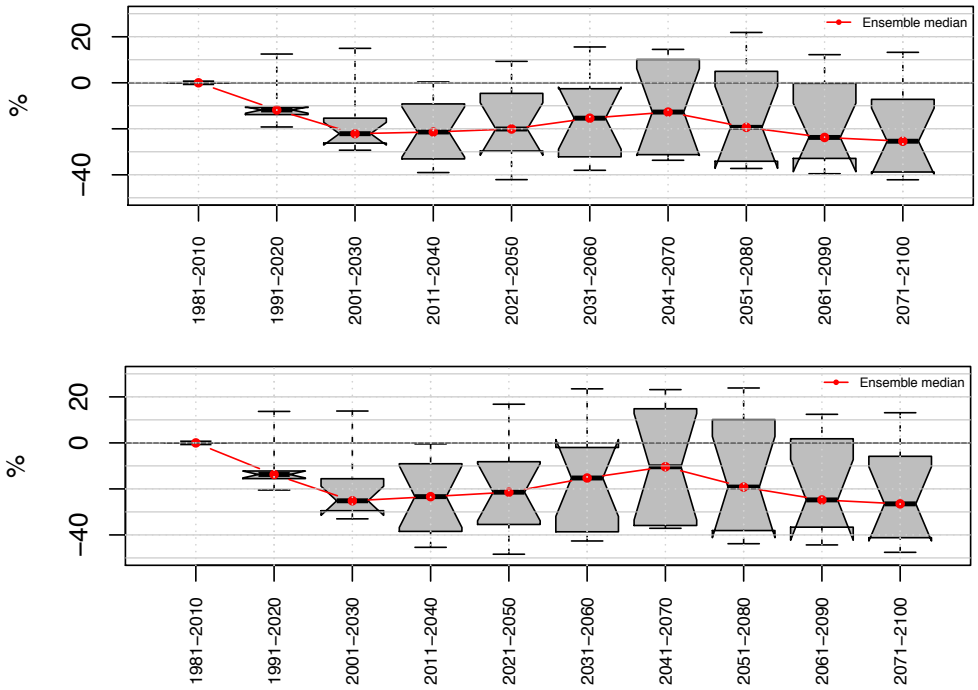

Fig. XI-4: Catchment vhm48, RCP8.5 emission scenario: Projected changes (in percent) in the magnitude of the 10-year flood (top) and 100-year flood (bottom) relative to the reference period (1981-2010). The notches give an estimate of the 95% confidence interval (CI) of the median. The 95% CI sometimes exceeds the interquartile range.

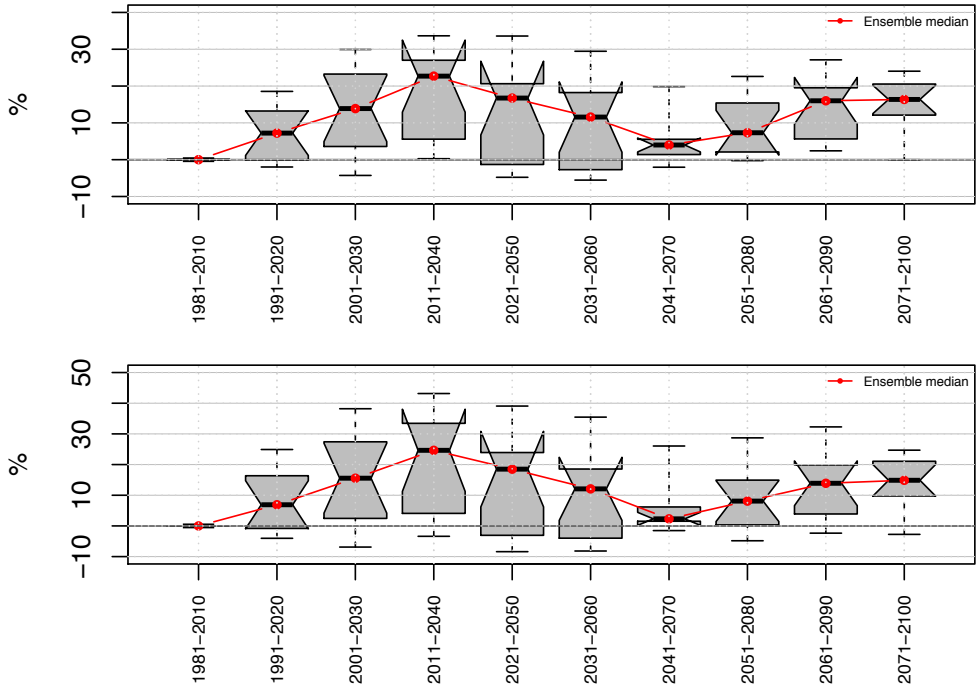

Fig. XI-5: Catchment vhm149, RCP4.5 emission scenario: Projected changes (in percent) in the magnitude of the 10-year flood (top) and 100-year flood (bottom) relative to the reference period (1981-2010). The notches give an estimate of the 95% confidence interval (CI) of the median. The 95% CI sometimes exceeds the interquartile range.

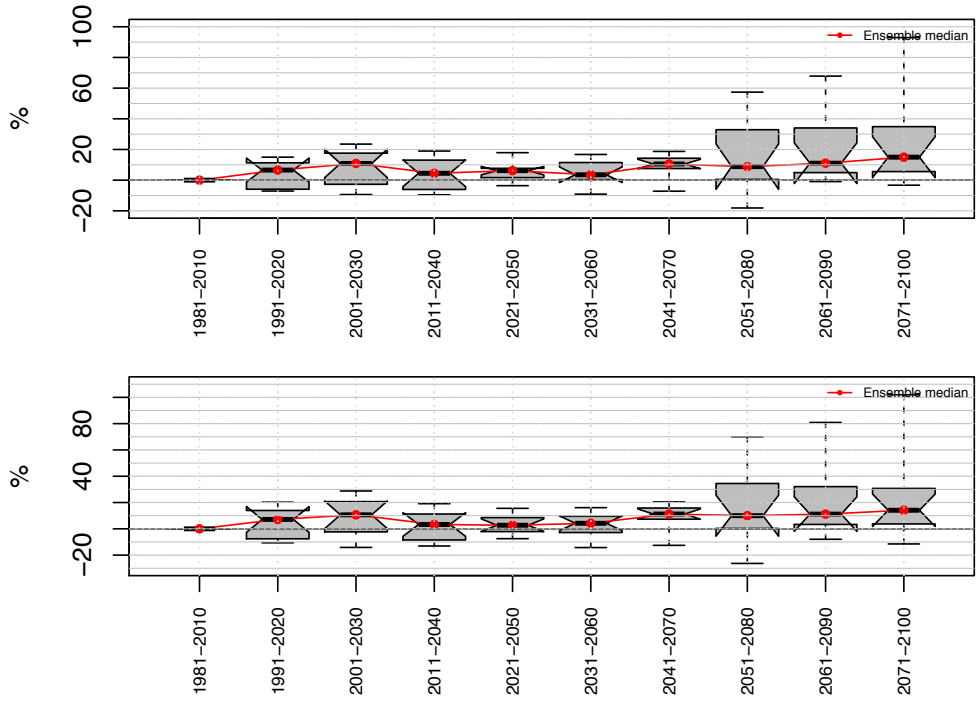

Fig. XI-6: Catchment vhm149, RCP8.5 emission scenario: Projected changes (in percent) in the magnitude of the 10-year flood (top) and 100-year flood (bottom) relative to the reference period (1981-2010). The notches give an estimate of the 95% confidence interval (CI) of the median. The 95% CI sometimes exceeds the interquartile range.